THE UNIVERSITY
of EDINBURGH

MicroRNAs in the regulation of alternatively activated macrophages

Divya Malik

A thesis submitted in fulfilment of requirements for the degree of

Doctor of Philosophy – Immunology and Infection Research

The University of Edinburgh

2016

Contents

List of Figures and Tables

Declaration

I hereby declare that the work presented and described in this thesis is my own unless otherwise acknowledged. This thesis has not been submitted for any other degree or professional qualification except to The University of Edinburgh for the degree of Doctor of Philosophy.

Divya Malik

Date:

Acknowledgements

First and foremost, I'd like to express my appreciation and gratitude for both my supervisors, Prof. Judith Allen and Dr. Amy Buck.

Judi, your constant advice, support and encouragement have meant the world to me these last four years. Thank you for always being there – be it for a quick chat and planning experiments or for listening to my frustrations over negative data. Thank you for not just being there, but for always going one step beyond. Without your constant presence, I would not have made it this far and for that, I will forever be grateful.

Amy, thank you for being the pushing force behind me constantly encouraging me to do my best. For challenging and helping me narrow my haywire stream of thought. I'd like to express my immense gratitude for your support, guidance and for always taking time out to meet, reassure and encourage. Thank you, for everything.

I am extremely thankful to the members of both the Allen and Buck labs. I'd like to especially acknowledge Dominik for providing his microarray data, without which this project would not exist. Beyond that, thank you for mentoring me initially and for being the most patient teacher ever. Thank you for your precious time, patience, help, advice and constant support. Tara, thank you for sharing your expertise for my *in vivo* lung experiments and for always "having a minute". Kat, thank you for so much more than just your amazing technical advice and troubleshooting skills. Nicola and Sheelagh, thank you for all your help and good times with the harvests. Martin, for all those hours teaching and helping with FACS. Many thanks to all the wonderful members, past and present, of both labs for some great memories. There are too many names to type here but you all know who you are!

To my family – mummy, papa, Mohit and Madhu maasi. Thank you for your unconditional love and encouragement. You were my rocks, always there night and day whenever I needed it. I would not have been through this long journey without your support.

Lastly, to my friends Farhin, Afreen, Lek, Asman, Bette, Shatakshi, Kamila, Ritu, Pooja, Carlos and Desmond (and the rest of the gang!). Here's to all the good (and bad) times, the amazing memories and for all backing these last few years.

Abstract

Macrophages play a key role in maintaining the balance and efficiency of the immune response. T_H2 cytokines IL-4 & IL-13, through shared IL-4Rα signalling, trigger a state of alternative activation in macrophages and also drive their proliferation. Alternatively activated macrophages (AAMΦ) are involved in the control of helminth infections and have also been implicated in tissue repair. However, T_H2 weighted imbalance can result in inflammatory disorders such as asthma and fibrosis. Hence, macrophage responses must be tightly regulated. MicroRNAs, a short (~22nt) class of non-coding RNA, are one such immunomodulatory feedback mechanism that can regulate gene expression by targeting the 3' UTR of mRNA resulting in destabilisation of the mRNA and/or inhibition of translation. With their ability for vast gene regulation, it was hypothesised that microRNAs could play a crucial role in the regulation of AAMΦ by targeting genes and pathways critical for their induction, maintenance & proliferation.

Previously generated microarrays in the lab have allowed us to identify microRNAs differentially expressed in AAMΦ. In an effort to determine which microRNAs are genuinely associated with alternative activation, the first part of this project examined the expression profiles of ten shortlisted microRNA candidates under varying conditions of alternative activation, ranging from a reductionist *in vitro* IL-4/13 stimulation of macrophage cell lines to a complex *in vivo* T_H2 mouse model of filarial infection. Profiling of microRNA expression under these conditions revealed that the expression of two IL-4Rα dependent microRNAs, namely miR-199b-5p and miR-378, along with another microRNA, miR-146, was highly regulated and consistently associated with alternative activation. The subsequent chapters of this thesis investigated the contribution of these microRNAs in regulating AAMΦ responses.

Interestingly, we identified miR-199b-5p as being highly expressed in AAMΦ *in vivo* but not *in vitro*. Pathway analysis identified insulin signalling and other proliferative pathways such as PI3K/AKT as being highly targeted by miR-199b-5p. Overexpression of miR-199b-5p in RAW 264.7 cells resulted in a reduction in the rate of proliferation and a change in the levels of Insulin Receptor Substrate -1 (IRS-1), suggesting that miR-199b-5p might regulate macrophage proliferation via insulin signalling. An alteration in the

expression of YM-1 and RELM-α, markers characteristic of alternative activation, was also observed. MiR-199b-5p was successfully delivered to the lung and overexpressed in alternatively activated alveolar macrophages. No effect was observed on IL-4 induced proliferation, potentially due to the lack of significant insulin receptor and IRS-1 expression in alveolar macrophages. However, secreted levels of YM-1, but not RELM-α, were significantly reduced.

MiR-378 is a microRNA that has previously been shown to be associated with AAMΦ through targeting of AKT-1; however, a direct influence of this microRNA on the regulation of this phenotype is yet to be determined. In this thesis, we have provided direct evidence of the impact of miR-378 deficiency on the regulation of AAMΦ and their responses using miR-378 KO mice. The ability of macrophages isolated from WT and KO animals to alternatively activate was studied in various systems both *in vitro* and *in vivo*. The influence of miR-378 deficiency on IL-4 induced proliferation was also addressed *in vivo*. Although the lack of miR-378 had no significant effect on IL-4 driven macrophage proliferation, results from this chapter support a role for miR-378 in the regulation of alternative activation through regulation of YM-1 and RELM-α expression. Lastly, to determine whether this regulation by miR-378 had functional consequences, we also utilised *Litomosoides sigmodontis*, a murine model of filarial infection. Due to experimental limitations, a concrete role for miR-378 in the context of infection could not be established.

The final chapter of this thesis focuses on examining the role of miR-146 in the regulation of AAMΦ. MiR-146a is a highly studied microRNA that has previously been linked strongly to T_H1 immune responses, especially classical activation of macrophages. However, a role for this microRNA in regulating AAMΦ is yet to be determined. Expression levels of miR-146a and miR-146b, the two isoforms of miR-146, were found to be differentially regulated upon alternative activation, with a decrease in miR-146a and increase in miR-146b expression in response to IL-4 both *in vitro* and *in vivo*. Based on this difference in expression and their known functions in suppressing excessive proinflammatory responses, it was hypothesised that miR-146a/b serve to regulate proinflammatory molecules (and signals) in a fine balance to allow efficient alternative activation to occur. However, the high sequence similarity between these two isoforms proved to be a hindrance to test this hypothesis in terms of shared targets. Therefore, the

latter half of this chapter was devoted to the generation and optimisation of a stable cell line for the identification of microRNA targets using CLASH (cross-linking, ligation and sequencing of hybrids).

In summary, the results from this thesis provide an important foundation for further studies of the functional role of microRNAs in the regulation of AAMΦ. Firstly, it characterises the expression profiles of ten different microRNAs differentially expressed during alternative activation. Secondly, for the first time, it identifies a role for miR-199b-5p in the regulation of macrophage proliferation and activation. Thirdly, this thesis has provided direct evidence for the effect of miR-378 deficiency on AAMΦ responses. Lastly, it identifies and demonstrates the robust differential expression of two separate isoforms of the same microRNA (miR-146) under varying conditions of alternative activation, whose functional properties as regulators of the AAMΦ phenotype await further investigation.

Abbreviations

°C	Degrees Celsius
~	Approximately
AAMϕ	Alternatively activated macrophage
AGO	Argonaute
AKT	V-Akt murine thymoma viral oncogene homolog
ANOVA	Analysis of variance
APC	Antigen presenting cell
APS	Ammonium persulfate
ATP	Adenosine triphosphate
bp	Base pairs
CAMϕ	Classically activated Macrophage
CCR4-NOT C-C	Chemokine receptor 4-NOT transcription complex
CD	Cluster of differentiation
CD4	Cluster of differentiation 4
CD8	Cluster of differentiation 8
cDNA	Complementary deoxyribonucleic acid
CDS	Coding sequence
CLASH	Cross-linking, ligation and sequencing of hybrids
CLIP	Cross-linking and immunoprecipitation
CNE1	Cyclin E1
CO_2	Carbon dioxide
CSF-1/2	Colony stimulating factor -1/2
CSF1R	Colony stimulating factor 1 receptor
DC	Dendritic cells

ddH20	Double-distilled water
DGCR8	DiGeorge Syndrome Critical Region 8 Protein
DMEM	Dulbecco's modification of eagle's medium
DNA	Deoxyribonucleic acid
dNTP	Deoxynucleotide triphosphate
ECL	Enhanced chemiluminescence
ECM	Extracellular matrix
EDTA	Ethylenediaminetetraacetic acid
eIF4E	Eukaryotic translation initiation factor 4E
eIF4F	Eukaryotic translation initiation factor 4F
eIF4G	Eukaryotic translation initiation factor 4G
ELISA	Enzyme-linked immunosorbent assay
ESC	Embryonic stem cell
FACS	Fluorescence-activated cell sorting
FC	Fold change
FCS	Foetal calf serum
g	Gravitational force
G-MCSF	Granulocyte macrophage colony stimulating factor
GAPDH	Glyceraldehyde-3-phosphate dehydrogenase
gm	Grams
GW182	Glycine-tryptophan protein of 182 kDa
HEK	Human Embryonic Kidney
HI-CS	Heat-inactivated calf serum
HI-FBS	Heat-inactivated foetal bovine serum
HSC	Haematopoietic stem cell
IFN	Interferon
IGF	Insulin growth factor

IgG	Immunoglobulin G
IL	Interleukine
iNOS	Inducible nitric oxide synthase
IPA	Ingenuity pathway analysis
IR	Insulin Receptor
IRES	Internal ribosome entry site
IRS-1	Insulin Receptor substrate
ISG	Interferon-stimulated gene
kb	Kilobase
kDa	Kilodalton
M	Molar
m7G	7-methylguanosine (m7G) cap
MAPK	Mitogen-activated protein kinase
MHC	Major histocompatibility complex
miR	microRNA
ml	Millilitre
mM	Millimolar
MOI	Multiplicity of infection
mRNA	Messanger RNA
Ncapg2	Non-SMC condensin II complex subunit G2
NFκB	Nuclear Factor κB
ng	Nanogram
nM	Nanomolar
nt	Nucleotides
ORF	Open reading frame
PABP1	Poly(A)-binding protein 1
PACT	Protein kinase R-activating protein

PAMP	Pathogen Associated Molecular Patterns
PAN2	Poly(A) specific ribonuclease subunit homolog
PBS	Phosphate buffered saline
PCR	Polymerase chain reaction
pH	Measure for the hydrogen ion concentration
PI3K	Phosphatidylinositol 3-kinase
PIK3R1	Phosphoinositide-3- kinase, regulatory subunit 1
Pol	Polymerase
PPAR-α	Peroxisome proliferator activated receptor-alpha
PPAR-γ	Peroxisome proliferator-activated receptor gamma
Pre-miRNA	Precursor microRNA
Pri-miRNA	Primary microRNA
qRT-PCR	Quantitative real time polymerase chain reaction
Rb	Retinoblastoma like 1
RBC	Red blood cells
RELM	Resistin Like Molecule
RISC	RNA-induced silencing complex
RNA	Ribonucleic acid
ROR	RAR related orphan receptor
SD	Standard deviation
SDS	Sodium dodecyl sulfate
SDS-PAGE	Sodium dodecyl sulfate polyacrylamide
SEM	Standard error mean
SHIP1	SH2 domains of inositol polyphosphate 5-phosphatases
siRNA	Small interfering ribonucleic acid
SOCS1	Suppressor of cytokine signaling1
STAT	Signal transducer and activator of transcription

TBE	Tris-borate-EDTA
TBS-T	Tris-buffered saline-Tween
TCA	Trichloroacetic Acid
TCR	T cell signalling pathway
TGF-β	Transforming growth factor-beta
T_H	T helper
Tk1	Thymidine Kinase 1
TLR	Toll Like Receptors
TNF-α	Tumour necrosis factor alpha
TRBP	Transactivation-response RNA-binding protein
U	Unit
U6 snRNA	Small nuclear RNA U6 (RNU6B)
UTR	Untranslated region of mRNA
XRN1	Exoribonuclease enzyme 1
µ	Micro
µg	Microgram
µl	Microliter
µM	Micromolar

Chapter 1: Introduction

1.1 The immune system and the T helper cell paradigm

The immune system has evolved to protect the host against a plethora of pathogens that range from microscopic organisms such as bacteria and viruses to far larger multicellular parasites such as helminths. Different pathogens utilise distinct methods of growth, survival and immune evasion resulting in insult and injury to the host. This necessitates the employment and activation of diverse effector mechanisms by the host to mount a response effective enough to contain and/or eliminate the foreign pathogen, whilst at the same time maintaining tolerance to self and limiting collateral damage (Parkin and Cohen, 2001, Graham et al., 2005a). The immune system has been classified into the innate and adaptive immune systems. The innate immune system initially detects foreign invasion through the recognition of common components/molecular patterns of pathogens and provides the first line of defence in a relatively non-specific manner. However, innate immunity is not always sufficient to recognise and eliminate all infectious agents. To deal with organisms that survive and/or escape this initial response, the adaptive immune system comprising B and T lymphocytes has evolved to provide a more versatile means of defence involving pathogen recognition in an antigen specific manner, but is still reliant on innate effectors (Dempsey et al., 2003, Paul, 2011).

T lymphocytes play a central role in immunostimulation and immunomodulation. T helper (T_H) cells, which express the cell surface marker CD4, orchestrate the employment of an appropriate immune response by differentiating into discrete subsets and secreting distinct cytokines. Based upon their cytokine profiles, these $CD4^+$ helper T cells were initially classified into one of two subsets by Mosmann and Coffman (Mosmann et al., 1986). Subsequently, transcriptional regulators were identified that verified this subset distinction. T helper type 1 (T_H1) cells are characterised by the transcription factor T-bet and expression of Interferon-γ (IFN- γ) and Tumour Necrosis Factors (TNFs) and considered to be mediators of immunity against intracellular pathogens. In contrast, T_H2 cells are distinguished by their

expression of the transcription factor GATA-3 and production of the cytokines IL-4, IL-5 and IL-13 (Romagnani, 1997, Kidd, 2003, Kaiko et al., 2008) among others. This original T_H1/ T_H2 paradigm has now developed into the T_H1/ T_H2/ T_H17 paradigm with the addition of the third T_H17 subset that requires the transcription factors ROR and STAT3 and an extensive network of cytokines such as the differentiation factors TGF-β, IL-6 and IL-21, and IL-23 for growth and stability (Steinman, 2007, Korn et al., 2009, Peck and Mellins, 2010). T_H17 cells mediate host defensive mechanisms to various infections, especially extracellular bacterial infections, and are characterised by their preferential production of IL-17, IL-21 and IL-22 (Ouyang et al., 2008, Korn et al., 2009). T_H17 cells are also involved in the pathogenesis of many autoimmune diseases (Waite and Skokos, 2012, Noack and Miossec, 2014, Yang et al., 2014). Another distinct lineage of $CD4^+$ T cells whose differentiation is also induced by TGF-β are T regulatory (T_{reg}) cells, identified according to their high expression of CD25 and the transcription factor Foxp3, and their ability to negatively regulate excessive and aberrant immune responses (Vignali et al., 2008, Saito et al., 2010, Josefowicz et al., 2012).

In addition to recognition mechanisms that have evolved to overcome the constraints faced by the innate immune system, adaptive immunity also provides increased protection against subsequent reinfection with a pathogen previously encountered by the host. However, the cells of the innate immune system play a crucial role in the initiation and subsequent direction of these adaptive immune responses, besides participating in the removal of pathogens targeted by the adaptive immune response. Mounting of an effective immune response thus depends on careful interplay between the innate and adaptive immune arms.

1.2 Macrophages

Macrophages sit at the interface of innate and adaptive immunity and are crucial for maintaining the balance and efficiency of the immune response. Macrophages are mononuclear phagocytes essential for the maintenance of homeostasis and are also involved in both the initiation and resolution of inflammatory responses.

Macrophages are present in essentially all tissues of the body. Until recently, the majority of the tissue resident macrophages were believed to originate from bone marrow derived blood monocytes (Davies et al., 2013a). However, recent evidence suggests that adult tissue macrophages in most tissues originate during development and not from circulating monocytes (Hashimoto et al., 2013, Epelman et al., 2014). Work from the Geissmann lab has shown that populations of tissue resident macrophages can arise from embryonic yolk sac precursors (Schulz et al., 2012, Gomez Perdiguero et al., 2015) and others have shown that they can also be foetal monocyte derived (Guilliams et al., 2013). Macrophages are dependent on either Colony-Stimulating Factor 1 (CSF-1, M-CSF) (Cecchini et al., 1994, Pixley and Stanley, 2004) or IL-34 (Wang et al., 2012), both of which signal via the CSF-1 receptor (CSF1R, *Csf1r,* CD115) (Hume and MacDonald, 2012) and are essential for macrophage development and survival. However, it has been shown that alveolar macrophages self-maintain via Granulocyte Macrophage Colony Stimulating Factor instead (GM-CSF, CSF-2) (Guilliams et al., 2013, Hashimoto et al., 2013). Besides differences in their origin, it has now also been demonstrated that the tissue environment in itself is a major controller of macrophage phenotype and can be a key determinant influencing the expression of several genes regardless of origin (Davies and Taylor, 2015).

Since macrophages are so widely distributed in various tissues throughout the body, they provide a first line of defence against invading pathogens. As part of the innate immune system, macrophages have the ability to recognise, engulf and kill potential pathogens (Gordon, 2007, Zhang and Mosser, 2008). At the same time, through their function as Antigen Presenting Cells (APC), macrophages bridge the gap between innate and adaptive immunity (Unanue, 1984). Heterogeneity and plasticity are hallmarks of macrophages. With such diverse characteristics, it is not surprising that macrophages display a range of functional phenotypes depending on the environmental cues and stimuli that they encounter (Mosser and Edwards, 2008).

1.2.1 Classical activation of macrophages

Also referred as M1 activation, classical activation is the best-documented mode of macrophage activation. Classically activated macrophages (CAMΦ) are the major effector cells of the T_H1 response and their prime functional focus is microbial destruction. CAMΦ are induced by exposure to a combination of two signals, the cytokine IFN-γ in concert with microbial products such as lipopolysaccharide (LPS) (Nathan, 1991, Wherry et al., 1991, Dalton et al., 1993, Mantovani et al., 2005). Signalling via IFN-γ is often termed the "priming step" that activates the transcription factor STAT1, which binds to Gamma-Activated Sequences (GAS) found in several immune effector genes. The second stimulus is ligation of one of the Toll Like Receptors (TLRs) with ligands typically expressed on pathogens termed Pathogen Associated Molecular Patterns (PAMPs). Activation of TLRs induces the MyD88 dependent production of Tumour Necrosis Factor (TNF-α), a cytokine that co-operates with IFN-γ and acts in an autocrine manner to stimulate macrophages (Mosser and Edwards, 2008, Mosser and Zhang, 2008). Whilst IFN receptor ligation activates STAT molecules, Nuclear Factor κB (NFκB) and Mitogen Activated Protein Kinases (MAPKs) are activated in response to TLR or TNF receptor ligation. Of note, TLR signalling through the adaptor molecule Toll IL-1 Receptor domain-containing adaptor-inducing IFN-beta (TRIF) can induce the production of IFNβ. This IFNβ can replace IFN-γ, thereby overcoming the need for two signals for activation (Mosser and Zhang, 2008).

CAMΦ are identified by virtue of their generation of a wide variety of oxygen and nitrogen derived radicals with antimicrobial properties, such as hydrogen peroxide (H_2O_2), superoxide ($O2^-$) anions and hydroxyl (OH) radicals (Nathan et al., 1983, Ding et al., 1988). Inducible nitric oxide synthase (iNOS, *Nos2*) is responsible for the production of the primary reactive nitrogen intermediate, nitric oxide (NO)(MacMicking et al., 1997, Mori and Gotoh, 2000). These reactive radical based cytotoxic pathways are triggered as a result of proinflammatory cytokine production (Parameswaran and Patial, 2010), which are generally the result of TLR ligation (Mosser and Zhang, 2008). TLR ligation also results in the production of other pro-inflammatory cytokines that are an

important component of host defence, but can also cause extensive damage to host physiology. For example, CAMΦ produce IL-1, IL-6 (Figure 1.1) and IL-23 (Mosser and Edwards, 2008) that have been associated with the development and expansion of T_H17 cells (Bettelli et al., 2006, Veldhoen et al., 2006), which have implicated roles in several autoimmune disorders (Langrish et al., 2005, Waite and Skokos, 2012).

1.2.2 Alternative activation of macrophages

Similar to the T_H1/T_H2 paradigm, an M1/M2 activation paradigm has been proposed for macrophages [reviewed in (Martinez and Gordon, 2014)]. However, the differentiation of macrophages into the M1 and M2 phenotypes is presumed to be more flexible than the differentiation of T helper cell subsets. Although M1/classical activation has a fairly clearly defined effector role and phenotype, the M2 activation phenotype of macrophages is less clear-cut. As such, M2 cells have been further sub-categorised into three polarised populations (Mantovani et al., 2004):

- **M2a**: induced by the cytokines IL-4 and IL-13 (hereafter referred to as "alternatively activated macrophages" in this thesis)
- **M2b**: induced by exposure to immune complexes and agonists of TLRs or IL-I receptor (IL-1R)
- **M2c**: induced by IL-10 and glucocorticoid (GC) hormones

Due to the complex nature of terminology utilised with regards to mediators involved in the generation of different polarised macrophage populations, Murray *et al* (2014) proposed the adoption of a uniform nomenclature that is linked to the activating stimulus concerned (Murray et al., 2014). In line with this, the M2a-c states of macrophage activation are addressed as M(IL-4), M(Ig)/M(LPS)/M(IFN-γ) and M(IL10)/ M(GC) respectively instead.

The Allen lab follows Siamon Gordon's description of alternative activation of macrophages and defines alternative activation [M(IL-4)] as a state of activation

induced by the T_H2 cytokines IL-4 and IL-13 (Gordon and Martinez, 2010).Therefore, for the purpose of this thesis, all references made to alternative activation refer to the M(IL-4) or M2a state of activation.

In contrast to CAMΦ being elicited in response to T_H1 stimuli, alternatively activated macrophages (AAMΦ) are potently induced during T_H2 responses. Macrophage function in large part is determined by stimuli they encounter from the local environment. Of utmost importance are cytokine signals from cells that are also recruited or present at the site of insult and injury. IL-4 and IL-13 signal through a shared IL-4 receptor (IL-4Rα) chain (Heller et al., 2008) that is absolutely required for the induction of AAMΦ. The IL-4Rα forms heterodimers with either the gamma chain (γC subunit) to form the Type I receptor or the IL-13Rα1 subunit to form the Type II receptor (Gordon, 2003, Heller et al., 2008, Gordon and Martinez, 2010). Thus, IL-4 has the ability to activate both Type I & II receptors whereas IL-13 activates Type II receptors only. In addition, the IL-21 receptor has been shown to augment the AAMΦ phenotype, mainly by increasing IL-4Rα and IL-13Rα expression (Pesce et al., 2006). Furthermore, IL-33 (ST2) is also known to contribute to the polarisation of AAMΦ by upregulating the expression IL-4Rα and promoting type 2 chemokine production (CCL24 and CCL17) (Kurowska-Stolarska et al., 2009). A role for the IL-33 receptor has also been implicated in IL-13 production that induces alternative activation of macrophages (Yang et al., 2013, Piehler et al., 2015).

Signalling via either IL-4 or IL-13 promotes phosphorylation of the IL-4Rα subunit, resulting in the activation of the transcription factor Signal Transducer and Activator of Transcription 6 (STAT6) (Hou et al., 1994, Goenka and Kaplan, 2011). Phosphorylation and subsequent activation of STAT6 drives alternative activation through the upregulation of several genes including *Arginase-1* (Arg-1), *Chi3l3* (Chitinase 3 like 3, YM-1) and *Retnla* (Resistin like alpha, RELM-α), considered to be hallmarks of AAMΦ (Modolell et al., 1995, Munder et al., 1999, Loke et al., 2002, Stutz et al., 2003). AAMΦ can be derived from both tissue resident macrophages and from recruited inflammatory monocytes. However, Gundra *et al* showed that these different sources generate AAMΦ that are transcriptionally distinct

(Gundra et al., 2014). Whilst Arg-1, YM-1 and RELM-α are expressed in AAMΦ regardless of origin, molecules such as the Mannose Receptor (MR, CD206) (Stein et al., 1992), Retinal Dehydrogenase 2 (Raldh2) (Broadhurst et al., 2012) and Programmed Death Ligand 2 (PD-L2) (Huber et al., 2010) that are also potently enhanced in response to IL-4 and strongly associated with AAMΦ have now been shown to be highly upregulated predominantly by AAMΦ of blood monocyte origin (Gundra et al., 2014).

1.2.2.1 Markers characteristic of alternatively activated macrophages

YM-1 and RELM-α were initially found to be major targets of IL-4 action and abundantly expressed in AAMΦ isolated from *Brugia malayi* infection in mice (Loke et al., 2002, Nair et al., 2003). Both YM-1 and RELM-α can also be induced in response to IL-4 and IL-13 *in vitro* (Raes et al., 2002, Nair et al., 2003, Edwards et al., 2006). YM-1 is an enzymatically inactive chitinase-like lectin found in mice that belongs to the chitinase-like protein (CLP) family (Jin et al., 1998, Chang et al., 2001). CLPs are amongst the most abundant proteins found under conditions of T_H2 activation but their functions are still poorly understood. In agreement with this, YM-1 expression is enhanced during a wide range of pathologies and it has previously been identified as a mediator of T_H2 inflammation in allergy (Webb et al., 2001, Welch et al., 2002). More recently, our lab has shown that YM-1 promotes IL-17 mediated neutrophilia that is essential for limiting parasite survival during *Nippostrongylus brasiliensis* infection in the lung (Sutherland et al., 2014). YM-1 was first described as an eosinophil chemotactic factor produced by CD8 lymphocytes (Owhashi et al., 1998). However, this finding has not been subsequently verified.

RELM-α is a member of the secreted cysteine-rich resistin-like molecules (RELM) family of proteins that was first identified in the lavage fluid of mice with experimentally induced asthma (Holcomb et al., 2000). Like YM-1, RELM-α has also been strongly associated with type 2 immune responses. However, the functions of RELM-α in T_H2 mediated settings such as helminth infection still remain to be

elucidated. During type 2 inflammation, a role for RELM-α has been implicated as a negative regulator by limiting pathogenesis of T_H2 cytokine mediated pulmonary inflammation (Nair et al., 2009). Additionally, recombinant RELM-α has also been reported to antagonise the effects of nerve growth factor (NGF), a protein associated with the exacerbation of allergic pulmonary responses (Holcomb et al., 2000). In contrast, RELM-α also exhibits various pro-fibrotic functions. These are discussed more in depth later on along with other effector functions of AAMΦ.

AAMΦ and their responses are widely considered to be "anti-inflammatory" in contrast to the pro-inflammatory CAMΦ (Martinez and Gordon, 2014). The induction of *Arginase-1* (Arg-1) by AAMΦ, another marker characteristic of alternative activation, exemplifies this functional antagonism between the two phenotypes (Modolell et al., 1995). Whereas AAMΦ produce Arg-1, CAMΦ synthesise inducible nitric oxide synthase (iNOS). The induction of either Arg-1 or iNOS is usually coupled with suppression of the opposing enzyme, indicating a competitive nature in these alternative states of macrophage metabolism (Modolell et al., 1995). Both Arg-1 and iNOS compete for a common substrate, L-arginine (Figure 1.1). Whilst CAMΦ utilise this L-arginine to produce nitrosative intermediates crucial for microbial killing, the same is converted to L-Ornithine and urea by AAMΦ (Munder et al., 1998, Munder, 2009). This L-Ornithine produced by AAMΦ is the substrate for two additional enzymes, namely ornithine decarboxylase (ODC) and ornithine aminotransferase (OAT). These enzymes further metabolise L-Ornithine to polyamines and proline respectively, which are vital for cell proliferation and collagen production (Albina et al., 1993, Igarashi and Kashiwagi, 2000, Bronte and Zanovello, 2005, Yeramian et al., 2006). Consistent with this function of *Arginase-1*, a role for AAMΦ has been implicated in wound repair and this is discussed later on.

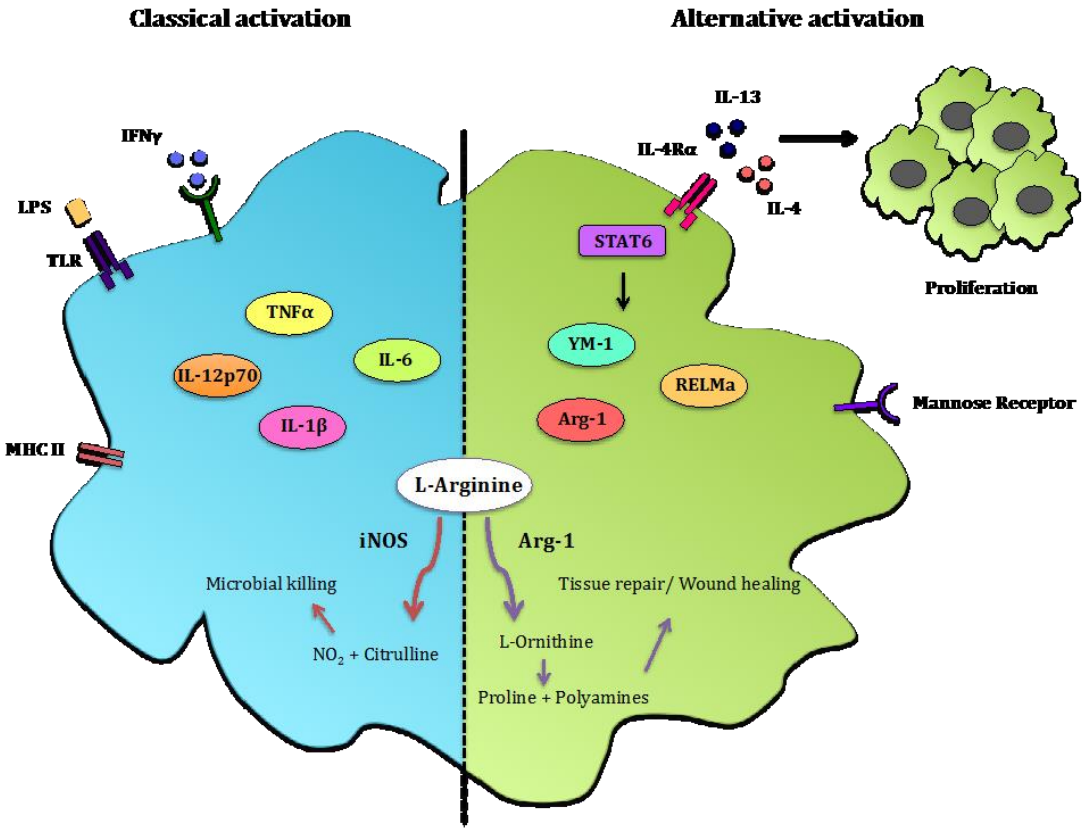

Figure 1.1 Differential metabolism of L-arginine during classical and alternative macrophage activation.

1.3 Macrophage proliferation

In addition to inducing a state of alternative activation, IL-4 (and also IL-13) also drives the proliferation of AAMΦ. IL-4 driven proliferation of macrophages was first discovered by the Allen lab in a study involving the filarial nematode *Litomosoides sigmodontis* (Jenkins et al., 2011), which resides in the pleural cavity of infected mice. In this study, a time course assessment over the first 10 days of infection demonstrated that although there was a steady increase in macrophage numbers in the pleural cavity, their overall profile, as determined by flow cytometry, remained identical to that of naïve mice. Further, depletion of blood monocytes did not alter expansion of the F4/80^{hi} population. This suggested that the resident F4/80^{hi} macrophage population in the pleural cavity was expanding by means other than blood monocyte recruitment. Using Ki67 and BrdU staining as measures of

proliferation, it was found that the resident macrophage population was actively proliferating (Jenkins et al., 2011). This nematode-induced macrophage proliferation was found to be significantly reduced in IL-4$^{-/-}$ mice. Prior to this, the survival and expansion of macrophages in the serous cavities had been associated with CSF1R signalling (Hume et al., 1988, MacDonald et al., 2010, Tagliani et al., 2011). In the study by Jenkins *et al*, IL-4 complex (IL-4c), which is a combination of recombinant IL-4 complexed to an anti-IL-4 antibody, was injected in the peritoneal cavity of mice resulting in a significant increase in macrophage proliferation. Remarkably, proliferation of macrophages was not restricted to the serous cavities, but also observed in other organs such as the liver and spleen. In a subsequent study from our lab, it was revealed that macrophage expansion following IL-4c delivery was independent of the adaptive immune system (using RAG$^{-/-}$ mice). However, the same result could not be achieved in mice deficient in either STAT6 or IL-4Rα (Jenkins et al., 2011, Jenkins et al., 2013). Additionally, using macrophage intrinsic bone marrow chimeras that included reconstitution of WT Ly5.1^{+} mice with a 1:1 mix of Ly5.1^{+} WT and Ly5.2^{+} IL-4Rα$^{-/-}$ cells, Jenkins and colleagues demonstrated that IL-4 acts directly on macrophages and that IL-4Rα is essential to drive proliferation. However, it was identified that as opposed to IL-4Rα$^{-/-}$ cells that failed to incorporate BrdU following IL-4c injection, these IL-4Rα$^{-/-}$ cells during early stages of *L. sigmodontis* infection did in fact incorporate BrdU, but at levels lower than WT cells (Jenkins et al., 2013). This led to the finding that this residual proliferation observed in IL-4Rα$^{-/-}$ cells during *L. sigmodontis* infection was driven by the canonical macrophage mitogen CSF-1. Since IL-13 also signals through a shared IL-4Rα chain, Jenkins *et al* also tested the ability of IL-13 to drive macrophage proliferation. Delivery of IL-13 complex to the peritoneal cavity in a manner similar to IL-4c resulted in IL-13 driving macrophage proliferation comparable to IL-4 (Jenkins et al., 2013).

In addition to IL-4 induced macrophage proliferation being STAT6 dependent, another study from our lab has demonstrated that intact PI3K/AKT signalling is also essential (Ruckerl et al., 2012). Ruckerl *et al* showed that chemical inhibition of AKT completely abrogates IL-4 induced macrophage proliferation. Notably,

proliferation of macrophages *in vitro* in response to IL-4 or IL-13 is very limited, suggesting that IL-4Rα signalling alone is not sufficient to induce macrophage proliferation and that a secondary factor may be needed.

This process of IL-4 (and IL-13) induced proliferation is of particular importance in scenarios of infection wherein recruitment of inflammatory macrophages can be detrimental to host pathology. The proliferation and local expansion of tissue resident macrophages in response to IL-4 may negate the need for coincident accumulation of inflammatory cells recruited from the blood – a key contributory factor to excessive inflammation and tissue damage.

1.4 Functions of alternatively activated macrophages

1.4.1 Helminth Infections

The importance of AAMΦ in a T_H2 environment is strongly suggested by their prevalence in chronic T_H2 settings like multicellular helminth infections. Helminths are a group of metazoan parasites comprising nematodes, trematodes and cestodes that elicit broadly similar immune responses in mammalian hosts (Jenkins and Allen, 2010, Allen and Maizels, 2011). Increasing evidence points to a role for macrophages during helminth infections in imposing slow death by compromising worm vitality and fecundity. For example, during infection with the gut dwelling nematode *Heligmosoides polygyrus*, AAMΦ are involved in impairment of the larval parasite health and mobility, thereby contributing to the expulsion of adult worms (Anthony et al., 2006). In this study, macrophages were depleted in mice during *H. polygyrus* infection using clodronate-loaded liposomes. These mice had impaired worm expulsion and also significantly greater larvae in comparison to mice treated with PBS-loaded liposomes. Moreover, inhibition of Arginase also yielded high parasite burdens and enhanced larval recovery suggesting an essential role for AAMΦ in the development of a protective immune response against *H. polygyrus* (Anthony et al., 2006). In a recent study, expression of AAMΦ markers Arginase-1, YM-1 and RELM-α also strongly correlated with the elimination of *H. polygyrus*. In

the same study, macrophage depletion by clodronate also compromised resistance to infection in BALB/c mice and slowed down worm expulsion (Filbey et al., 2014). A role for arginase was directly implicated in nematode killing during secondary *H. polygyrus* infection by Esser-von Bieren and colleagues (2013). In this study, using mice lacking antibodies or activating Fc receptors, the authors demonstrated that antibodies activate macrophages to trap and immobilise infective larvae. Although the ability of antibodies to induce Arginase expression for worm killing was found to be IL-4Rα independent, the lack of IL-4Rα resulted in a failure of macrophages to accumulate at the site of infection suggesting that certain processes may require macrophage expansion independent of IL-4Rα dependent molecular functions (Esser-von Bieren et al., 2013). Esser-von Bieren and colleagues also showed that L-ornithine and polyamines, which are products derived from arginine catabolism by Arginase-1, reduce the migratory capacity of *H. polygyrus* larvae *in vitro*. In line with these findings, inhibition of Arginase-1 has also been associated with reduced retention and trapping of *Nippostrongylus brasiliensis* larvae in the skin of infected mice (Obata-Ninomiya et al., 2013). Proline, another byproduct of arginine metabolism and the building block of collagen (and thus, extracellular matrix), is found in abundance in *Schistosoma mansoni* induced liver granulomas and considered to be potentially important in restricting larval migration (Morris, 2007).

Delivery of IL-4 and/or IL-13 alone has been reported to trigger mucous production, smooth muscle contraction and epithelial cell turnover, all of which are sufficient to mediate worm expulsion from the gut (Finkelman et al., 2004). AAMΦ have also been implicated in expulsion of parasites by increasing the hypercontractility of intestinal smooth muscles in primary *Nippostrongylus brasiliensis* infection (Zhao et al., 2008). Roles for both IL-4Rα and STAT6 have been implicated in this expulsion (Urban et al., 1998). Eosinophilia is a distinct protective feature of helminth infections (Behm and Ovington, 2000) and mice implanted with the filarial nematode *Brugia malayi* and deficient in AAMΦ display reduced recruitment of eosinophils (Loke et al., 2007). Consistent with these findings, Thomas *et al* have showed that AAMΦ produce CCL24, CCL8 and TxA2 (a bioactive precursor of TxB2), all of which are eosinophil chemoattractants, following *B. malayi* implant in the peritoneal

cavity of mice (Thomas et al., 2012). Interference with macrophage function through injection of carbon particles or carrageenan also enhances the survival of *B. malayi* and *B. pahangi* larvae in the peritoneal cavity of mice (Nakanishi et al., 1989, Rao et al., 1992).

Multinucleated giant cell formation is a feature of AAMΦ that has previously been described (Gordon, 2003). It is thought that fusion of macrophages and giant cell formation may be vital for worm encapsulation and granuloma formation and that this entrapment might be important for allowing the immune system enough time to deploy additional defence mechanisms. Additionally, these fused macrophages are considered to create restricted environments for the secretion of effective killing molecules and/or for the removal of essential nutrients to starve the parasite, thereby limiting parasite survival [reviewed in (Ruckerl and Allen, 2014). In support of this, RNAseq data generated in our lab using *B. malayi* implant has shown that a dramatic change in metabolic pathways utilised by macrophages occurs post infection. This data identified pathways linked with the degradation and processing of many amino acids, thereby suggesting that AAMΦ may withhold essential nutrients from the surrounding environment. Furthermore, upregulation of transporters for amino acid uptake by IL-4Rα was also reported (Thomas et al., 2012). However, it is still debatable whether these mechanisms exist to affect worm vitality or for host metabolic processes.

1.4.1.1 Filariasis

It is estimated that one third of the global human population is infected by helminths, with the most common helminthiases being caused by infection with intestinal helminths such as hookworms (Hotez et al., 2008). Beyond the abundant soil-transmitted infections, helminths are also the causative agents of vector-borne diseases such as Elephantiasis (lymphatic filariasis) (Evans et al., 1993), river blindness (Onchocherciasis) (Davies, 1994) and schistosomiasis (Chitsulo et al., 2000). Filariasis is an infectious disease of the lymphatics and subcutaneous tissues caused by nematodes (roundworms) or filariae that belong to the Filarioidea

superfamily and are transmitted by blood-feeding black flies and mosquitoes. Filariasis is further classified into groups depending on the niche that the parasites inhabit within the body:

1. Lymphatic filariasis – This is caused by parasites that occupy the lymphatic system such as *Wuchereria bancrofti* and *Brugia malayi*.
2. Subcutaneous filariasis – This includes parasites that inhabit the subcutaneous layer of the skin such as *Onchocerca volvulus* and *Loa loa*.
3. Serous cavity filariasis – Includes worms that dwell in the serous cavity of the abdomen such as some *Mansonella* species.

Lymphatic filariasis is an endemic disease estimated to affect approximately 83 countries around the world and ~1.3 billion people are projected to be at risk of developing this disease. The infected patients have a high risk of developing chronic symptoms such as lymphedema, elephantiasis and/or blindness that can result in decreased productivity, quality of life and in some cases also lead to life threatening infections (Mendoza et al., 2009, Ruckerl and Allen, 2014). The life cycles of all filariae are similar, beginning with infective larvae that are transmitted by the relevant vector through a blood meal. The larvae then migrate to the specific niches in the host where they develop into adults and mate. Microfilariae are then released into the blood stream or the skin by female worms, depending on the parasite involved. The transmission vector then takes up the microfilariae during a subsequent blood meal, where they progress onto infective larval stages [reviewed in (Mendoza et al., 2009)].

Models of lymphatic filariasis were utilised in this project and data from these infection models has been discussed in this thesis. The first of these is modelled by the human parasite *Brugia malayi* (McSorley and Maizels, 2012). However, the infective L3 larval stage of *B. malayi*, which is transmitted from the arthropod vector to the mammalian host, does not readily progress to the adult worm stage in mice. Instead, the Mongolian Jird (*Meriones unguiculatus*) serves as an intermediary and adult worms are extracted from the peritoneal cavity of the jird and subsequently implanted surgically into the peritoneal cavity of mice (MacDonald et al., 1998).

Although not the natural host or route of infection, this has served as an effective tool to study T_H2 immune responses mounted against the adult worms.

1.4.1.1.1 *Litomosoides sigmodontis* model of filarial infection

Despite the existence of the *B. malayi* implant model, work in filariasis was constrained by the absence of a model that allows the investigation of both the immunology and natural migration of filarial parasites. In recent years, rodent adapted models have been developed to represent filarial models of human infection. Reflecting lymphatic filariasis and Onchocerciasis (river blindness), *Litomosoides sigmodontis*, developed by Odile Bain's group in Paris, is a mouse model of filarial infection that has also been used in this thesis. This natural parasite of the cotton rat has the added advantage of completing developmental progression from the infective L3 larvae to adult worms (and microfilariae) within mice (Hubner et al., 2009). Depending on the strain of mice used, this model provides the opportunity to elucidate the mechanisms, immunological and otherwise, that determine whether this nematode can establish a successful infection or is rejected by the host. Whilst C57BL/6 mice are largely resistant to infection, BALB/c mice are susceptible allowing the development of patent infection (Le Goff et al., 2002, Babayan et al., 2003b). This patent infection is characterised by the presence of circulating microfilariae in the bloodstream (Hoffmann et al., 2000). The lifecycle of *L. sigmodontis* in mice involves subcutaneous infection with infective L3 larvae (Figure 1.2). These larvae migrate through the lymphatic system to the pleural cavity between 4 to 6 days and induce a strong T_H2 response. Following migration, moulting to the L4 larval stage occurs and by day 28, development progresses to the adult worm stage. In the resistant C57BL/6 mice, these adult worms are killed prior to the onset of sexual maturation (~ day 50 post infection). In comparison, patency is established in the susceptible BALB/c mice with the onset of microfilariae production around day 55 post infection (Hoffmann et al., 2000, Le Goff et al., 2002, Babayan et al., 2003b). In both C57BL/6 and BALB/c mice, alternative activation of macrophages, as characterised by YM-1 and RELM-α production, and IL-4 induced

macrophage proliferation are both observed during infection (Babayan et al., 2003a, Jenkins et al., 2011).

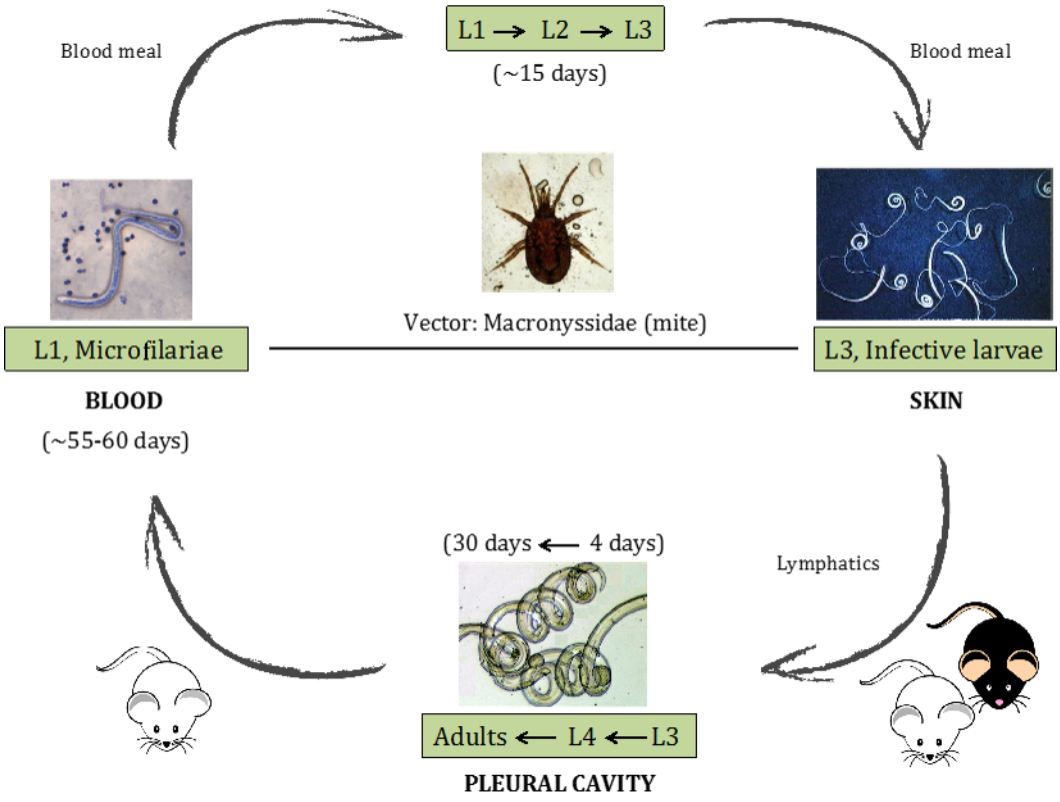

Figure 1.2 Lifecycle of the filarial nematode Litomosoides sigmodontis in resistant C57BL/6 and susceptible BALB/c mice (adapted from http://www.oncholab-sokode.de/forsch.htm).

The direct contribution of AAMΦ during *L. sigmodontis* infection still remains unclear. However, the importance of IL-4 in this model of infection was established by Le Goff et al. (2002) using IL-4 knockout animals on the resistant C57BL/6 background. The major finding from this study was that two months post infection, adult worm recovery and the percentage of microfilaraemic mice in infected IL-4 deficient C57BL/6 groups were comparable with those of the susceptible BALB/c mice (Le Goff et al., 2002). In another study, using susceptible BALB/c mice, Volkmann *et al* (2001) showed that mice lacking IL-4 exhibited up to a 100 fold higher and significantly prolonged microfilaraemia compared to wild type BALB/c mice. Whilst adult worm development and persistence were unaffected, the fertility

and length of adult female worms in mice deficient in IL-4 was clearly enhanced (Volkmann et al., 2001). Data from our lab has provided some evidence for IL-4Rα mediated macrophage activation during *L. sigmodontis* infection. Infected LysMCre IL-4Rα$^{flox/-}$ mice exhibit increased numbers of circulating microfilariae during late stages of infection suggestive of a role for AAMΦ in hampering circulating microfilariae or impairing female worm fecundity. However, the relatively inefficient deletion of the floxed IL-4Rα gene and lack of differences in activation markers at later stages of infection, presumably due to chronic IL-4 exposure and increase in IL-4Rα expression, made interpretation of results challenging (Ruckerl and Allen, 2014).

1.4.2 Wound healing and tissue repair

The type 2 response is host protective in part because it results in the reduction of parasites either through direct killing or expulsion. However, during the progression of infection, damage to the host also occurs as these parasites migrate through the body. Thus, an essential function of type 2 immunity is to also protect the host against damage mediated by these large multicellular parasites through resolution of inflammation and wound repair. Macrophages are present in every stage of repair following tissue injury – from the initial inflammatory phase, proliferation and angiogenesis to matrix deposition and tissue remodelling (Lucas et al., 2010, Sindrilaru and Scharffetter-Kochanek, 2013). In the initial stages of repair, macrophages produce pro-fibrotic mediators such as Transforming Growth Factor β (TGF-β) and Platelet-Derived Growth Factor (PD-GF) that recruit and activate myofibroblasts. AAMΦ also secrete Insulin-Like Growth Factor 1 (IGF-1), which stimulates the proliferation and survival of myofibroblasts (Wynn and Barron, 2010). The importance of IGF-1 and AAMΦ in tissue repair was illustrated by a study that showed IGF-1 producing AAMΦ are needed to repair the damage caused by *N. brasiliensis* larvae in the lung (Chen et al., 2012a). In addition, AAMΦ are also known to produce matrix metalloproteases (MMPs) and tissue inhibitors of matrix metalloproteases (TIMPs) that control extracellular matrix (ECM) turnover. As

professional phagocytes, macrophages also terminate inflammation through uptake of debris and dead cells.

Parasite killing and tissue repair (as a consequence of worm damage) are flip sides of the same coin (Allen and Sutherland, 2014). For example, arginase is involved in both parasite killing and wound repair. As described earlier, L-arginine metabolism via Arginase-1 activity results in the production of proline and polayamines that are involved in collagen production and cell proliferation (Figure 1.1). These properties of AAMΦ originally led to the hypothesis that wound healing is a function of this phenotype (Hesse et al., 2001, Wynn, 2004). Alternative activation by IL-4 and IL-13 has been described as an innate and rapid response to tissue injury that takes place even in the absence of an infectious agent (Loke et al., 2007). IL-13, in particular has been described as being potently pro-fibrotic (Wynn, 2004). Increasing evidence supports the involvement of AAMΦ in host protection, wound healing and tissue remodelling (Sandler et al., 2003, Wynn, 2004, Loke et al., 2007). For example, AAMΦ in schistosomiasis are essential for protection against organ injury. IL-4Rα$^{-/-}$ and LysMCreIL-4Rα$^{-/flox}$ mice infected with *S. mansoni* are unable to survive acute schistosomiasis and die from overwhelming inflammatory responses in the intestine and leakage of bacteria into the blood (Herbert et al., 2004). In this model, T_H2 progression confers AAMΦ dependent protection and their absence results in a T_H1 response instead. Moreover, this data shows that in the absence of AAMΦ, the host is unable to repair damage caused by egg migration through the intestinal wall. The association of AAMΦ with egg-induced liver granulomas during *Schistosoma mansoni* in mice also suggests an effector function for this phenotype (Herbert et al., 2004). During schistosomiasis, AAMΦ account for 20-30% of egg induced liver granulomas, and are thought to contribute to hepatic fibrosis. Infected mice treated with IL-12, a cytokine that results in classical activation of macrophages and NO production, exhibit much less fibrosis (Hesse et al., 2001). In a different model of silica-induced lung fibrosis, AAMΦ were found to be critical for the induction and maintenance of $CD4^+$ T_H2 response necessary to trigger fibrosis (Migliaccio et al., 2008, Wynn and Barron, 2010).

1.4.3 Alternative activation proteins in tissue repair and fibrosis

The anti-inflammatory properties of AAMΦ combined with their pro-angiogenic and tissue remodelling abilities that are predicted to facilitate wound repair and tissue regeneration (Martinez et al., 2009, Wynn and Barron, 2010, Allen and Wynn, 2011). The specific contribution of IL-4Rα signalling in repair and wound healing processes still remains elusive. However, there is growing evidence that IL-4Rα signalling in macrophages has an important contribution in tissue repair through the elucidation of the potential functional roles of the three most abundant proteins produced by AAMΦ, namely Arginase-1, YM-1 and RELMα. However, it is important to note that a current hurdle in delineating the direct effector functions (and otherwise) of AAMΦ is that many of the molecular signatures associated with AAMΦ are not restricted to macrophages.

Proline, an amino acid essential for collagen synthesis, is produced in abundance by AAMΦ in an Arginase-1 dependent mechanism; because Arginase-1 is predominantly expressed by macrophages, this pathway has been singled out as central to their putative role in wound healing and tissue repair. (Wynn and Barron, 2010, Hesse et al., 2001). The process of tissue remodelling is dependent on the timely removal and remodelling of pre-existing collagen scaffolds. Madsen *et al* showed collagen uptake through the mannose receptor and its subsequent degradation by AAMΦ (Madsen et al., 2013). Suppression of inflammatory responses is one of the key functions of Arginase-1, and an essential part of tissue repair. Suppressive effects of Arginase-1 are mediated through competition with iNOS but also direct effects on T cells. T cells are extremely sensitive to arginine concentration and AAMΦ deplete arginine in the surrounding environment through the activation of Arginase-1, thereby impairing T cell function (Zhu et al., 2014). Due to the conversion of arginine to polyamines and proline by Arginase-1, it has frequently been associated with the progression of fibrosis and it is believed to contribute to pathological tissue remodelling, particularly in asthma (Maarsingh et al., 2009). Although Arginase-1 is considered to be mostly pro-fibrotic, it can also suppress repair. Dysregulated and extensive repair results in fibrosis and AAMΦ have been reported to compete for extracellular arginine with fibroblasts during

inflammatory processes, thereby limiting fibrosis by restricting proline availability (Pesce et al., 2009a).

No specific function for YM-1 has been defined in tissue remodelling yet, however, CLPs including YM-1 are known to bind to extracellular matrix (Hung et al., 2002) and are often expressed in injury environments. Although a functional role of YM-1 is yet to be elucidated in tissue repair, other members of the chitinase family such as Acidic Mammalian Chitinase (AMCase) that are also expressed by AAMΦ, have been shown to ameliorate airway remodelling through inactivation of the downstream processes of IL-13 in an aeroallergen asthma model (Zhu et al., 2004). AMCase and BRP-39, also members of the CLP family, are also increased in livers of mice embedded with *S. mansoni* eggs, suggesting a potential involvement in the development of IL-13 dependent fibrosis in the context of infection [reviewed in (Wynn and Barron, 2010)].

In contrast, there is considerably more evidence for a pro-repair role for RELM-α with its well-established angiogenic and mitogenic properties (Teng et al., 2003). However, since RELM-α is a known negative regulator of T_H2 responses, delineating its contribution in wound healing and tissue repair is contradictory to its role in controlling fibrosis (Nair et al., 2009, Pesce et al., 2009b). Unpublished data from our lab suggests that the amount of RELM-α together with the extent of damage may determine whether RELM-α promotes or inhibits fibrosis. Both RELM-α and YM-1 are transiently but abundantly expressed in response to wounding (Loke et al., 2007). Circumstantial evidence suggests that RELM-α might be involved in fibrogenesis by promoting the differentiation and survival of myofibroblasts. For example, RELM-α is highly induced in the lung in the bleomycin model of fibrosis during fibrogenesis and RELM-α expressing cells activate Type I collagen and actin expression in fibroblasts (Liu et al., 2004b, Liu et al., 2009b). Furthermore, instillation of RELM-α in the lungs of mice induces a phenotype that is similar to that seen following a pneumonectomy with increased epithelial cell proliferation and hyperplasia (Li et al., 2005). Ablation of RELM-α in mice also exacerbates IL-13 mediated liver fibrosis in response to *S. mansoni* eggs (Pesce et al., 2009b), suggesting a protective function. This is in line with its function as a negative regulator of the T_H2 response (Nair et

al., 2009). More recently, Knipper et al provided the first direct evidence for the involvement of IL-4Rα dependent macrophage activation in controlling collagen assembly important for effective repair at the cost of pro-fibrotic side effects. It was found that following mechanical skin injury, macrophages switched from an inflammatory to a resolution phenotype in an IL-4Rα dependent manner. IL-4Rα$^{fl/-}$ Lyz2-Cre mice failed to initiate essential repair programmes. The study identified RELM-α as a key player for the induction of LH2 in fibroblasts, an enzyme responsible for directing collagen cross links (Knipper et al., 2015).

1.5 Macrophage plasticity

Classical and alternative activation of macrophages are two extremes of a wide spectrum of overlapping activation phenotypes. In a reflection of dynamic changes and complex tissue-derived signals, the existence of macrophage plasticity and coexistence of cells in different activation states has been suggested. A growing body of evidence supports the theory that macrophages are highly plastic and rarely adopt a fixed phenotype (Biswas and Mantovani, 2010, Sica and Mantovani, 2012, Mantovani et al., 2013). Macrophages have been suggested to readily adapt and reprogram to changing microenvironments (Stout and Suttles, 2004, Stout et al., 2009). The lack of a concrete phenotype is evidenced by data showing that once the stimulating agent driving a particular macrophage phenotype is removed, macrophages tend to rapidly lose their activation status (Ruckerl and Allen, 2014). This is further supported by the fact that macrophages isolated from one environment when subject to an opposing stimulus readily adopt activation features of the new stimulus (Stout et al., 2009). For example, macrophages isolated from mice implanted with the T_H2-inducing nematode *B. malayi* if subject to stimulation with LPS and IFNγ begin to express a pro-inflammatory cytokine profile that includes IL-6 and TNF (Mylonas et al., 2009). In a related study, it was shown that macrophages isolated from *B. malayi* infected mice expressed a different cytokine profile depending on the stage that they were isolated at. Whilst early isolation was associated with a T_H2 profile, macrophages isolated at later stages exhibited

increased proinflammatory cytokine production (Whyte et al., 2011). Of note, even though plasticity between macrophage phenotypes exists, studies have reported that in certain cases the switch between phenotypes is not always absolute. For example, in the study by Mylonas *et al,* it was observed that despite production of iNOS and other proinflammatory cytokines by *B. malayi* isolated macrophages following stimulation with LPS/IFNγ, they were unable to detect the release of IL-12, a hallmark of classically activated macrophages (Mylonas et al., 2009). This may, in part, be explained by recent reports of macrophage regulation by epigenetic mechanisms that can also govern macrophage phenotype and are induced early on during development, thereby restricting the extent of macrophage plasticity (Ishii et al., 2009, Satoh et al., 2010).

From existing literature it is evident that AAMΦ have the potential to exert both beneficial and detrimental effects on host physiology. It is also clear that macrophage function and diversity of phenotypes seem to be regulated by extremely complicated networks and factors that are capable of acting individually or in conjunction. Therefore, it is essential to understand the molecular mechanisms underlying the regulation of these different macrophage phenotypes that govern their overall function. Although there has been striking progress in understanding the underlying mechanisms that regulate AAMΦ function, much remains yet to be discovered.

1.6 MicroRNAs

MicroRNAs have gained importance over the last decade as regulators of immune cells and their responses and as such are prime candidates for involvement in macrophage function. MicroRNAs are a class of short (~19-24nt), single stranded, non-coding RNA that are known to negatively regulate gene expression at the post transcriptional level. This is achieved typically by binding to the 3' untranslated region (UTR) of target messenger RNAs (mRNAs) resulting in translational repression and/or destabilisation of the mRNA (Bartel, 2004, Wilczynska and Bushell, 2015). Back in 1993, the first evidence for the existence of microRNAs was obtained from the labs of Victor Ambros and Gary Ruvkun with discovery of the small endogenous RNA lin-4 in the nematode *Caenorhabditis elegans*. They showed that the *lin-4* gene did not encode a protein; instead it gave rise to two small RNA transcripts of 22nt and 61nt respectively that were complementary to the 3' UTR of *lin-14* mRNA, a transcription factor critical for larval stage progression in *C. elegans*, and also bound to lin-14 mRNA in an antisense manner (Lee et al., 1993, Wightman et al., 1993). Later in 2000, Reinhart *et al* discovered let-7, a 21nt long microRNA that controls the L4 to adult transition of larval development in *C. elegans* via the regulation of *lin-41* (Reinhart et al., 2000). It was also discovered that this microRNA is conserved in other animals, including mammals (Pasquinelli et al., 2000), resulting in the assumption that more such small RNAs were likely to exist. Subsequently, hundreds of microRNAs have been identified in animals, plants and also viruses (Griffiths-Jones et al., 2008) and mirBase (http://www.mirbase.org), an online database was established to facilitate classification of microRNAs (Griffiths-Jones et al., 2008, Kozomara and Griffiths-Jones, 2011, Kozomara and Griffiths-Jones, 2014). As of June 2014, version 21 of mirBase describes 28,645 microRNA loci expressing 35,828 mature microRNAs spanning across 223 species. Typically, microRNAs do not require perfect complementarity with their targets and each microRNA is, therefore, predicted to bind several hundreds of targets (Bartel, 2009, Friedman et al., 2009), making microRNAs complex regulators of cellular gene expression. Furthermore, different cell types express different microRNA signatures and thus, different combinations of microRNAs may be important in

different contexts (Krek et al., 2005). Taking together the gene regulatory capacity of microRNAs along with their diversity, microRNAs are involved in nearly all developmental and pathological processes and it is difficult to find a cellular pathway that is not regulated by microRNAs at some level.

1.7 Biogenesis of microRNAs

Approximately 50% of the genes encoding microRNAs in mammals are localised in intergenic spaces. Of the remaining microRNA-coding genes, ~40% are found within introns and ~10% are encoded within exons of protein coding genes (O'Carroll and Schaefer, 2013). Most of the intergenic microRNAs are autonomously expressed and possess their own enhancer and promoter elements whereas transcription of intronic microRNAs and those found within exons (if encoded in the sense direction) is thought to be tightly co-ordinated with the transcription of the protein-coding parent genes [(Corcoran et al., 2009), reviewed in (O'Carroll and Schaefer, 2013, Ha and Kim, 2014)]. Furthermore, microRNAs with highly related sequences (termed isoforms) and consequently, similar targets, are classified into the same microRNA families. Of note, microRNAs are often redundant in function with isoforms of the same microRNA located on different chromosomes. These relationships are annotated by alphanumeric descriptions. For example, in mice, the microRNA let-7 family comprises members ranging from let-7a to let-7k located on different chromosomes. Some of these family members are also redundant in function. For instance, mature let-7a can be derived from two separate chromosomal locations and is termed let-7a-1 or let-7a-2 depending on its origin. In addition to the individual loci, microRNA genes can also be organised in clusters giving rise to dicistronic or polycistronic microRNAs that can either be co-expressed/co-transcribed or expressed independently of each other (Altuvia et al., 2005, Baskerville and Bartel, 2005, Song and Wang, 2008, Ramalingam et al., 2014). The *mir-125a/let-7e/99a*, *miR-125b-1/let-7a-2/miR-100* and *miR-99a/let-7c/miR-125b-2* clusters exemplify these complex microRNA cluster relationships. Regardless of their genomic localisation, the canonical biogenesis of mature microRNAs occurs in a highly conserved process

comprising processing of the primary microRNA transcript in the nucleus followed by further processing of the precursor microRNA in the cytoplasm (Figure 1.3).

1.7.1 MicroRNA transcription in the nucleus

The majority of the microRNAs are transcribed in the nucleus by RNA polymerase II (Lee et al., 2004, Schanen and Li, 2011), with a small subset being transcribed by RNA polymerase III (Cai et al., 2004, Pfeffer et al., 2005, Borchert et al., 2006, Canella et al., 2010). Transcription by RNA polymerase II results in the generation of a long primary transcript, usually several kilobases in length, which forms a local hairpin structure within which the microRNA sequences are embedded. A typical primary microRNA (pri-miRNA) consists of a 33-35bp stem, a terminal loop and flanking single stranded RNA segments on 5' and 3' ends. When clustered, pri-miRNA transcripts can form highly complex structures containing several sequential multiple stem loops (O'Carroll and Schaefer, 2013). The pri-miRNAs generated via RNA Polymerase II have a 7-methylguanosine cap (m^7Gppp) at the 5' end and a poly(A) tail at the 3' end (Cai et al., 2004). The pri-miRNA is recognised by the nuclear microprocessor complex encompassing two core proteins, namely Drosha and DiGeorge syndrome Critical Region 8 (DGCR8, referred to as PASH-1 in *C.elegans* and Pasha in *Drosophila melanogaster*) (Lee et al., 2003, Denli et al., 2004, Gregory et al., 2004, Han et al., 2004, Landthaler et al., 2004, Wang et al., 2007). DGCR8 recognises and binds to the stem region of the pri-miRNA followed by the recruitment the nuclear RNase III Drosha, which initiates the processing of the pri-miRNA by cropping the stem-loop to release a small hairpin RNA termed the precursor microRNA (pre-miRNA). The pre-miRNAs are generally ~65-70nt in length and possess a 5' phosphate and 3' –OH with a 2-3nt overhang (Lee et al., 2003, Zeng et al., 2005). In addition to the canonical microRNA biogenesis involving the microprocessor complex (Drosha/DGCR8), a non-canonical pathway for pre-miRNA generation termed the "Mirtron pathway" has also been described. Mirtrons are short intronic hairpins found in protein coding genes with the ability to debranch and become pre-miRNAs independent of Drosha and DGCR8 (Berezikov

et al., 2007, Babiarz et al., 2011). The nascent pre-miRNAs (including mirtrons) are then exported to the cytoplasm in a GTP-dependent manner by Exportin-5 (EXP5). EXP5 is a karyopherin protein family member that forms a transport complex with the nuclear protein RAN-GTP and recognises the 2-3nt 3' overhang left by Drosha at the base of the pre-miRNA stem (Bohnsack et al., 2004, Lund et al., 2004, Tomari and Zamore, 2005). The maturation of the exported pre-miRNA is then completed in the cytosol.

1.7.2 MicroRNA maturation and RISC assembly in the cytoplasm

Upon export to the cytoplasm, the pre-miRNA is cleaved by the RNase III enzyme Dicer, which binds to the pre-miRNA with a preference for the 3' overhang generated by Drosha, resulting in the liberation of a small (~22nt) microRNA:microRNA* duplex (Bernstein et al., 2001, Grishok et al., 2001, Hutvagner et al., 2001, Ketting et al., 2001). Like Drosha is a component of the microprocessor complex, Dicer also functions as part of a large complex called the RISC (RNA Induced Silencing Complex) Loading Complex (RLC) and interacts with Transactivation Response RNA-Binding Protein (TRBP) and Protein Activator of PKR (PACT) (Chendrimada et al., 2005, Haase et al., 2005, Lee et al., 2006). Although not essential for Dicer-mediated cleavage, TRBP facilitates the stability of Dicer and acts as a sensor for thermodynamic asymmetry within a microRNA duplex. Additionally, both TRBP and PACT participate in the recruitment of an Argonaute protein to the RLC (Chendrimada et al., 2005, Lee et al., 2006). Following cleavage by Dicer, the double stranded microRNA:microRNA* duplex is separated into the functional "guide" strand and the "passenger (*)" strand. The guide or lead strand is preferentially loaded on to the Argonaute protein, which forms part of the RISC complex, whereas the passenger (*) strand is usually degraded (Khvorova et al., 2003, Schwarz et al., 2003, Bartel, 2004, Castilla-Llorente et al., 2013) [reviewed in (Winter et al., 2009)]. According to current nomenclature, the mature microRNA originating from the 5' arm of the pre-miRNA stem is termed the

5p microRNA and that arising from the 3’ arm of the stem is referred to as the 3p microRNA.

Argonaute proteins are central components of RISC and essential for microRNA mediated gene silencing. In mammals, the prevalence of four Argonaute (1-4) proteins has been reported with no obvious affinity or bias for specific microRNAs (Burroughs et al., 2011, Czech and Hannon, 2011), although some reports suggest specificity in the microRNAs associated with differents Agos (Li et al., 2014). Shared N-terminal, Piwi-Argonaute-Zwille (PAZ), C-terminal love containing MID domain and P-element Induced WImpy estis (PIWI) domains are hallmarks of all Argonaute proteins (Song et al., 2004, Elkayam et al., 2012, Schirle and MacRae, 2012). Whilst the N domain mediates loading and unwinding of the microRNA:microRNA* duplex, the PAZ and MID domain anchor the 3’ and 5’ ends of the microRNA respectively (Jinek and Doudna, 2009). Although all four Argonaute proteins function in a similar manner, only Argonaute 2 possesses endonucleolytic activity such that it can cleave target mRNAs with perfect complementarity to the mature microRNA (Diederichs and Haber, 2007, Hutvagner and Simard, 2008).

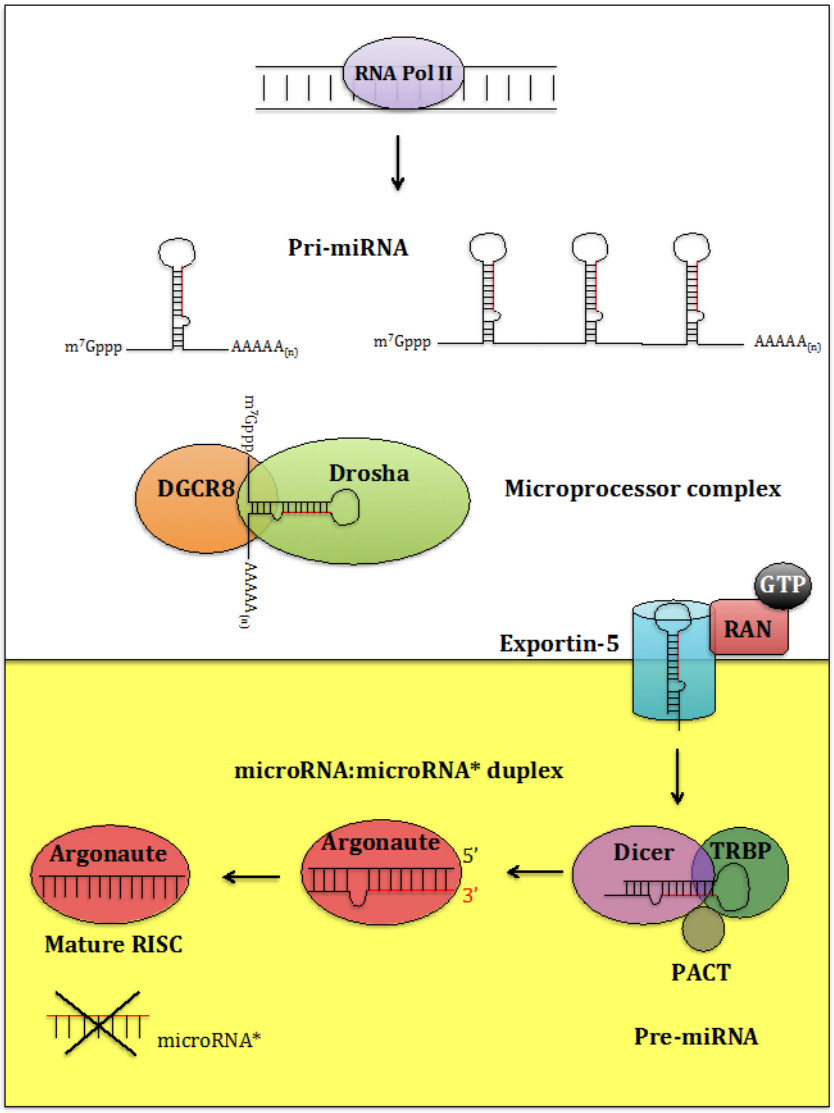

Figure 1.3 Biogenesis of microRNAs [adapted from Winter et al. (2009)].

Primary microRNAs (pri-miRNAs) containing a 7-methylguanosine cap (m7Gppp) and a 3' poly(A) tail are transcribed by RNA polymerase II in the nucleus. The pri-miRNAs are cleaved by the microprocessor complex comprising the endonuclease Drosha and its partner DGCR8 into ~70nt long precursor microRNAs (pre-miRNA). Exportin-5 exports the pre-miRNAs to the cytoplasm in a GTP dependent manner, where they are further cleaved by a complex consisting of the endonuclease Dicer and its interacting partners TRBP and PACT. This generates a ~22nt long microRNA:microRNA* duplex, which is incorporated into the RISC complex containing Argonaute protein. The guide/lead strand of the duplex remains associated with Argonaute, whereas the passenger strand (microRNA*) dissociates from the RISC and is subsequently degraded.

1.8 Mechanism of action

The targeting specificity of microRNAs is largely dictated by the "seed region" found between nucleotides 2 and 8 from the 5' end of the mature microRNA (Bartel, 2009). Perfect complementarity between the seed sequence of a microRNA and its target mRNA is the most common form of microRNA mediated target repression. Although the main mechanism of action for most microRNAs is based on their binding to the 3'UTR of the target mRNA, interactions between microRNAs and the 5' UTR or coding sequence (CDS) of mRNAs have also been reported (Zhou et al., 2009, Hausser et al., 2013). Other than complementarity with the seed region, pairing between the 3' UTR and microRNA at nucleotides 13 to 16 can reduce the off rate of RISC from the target mRNA and has been referred to as "supplementary" base pairing, which is suggested to improve target inhibition. Additionally, "compensatory" pairing between the 3' end of the microRNA and the 3' UTR of the mRNA can also compensate for mismatches within the seed region (Brennecke et al., 2005, Grimson et al., 2007, Shin et al., 2010). Furthermore, other features such as the presence of adenosine residues across from the first base of a microRNA, the position of the target site within 3' UTR and/or sequence motifs within microRNAs can affect the overall binding affinity of a microRNA to its target (Grimson et al., 2007, Obernosterer et al., 2008, Tafer et al., 2008). The interaction between a microRNA and its target mRNA within the RISC complex results in destabilisation of the mRNA and/or inhibition of translation. Although many studies have shown that microRNAs are capable of regulating gene expression post-transcriptionally, the exact mechanisms of microRNA mediated repression of targets still remain controversial. Several mechanisms have been proposed to be involved in translational inhibition at the initiation and elongation steps and mRNA destabilization and/or degradation [reviewed in (Huntzinger and Izaurralde, 2011, Ameres and Zamore, 2013)]. These are addressed in depth later on.

1.8.1 MicroRNA directed degradation of target mRNA

It is widely accepted that microRNA directed endonucleolytic cleavage of target mRNAs by Argonaute occurs in plants. This occurs at the site in the mRNA that pairs to nucleotides 10 and 11 in the microRNA and requires complete complementarity between the microRNA and its target (Llave et al., 2002, Rhoades et al., 2002, Yekta et al., 2004). However, in animals, microRNAs are only partially complementary to the binding sites within target mRNAs. In this case, the microRNA mediated mRNA degradation occurs via the 5' to 3' mRNA decay pathway (Figure 1.4). In this pathway, the target mRNA first undergoes deadenylation by the CAF1-CCR4-NOT deadenylase complex. The PAN2 and PAN3 deadenylase complexes are also required, although to a lesser extent [reviewed in (Wilczynska and Bushell, 2015)]. All these complexes are recruited by GW182, a protein characterized by the presence of glycine and tryptophan repeats (GW repeats) and essential for microRNA mediated target repression (Rehwinkel et al., 2005, Behm-Ansmant et al., 2006, Kuzuoglu-Ozturk et al., 2012). GW182, when physically associated with AGO, interacts with the Poly(A) Binding Protein (PABPC). PABPC binds the poly(A) tail of the target mRNA and recruits the CCR4-NOT deadenylase complex resulting in mRNA deadenylation (Behm-Ansmant et al., 2006, Chekulaeva et al., 2011). Following deadenlyation, the target mRNA is then decapped. The decapping enzyme DCP2, which further requires association with decapping activators and enhancers (DCP1, DDX6 and EDC4) for complete activity and stability, catalyses this removal of the 5' cap of the mRNA (Rehwinkel et al., 2005, Eulalio et al., 2007, Nishihara et al., 2013). This capping process has been shown to be independent of the deadenylation process (Fabian and Sonenberg, 2012). Subsequently, the 5'-3' exonuclease XRN1 degrades the deadenylated and decapped target mRNA (Orban and Izaurralde, 2005).

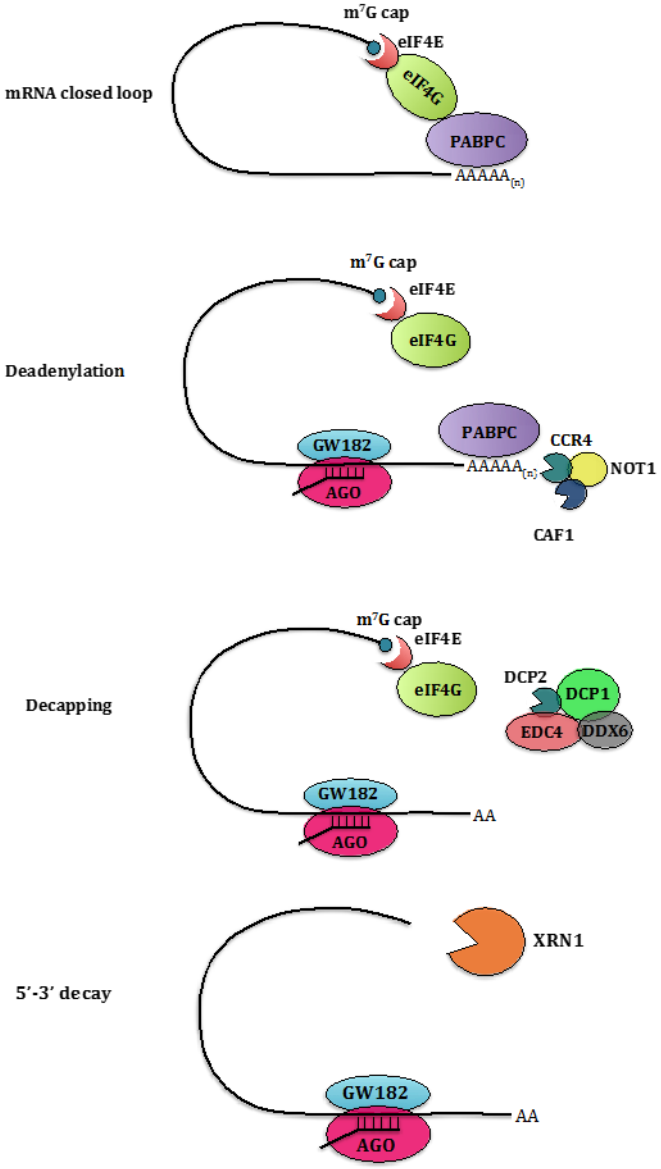

Figure 1.4 MicroRNA mediated mRNA decay [figure adapted from Huntzinger & Izaurralde (2011)].

The eIF4F complex (eIF4G, eIF4E and eIF4F) binds to the 5' cap of the mRNA. eIF4G also interacts with PABPC, which binds to the poly(A) tail forming a closed mRNA loop for translation. MicroRNAs contained within the RISC complex bind to partially complementary sites within the 3' UTR of target mRNA. GW182 associated Argonaute (AGO) interacts with PABPC resulting in the recruitment of the CCR4-NOT complex, which deadenylates the target mRNA. Following deadenylation, the mRNA undergoes decapping through the recruitment and activity of DCP2 bound to various co-factors (DDX6, DCP1 and EDC4). Subsequently, the target mRNA is further degraded by the 5'-3' exonuclease XRN1.

1.8.2 MicroRNA mediated translational repression

Translational repression is a key feature of microRNA directed gene regulation. Previously, next-generation sequencing and ribosome profiling data have revealed that the decrease in protein level observed in microRNA-mediated regulation of target mRNAs is primarily due to mRNA decay and only in some (11-16%) cases derived from translational inhibition (Guo et al., 2010). However, accumulating evidence in recent years suggests that translational repression of microRNA targets is the primary event and recent studies have suggested that repression can occur without the necessity for mRNA degradation (Mathonnet et al., 2007, Fabian et al., 2009, Bazzini et al., 2012, Bethune et al., 2012, Djuranovic et al., 2012, Meijer et al., 2013). Studies have also investigated whether these mechanisms of regulation are mutually exclusive and if mRNA degradation is a consequence of translational repression. mRNA translation consists of three distinct steps: initiation, elongation and termination. Different studies suggest that microRNAs can repress translation at both the initiation and post initiation steps in four distinct ways: inhibition of translation initiation, inhibition of translation elongation, co-translational protein degradation and premature termination of translation [reviewed in (Huntzinger and Izaurralde, 2011, Wilczynska and Bushell, 2015).

Translation requires numerous factors that are involved in the recruitment of the ribosomal subunits to the mRNA and that ensure initiation at the correct initiation codon, and subsequently proper elongation and termination. Initiation of translation involves the recognition of the 5' terminal m^7G cap by the eIF4F (eukaryotic translation initiation factor) complex comprising eIF4E, eIF4G and eIF4A. Whilst eIF4A is a helicase, eIF4E binds the mRNA cap and eIF4G provides a scaffold for the assembly of the entire complex. eIF4G, together with eIF3, facilitates the recruitment of the 40S ribosomal subunit (Kapp and Lorsch, 2004). Additionally, eIF4G also interacts with PABP1 [Poly(A) binding protein 1], which binds the poly(A) tail of the mRNA, resulting in the circularization of mRNA that is efficiently translated and protected from degradation (Derry et al., 2006). Initiation of translation occurs at the AUG (methionine) codon, with assembly of the 60S ribosomal subunit and progression on to the elongation phase.

Several studies have demonstrated that microRNAs interfere with the functioning of the eIF4F complex and PABPC during translation. For example, studies involving repression of *lin-14* and *lin-28* by the lin-4 microRNA reported the detection of these mRNAs in polysomes suggesting that repression occurred after the initiation of translation (Olsen and Ambros, 1999, Seggerson et al., 2002). These findings were further supported by the fact that upon sucrose gradient sedimentation, microRNAs and their targets were found to be associated with polysomes. These appeared in the actively translated fraction, however, the corresponding protein was undetectable (Maroney et al., 2006, Nottrott et al., 2006, Petersen et al., 2006). These findings were explained via different hypotheses including degradation of the nascent polypeptide chain co-translationally (Nottrott et al., 2006) and premature dissociation of ribosomes (Petersen et al., 2006). The study carried out by Petersen *et al* also showed that microRNA-associated polysomes, when treated with a translational inhibitor, dissociated more rapidly in comparison to polysomes associated with a control unrepressed mRNA. Furthermore, Petersen and colleagues observed an ability for microRNAs to silence translation initiated independently of the cap structure via an Internal Ribosome Entry Site (IRES) (Petersen et al., 2006), thus providing further evidence for translational repression by microRNAs post initiation.

At the same time, a conflicting study reported that in the presence of cognate microRNAs, target mRNAs do not co-sediment with the polysomal fraction during sucrose gradient sedimentation; instead they are found in lighter fractions that contain fewer ribosomes (Pillai et al., 2005). Pillai *et al* and other related studies stated that mRNAs translated through an IRES were refractory to repression by microRNAs, suggesting that the mechanism for microRNA inhibition involved cap dependent translation initiation (Humphreys et al., 2005, Pillai et al., 2005). Consistent with this finding, studies involving cell free extracts demonstrated that microRNAs silenced m^7Gppp-capped mRNAs but not mRNAs with artificial Appp caps and failed to silence transcripts in IRES driven translation (Mathonnet et al., 2007, Wakiyama et al., 2007). In further agreement with these results, target silencing was suppressed with increasing concentrations of purified eIF4F in extracts from mouse tumour cells (Wakiyama et al., 2007). The idea that microRNAs

interfere with the functioning of the cap binding complex, thereby repressing initiation, was also supported by a bioinformatic analysis that revealed that mRNAs containing miRNA target sites are more likely to have highly structured 5' UTRs (Meijer et al., 2013).

1.8.3 Evidence for microRNA mediated mRNA degradation

Evidence for the finding that microRNAs can induce target degradation comes from transcriptomic studies showing that the levels of mRNA targets correlate inversely with microRNA abundance [reviewed in (Huntzinger and Izaurralde, 2011)]. These transcriptomic profiles reveal that cells transfected with specific microRNAs show a reduction in transcripts containing complementary binding sites for these microRNAs. The finding that the levels of microRNA targets increase when these factors are depleted supports a role for mRNA decay factors in microRNA mediated mRNA destabilisation. For example, depletion of components of the CAF1-CCR4-NOT deadenylase complex results in the upregulation of most microRNA targets suggesting that deadenylation is a widespread consequence of microRNA regulation (Behm-Ansmant et al., 2006, Eulalio et al., 2007). Additionally, Guo *et al* showed that reduction of protein in a microRNA-mediated fashion is a result of mRNA degradation. In this study, ribosomal profiling was carried out that involves sequencing of ribosome-protected mRNA fragments (RPFs) to evaluate the effects of microRNAs on protein production along with simultaneous measurement of mRNA levels. The effect of a specific microRNA on protein production was calculated as a ratio of RPFs and mRNA levels. It was found that the decrease in mRNA levels accounted for more than 84% of the decrease in protein production, suggesting that microRNA mediated destabilisation/degradation of mRNAs may be accountable for the protein reduction (Guo et al., 2010).

Although mechanisms of microRNA action remain controversial, the most wide-spread current opinion is that microRNA-mediated translational repression is a prerequisite for target mRNA degradation (Wilczynska and Bushell, 2015). In light of this, kinetic studies in *Drosophila melanogaster* and mammalian cells have

demonstrated that microRNAs function through initial repression of target translation prior to triggering mRNA decay (Bethune et al., 2012, Djuranovic et al., 2012). Furthermore, in Zebrafish, inhibition of translation has been shown to cause mRNA degradation. Using ribosomal profiling it was found that miR-430 reduced the ribosomal occupancy on target mRNAs with subsequent mRNA decay (Bazzini et al., 2012).

1.8.4 Novel functions of microRNAs

Normally, an anti-correlation in expression would be expected for a true miRNA–mRNA pair. However, besides translational repression and mRNA destabilisation, microRNAs have also been linked to translational activation in specific circumstances. For example, upon cell cycle arrest in serum starved cells, AU-rich elements (AREs), present specifically in TNFα mRNA are transformed into an activation signal for translation. This results in the recruitment of AGO and miR-369-3 directs its association with the AREs to activate translation (Vasudevan et al., 2007). Vasudevan *et al* also showed that whilst let-7 represses translation in proliferating cells, it could also induce translational activation in a similar manner during cell cycle arrest. In another study, miR-373 has been reported to induce the expression of E-cadherin by targeting a site in the promoter. In the same study, expression of Cold-Shock Domain-Containing protein C2 (CSDC2) was also induced in response to miR-373 (Place et al., 2008). However the exact mechanisms of how microRNAs result in translational activation are still unknown.

Additionally, Eiring *et al* have suggested a novel function for microRNAs as decoys for regulatory RNA-binding proteins. They showed that miR-328 is bound by hnRNP E2 and sequesters it away from its mRNA targets. This interaction with hnRNP E2 is independent of the microRNA seed sequence and results in the release of the key myeloid differentiation factor CEBPA mRNA from hnRNP E2 mediated translational inhibition. Patients with chronic myeloid leukaemia were found to have decreased expression of miR-328, meaning that there is less competition for hnRNP E2. As a result, hnRNP E2 is free to induce the translational inhibition of CEBPA

(Eiring et al., 2010). Another study by Balkhi *et al* also showed a similar relationship between HuR and miR-29, which prevents the protein from repressing the mRNA of tumour suppressor A20 by acting as a decoy (Balkhi et al., 2013). At the same time, recent works propose that mRNA targets can also act as competitive inhibitors ("sponges") of microRNAs and therefore, affect the concentration of microRNAs (Ebert et al., 2007, Ebert and Sharp, 2010, Hansen et al., 2013). This adds another layer of complexity to the already existing complex microRNA networks mediating posttranscriptional gene regulation.

Although the varied mechanisms of microRNA-mediated gene regulation are still being elucidated, based on their wide-spread functions in the regulation of gene expression microRNAs are important fine tuners of a variety of cellular processes, including immune responses.

1.9 MicroRNAs in immune responses

In the past decade, there has been great insight into the intersection between the fields of immunology and microRNA biology. The contribution of microRNAs in the regulation of the immune system is highlighted by their importance in various processes such as haematopoietic development (Bissels et al., 2012, Undi et al., 2013, Montagner et al., 2014), maintenance of immune homeostasis (Lian et al., 2012, Runtsch et al., 2014, Pauley et al., 2009), cancer (Hayes et al., 2014, Lee and Dutta, 2009, Jansson and Lund, 2012, Lin and Gregory, 2015) and autoimmunity (Pauley et al., 2009, Ceribelli et al., 2012, Singh et al., 2013, Qu et al., 2014, Simpson and Ansel, 2015). The earliest studies involving microRNAs focused on their impact on the functioning of the immune system as a whole. More recently, advancement in profiling methods has allowed for the identification and contribution of specific microRNAs in the regulation of distinct immune cell populations and their responses.

Knocking out of Dicer, which is essential for microRNA biogenesis, is embryonically lethal, with *Dicer1* null embryos depleted of stem cells entirely (Bernstein et al., 2003). In addition, Homeobox (HOX) genes are critical in regulating haematopoietic stem cell (HSC) homeostasis (Argiropoulos and Humphries, 2007). MicroRNAs belonging to the miR-196 and miR-10 families are not only located in the HOX loci, but also have the capacity to directly repress HOX family expression (Yekta et al., 2004, Garzon et al., 2008). MiR-196b is specially expressed in mouse HSCs and modulates HSC homeostasis and lineage commitment (Popovic et al., 2009), whereas miR-126 regulates the expression of HOXA9 and PLK2 and is involved in the production of downstream progenitors by HSCs (Li et al., 2008). MiR-221 and miR-222, on the other hand inhibit KIT expression of stem cells resulting in impaired cell proliferation (Felli et al., 2005).

Since mice lacking Dicer do not survive, follow on studies utilised conditional Dicer knockout systems. Specific deletion of Dicer in the T cell lineage results not only in defective T cell development, but also irregular T_H cell differentiation and cytokine production (Cobb et al., 2005, Muljo et al., 2005, Seo et al., 2010, Zhang and Bevan, 2010, Podshivalova and Salomon, 2013). Whilst Dicer deletion in mature CD8 T cells results in enhanced activation but defective survival and migration to peripheral tissues (Zhang and Bevan, 2010), global microRNA knockout (*Dicer* $^{-/-}$) in CD4 T cells deletion leads to reduced proliferation and abnormal T_H1 cytokine production (Muljo et al., 2005, Chong et al., 2008). Despite these aberrations, Dicer appears to be dispensable for CD4 and CD8 lineage commitment in the thymus (Cobb et al., 2005). Additionally, regulatory T cells lacking Drosha or Dicer lose their suppressor function and fail to prevent autoimmunity in mice and this fatal autoimmunity is indistinguishable from that caused by deficiency in Foxp3, the master regulator of T_{reg} differentiation (Chong et al., 2008, Liston et al., 2008, Zhou et al., 2008).

T cells are one of the most widely studied cell type in the context of regulation by specific microRNAs. MiR-181a has been shown to positively regulate the T cell receptor (TCR) mediated response to antigen in $CD4^+$ T cells through the amplification of signal strength and subsequent cytokine release (Li et al., 2007). In the same study, Li and colleagues showed that miR-181a acts like a rheostat through

the coordinated downregulation of multiple phosphatases downstream of this surface receptor and was thus implicated in the regulation of positive and negative selection of T cells during thymic development (Li et al., 2007, Ebert et al., 2009). Unwanted T cell clones are commonly disposed of via apoptosis. The miR-17 to miR-92 cluster of microRNAs is involved in the regulation of T cell survival through the repression of BIM and PTEN, factors involved in the potentiation of cell death. At the same time, overexpression of this microRNA cluster in transgenic mice results in T cell populations that are hyperproliferative and resistant to cell death (Xiao et al., 2008). Interestingly, CD4 T cell display mRNA with shorter 3' UTRs upon activation (Sandberg et al., 2008). Sandberg *et al* showed that truncation of the UTR results in loss of specific microRNA binding sites, thus protecting transcripts from microRNA mediated degradation and implicating a role for microRNAs in T cell activation. Activated $CD4^+$ T cells express miR-155 and deficiency of this microRNA results in a T_H2 bias under neutral conditions *in vitro* (Rodriguez et al., 2007, Thai et al., 2007). Mice lacking miR-155 are also defective in their capacity to produce T_H1 and T_H17 cells in mouse models of autoimmune inflammation such as Experimental Autoimmune Encephalomyelitis (EAE) (O'Connell et al., 2010), colitis (Oertli et al., 2011) and Collagen Induced Arthritis (CIA) (Kurowska-Stolarska et al., 2011). MiR-326 is also a promoter of T_H17 responses and EAE development through targeting of the transcription factor Ets1, an established repressor of T_H17 development (Du et al., 2009). Furthermore, the clonal expansion of T cells is repressed by the suppression of Foxo1 by miR-182, a microRNA that is induced in response to IL-2, a cytokine produced by activated T cells (Stittrich et al., 2010). In contrast to miR-182, miR-214 is a microRNA that promotes T cell proliferation through the repression of PTEN, an established inhibitor of the PI3K pathway (Jindra et al., 2010). Absence of the microRNA miR-146a in T cells leads to the elevated expression of STAT1 and an uncontrolled T_H1 response. Moreover, miR-$146a^{-/-}$ mice succumb to a chronic inflammatory disorder with a reduced life span (Lu et al., 2010). These studies are only a few selected examples from the extensive literature describing the functional role of microRNAs in T cells.

A deficiency in microRNAs also affects B cell development, as first reported by the conditional deletion of AGO2 in haematopoietic cells. This resulted in a partial deficiency in microRNA function and compromised the development of B and erythroid cells (O'Carroll et al., 2007). Furthermore, a B cell lineage specific deletion of Dicer hampers B cell development and an almost complete block at the pro to pre-B cell transition due to apoptosis of *Dicer-/-* pre-B cells (Koralov et al., 2008). The miR-17~92 cluster was shown to peak in these pre-B cells and was also accountable for the inhibition of cell death through downregulation of the proapoptotic protein Bim. This block in B cell development could be overcome by transgenic expression of BCL-2, but the mature B cells still had abnormal distributions of VDJ rearrangements, suggesting that there was a considerable defect in the regulation of B cell selection. Significantly, mice lacking the miR-17~92 microRNA cluster are also non viable at birth with severe defects in the lung and heart (Ventura et al., 2008). *Dicer* ablation in mature B cells also skews the cells towards transitional and marginal zone phenotypes in the spleen with a concomitant reduction in follicular B cells (Koralov et al., 2008). MiR-155 is induced during LPS activation of B cells and is critical in the regulation of B2 cell responses in germinal centres. Mice deficient in miR-155 show marked defects in both antibody secretion and class switching and these changes are a result of miR-155 mediated repression of >60 target genes (Thai et al., 2007, Vigorito et al., 2007). In addition to B2 cells, mice deficient in miR-150 show abnormal expansion of B1 cells accompanied by dramatic increases in steady state immunoglobulin levels. Constitutive expression of miR-150 also arrests cells at the pro-B cell stage. These defects were explained by dysregulation of c-Myb expression (Xiao et al., 2007, Zhou et al., 2007). In contrast, constitutive expression of miR-34a perturbs B cell development through increased cell numbers during pro-B to pre-B cell transition by targetting the transcription factor *Foxp1*, which regulates expression of the recombination-activating genes *Rag1/2* (He et al., 2007).

Granulocytes arise from granulocyte-monocyte progenitors and this process is controlled by the transcription factor GFI1 (Velu et al., 2009). Overexpression of miR-21 and miR-196b blocks granulopoiesis and, in agreement with this, it was found that GFI1 binds to the promoter regions of pri-miR-21 and pri-miR-196b,

thereby repressing their expression (Hock et al., 2003). Sustained expression of miR-155 can also increase granulocyte numbers *in vivo* by targeting SHIP1 (O'Connell et al., 2008, O'Connell et al., 2009). Besides regulating granulocyte development, microRNAs also have the ability to regulate granulocyte function. The myeloid transcription factors PU.1 and C/EBPβ are known to induce expression of miR-223 (Fukao et al., 2007). MiR-223 negatively regulates both the activation and proliferation of neutrophils, and neutrophils lacking miR-223 have been shown to undergo an increased oxidative burst and efficiently kill *Candida albicans* in comparison to wild type cells (Johnnidis et al., 2008). This was the first report that genetic ablation of microRNAs can influence myeloid cell development and function *in* vivo. In the same study, it was shown that miR-223 also directly targets MEF2C, a transcription factor which promotes myeloid progenitor differentiation, is also important for the increased neutrophil expansion observed in miR-223 deficient mice. MiR-223 null mice also develop inflammatory lung pathology and exacerbated tissue destruction following endotoxin challenge suggesting that miR-223, like miR-146a and miR-155, is also an integral component of the homeostatic maintenance machinery (Johnnidis et al., 2008).

1.9.1 MicroRNAs in the regulation of monocytes, macrophages and dendritic cells

A number of studies have also implicated roles for specific microRNAs in the regulation of transcription factors involved in monocytopoiesis. During differentiation of human haematopoietic progenitors into monocytes, the expression levels of members of the miR-17~92 and the related miR-106a~92 families are significantly reduced, resulting in the de-repression of the transcription factor RUNX1. This increase in RUNX1 leads to the promotion of monocyte differentiation through an increase in CSF1R expression. Moreover, RUNX1 also binds to the promoter region of these microRNA families, thus creating a mutual negative feedback loop (Fontana et al., 2007). PU.1 is a transcription factor essential for monocyte and macrophage differentiation. PU.1 has been shown to up-regulate miR-

424 expression, which promotes TPA (12-O-tetra-decanoylphorbol-13-acetate) mediated monocyte differentiation of NB4 cells (Rosa et al., 2007), a human acute promyelocytic leukemia derived cell line, thereby increasing the numbers of $CD11b^{+}$ and $CD14^{+}$ expressing cells. This is achieved through the suppression of the nuclear factor I/A (NFIA), a transcription factor important for myeloid cell differentiation (Fazi et al., 2005). Furthermore, expression levels of miR-146a, miR-155, miR-342 and miR-338 are also increased under the influence of PU.1 and ectopic expression of miR-146a is sufficient to direct HSC differentiation and commitment to the myeloid cell lineage in mouse transplantation assays (Ghani et al., 2011).

Monocytes comprise two functionally distinct subsets: inflammatory Ly-$6C^{hi}$ (human $CD14^{hi}$) and patrolling Ly-$6C^{lo}$ (human $CD14^{lo}/CD16^{+}$) cells. Whilst miR-146a is constitutively expressed by Ly-$6C^{lo}$ monocytes, following inflammatory challenge, Ly-$6C^{hi}$ monocytes selectively induce miR-146a expression. MiR-146a limits the expansion of these cells in the bone marrow, thereby limiting the magnitude of the inflammatory response mediated by these cells (Etzrodt et al., 2012). Because of this, *miR-146a*$^{-/-}$ mice exhibit chronic myeloproliferation and develop malignancies (Zhao et al., 2011). Additionally, miR-146a impairs CCR2 (Chemokine CC Ligand CCL2 Receptor) expression, which is essential for the recruitment of Ly-$6C^{hi}$ monocytes to sites of insult and injury, where they differentiate into macrophages. This miR-146a mediated regulation in monocytes is cell autonomous and dependent on RELB, a direct target of this microRNA (Etzrodt et al., 2012).

There are a number of microRNAs known to modulate macrophage activation and function. MiR-9, miR-21, miR-146, miR-147 and miR-155 have all been shown to be upregulated in macrophages in response to infection (O'Connell et al., 2008, Taganov et al., 2006, Sheedy et al., 2010, Liu et al., 2009a, Bazzoni et al., 2009). Specifically, miR-155 expression is induced in mouse bone marrow derived macrophages through TLR ligation and also by the proinflammatory cytokine TNFα and interferons (O'Connell et al., 2008). The primary transcript that encodes miR-155 has also been shown to be activated by NF-κB (O'Connell et al., 2008, Thai et al., 2007, Gatto et al., 2008, Yin et al., 2008). MiR-146 expression is induced in macrophages by cognate ligands for TLRs and the cytoplasmic sensor RIG-1 in an

NF-κB dependent manner (Taganov et al., 2006, Hou et al., 2009). In humans, miR-9 is upregulated by pro-inflammatory signals that are dependent on LPS activation of MYD88 and NF-κB (Bazzoni et al., 2009). Induction of miR-9 is also mediated by the proinflammatory cytokines IL-1β and TNF-α, but not by IFN-γ. These microRNAs all appear to be transcriptionally regulated in a manner similar to other inflammatory genes but can negatively influence the activation of inflammatory pathways in myeloid cells. For example, miR-146 is induced by NF-κB and directly targets several signalling molecules downstream of TLRs that promote inflammation, such as the adaptor molecules IRAK1, IRAK2 and TRAF6 in the TLR/ NF-κB pathway, in a negative feedback loop (Taganov et al., 2006, Hou et al., 2009). In contrast to miR-146a limiting proinflammatory responses, a model for miR-9 preventing the negative regulation of NF-κB signalling in monocytes has been proposed. miR-9 represses *NFKB1* to help maintain NF-κB protein levels and proinflammatory action during TLR4 mediated activation of monocytes (and neutrophils) (Ma et al., 2011).

MiR-155 provides an example of a microRNA with complex effects on myeloid activation. Overexpression of miR-155 in the bone marrow of adult mice results in a myeloproliferative phenotype mirroring that observed following LPS injection (O'Connell et al., 2008). SHIP1 is a negative regulator of TLR signalling and the PI3K/AKT pathway (Sly et al., 2004, Costinean et al., 2009, O'Connell et al., 2009). MiR-155 has been shown to negatively regulate SHIP1, thereby countering the negative influence of SHIP1 and increasing downstream AKT1 signalling. In macrophages, AKT signalling has interestingly been shown to repress miR-155 expression, indicating the existence of a negative feedback loop (Androulidaki et al., 2009). Moreover, macrophages deficient in AKT that are stimulated with LPS express higher levels of miR-155 and also miR-125b in comparison to wild type controls and these $Akt^{-/-}$ macrophages are more sensitive to LPS. In this study, miR-155 was shown to directly target SOCS1, another native regulator of the TLR pathway. This sensitisation to LPS was achieved in combination with a reduction in levels of let-7e, which downregulates the expression of the LPS receptor TLR4. In

agreement with these findings, *Akt*$^{-/-}$ mice display a lower tolerance when challenged with LPS (Androulidaki et al., 2009).

In addition to macrophages, miR-155 is also known to fine tune the functioning of dendritic cells (DCs). In human DCs, knockdown of miR-155 expression results in a significant increase in the expression of the pro-inflammatory cytokine IL-1β. Consistent with its role in regulating pro-inflammatory responses, miR-155 was also reported to repress the expression of an NF-κB reporter and TAB2, an important signal transduction molecule, in the same study (Ceppi et al., 2009). Furthermore, DCs from *Bic*$^{-/-}$ mice that are deficient in miR-155 are defective in their ability to present antigens, despite normal MHC Class II expression and other co-stimulatory molecules (Rodriguez et al., 2007). MiR-155 also downregulated the expression of the DC specific molecule DC-SIGN (CD209), which is a C-type lectin that binds to pathogens, thus implicating a role for microRNAs in pathogen uptake (Martinez-Nunez et al., 2009). Taken together, these results suggest that microRNAs are important regulators of inflammation and key players in the maintenance of a balanced response to pathogens and stimuli.

Owing to the diversity of microRNA targets, the roles of microRNAs can be extremely complex and context dependent with microRNA targets and functions at times specific to a particular cell type and activation status. For example, miR-125 is a microRNA that is rapidly induced in macrophages by TLR ligands. The miR-125 family is composed of the miR-125a/b-1 and miR-125b-2 members, which are mammalian homologues of the first discovered microRNA, lin-4, in *C. elegans*. Bone marrow derived macrophages express high levels of both miR-125a and miR-125b. Whilst miR-125a is upregulated, miR-125b is downregulated in response to LPS (Tili et al., 2007, Androulidaki et al., 2009, Graff et al., 2012b). Nevertheless, evidence suggests that both microRNAs enhance NF-κB signalling through the repression of the NF-κB regulator TNFAIP3 (Kim et al., 2012). In agreement with these findings, macrophages overexpressing miR-125b are highly responsive to IFNγ (Chaudhuri et al., 2011). In addition, miR-125b also directly targets and destabilises the TNFα mRNA transcript and downregulation of miR-125b in response to LPS

results in enhanced TNFα production (Androulidaki et al., 2009). Moreover, miR-125b is involved in the sustenance of classical activation by targeting the transcription factor IRF4, which is a mediator of alternative macrophage activation (Chaudhuri et al., 2011).

As mentioned earlier, miR-223 is a microRNA preferentially expressed in the myeloid lineage. Recent studies have suggested that miR-223 is induced in response to LPS and acts to limit inflammatory activation of macrophages. Consistent with this finding, bone marrow macrophages lacking miR-223 express significantly higher levels of IL-1β, IL-6 and TNFα (Zhuang et al., 2012).

1.9.2 MicroRNAs in alternative activation

As opposed to the well-studied roles of microRNAs in the regulation of classically activated macrophages and proinflammatory responses, existing literature implicating functional roles of microRNAs in alternative activation is relatively sparse [reviewed in (Squadrito et al., 2013)]. The expression of several microRNAs has been reported to be altered in response to IL-4 in bone marrow derived macrophages, however, the functional significance of these microRNAs is still unknown (Squadrito et al., 2014). To date, three studies delineating the functional roles of microRNAs in alternative activation have been reported.

The first of these came from our lab and was reported by Ruckerl *et al* (2012). Using an *in vivo* model of *B. malayi* implant in the peritoneal cavity of mice, the authors identified the differential expression of four different microRNAs in helminth induced alternatively activated macrophages, namely miR-125b-5p, miR-146a-5p, miR-199b-5p and miR-378-3p. Of these, miR-378-3p was specifically identified as being induced by IL-4 and shown to target the IL-4 induced PI3K/AKT proliferative pathway. MiR-378-3p is encoded within the first intron of the *Ppargc1b* gene, which has previously been shown to be associated with the alternative activation phenotype. The expression of miR-378-3p was confirmed as being IL-4Rα dependent and strongly associated with alternative activation. MiR-378 was hypothesised to operate in a negative feedback loop to limit IL-4 induced macrophage proliferation. To this

end, AKT1 was established as a direct target of this microRNA *in vitro*, although analysis of inhibition of AKT1 by miR-378-3p could not be achieved *in vivo* due to technical hurdles (Ruckerl et al., 2012).

Work by other labs has also linked other microRNAs to alternative macrophage activation, although not strictly with the M(IL-4) phenotype. The use of microRNA sensor lentiviral vectors has shown that miR-511-3p is upregulated in AAMϕ. However, functionally miR-511-3p has only been shown to downregulate genes with a pro-tumoural effector function in Tumor Associated Macrophages (TAMs). Of note, miR-511-3p has been indirectly linked to AAMϕ through the suppression of ROCK2, a kinase that phosphorylates IRF4, which is a transcription factor involved in the promotion of alternative activation (Squadrito et al., 2012).

Lastly, miR-223 has been studied as a mediator of PPARγ regulated alternative macrophage activation. In this study, the expression of miR-223 was enhanced directly by PPARγ upon exposure to T_H2 stimuli through binding of regulatory elements upstream of the pre-miR-223 coding region. Moreover, deletion of miR-223 impaired alternative activation *ex vivo* and also in mice fed a high fat diet. These effects were mediated by direct targeting of *Rasa1* and *Nfat5*, genes essential for PPARγ dependent alternative activation (Ying et al., 2015).

1.10 Hypotheses and aims of this thesis

As described earlier, AAMϕ are involved in a range of effector functions that range from helminth infections to T_H2 weighted disorders such as asthma and fibrosis. Although our knowledge of macrophage function in a T_H2 environment is rapidly increasing, a number of questions still remain to be addressed about the regulation of the AAMϕ phenotype, particularly by microRNAs.

We, therefore, hypothesised that:

- MicroRNAs are altered in response to IL-4 and IL-13 in macrophages.
- With their ability for vast gene regulation, microRNAs could target genes and pathways critical for the induction, maintenance and proliferation of the AAMϕ phenotype.

To test these hypotheses, the following aims were addressed in this project:

1. Identification of microRNAs associated with alternative activation.
2. Investigation of the functional role of lead microRNA candidates *in vitro* and *in vivo.*
3. Biochemical identification of direct targets of microRNA candidates.

Chapter 2: Identification and selection of microRNAs for further study

SUMMARY:

In this chapter, in light of the increasing evidence that microRNAs are involved in the regulation of different macrophage phenotypes, we determined the expression profiles of microRNAs that are highly regulated during IL-4Rα dependent alternative activation. To this end, we utilised microarray data previously generated in the lab to identify microRNAs differentially expressed in AAMΦ. This included a two-way comparison of AAMΦ elicited in response to a nematode *B. malayi* with macrophages from IL-4Rα deficient animals (IL-4Rα$^{-/-}$) and inflammatory thioglycollate-elicited macrophages (Thio MΦ) from wild type animals. Additionally, a second microarray dataset identified microRNAs that were altered in response to IL-4 stimulation of bone marrow derived macrophages. The ten most significantly regulated microRNAs identified as being differentially expressed in AAMΦ and/or common to both datasets were selected for further study. The expression profiles of these ten microRNAs were then validated under a range of conditions of alternative activation ranging from a complex *in vivo* T_H2 infection to *in vitro* stimulation of macrophage cell lines with IL-4 and IL-13. Based on consistency in expression profiles across the range of these conditions of alternative activation, microRNA candidates were selected for further study in the subsequent chapters to determine their contribution to the induction, maintenance and proliferation of AAMΦ.

2.1 Introduction

Depending on the external stimuli and environmental cues encountered, macrophages can develop into various highly distinct functional phenotypes (Mantovani et al., 2004, Mantovani et al., 2005, Mosser and Edwards, 2008, Sica and Mantovani, 2012, Gordon and Martinez, 2010). CAMΦ and AAMΦ represent two highly polarised activation states that, when uncontrolled, can lead to either excessive inflammation and tissue destruction or T_H2 weighted inflammatory disorders such as asthma and fibrosis respectively (Gordon, 2003, Wynn, 2004, Gordon and Martinez, 2010). Hence, macrophage responses must be tightly regulated for the maintenance of homeostasis both during and after infection and tissue injury. As previously mentioned in the introductory chapter, several mechanisms are involved in the regulation of the functional polarisation and activation of macrophages. Besides signalling cascades essential for triggering an activation state, it has been shown that transcriptional and chromatin-mediated control are the key players that determine macrophage identity (Sica and Mantovani, 2012, Martinez and Gordon, 2014). These include regulation via transcription factor families such as STAT proteins (Hu et al., 2008, Blanc et al., 2013), IRFs (Dror et al., 2007, Gunthner and Anders, 2013), PPARs (Odegaard et al., 2007, Chawla, 2010, Szanto et al., 2010) and others such as GATA6 (Okabe and Medzhitov, 2014, Rosas et al., 2014). Additionally, chromatin remodelling and histone demethylation (Bowdridge and Gause, 2010), the tyrosine kinase receptor STK/RON (Iwama et al., 1996, Liu et al., 1999), retinoic acid (Manicassamy and Pulendran, 2009), adenosine (Csoka et al., 2012, Hasko and Cronstein, 2013) and cell death by apoptosis (Munn et al., 1995) have all been implicated in the functional regulation of macrophage responses.

MicroRNAs are a class of naturally occurring, short (~22nt), non coding RNA that have the potential for vast gene regulation by binding target messenger RNAs (mRNAs) resulting in the inhibition of translation and/or mRNA destabilization (Bartel, 2009, Fabian and Sonenberg, 2012). Most microRNAs bind to the 3' UTR of the target mRNA via a conserved "seed" site, which is defined as nucleotides (nt) 2-8nt at the 5' end of a microRNA (Bartel, 2004, Doench and Sharp, 2004, Brennecke et al., 2005). Although outside of this seed region perfect complementarity between

the microRNA and its target is not required, additional supplementary and compensatory pairing mechanisms can enhance target inhibition (Grimson et al., 2007, Bartel, 2009). Additionally, interactions between microRNAs and the 5'UTR or coding sequences of target mRNAs have also been reported (Zhou et al., 2009). Directly or indirectly, a single mature microRNA has the capacity to regulate multiple components within complex regulatory networks. In recent years, microRNAs have gained importance as immunomodulatory regulators. Genetic ablation of the microRNA processing or functional machinery, or deregulation of certain individual microRNAs can severely compromise immune development and responses leading to several immune disorders (Xiao and Rajewsky, 2009).

The role of microRNAs in the functional regulation of macrophage responses has been widely studied. MicroRNAs have been shown to be key players right from the early stages of macrophage development and production to the later stages involving macrophage polarisation and maintenance of activation (Graff et al., 2012b, Liu and Abraham, 2013b, Squadrito et al., 2013). TLR signalling is a key feature of CAMΦ involved in microbial killing (Mosser, 2003, Mosser and Edwards, 2008, Mosser and Zhang, 2008, Martinez and Gordon, 2014). MicroRNAs are known to be fine tuners of TLR signalling and hence can act as regulators of CAMΦ to limit excessive inflammation during infection [reviewed in (O'Neill et al., 2011)]. In this regard, miR-146 and miR-155 are the best examples of microRNAs that are well-established regulators of classical activation. MiR-146a is rapidly induced in macrophages in an NF-κB dependent manner in response to LPS stimulation and has been shown to modulate classical activation through a negative feedback regulatory loop (Taganov et al., 2006, Rusca and Monticelli, 2011). A more specific role for miR-146a has also been suggested in the regulation of IL-6 production in response to LPS (He et al., 2014c). MiR-155 is a microRNA whose expression is induced in macrophages in response to a broad range of inflammatory mediators (O'Connell et al., 2007). Deficiency of miR-155 in macrophages also has a direct influence on the expression levels of other microRNAs (Dueck et al., 2014).

Besides miR-146 and miR-155, roles for other microRNAs have also been implicated in regulating macrophage activation. For example, macrophages,

compared to other immune cells, are enriched in the expression of miR-125b, which is known to potentiate classical activation through suppression of IRF4 leading to enhancement of costimulatory factors and increased responsiveness to IFN-γ (Chaudhuri et al., 2011). Like miR-146a, miR-125b is also transcriptionally induced by NF-κB and promotes a positive self-regulatory loop that prolongs NF-κB activity, thereby prolonging macrophage activation (Kim et al., 2012). Macrophages are also involved in the progression of tumours and metastasis (Pollard, 2004, Solinas et al., 2009, Noy and Pollard, 2014) and defined microRNA signatures have been shown to be associated with this progression (Squadrito et al., 2013). MiR-125b is also a known oncomir that promotes tumorigenesis, also through the repression of IRF4, in line with the finding that microRNAs involved in cancers can function via dual mechanisms (Fabbri et al., 2007, So et al., 2014).

In contrast to the fairly extensive literature on microRNAs in the regulation of CAMΦ, there is still a gap in the existing literature and current understanding of how microRNAs regulate IL-4Rα dependent AAMΦ and their responses. Although the expression profiles of several microRNAs have been implicated with the M2 phenotype, currently only a few microRNAs are associated with the functional regulation of AAMΦ. Of these, miR-223 and miR-124a serve as regulators of M2 polarisation (Zhuang et al., 2012, Veremeyko et al., 2013) while miR-7a-1 is involved in IL-4 directed giant cell formation (Sissons et al., 2012). Additionally, a study from our lab has shown the functional relevance of miR-378 as a negative modulator of IL-4 induced macrophage proliferation (Ruckerl et al., 2012).

AAMΦ have been implicated in a wide range of processes including homeostasis, thermoregulation, malignancy, wound healing and tissue repair. This is in addition to the established role of AAMΦ during infection with multicellular parasitic (helminths), allergy, metabolic functions and inflammatory disorders such as fibrosis (Fairweather and Cihakova, 2009, Gordon and Martinez, 2010). Given their association with such a diverse range of functions, it is likely that the current knowledge and understanding in terms of microRNA regulation of AAMΦ is only the tip of the iceberg. Thus, investigating the role of microRNAs in the regulation of AAMΦ could have important implications for therapeutic targeting of macrophages

in not only the context of disease and disorders, but also for a greater understanding of how microRNAs in general contribute towards maintenance of the balance and efficiency of the immune response.

The purpose of the work described in this chapter was to identify microRNAs associated with AAMΦ under a range of conditions and to select the most appropriate microRNA candidates for further study in the subsequent chapters.

2.2 Results

2.2.1 Identification of microRNAs associated with alternative activation

In order to identify microRNAs associated with AAMΦ, microarray datasets previously generated by Dominik Ruckerl in our lab were utilised. These datasets provide information on the differential regulation of microRNAs under two distinct conditions of alternative activation:

1. **Macrophages generated via *in vitro* stimulation of bone marrow derived macrophages.**

   Cells were harvested from the bone marrow of WT C57BL/6 mice and cultured *in vitro* in M-CSF/CSF-1 containing medium for 7 days to obtain bone marrow derived macrophages (BMDMs) (Weischenfeldt and Porse, 2008). These differentiated BMDMs were either left untreated as an unstimulated control or stimulated with either IL-4 or LPS for 24 hours. Stimulation with LPS generated classically activated BMDMs whereas IL-4 treatment resulted in alternative activation of these macrophages (Figure 2.1). Total RNA was extracted from these distinct treatment groups and a microRNA array screen (Dharmacon/Thermofisher Agilent array) was carried out to identify microRNAs that are differentially expressed between the samples. Microarray analysis of these BMDMs stimulated with either LPS or IL-4 compared with the unstimulated control identified 118 microRNAs that were differentially expressed upon treatment (unpublished data, D.Ruckerl).

Changes in the expression profiles of these 118 microRNAs were further categorised into three groups:

a. **LPS or IL-4:** microRNAs differentially expressed in BMDMs in response to LPS only were deemed to be associated with classical activation while microRNAs whose expression was altered upon stimulation with IL-4 only were considered to be associated with alternative activation.

b. **LPS = IL-4:** microRNAs that exhibited similar changes in expression, i.e. either upregulated or downregulated, in response to both LPS and IL-4. These microRNAs were excluded from further consideration based on the assumption that they were more likely to be associated with general macrophage function and activation rather than being associated with a particular phenotype.

c. **LPS ≠ IL-4:** microRNAs whose expression was altered in response to both LPS and IL-4, but differentially, were designated as being associated with either the classical or alternative activation phenotype and included for further study (Figure 2.1).

Taking into consideration microRNAs that were altered in BMDMs in response to IL-4 treatment only or in response to both LPS and IL-4, but differentially, 15 microRNAs were identified to be potentially associated with alternative activation (summarised in Table 2.1).

2. AAMϕ elicited in response to *Brugia malayi* implant in the peritoneal cavity

B. malayi is a parasitic nematode that results in a strong T_H2 response when adult worms are implanted in the peritoneal cavity of mice. This leads to the accumulation of AAMΦ at the site of implantation. In a study carried out by Ruckerl *et al.* (2012) from our lab, AAMΦ elicited upon exposure to *B. malayi* were harvested from the peritoneal cavity of wild type (WT) mice 3 weeks post implant. Additionally, IL-4Rα deficient animals (IL-4Rα$^{-/-}$), which fail to produce AAMΦ, were also implanted with *B. malayi* adults. As a secondary comparison, WT mice were subject to sham surgery and injected with thioglycollate 3 days prior to necropsy. These thioglycollate-elicited macrophages (Thio MΦ) are monocyte-derived macrophages that are not alternatively activated and not associated with helminth infection. Total RNA was extracted from these three distinct cell populations and subject to a microRNA array screen (Exiqon miRCury 8.1 platform) to identify microRNAs that are differentially expressed between the samples. Comparison of the WT *B. malayi* elicited AAMΦ with macrophages from IL-4Rα$^{-/-}$ mice identified IL-4Rα dependent microRNAs. An additional comparison between the WT AAMΦ elicited in response to *B. malayi* implant and Thio MΦ identified microRNAs that were altered only in response to *B. malayi* and not in Thio MΦ (Figure 2.2). Together, these two comparisons revealed differential expression of 19 microRNAs (cut off > 2 fold) in the *B. malayi* elicited AAMΦ compared with macrophages either from IL-4Rα$^{-/-}$ mice or Thio MΦ (summarised in Table 2.2).

2.2.2 Identification of microRNAs consistently associated with alternative activation

Tables 2.1 and 2.2 list microRNAs that were identified as being associated with AAMΦ through analyses of two different microarray datasets from macrophages generated following IL-4 stimulation of BMDMs and *B. malayi* implants in mice respectively. Based on rationales explained below and considering microRNA isoforms as single microRNAs, these tables were then assessed to generate a final list of ten microRNAs either common to both datasets or other interesting candidates that may potentially be associated with AAMΦ.

Analysis of Tables 2.1 and 2.2 revealed four microRNAs that were common to both datasets – namely miR-125a-5p, miR-146a, miR-199b-5p and miR-378. Three of these microRNAs were also identified as being IL-4Rα dependent (Table 2.2) and therefore, selected for further study. Moreover, these four microRNAs were the most likely to be associated with AAMΦ being differentially expressed under two separate conditions of alternative activation. Although miR-378 was not significantly altered in BMDMs in response to IL-4 according to our cut-off values (Table 2.1), given its known association with AAMΦ (Ruckerl et al., 2012), it was selected as a positive control for future experiments regardless.

MiR-125b-5p, miR-146b and miR-199a-5p are isoforms of miR-125a-5p, miR-146a and miR-199b-5p respectively. Isoforms share identical seed sequences and hence are predicted to bind the same target mRNA 3' UTRs. These isoforms were identified as being differentially expressed in Table 2.1 and were therefore, also selected for further analysis. Moreover, as discussed earlier in the introduction for this chapter, miR-125b and miR-146a/b already play established roles in regulating CAMΦ. Thus, it would be interesting to try and dissect their functional roles and association with AAMΦ. MiR-199-3p, which arises from the same microRNA precursor and is transcribed at the same time as miR-199a/b-5p (reviewed later in Chapter 3) was identified as being differentially expressed in response to IL-4 in BMDMs (Table 2.1). For this reason, miR-199-3p was also selected as a potential candidate.

As shown in Table 2.1 both miR-99b and miR-99b* are regulated by IL-4. Interestingly, miR-99 and miR-99b* are derived from the same precursor microRNA that also forms a microRNA cluster with miR-125a-5p, which was identified as being common to both datasets. Majority of the times clustered microRNAs tend to be regulated and transcribed together (Bartel, 2004, Altuvia et al., 2005). Hence, both miR-99b and miR-99b* appeared to be interesting candidates given their association with miR-125a-5p and were also selected for further analysis.

MiR-223 has recently been shown to play a role in macrophage polarisation (Zhuang et al., 2012). It was also identified as being IL-4 receptor dependent (Table 2.2). Moreover, miR-223 was also regulated by IL-4 according to the BMDM microarray results, however, below our threshold (cut off > 2 fold) and hence does not feature in Table 2.1. Based on the above reasoning, miR-223 was also included for further study.

Finally, miR-221 and miR-222 are paralogues that were also identified as being differentially expressed in AAMΦ (Table 2.2). Both miR-221 and miR-222 have been classified as oncogenic microRNAs with great involvement in the progression of several kinds of tumours (Garofalo et al., 2012). Since a role for M2 polarised macrophages has been implicated in tumour progression (Solinas et al., 2009, Gocheva et al., 2010, Wang and Joyce, 2010), these microRNAs were also considered as interesting candidates for further analysis.

All of these microRNA candidates selected for further study are listed in Table 2.3. We then set out to identify which of these ten microRNAs (classifying isoforms as single microRNAs) were consistently associated with the alternative activation phenotype. To do this, their expression profiles were studied in different conditions of alternative activation ranging from a reductionist *in vitro* IL-4/13 stimulation of macrophage cell lines to a complex *in vivo* T_H2 infection to (Figure 2.3) as outlined below.

2.2.2.1 *In vitro* stimulation of macrophage cell lines RAW 264.7 and J774A.1

Having identified ten microRNAs that were differentially expressed and potentially associated with two different models of alternative activation, we set out to validate the association of these microRNAs with alternative activation. As a starting point, we used two different macrophage cell lines, RAW 264.7 and J774A.1. We decided to study the expression profiles of these microRNAs in cell lines initially as they provide a homogenous/pure cell population that is cost effective and easy to manipulate. Both RAW 264.7 and J774A.1 are functional monocytic macrophage cell lines derived from BALB/c mice, with RAW 264.7 being transformed by Abelson leukaemia virus (Raschke et al., 1978) while J774A.1 cells were isolated from a reticulum cell sarcoma (Ralph et al., 1976).

Prior to utilisation of these cell lines as *in vitro* models representative of alternative activation, it was essential to establish the individual ability of both RAW 264.7 and J774A.1 cells to alternatively activate. Both RAW 264.7 and J774A.1 cells were stimulated with IL-4 and/or IL-13 to compare the capacity of these two macrophage cell lines to alternatively activate. Additionally, a secondary aim of these experiments was to compare and select one of the two cell lines as an *in vitro* system for the identification of microRNA targets. This aligned with the aim of Chapter 5, which involves the use of immunoprecipitation of the RISC complex to identify microRNA targets in a macrophage cell line.

Both RAW 264.7 and J774A.1 cells were either left untreated or stimulated with 10ng/mL of IL-4 and IL-13. Supernatants were harvested for ELISAs and cells lysed for extraction of RNA. The parameters measured were primarily the production of the characteristic markers of alternative activation - YM-1 (*Chi3l3*), RELM-a (*Retnla*) and Arginase-1 (*Arginase-1*) (Gordon, 2003, Martinez and Gordon, 2014). Changes in RNA expression and expression of mRNA transcripts were quantified by qRT-PCR (Figure 2.4A). At 4hr post stimulation with IL-4 and IL-13, no alternative activation was observed as measured by transcript levels of *Arginase-1, Chi3l3* and *Retnla* for RAW 264.7 cells. Although no changes were observed in the expression levels of *Arginase-1* and *Chi3l3* in J774A.1 cells, *Retnla* levels were elevated by 5

fold at 4hr. At 24hr post stimulation, a 2 fold, 6 fold and 5 fold increase (relative to *Gapdh*) was observed in the expression of *Arginase-1*, *Chi3l3* and *Retnla* in RAW 264.7 cells. No significant changes in expression of these markers of activation were observed in J774A.1 cells, except for *Retnla*, which showed ~10 fold increase in expression relative to *Gapdh*. At 48hr post stimulation, this increase in *Retnla* expression was not noticeable in J774A.1 cells and the increase in *Chi3l3* expression had also subsided. Only *Arginase-1* levels were still increased by 2 fold at 48hr in this cell line. In contrast, activation was at its peak in RAW 264.7 cells at 48hr post IL-4/IL-13 stimulation, with ~6 fold increase in expression of both *Arginase-1* and *Chi3l3* (Figure 2.4A). Secreted protein concentrations of YM-1 and RELM-α were also measured by ELISA. Only YM-1 was detected in the supernatant (Figure 2.4B). No RELM-α was detected in the supernatant for both RAW 264.7 and J774A.1. We also assessed the capacity of these cell lines to express other markers of alternative activation and to exhibit classical activation markers (described in Appendix 1).

Having confirmed the ability of both RAW 264.7 and J774A.1 cells to alternatively activate, we next sought to validate the expression of the selected microRNAs (Table 2.3) in these alternatively activated cell lines. To validate the association of these ten shortlisted microRNAs from the microarray datasets with alternative activation, both RAW 264.7 and J774A.1 cells were either left untreated or stimulated with a combination of both IL-4 and IL-13. Cells were harvested and RNA was extracted 48 hours post stimulation. As previously mentioned, both IL-4 and IL-13 signal through a shared IL-4Rα chain (Gordon, 2003) and we have shown above that alternative activation in these cell lines is mainly IL-4 driven (Appendix 2). However, the addition of IL-13 to the culture medium enhances the state of alternative activation and was therefore used in combination with IL-4 in this experiment (Appendix 2). Of the ten microRNAs selected, three that were identified as being common to both microarray datasets and/or IL-4Rα dependent were selected for initial quantification by qRT-PCR. These included miR-125b, miR-146a and miR-378. Additionally, miR-146b, an isoform of miR-146a that shares the same seed sequence and hence functional overlap through shared targets, was included for the quantification as it was also differentially regulated in response to IL-4 in BMDM.

Consistent with the array results, there was an increase in the levels of miR-125b and miR-146b and a reduction in the expression of miR-146a in response to IL-4 and IL-13 in both RAW 264.7 and J774A.1 cell lines (Figure 2.4C). However, miR-378, whose expression was previously shown to be IL-4Rα dependent and upregulated in response to IL-4 (Ruckerl et al., 2012), was not altered in either of the cell lines upon treatment with IL-4 and IL-13 (Figure 2.4C). This can potentially be explained by the fact that both RAW 264.7 and J774A.1 are immortalised tumour cell lines that are constantly proliferating and it is probable that microRNAs such as miR-378, which are involved in the regulation of macrophage proliferation, are dysregulated in such modified cell lines. The lack of miR-378 regulation exposed a serious limitation in the use of these cell lines for subsequent analysis of microRNAs involved in the regulation of AAMΦ.

2.2.2.2 Analysis of microRNA expression levels in BMDM stimulated with IL-4 and IL-13 *in vitro*

Due to the limitations involved in the use of macrophage cell lines, exemplified by the lack of differential expression of miR-378, we next sought out to study the expression profiles of the ten shortlisted microRNAs (Table 2.3) in primary macrophages. Additionally, although microarrays are a powerful tool for studying simultaneous expression profiles on a scale that is impossible using conventional analysis, occasionally reliability and reproducibility issues are still encountered. Hence, validation of these ten microRNAs in alternatively activated BMDM *in vitro* also provided a secondary confirmation of the differential expression observed in the aforementioned microarray dataset. To do this, we generated BMDM as previously described (Weischenfeldt and Porse, 2008) and stimulated these BMDM with IL-4 and IL-13 *in vitro* or left them untreated for 24 and 48 hours. In the microarray described in section 2.3.1, BMDM were stimulated with IL-4 only. It is possible that IL-4 and IL-13 exert different effects downstream and regulate the transcription of different microRNAs. To account for this, a combination of both IL-4 and IL-13 was used as a stimulus for the activation of BMDM. In order to examine their association

with alternative activation, the expression levels of the ten shortlisted microRNAs (Table 2.3) were validated by qRT-PCR at both 24 and 48 hours post stimulation with IL-4 and IL-13. The data were normalised to RNU6B, which displayed stable expression in BMDM (data not shown). Of the ten microRNAs examined, all except miR-99b* and miR-199-3p were differentially expressed between untreated and BMDM treated with IL-4 and IL-13 (Figure 2.5A). Of note, the expression of miR-199-5p was not detectable in BMDM (C_t value > 38). MiR-125b, miR-146b, miR-221, miR-222 and miR-378 were all upregulated. Of these, miR-378 was found to be the most differentially regulated with an average of a 3-fold change in expression at 48 hours post stimulation. Conversely, miR-99b, miR-125a, mir-146a and miR-223 showed a reduction in expression levels by 48 hours. The changes in the expression of these microRNAs correlated with an increase in alternative activation over time, with greatest changes observed at peak of activation at 48 hours (Figure 2.5B). Additionally, thioglycollate elicited macrophages stimulated with IL-4 and IL-13 *in vitro* also displayed similar expression profiles of the ten selected microRNAs (Appendix 3). These results demonstrate that the altered expression of the majority of these microRNAs appears to be associated with alternative activation of macrophages.

2.2.2.3 Expression profiles of microRNAs upon IL-4 complex injection in the peritoneal cavity of mice

Although primary macrophages were a reliable source for validation of the micro-array analysis, often *in vitro* systems fail to represent *in vivo* biological systems in terms of complexity. Hence, following validation of the ten shortlisted microRNAs with *in vitro* alternative activation of primary BMDM, we next sought to examine the consistency of their association with AAMΦ in *in vivo* conditions. IL-4 complex (IL-4c) injection into the peritoneal cavity of mice involves the delivery of recombinant IL-4 complexed to an anti IL-4 monoclonal antibody. Slow dissociation of the complex allows release of IL-4 from the anti-IL-4 antibody over time (Jenkins et al., 2013). This results in the proliferation and accumulation of tissue resident

macrophages that are also alternatively activated in the peritoneal cavity. Total macrophages were isolated from the peritoneal cavity and sorted by flow cytometry 24 hours post either PBS or IL-4c injection based on the hallmark signatures of macrophages, namely F4/80 and CD11b. RNA was then extracted from the sorted macrophages and the expression profiles of the ten shortlisted microRNAs examined by qRT-PCR. Consistent with the array results, miR-99b*, miR-146b, miR-199b-5p, miR-199-3p, miR-221, miR-222 and miR-378 were all found to be upregulated in response to IL-4c. MiR-378, which is known to be associated with AAMΦ and has been shown to target AKT-1 and thought to negatively regulate IL-4 induced proliferation, displayed the largest fold change amongst all the microRNAs whose expression was enhanced (Ruckerl et al., 2012). On the other hand there was a reduction in the expression of miR-125a, miR-125b, miR-146a and miR-223. MiR-99b was the only microRNA that did not display differential expression upon treatment (Figure 2.6). This data demonstrated consistency in the alteration of expression of the majority of the selected microRNAs in AAMΦ both *in vitro* and *in vivo*.

2.2.2.4 Differential expression of microRNAs during *Litomosoides sigmodontis* infection time course

We had now validated differential expression of the selected microRNAs under three different conditions of alternative activation with increasing complexity. However, these conditions were restricted to *in vitro* IL-4/IL-13 stimulation or IL-4c injection in the peritoneal cavity. None of these represented a natural physiological system. Although delivery of IL-4c to the peritoneal cavity provides information about the expression of these microRNAs in a biological system, it is still a reductionist approach that utilises levels of IL-4 that may not be physiological, especially in the absence of tissue-specific signals that may normally operate. Additionally, even though the expression of these microRNAs was altered in response to *B. malayi* implant, it is possible that the change in their expression following implant was infection specific. Hence, to investigate whether in a more complex scenario and in a

completely distinct T_H2 infection setting these microRNAs would still be differentially expressed and associated with alternative activation, we used *Litomosoides sigmodontis,* a murine model of filarial nematode infection.

Mice were injected subcutaneously with either infective *L. sigmodontis* L3 larvae or injected with control RPMI medium. As the larvae migrate to the pleural cavity between day 4 and 6, a T_H2 biased immune response is mounted. This was characterised by the presence of alternative activation markers, YM-1 and RELMα, from day 8 onwards (Figure 2.7), as previously shown (Nair et al., 2005, Jenkins et al., 2011). As the infection progressed over time, this state of alternative activation continued to rise peaking at day 14 and was maintained until day 28 thereafter. During this 28 day period, the lifecycle of the nematode progresses from the L3 larval stage through to the development into adult worms at day 28 with moulting to the L4 stage in between (reviewed in Chapter 1). We utilised C57BL/6 mice for this experiment and the time course was allowed to progress until day 28 and no further as C57BL/6 mice have been shown to be resistant to *L. sigmodontis* infection; the fecundity of adult worms is largely affected and no microfilariae are produced (Marechal et al., 1997, Babayan et al., 2003b). With the core aim of this study being the identification of microRNAs associated with AAMΦ and with alternative activation being well established by day 14 post infection (Figure 2.7), the need for a long-term patent infection was eliminated.

It has previously been shown that besides alternative activation, the resident pleural macrophages also undergo proliferation (Jenkins et al., 2011). Although the initial burst of proliferation is CSF-1 dependent, it is mainly IL-4 dependent mechanisms that drive the expansion of the tissue resident population with the progression of infection (Jenkins et al., 2011, Jenkins et al., 2013). Consistent with the published data, we observed a peak in this IL-4 driven proliferation at day 11 as shown in Figure 2.7. Contrary to the maintenance of alternative activation during the time course, proliferation steadily declined to baseline levels by day 18. A second burst of proliferation was observed at day 28, presumably to return to homeostatic levels of steady state proliferation.

Having determined that the infection progressed as expected through analysis of characteristic markers of alternative activation and proliferation through FACS (Figure 2.7), we next sought to examine the expression profiles of the ten selected microRNAs over the course of *L. sigmodontis* infection. At each selected time point, macrophages were isolated from the pleural lavage through adherence purification and RNA extracted. Changes in microRNA expression levels were measured through qRT-PCR and normalised to RNU6B expression. Fold changes were calculated as a ratio of values from infected versus naïve mice. As shown in Figure 2.8, consistent with our previous findings and in line with the microarray data, expression profiles of all the selected microRNAs were altered. Expression levels of miR-99b*, miR-146b, miR-199b-5p, miR-221, miR-222, miR-223 and miR-378 were significantly enhanced. Once again, miR-378 showed the greatest fold change amongst all the microRNAs with increased expression levels. Downregulation in the expression of miR-99b, miR-125a, miR-125b and miR-146a was observed. Besides examining the consistency of expression of the selected microRNAs in this infection model, a secondary aim of this infection time course was to gain insight into the expression kinetics of these microRNAs over the course of infection and to compare them to the expression of characteristic markers of alternative activation and proliferation. This data provides some insight regarding the expression levels of several microRNAs in relation to the activation and proliferative state of macrophages at specific time points over the course of infection.

2.3 Discussion

MicroRNAs play a critical role in the regulation of cellular processes. Numerous studies have shown that microRNAs participate in immune responses and specifically in the regulation of CAMΦ. However, it is less clear how microRNAs regulate AAMΦ and their responses. The primary objective of this chapter was to identify microRNAs differentially expressed in AAMΦ under a range of conditions and to select the most appropriate microRNA candidates for further study. Utilising microarray datasets previously generated in the lab by Dominik Ruckerl, we

identified microRNAs that are highly regulated by IL-4 in either BMDMs *in vitro* or in a *B. malayi* implant model in mice. In the first microarray dataset obtained through stimulation of BMDMs with either IL-4 or LPS, a total of a 118 microRNAs were differentially expressed. Based on the selection criteria detailed in section 2.3.1, 15 microRNAs were deemed to be differentially expressed in response to IL-4 and considered for further study (Table 2.1). A recent study conducted by (Squadrito et al., 2014), although primarily focused on exosomes, also studied changes in microRNA expression levels following IL-4 stimulation of BMDMs. They identified 29 microRNAs that were significantly regulated by IL-4. Of note, 18 of these microRNAs also featured in our BMDM microarray data (data not shown). However, only 4 of these microRNAs were shortlisted based on our selection criteria – namely miR-125a-5p, miR-146a-5p, miR-149 and miR-378 (summarised in Table 2.1). The other 14 had not been considered to be as interesting because their expression levels were below our selected threshold (> 2 fold) or because similar changes in their expression was observed in response to both IL-4 and LPS. Our focus was to identify microRNAs strictly associated with alternative activation; changes in expression levels in response to both IL-4 and LPS would suggest a greater likelihood for the microRNA function to be associated with macrophage activation in general.

The information for the second microarray dataset available to us was taken from the study performed by Ruckerl *et al.* in 2012 (Supplementary table 1). This involved the use of 19 microRNAs that were identified as being differentially expressed in AAMΦ isolated from mice implanted with the nematode *B. malayi*. Some of these microRNAs were also identified as being IL-4Rα dependent (reviewed in Table 2.2). Having identified microRNAs differentially expressed in response to IL-4 under two distinct conditions of alternative activation, based on our reasoning in section 2.3.2, we shortlisted ten microRNA candidates potentially associated with AAMΦ for further study. These shortlisted microRNA candidates are listed in Table 2.3.

To validate the microarray data and to examine the consistency in their expression and association with AAMΦ, the expression profiles of these selected microRNA candidates were studied under different conditions of alternative activation ranging from a complex T_H2 infection setting to a reductionist IL-4/IL-13 stimulation of

macrophage cell lines. Due to the limitations involved with the use of macrophage cell lines, demonstrated by the lack of differential expression of microRNAs with known function, data generated using these cell lines was excluded from the final analysis for selection of candidates for further study in the subsequent chapters (Figure 2.9).

Among these microRNAs, miR-378, which has previously been shown to directly target AKT-1, crucial for the modulation of IL-4 induced proliferation in AAMΦ by our lab (Ruckerl et al., 2012), consistently displayed the highest fold change increase in its expression. MiR-378 has previously been linked to adipogenesis (Gerin et al., 2010, Pan et al., 2014, Kulyte et al., 2014, Huang et al., 2015). In relation to this, a role for AAMΦ has also been implicated in thermogenesis (Odegaard et al., 2007, Kang et al., 2008, Chawla, 2010, Nguyen et al., 2011). Hence, it is possible that besides proliferation, miR-378 might regulate other functions of AAMΦ. Given the strong association of miR-378 with the alternatively activated phenotype as demonstrated in this chapter along with it's previously published role in their regulation, miR-378 was selected for further study in Chapter 4 to delineate its role in regulating AAMΦ responses other than proliferation.

Besides miR-378, two other microRNAs miR-125a-5p and miR-146a also showed a consistent downregulation in their expression under all the different conditions of alternative activation that were analysed. MiR-125a-5p has previously been shown to suppress TLR4 mediated proinflammatory responses and promote macrophage polarisation towards the M2 phenotype (Banerjee et al., 2013a). In their study, Banerjee *et al.* show that the induction of miR-125a-5p expression is NF-κB and MYD88 dependent. Inhibition of miR-125a-5p enhances levels of TNF-α, IL-12 and iNOS. Induction of miR-125a-5p expression upon LPS stimulation is in agreement with our results (Table 2.1). However, contrary to our results in terms of alternative activation, Banerjee *et al.* suggest that expression of miR-125a-5p is higher in M2 macrophages and enhances Arginase-1 levels. Arginine metabolism is a shared characteristic of both AAMΦ and CAMΦ. There are circumstances in which Arginase-1 expression can be induced by pro-inflammatory signals (El Kasmi et al., 2008, Mylonas et al., 2009). Hence, solely using Arginase-1 as a marker for

enhanced M2 polarisation may not be reliable. Ruckerl *et al.* (2012) previously found the expression of miR-125a-5p to be IL-4Rα dependent. IL-4 has been shown to inhibit alternative NF-κB signalling and with miR-125a-5p expression being NF-κB dependent (Lawrence, 2009, Sun et al., 2013), the downregulation of miR-125a-5p seen in our different models of alternative activation could possibly be explained.

Besides miR-378 and miR-125a-5p, miR-146a was the third microRNA that was consistently downregulated in all conditions of alternative activation that were studied. MiR-146a is one of the most widely studied microRNAs and a well-known mediator of inflammation, especially in T-cell responses (Curtale et al., 2010, Rusca and Monticelli, 2011, Labbaye and Testa, 2012, Yang et al., 2012, Baumjohann and Ansel, 2013). As for macrophages, miR-146a is a key player in controlling inflammation, myeloproliferation and oncogenic transformation (Taganov et al., 2006, Boldin et al., 2011, O'Neill et al., 2011). It is known to regulate IL-6 production and is a known inhibitor of TRAF6 and IRAK1 involved in the regulation of TLR signalling in a negative feedback loop (Taganov et al., 2006, He et al., 2014c). However, a role for miR-146a in the regulation of AAMΦ is yet to be determined. We observed a consistent reduction in the expression of miR-146a in response to IL-4 both *in vitro* and *in vivo*. Conversely, expression of miR-146a was significantly enhanced upon LPS stimulation. Like miR-125a-5p, expression of miR-146a is also NF-κB dependent (Taganov et al., 2006). Both AAMΦ and CAMΦ activation states promote changes in patterns of macrophage gene expression that are transcriptionally distinct. Keeping this in mind and with the knowledge that IL-4 can also inhibit alternative NF-κB signalling, the observed reduction in miR-146a in our different models of alternative activation can potentially be explained through the NF-κB dependent downregulation of miR-146a by IL-4.

While expression of miR-146a was reduced in AAMΦ, there was a significant increase in the levels of miR-146b, an isoform of miR-146a, under the same conditions of alternative activation except in response to *B. malayi* implant, wherein no significant alteration in miR-146b expression was observed. In addition to a Th2 immune response, exposure to helminths results in complex changes in the surrounding environment (MacDonald et al., 2002, Anthony et al., 2007, McSorley

and Maizels, 2012). Furthermore, the immune response following an implant is much more inflammatory than other infections such as *L. sigmodontis* because of the initial surgery. Hence, there is the possibility that the expression of miR-146b is masked by other factors with a stronger influence in this particular scenario. As mentioned previously, microRNA isoforms share identical seed sequences (2-8nt) and are predicted to bind the same targets and hence, functionally overlap. Like miR-146a, miR-146b also regulates TRAF6 and IRAK1 function and is involved in a negative feedback loop downstream of TLR signalling (Taganov et al., 2006). Genes encoding these microRNAs are found on separate chromosomes. While miR-146a is known to be NF-κB dependent, miR-146b is STAT3 induced (Xiang et al., 2014). Whilst IL-4 can inhibit alternative NF-κB signalling, there have been reports that the shared IL-4Rα/ IL-13Rα can lead to STAT3 activation (Wery-Zennaro et al., 1999, Umeshita-Suyama et al., 2000, Bhattacharjee et al., 2013). Hence, the probability exists that these isoforms have evolved with redundancy in function, but are expressed in response to different environmental cues. This would explain our finding that whilst miR-146a expression is reduced in AAMΦ, expression of miR-146b is enhanced.

Ruckerl *et al.* (2012) identified miR-199b-5p as being the second most highly regulated by IL-4 after miR-378. Moreover, miR-199a-5p and miR-199-3p, which belong to the same family as miR-199b-5p, were also differentially expressed in AAMΦ according to our lab's microarray dataset. However, since miR-199b-5p and miR-199a-5p are isoforms with identical seed sequences, we decided to focus on miR-199b-5p because its expression was IL-4Rα-dependent (Table 2.1). Although a role for the miR-199 family has been suggested in several different cancers, the specific function of miR-199b-5p is still largely unknown (Sakurai et al., 2011, Alexander et al., 2013, Yi et al., 2013, He et al., 2014c, Hashemi Gheinani et al., 2015). Our investigation of the expression profile of this microRNA under various conditions of alternative activation revealed an increase in its expression *in vivo.* MiR-199b-5p was upregulated both in response to IL-4 complex delivery i.p and during *L. sigmodontis* infection. Interestingly, the microarray data from BMDMs stimulated with IL-4 suggested a downregulation in the expression of miR-199b-5p in response to IL-4. However, upon validation of this data with *in vitro* stimulation of

BMDMs with IL-4 and IL-13, it was found that miR-199b-5p is not expressed very highly in these cells indicated by a C_t value >38. These results are in agreement with the finding of Ruckerl *et al.* (2012) that *in vitro* stimulation of Thio MΦ with IL-4 does not result in an increase in miR-199b-5p expression. Even though miR-199b-5p expression was enhanced in response to two different nematodes and IL-4 injection *in vivo*, the same was not true for stimulation with IL-4 *in vitro.* Additionally, these results might suggest that IL-4Rα signalling on its own is not sufficient to induce the expression of miR-199b-5p and that a secondary extrinsic factor that is only found in an *in vivo* environment may be needed. It may also suggest that IL-4Rα expression on the macrophage may not be required, but that some other IL-4Rα expressing cell type may be involved in the induction of this microRNA. These findings together rendered miR-199b-5p a very interesting candidate to pursue for further study as described in Chapter 3.

Next, we examined the expression levels of miR-125b-5p, an isoform of miR-125a-5p, which has been discussed earlier on in this section. Like miR-125a-5p, miR-125b-5p is a well-known oncomir known to potentiate macrophage activation (Chaudhuri et al., 2011, Kim et al., 2012, Sun et al., 2013, So et al., 2014). Contrary to the consistent downregulation of miR-125a-5p under all the different conditions of alternative activation, the expression of miR-125b-5p varied greatly. It was upregulated in the microarray data obtained from AAMΦ isolated following *B. malayi* implant in mice as well as in BMDMs stimulated with IL-4. The increased expression of this microRNA in BMDMs was further validated by qRT-PCR following *in vitro* stimulation with IL-4 and IL-13. However, expression of miR-125b-5p was reduced during the course of *L. sigmodontis* infection and also in response to IL-4c injection in the peritoneal cavity. A notable contrast to the expression profile miR-125b-5p were miR-221 and miR-222, whose pattern of expression was opposite to that of miR-125b-5p. MiR-221 and miR-222 showed elevated levels during *L. sigmodontis* infection and following IL-4 delivery to the peritoneal cavity. Their expression, on the other hand, was reduced in the arrays involving AAMΦ isolated from *B. malayi* implant in mice and IL-4 stimulation of BMDMs (also confirmed by *in vitro* stimulation by IL-4 and IL-13). As mentioned

previously, miR-221 and miR-222 are paralogs that have been strongly linked with angiogenesis and progression of tumours (Suarez and Sessa, 2009, Zhang et al., 2010b, Zhang et al., 2010a, Zhang et al., 2010d, Shah and Calin, 2011, Garofalo et al., 2012, Falkenberg et al., 2013, Gan et al., 2014). A role for AAMΦ has been implicated in tumour progression since tumour associated macrophages share many properties of AAMΦ (Gordon, 2003, Solinas et al., 2009, Gordon and Martinez, 2010, Wang and Joyce, 2010). Given that miR-125b-5p has been classified as an oncomir (Klusmann et al., 2010, Chaudhuri et al., 2012, Amir et al., 2013), it is plausible that these microRNAs are associated with the regulation of some of those tumour-promoting properties. What is potentially more interesting is the origin of the macrophages under the different conditions of alternative activation. AAMΦ elicited following *B. malayi* implant and BMDMs are both of blood monocyte derived macrophage origin whereas AAMΦ isolated during *L. sigmodontis* infection and in response to IL-4c injection in the peritoneal cavity are tissue resident macrophages (Ruckerl and Allen, 2014). It has recently been shown that AAMΦ derived from monocytes and tissue macrophages are phenotypically and functionally distinct (Gundra et al., 2014). Thus, it is intriguing that miR-125b-5p, miR-221 and miR-222 exhibit differential expression in macrophages based on their origin. Although these microRNAs were not selected for further study due to the main focus of this study being the association of microRNAs with alternative activation in general, dissecting the functional roles of these microRNAs in context of macrophage origin may be worth pursuing.

MiR-223, another IL-4Rα-dependent microRNA, plays a role in macrophage polarisation through suppression of proinflammatory activation (Zhuang et al., 2012). It is also known to play a critical role in haematopoiesis through the regulation of progenitor cell proliferation and granulocyte function (Johnnidis et al., 2008). We have shown that levels of miR-223 were increased in AAMΦ elicited in response to both *B. malayi* and *L. sigmodontis*. Conversely, a reduction in the expression of miR-223 was observed in response to IL-4 in peritoneal macrophages and BMDMs. Helminth infections create complex environments wherein several factors such as heterogeneous cell populations and varied environmental cues can

influence gene expression. In contrast, *in vitro* stimulation of cells and IL-4 delivery to the peritoneal cavity are relatively reductionist approaches restricted to cells expressing the IL-4Rα. Hence, it is likely that the enhanced levels of miR-223 in response to helminths may be infection specific and a result of interactions between the IL-4Rα and other parasite-induced signals.

In conclusion, we have identified several microRNAs that are differentially expressed in AAMΦ. A growing body of evidence discussed in this chapter suggests that some of these microRNAs are consistently associated with varying conditions of alternative activation. The aim of this study was to shortlist microRNA candidates for further study in the subsequent chapters. Of all the selected microRNAs, due to the consistency of their expression in AAMΦ under all the different conditions studied, miR-125a-5p, miR-146a and miR-378 were considered the most likely to play crucial roles in the regulation of this phenotype. Of these, given the importance of miR-146a as a mediator of inflammatory responses and the differential expression of its isoform miR-146b under the same conditions of alternative activation, we decided to evaluate the role of these isoforms in the regulation of AAMΦ in Chapter 5. With their recognised roles as suppressors of inflammatory responses, we hypothesised that under conditions of alternative activation, miR-146b suppresses genes otherwise targeted by miR-146a, so as to allow efficient alternative activation to occur. Additionally, miR-378 is a known regulator of IL-4 induced proliferation (Ruckerl et al., 2012). Given its strong association with the alternatively activated phenotype as shown in this chapter, miR-378 was also selected for further analysis of its role in fine tuning AAMΦ responses in contexts other than proliferation (discussed in Chapter 4). Lastly, the finding that miR-199b-5p is an IL-4 receptor dependent microRNA that appears to be expressed highly in AAMΦ only *in vivo* and not *in vitro* compelled us to investigate the contribution of this microRNA in the regulation of AAMΦ further in Chapter 3.

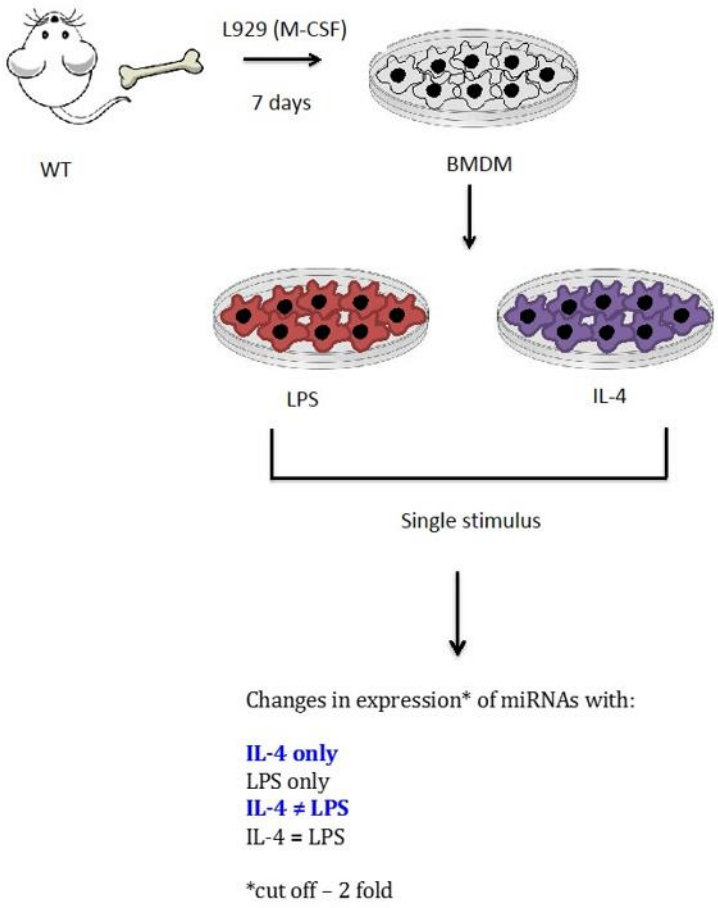

Figure 2.1 Generation of BMDM and identification of microRNAs differentially expressed in alternatively activated BMDM.

BMDM were obtained through *in vitro* differentiation of bone marrow precursors in M-CSF containing medium for 7 days. These BMDM were stimulated with either LPS or IL-4 only for 24 hours or preincubated with either LPS or IL-4 for 4 hours followed by treatment with either IL-4 or LPS overnight. A microarray screen was then performed with samples (n=3) from each treatment group to identify microRNAs differentially regulated in classical and alternative activation (Experiment designed, conducted and analysed by D. Ruckerl).

microRNA ID	IL-4 vs. media	LPS/IFN vs. media
mmu-miR-16-1*	-1.60	-0.92
mmu-miR-99b	**-1.00**	**0.28**
mmu-miR-99b*	**-2.56**	**0.57**
mmu-miR-125a-5p	**-1.00**	**0.71**
mmu-miR-139-5p	-1.03	0.38
mmu-miR-146a	**-1.09**	**0.77**
mmu-miR-146b	**1.32**	**0.90**
mmu-miR-149	1.70	0.00
mmu-miR-184	-1.43	2.20
mmu-miR-193	1.01	-0.25
mmu-miR-199a-5p	**-1.94**	**2.63**
mmu-miR-199a-3p	**-1.64**	**2.86**
mmu-miR-199b-5p	**-2.74**	**2.12**
mmu-miR-378	**0.81**	**0.95**
mmu-miR-551b	-1.32	3.72
mmu-miR-582-5p	1.04	-0.22

TABLE 2.1 Fold changes (Log2) of microRNAs altered in BMDMs in response to either IL-4 or LPS treatment 24 hours post stimulation.

Results adapted from unpublished microarray analysis carried out by D. Ruckerl. Data are representative of results obtained from analysis of a single microarray (n=3). MicroRNA selection was based on a minimum 2-fold (cut off value) change in expression post treatment. MiR-378 (highlighted in red) was included as an exception based on its previous association with alternative activation (Ruckerl *et al.*, 2012).

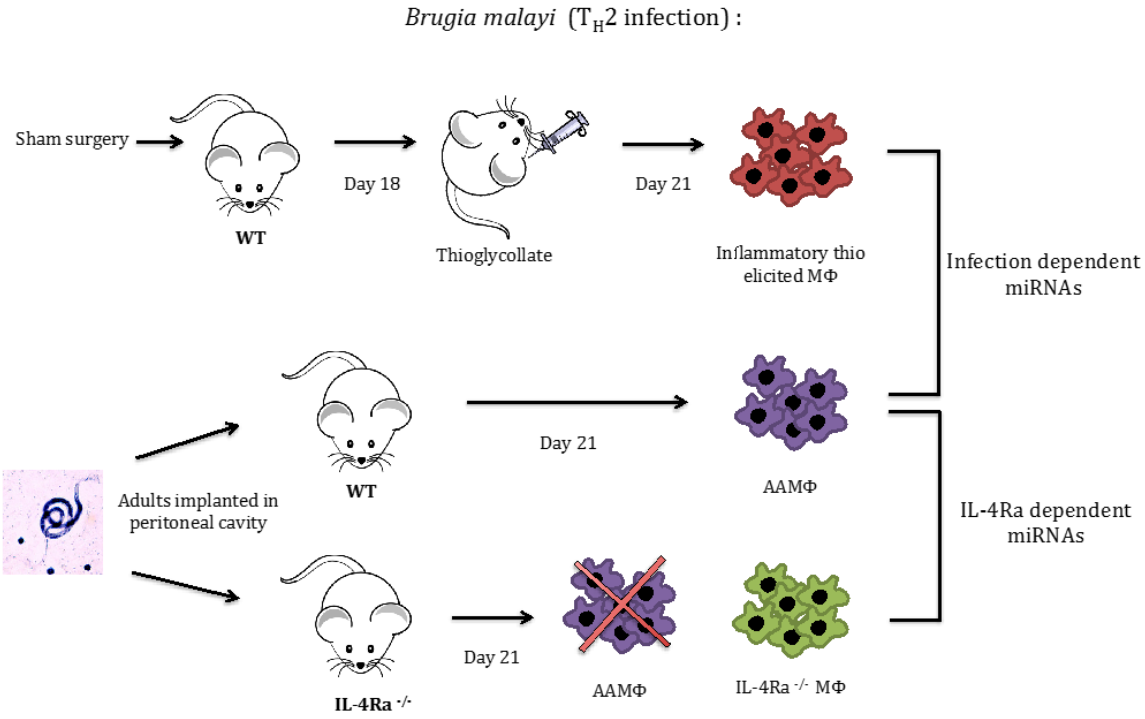

Figure 2.2 Identification of IL-4Rα dependent microRNAs during *B. malayi* infection.

Thioglycollate elicited macrophages or macrophages elicited in response to *B. malayi* infection from WT and IL-4Rα$^{-/-}$ mice (BALB/c) were harvested from the peritoneal cavity of mice and subject to a microRNA array screen. WT *B. malayi* elicited AAMΦ were compared to macrophages from IL-4Rα$^{-/-}$ animals also implanted with *B. malayi* to identify IL-4Rα dependent microRNAs. Additionally, WT *B. malayi* elicited AAMΦ were also compared to thio elicited MΦ to identify microRNAs expressed only in response to *B. malayi* and not in Thio MΦ (n=3).

microRNA-ID	AAMΦ vs. IL-4Rα$^{-/-}$	AAMΦ vs. Thio MΦ
miR-18a	-	-1.31
miR-20a	-0.6	-
miR-125a-5p	**-1.09**	**-**
miR-125b-5p	**1.91**	**-**
miR-141	-	-1.14
miR-146a	**-**	**-1.46**
miR-150	-1.97	-
miR-199b-5p	**2.04**	**-**
miR-221	**-**	**-1.53**
miR-222	**-**	**-1.27**
miR-223	**1.22**	**-**
miR-291a-5p	-0.75	-
miR-342-3p	-	-1.51
miR-378	**2.28**	**2.1**
miR-467b	-	-1.1
miR-689	-2.56	-
miR-710	-1.06	-
miR-720	1.03	-
miR-744	-0.85	-

TABLE 2.2 Log 2 ratios of microRNAs found to be significantly altered in WT mice implanted with *B. malayi* in comparison to either IL-4Rα$^{-/-}$ mice or Thio MΦ isolated from WT animals.

Data are representative of results obtained from a single microarray analysis (n=3).

**(data table adapted from Ruckerl *et al.*, 2012)

microRNA-ID	AAMΦ vs. IL-4Rα$^{-/-}$	AAMΦ vs. Thio MΦ	IL-4 vs. media	LPS/IFN vs. media
miR-99b	-	-	-1.00	0.28
miR-99b*	-	-	-2.56	0.57
miR-125a-5p	-1.09	-	-1.00	0.71
miR-125b-5p	1.91	-	-	-
miR-146a	-	-1.46	-1.09	0.77
miR-146b	-	-	1.32	0.90
miR-199a-5p	-	-	-1.94	2.63
miR-199a-3p	-	-	-1.64	2.86
miR-199b-5p	2.04	-	-2.74	2.12
miR-221	-	-1.53	-	-
miR-222	-	-1.27	-	-
miR-223	1.22	-	-	-
miR-378	2.28	2.1	0.81	0.95

TABLE 2.3 Log 2 ratios of microRNA candidates shortlisted for further validation in varying conditions of alternative activation.

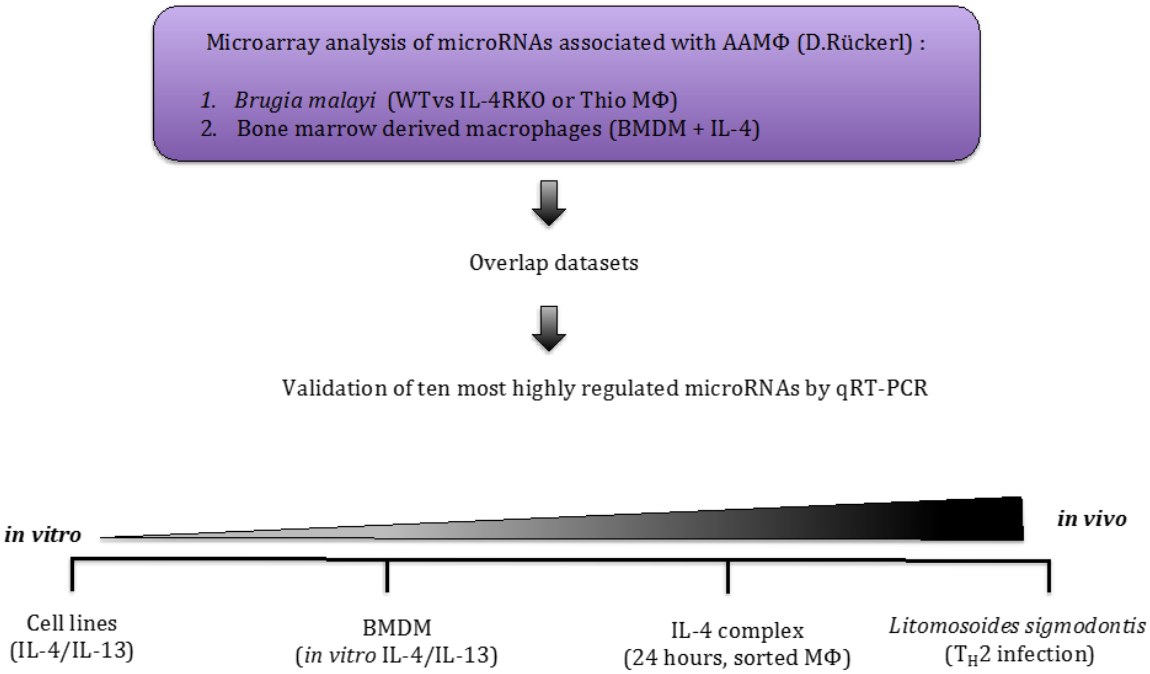

Figure 2.3 Identification of microRNAs consistently associated with alternative activation.

Previously generated microarray datasets from *B. malayi* implant and alternatively activated BMDMs were utilised to shortlist ten highly regulated microRNAs. The expression profiles of these ten microRNAs were then validated by qRT-PCR in four different conditions of alternative activation that included macrophage cell lines, BMDM stimulated *in vitro* with IL-4 and IL-13, peritoneal macrophages sorted from mice injected with IL-4 complex and macrophages isolated from the pleural cavity of mice infected with the nematode *Litomosoides sigmodontis*.

A.

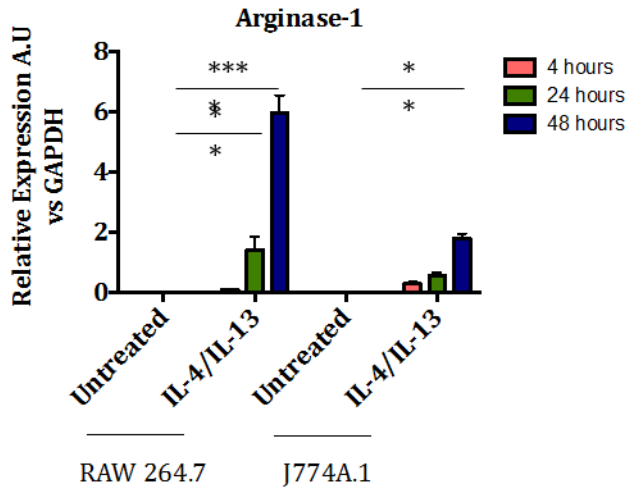
Arginase-1
Relative Expression A.U vs GAPDH
8
6
4
2
0
***
*
*
*
*
4 hours
24 hours
48 hours
Untreated
IL-4/IL-13
Untreated
IL-4/IL-13
RAW 264.7
J774A.1

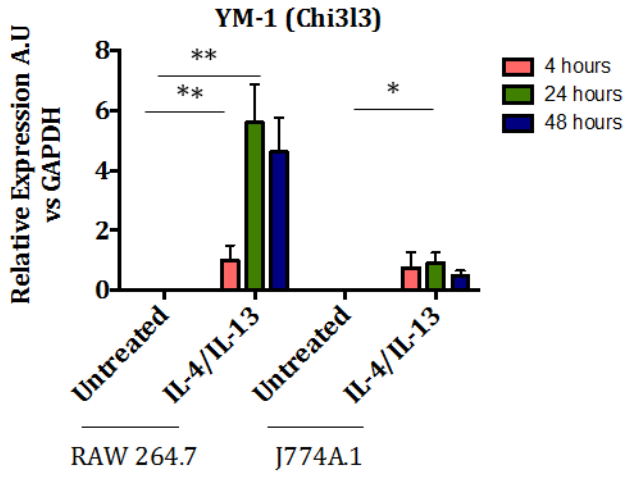
YM-1 (Chi3l3)
Relative Expression A.U vs GAPDH
8
6
4
2
0
**
**
*
4 hours
24 hours
48 hours
Untreated
IL-4/IL-13
Untreated
IL-4/IL-13
RAW 264.7
J774A.1

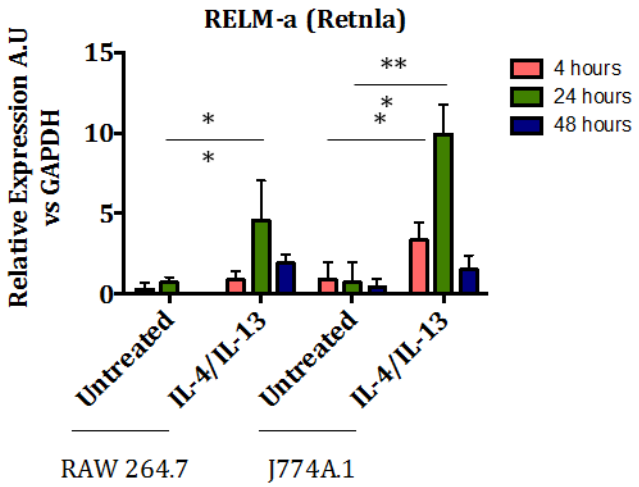
RELM-a (Retnla)
Relative Expression A.U vs GAPDH
15
10
5
0
*
*
**
*
*
4 hours
24 hours
48 hours
Untreated
IL-4/IL-13
Untreated
IL-4/IL-13
RAW 264.7
J774A.1

B.

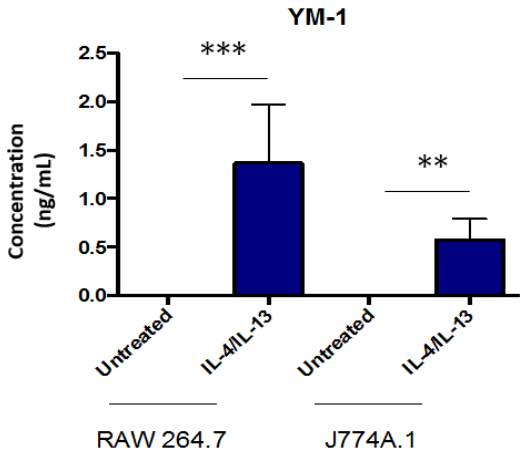

Figure 2.4 Comparison of the ability of macrophage cell lines to alternatively activate in response to IL-4 and IL-13 *in vitro*.

Macrophage cell lines RAW 264.7 and J774A.1 cells were stimulated with 10ng/mL of IL-4 and IL-13 for 24 and 48 hours. **A)** Their ability to alternatively activate was measured through quantification of characteristic markers of alternative activation, namely *Arginase-1* (Arg-1), *Chi3l3* (YM-1) and *Retnla* (Relm-a) by qRT-PCR. **B)** Secreted YM-1 protein was quantified by ELISA. RELMa was not detectable in the supernatants for either cell line. Data are presented as the mean fold change ± SEM and representative of two separate experiments (n=3). Statistical significance for differences between treated and untreated samples were determined using one-way ANOVA (Kruskal Wallis test) (* $P< 0.05$, ** $P< 0.01$, *** $P< 0.001$).

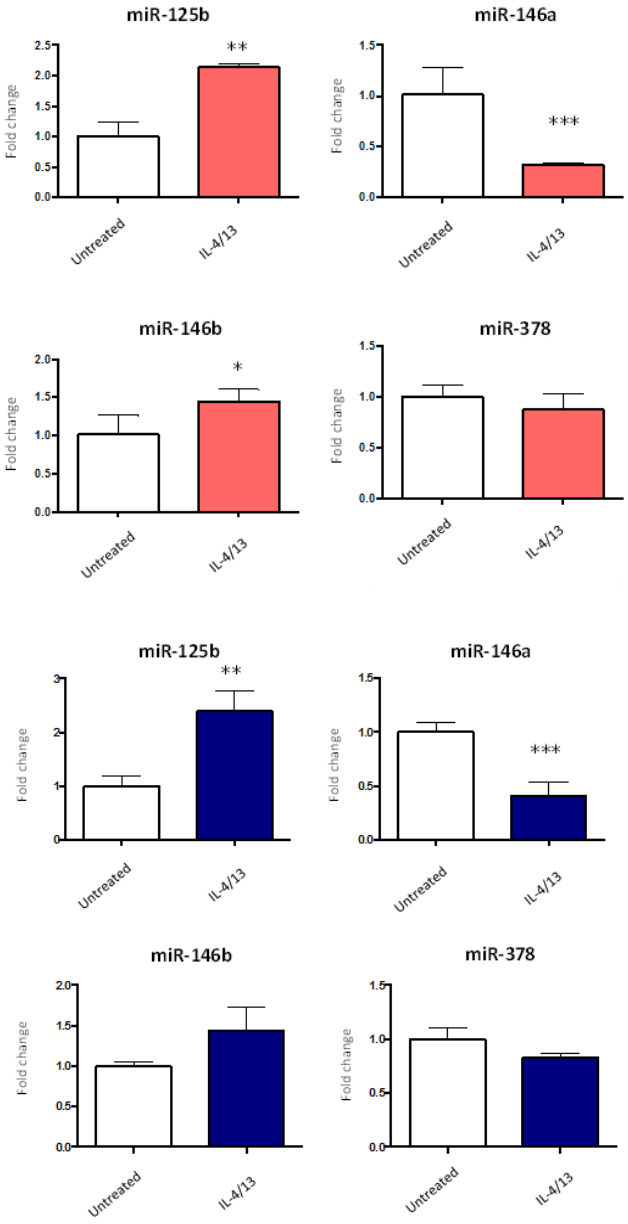

Figure 2.4C Analysis of microRNA expression levels in macrophage cell lines upon alternative activation *in vitro*. J774A.1 (coral) and RAW 264.7 (navy) cells were either left untreated or stimulated with 20ng/ml IL-4 and IL-13 for 48 hours. Samples were harvested for RNA extraction and microRNAs were quantified by qRT-PCR. *RNU6b* was used as a reference gene for normalisation and fold changes were calculated against untreated samples. Data are presented as the mean fold change ± SEM and representative of two separate experiments (n=3). Statistical significance for differences between treated and untreated samples were determined using a two-tailed unpaired student's T-test (* P< 0.05, ** P< 0.01, *** P< 0.001).

A.

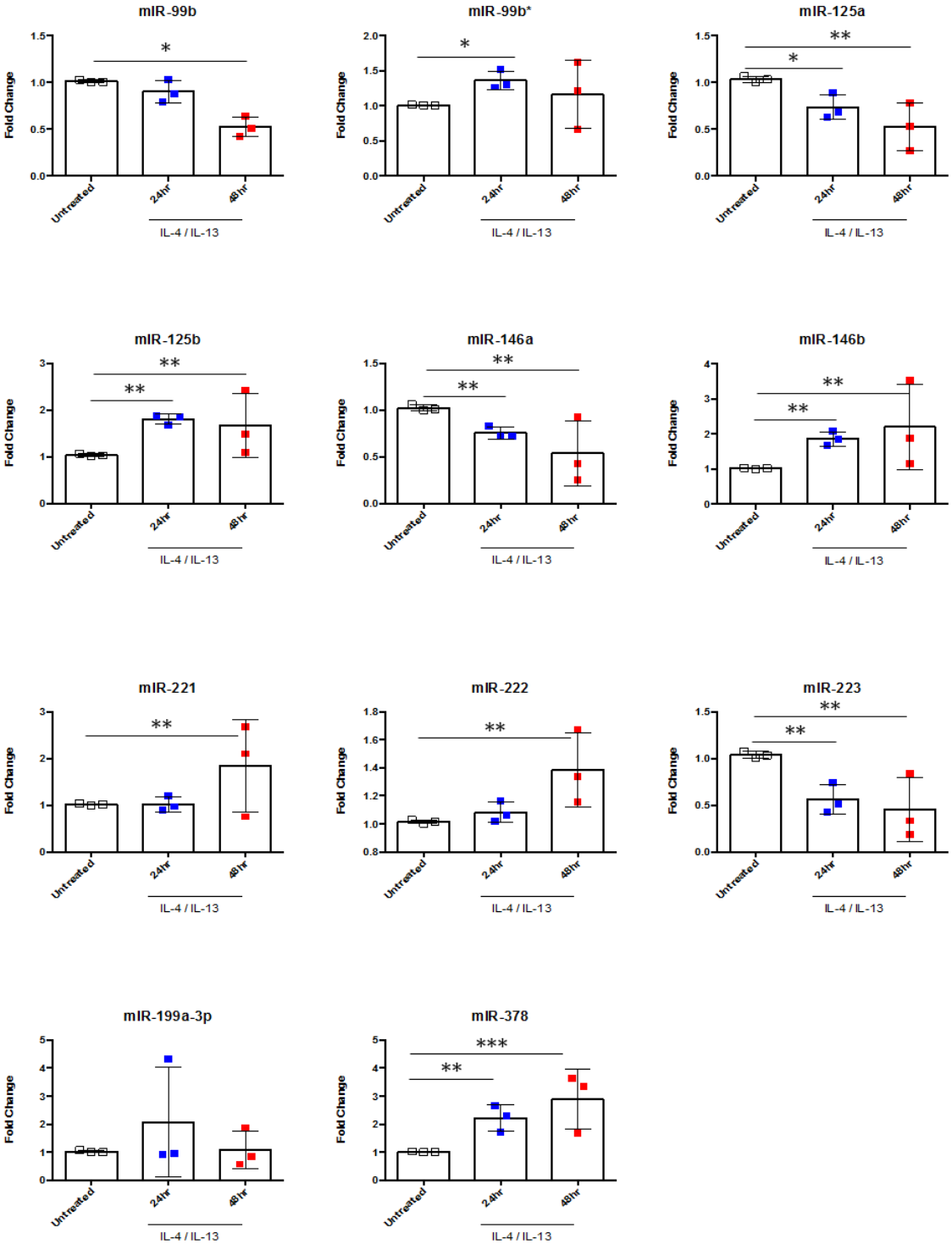
miR-99b
miR-99b*
miR-125a
miR-125b
miR-146a
miR-146b
miR-221
miR-222
miR-223
miR-199a-3p
miR-378
Fold Change
Untreated
24hr
48hr
IL-4 / IL-13

B.

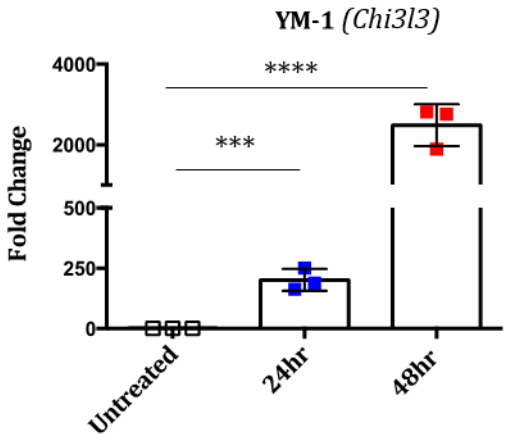

Figure 2.5 Differential expression of shortlisted microRNAs in BMDM 24 and 48hr post IL-4 and IL-13 stimulation.

Bone marrow precursors isolated from C57BL/6 mice were used to generate BMDM *in vitro* in culture media containing M-CSF for 7 days. **A)** BMDM were left untreated or stimulated with a combination of IL-4 and IL-13 at 20ng/ml for 24 and 48 hours. MicroRNAs were quantified by qRT-PCR and normalised using *RNU6b* as a reference gene. **B)** *Chi3l3* (YM-1) expression was quantified as a measure of alternative activation and normalised to *Gapdh* expression. Fold changes are calculated as the ratio of values from untreated samples versus samples stimulated with IL-4 and IL-13. Data are presented as the mean fold change ± SEM and representative of two separate experiments (n=3). Statistical significance for differences between treated and untreated samples were determined using one-way ANOVA (Kruskal Wallis test) (* P< 0.05, ** P< 0.01, *** P< 0.001).

A.

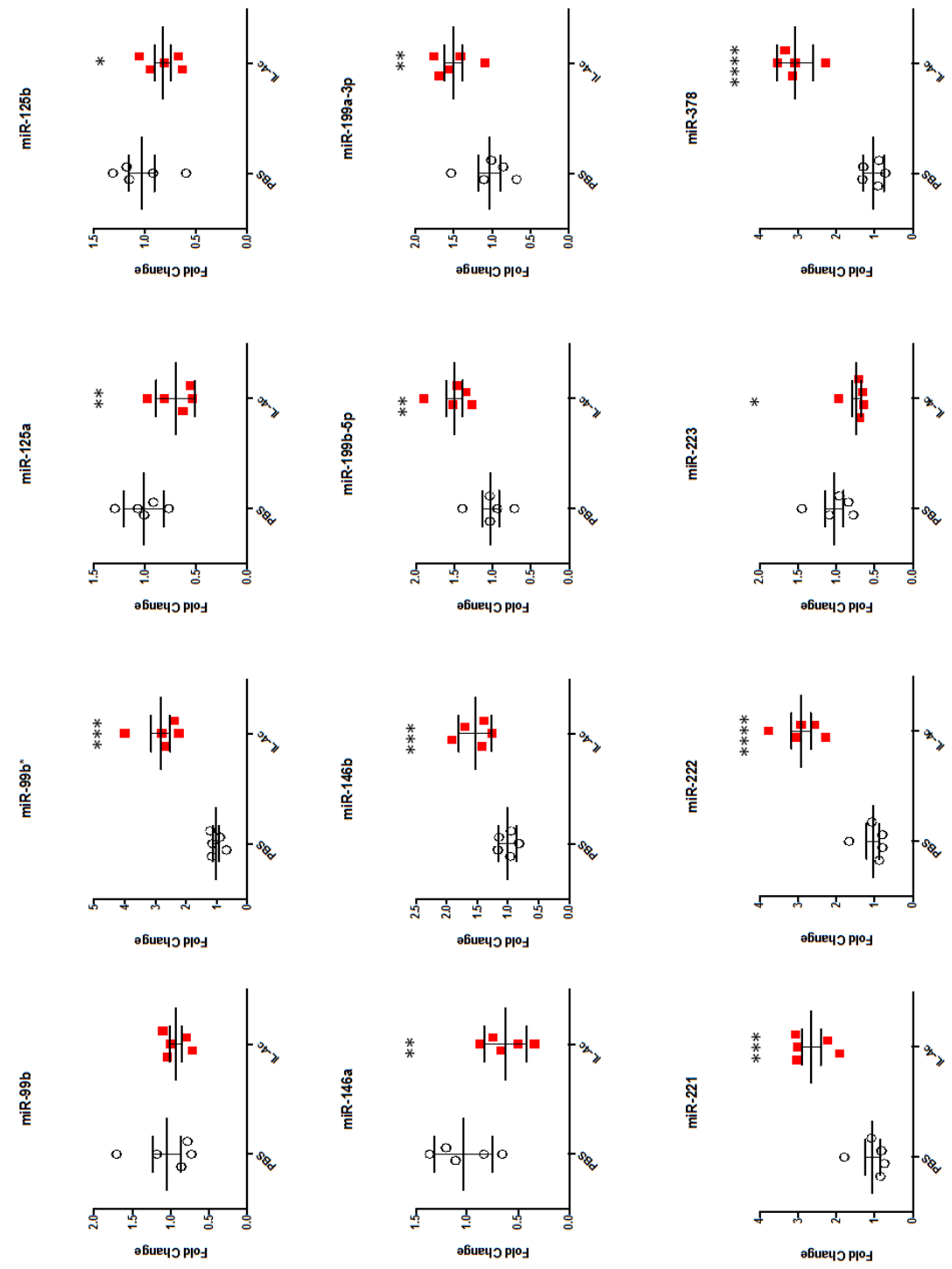
miR-125b
miR-199a-3p
miR-378
miR-125a
miR-199b-5p
miR-223
miR-99b*
miR-146b
miR-222
miR-99b
miR-146a
miR-221
Fold Change
PBS
IL-4

B.

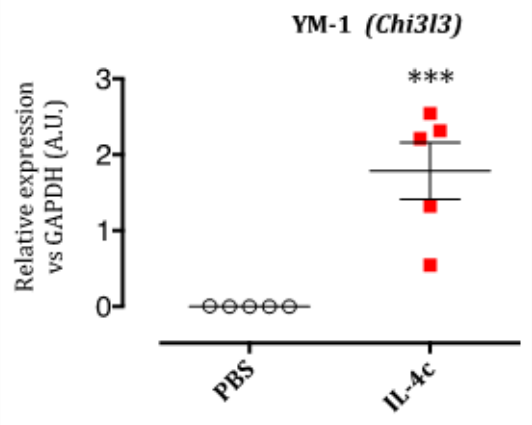

Figure 2.6 Expression profiles of the ten shortlisted microRNAs following injection of IL-4 complex in the peritoneal cavity of mice.

WT C57BL/6 mice were injected with either PBS or 5µg of IL-4 complexed with an anti IL-4 antibody intraperitoneally. Total macrophages were sorted from the peritoneal lavage based on F4/80 and CD11b expression. **A)** MicroRNAs were quantified by qRT-PCR and normalised to *RNU6b* expression. Fold changes are calculated as the ratio of values obtained from naïve mice vs. mice injected with IL-4c **B)** *Chi3l3* (YM-1) expression was quantified as a measure of alternative activation and normalised to *Gapdh* expression. Fold changes are calculated as the ratio of values from PBS treated mice versus mice injected with IL-4c. Data are presented as the mean fold change ± SEM and representative of three separate experiments (n=5). Statistical significance for differences between treated and untreated samples were determined using a two-tailed unpaired student's T-test [Mann Whitney] (* P< 0.05, ** P< 0.01, *** P< 0.001, **** P< 0.0001).

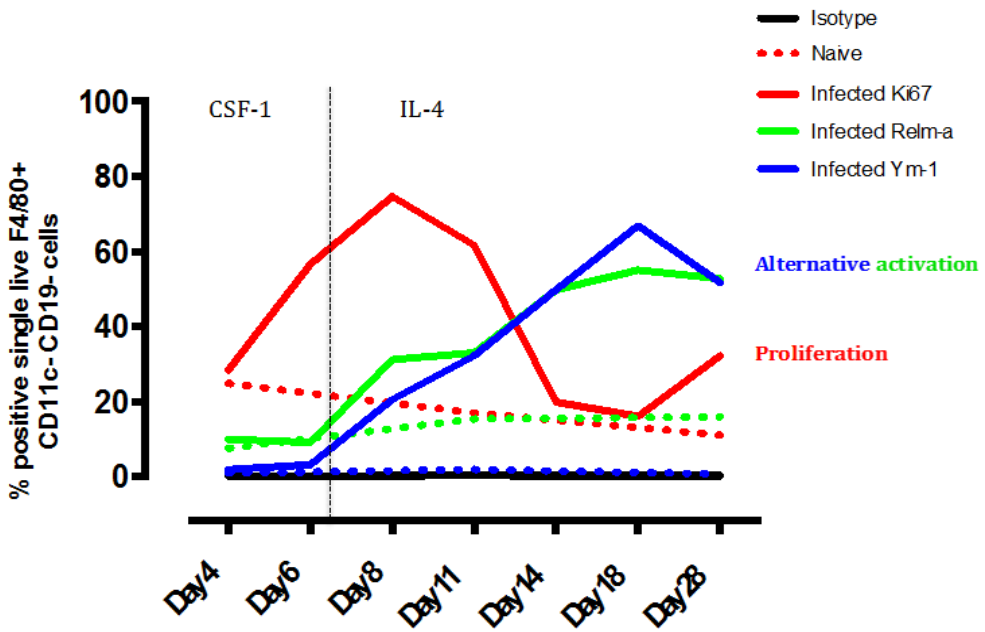

Figure 2.7 Expression kinetics of markers of alternative activation and proliferation during *L. sigmodontis* infection.

WT C57BL/6 mice were infected with infective L3 larvae subcutaneously. With the migration of larvae into the pleural cavity and progression of infection, the resident macrophage population alternatively activates as characterised by the expression of YM-1 (blue) and RELMα (green). At the same time, macrophages undergo proliferation (characterised by Ki67 expression in red), which switches from CSF-1 dependent to CSF-1 independent IL-4 driven mechanisms after day 6. While a state of alternative activation continues to be maintained throughout the infection, the rate of proliferation steadily declines to homeostatic levels at day 18. Data are presented as percentage of $Cd11b^{+}$ $F4/80^{+}$ macrophages positive for the markers described and representative of a single experiment (n=5).

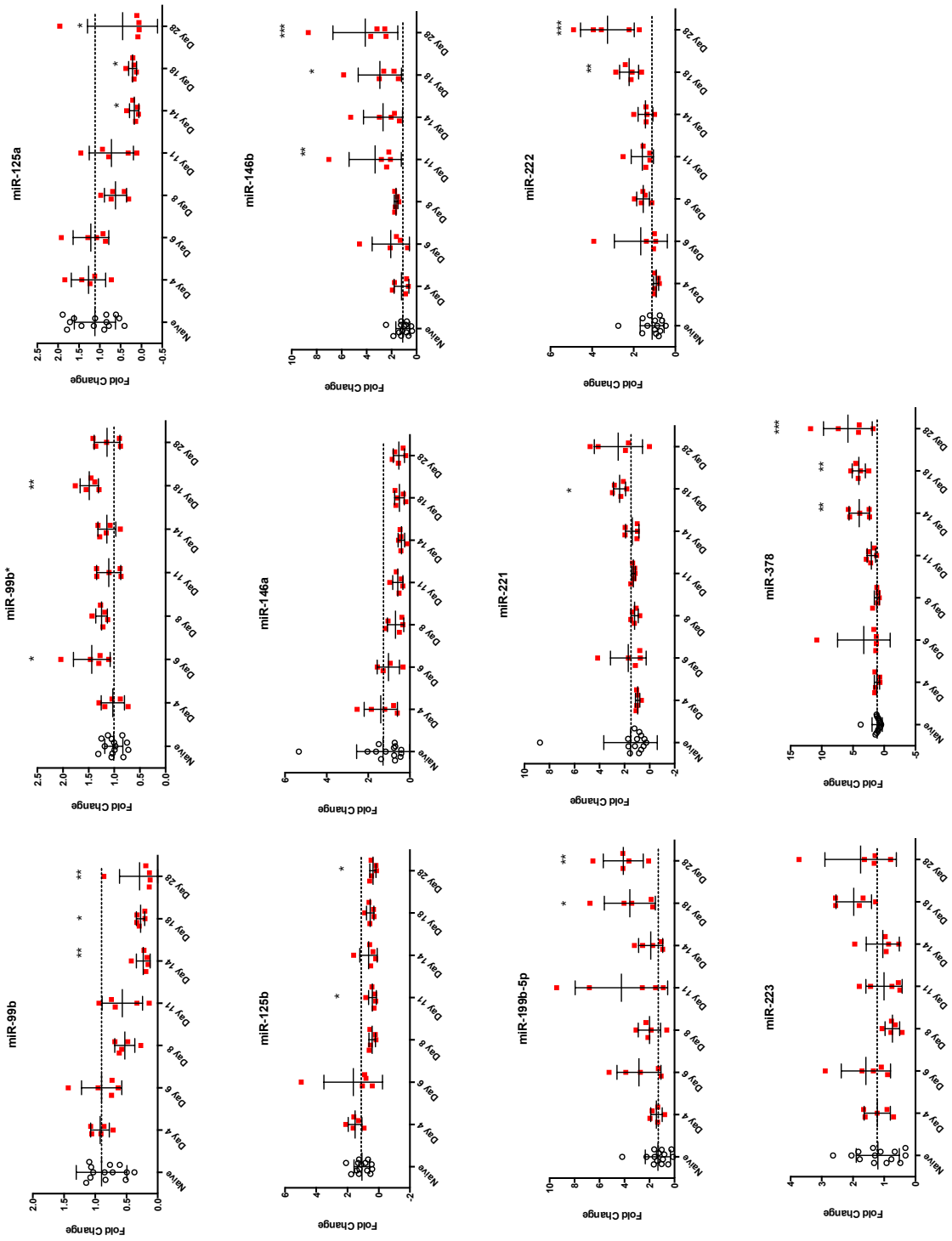
miR-125a
miR-146b
miR-222
miR-99b*
miR-146a
miR-221
miR-378
miR-99b
miR-125b
miR-199b-5p
miR-223
Fold Change
NaïVe
Day 4
Day 6
Day 8
Day 11
Day 14
Day 18
Day 28

Figure 2.8 Validation of expression profiles of selected microRNAs during *L. sigmodontis* infection.

Pleural macrophages were isolated from pleural exudate cells through adherence purification (4 hours) on days 4, 6, 8, 11, 14, 18 and 28 post infection. RNA was extracted and microRNAs quantified by qRT-PCR,. Expression was normalised to *RNU6B* and fold changes calculated in comparison to a pool of naïve animals from various time points (days 4, 11 and 18. Data are presented as the mean fold change ± SEM and representative of a single experiment (n=5). Statistical significance for differences between treated and untreated samples were determined using two-way ANOVA (* P< 0.05, ** P< 0.01, *** P< 0.001, **** P< 0.0001).

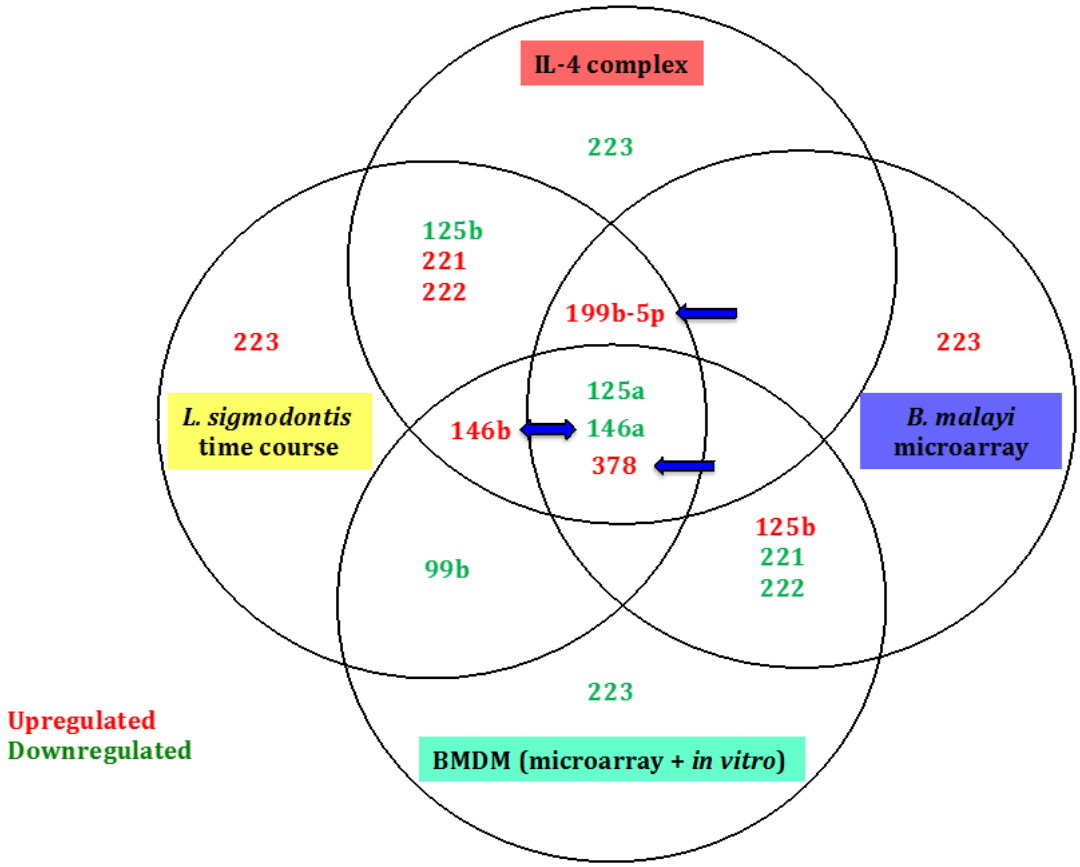

Figure 2.9 Venn diagram summary of microRNAs identified as being consistently associated with alternative activation across a range of *in vitro* and *in vivo* conditions

Chapter 3: Functional role of miR-199b-5p in the regulation of alternatively activated macrophages

SUMMARY:

Having identified the association of miR-199b-5p with alternative activation in macrophages in Chapter 2, this chapter focuses on elucidating the functional role of miR-199b-5p in the regulation of the AAMΦ phenotype. Our lab has previously shown that the expression of miR-199b-5p is IL-4Rα dependent. Interestingly, we also identified miR-199b-5p as being highly expressed in AAMΦ *in vivo* but not *in vitro*. Pathway analysis identified insulin signalling and other proliferative pathways such as PI3K/AKT as being highly targeted by miR-199b-5p. Overexpression of miR-199b-5p in RAW 264.7 cells resulted in a reduction in the rate of proliferation and a change in the levels of Insulin Receptor Substrate -1 (IRS-1), suggesting that miR-199b-5p might regulate macrophage proliferation via insulin signalling. In addition, miR-199b-5p overexpression also resulted in a decrease in secreted YM-1 and RELM-α proteins, although the effect was less profound than that on the rate of proliferation. To address whether these effects also translated *in vivo*, miR-199b-5p was injected in the peritoneal cavity of mice. Consequently, this resulted in an inflammatory influx and the disappearance of tissue resident macrophages. Subsequently, miR-199b-5p was successfully delivered to the lung and overexpressed in alternatively activated alveolar macrophages. No effect was observed on IL-4 induced proliferation, potentially due to the lack of insulin receptor and IRS-1 expression in alveolar macrophages. However, secreted levels of YM-1, characteristic of alternative activation, were significantly reduced.

3.1 Introduction

3.1.1 The miR-199 family

Genes encoding microRNAs can be intronic or exonic to annotated genes or reside in the intergenic regions in both sense and antisense orientations. The miR-199 family comprises three paralogs, namely *miR-199a-1, miR-199a-2* and *miR-199b*. All *miR-199* genes are located on separate chromosomes on strands opposite (antisense) to intronic regions of Dynamin genes, a family of microtubule binding GTPases, and are conserved across vertebrates. *MiR-199a-1* and *miR-199a-2* are located opposite to the intronic regions of Dynamin2 (*Dnm2*) and Dynamin3 (*Dnm3*) respectively whereas *miR-199b* is encoded antisense to the intronic region of *Dynamin 1 (Dnm1)* (Figure 1A). Of the miR-199 family, *miR-199a-2* is the only member known to cluster with another microRNA (*miR-214*).

Following transcription and further processing of the primary transcript, the precursor microRNAs (pre-miRNAs) derived from each *miR-199* gene give rise to two mature microRNAs – miR-199-5p and miR-199-3p. The 3' arm of all three miR-199 precursors (miR-199a-1, miR-199a-2 and miR-199b) gives rise to a mature microRNA product (miR-199-3p) that is identical in sequence and hence its origin can only be distinguished at the precursor microRNA or primary microRNA transcript levels. However, there are slight differences in the mature microRNA comprising the 5' arm. MiR-199a-1-5p and miR-199a-2-5p, which originate from *miR-199a-1* and *miR-199a-2* precursors respectively, are identical in sequence but differ from miR-199b-5p (derived from *miR-199b*) by one nucleotide. Nevertheless, the seed sequences (nucleotides 2-8 from the 5' end of the miRNA) of miR-199a-5p and miR-199b-5p are identical. Since the seed sequences are thought to be the key specificity determinants in target recognition (Bartel, 2009, Wang, 2014), these miRNAs are therefore predicted to bind to the same targets and presumably share significant overlap in function (Figure 1B).

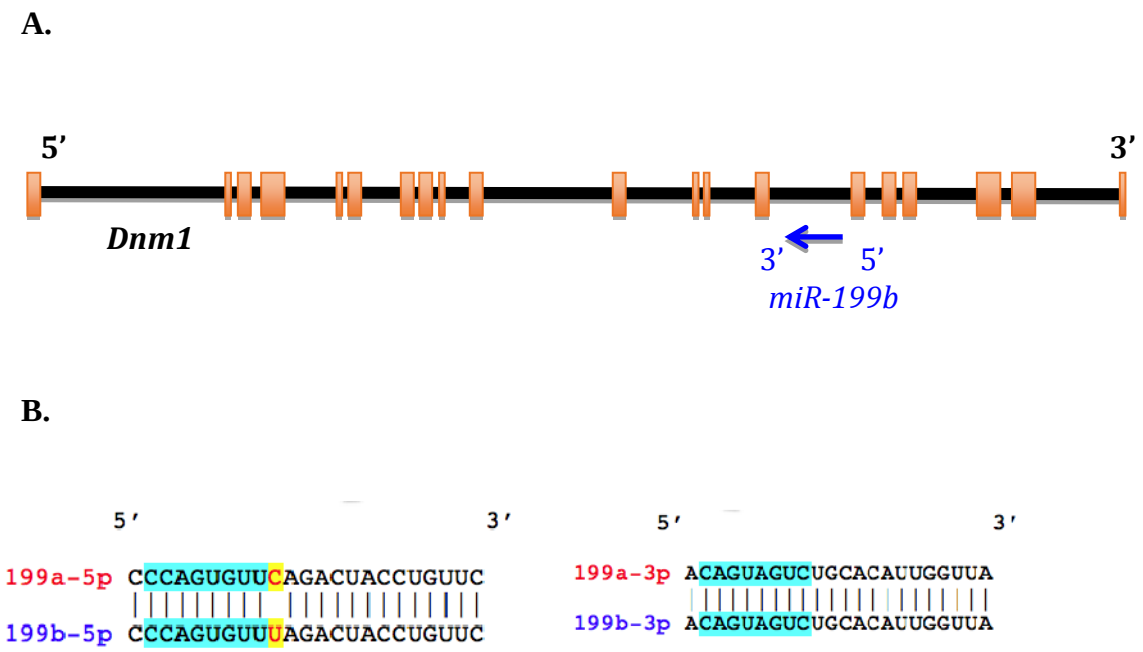

Figure 1. MiR-199b-5p is a member of the miR-199 family A) *MiR-199b* is encoded antisense to the intronic region of *Dynamin 1*. **B)** All *miR-199* genes are antisense to intronic regions of Dynamin genes on different chromosomes and give rise to highly related mature microRNA sequences. Alignment of 5' and 3' mature microRNA sequences derived from the three different miR-199 precursors suggests 100% homology in sequence of the 3' arm whereas the 5' arm differs by a single nucleotide (Identical seed regions are highlighted in blue and any differences in nucleotide sequences represented in yellow).

The chromosomal location of the miR-199 family members is distinct and thus, also their transcriptional regulation. Previous studies have suggested that STAT3 is involved in the regulation of *miR-199a*-1 (Haghikia et al., 2011), whilst *miR-199a-2* along with its clustered partner *miR-214*, are regulated by the transcription factor Twist-1 during development (Lee et al., 2009). On the other hand, the expression of miR-199b-5p has previously been associated with the transcription factors GATA-1 and NF-E2 (Rosas et al., 2014). Hence, despite their sequence similarity and overlap in function, the induction of each of the miR-199 family members appears to be

distinct. Both of the mature microRNAs originating from *miR-199a-1* and *miR-199a-2* (miR-199a-5p and miR-199a-3p) are fairly well characterised with implicated roles in several different pathways. *MiR-199b* on the other hand is less described in the literature. Expression of the miR-199 family members has been strongly linked with several different cancers (Chen et al., 2008, Song et al., 2010, Hou et al., 2011, He et al., 2014b, Chen et al., 2014a). MiR-199a has also been associated with the progression of liver fibrosis (Murakami et al., 2011, Hoy et al., 2014). MiR-199b specifically has been implicated as a therapeutic target in cardiac failure (da Costa Martins et al., 2010), as a regulator of the phenotypic switch during vascular cell differentiation (Chen et al., 2015) and is known to be involved in the control of receptor-mediated endocytosis (Aranda et al., 2015). In the context of macrophages, miR-199a-5p and miR-199a-3p were found to be dysregulated in RAW 264.7 macrophages upon silencing of CD14 that is involved in LPS induced proinflammatory cytokine release (Du et al., 2014). Furthermore, miR-199a-5p is involved in the inhibition of monocyte/macrophage differentiation (Lin et al., 2014). However, a role for miR-199b-5p in the regulation of macrophage responses is yet to be determined.

3.1.2 IL-4Rα dependent expression of miR-199b-5p

Ruckerl *et al.* (2012) previously showed the differential expression of miR-199b-5p in alternatively activated macrophages during *B. malayi* implant in the peritoneal cavity of mice. *B. malayi* implant results in a strong T_H2 response leading to the accumulation of alternatively activated macrophages. These *B. malayi* elicited AAMΦ were compared with macrophages isolated from animals also implanted with *B. malayi*, but lacking the IL-4 receptor (IL-4Rα) in order to distinguish IL-4Rα dependent microRNA expression. Mice lacking the IL-4Rα fail to produce AAMΦ. Microarray analysis to compare microRNA expression in these macrophage populations identified miR-199b-5p as significantly upregulated in the AAMΦ elicited in response to *B. malayi* implant. Additionally this study also examined the expression of miR-199b-5p in thioglycollate-elicited macrophages

(Thio MΦ) isolated from WT and IL-4Rα$^{-/-}$ animals to validate the findings from the microarray results. qRT-PCR analysis of alternatively activated Thio MΦ confirmed that the expression of mir-199b-5p is abrogated in mice deficient in the IL-4Rα indicating that macrophage expression of miR-199b-5p is IL-4Rα dependent. However, no significant change was observed in the expression of miR-199b-5p upon stimulation of Thio MΦ with IL-4 for 16 hours *in vitro* suggesting that the increase in expression of miR-199b-5p *in vivo* is not a direct effect of IL-4Rα signalling and possibly the induction of this miRNA involves a secondary factor (Ruckerl et al., 2012).

3.1.3 Aims of chapter

As described in Chapter 2, miR-199b-5p was validated as being differentially expressed in macrophages under a range of alternative activation conditions. However, the role of miR-199b-5p in regulating AAMΦ and their responses is still unknown. Thus, the focus of this chapter is aimed at determining the contribution of miR-199b-5p in the regulation of the AAMΦ phenotype. To this end, previously generated mRNA array data from the lab and algorithmic prediction software were utilised to identify potential targets of miR-199b-5p. The biological functions and signalling pathways associated with these potential targets were deduced using pathway analysis software. MiR-199b-5p was then synthetically overexpressed both *in vitro* and *in vivo* followed by target validation to provide further insight into the contribution of miR-199b-5p to the regulation of the AAMΦ phenotype.

3.2 Results

3.2.1 MiR-199b-5p is expressed highly in AAMΦ *in vivo* but not *in vitro*

In the study by D. Ruckerl *et al.* (2012), expression of miR-199b-5p was initially identified as being IL-4Rα dependent and associated with alternative activation, as described above. However, the levels of miR-199b-5p were found to be highly regulated only in AAMΦ isolated from the *B. malayi* implant *in vivo* but not in thioglycollate-elicited macrophages stimulated with IL-4 for 16 hours *in vitro*. We have already shown in Chapter 2 that the differential expression of miR-199b-5p is not restricted to *B. malayi* implant but was also seen during infection of mice with the nematode *L. sigmodontis* (Figure 2.8, Chapter 2). Moreover, miR-199b-5p was also upregulated in response to IL-4 complex injection in the peritoneal cavity (Figure 2.6, Chapter 2). All of these results suggested that miR-199b-5p is highly regulated *in vivo* under diverse conditions of alternative activation. In contrast, the expression of miR-199b-5p was not altered in bone marrow derived macrophages (BMDM) stimulated with IL-4 and IL-13 *in vitro* for up to 48 hours (Figure 3.1). This is consistent with the finding of Ruckerl *et al.* (2012) that miR-199b-5p is not regulated in thioglycollate-elicited macrophages stimulated with IL-4 *in vitro*. In fact, based on a C_t value >35 as measured by qRT-PCR, miR-199b-5p was expected to be present only at very low levels in BMDM (reviewed in Chapter 2). Additionally, no changes were observed in the expression of miR-199b-5p in RAW 264.7 cells in response to stimulation with IL-4 and IL-13 for 48 hours (Figure 3.1). Analysis of copy number determined by qRT-PCR using a synthetic standard revealed that miR-199b-5p was expressed at significantly lower levels *in vitro* than *in vivo* as shown in Figure 3.1. MiR-199b-5p was only expressed at 5-10 x 10^3 copies per ng of RNA in BMDM and RAW 264.7 cells and these numbers remained unchanged upon stimulation with IL-4/IL-13. On the other hand, levels of miR-199b-5p reached 100-200 x 10^3 copies/ng RNA in response to IL-4c delivery or during *L. sigmodontis* infection. In summary, though miR-199b-5p expression was highly

regulated *in vivo* in a T_H2 environment, this miRNA does not appear to be regulated in alternatively activated BMDMs and RAW 264.7 cells stimulated with IL-4/13 *in vitro*. These results are consistent with the hypothesis that the regulation of miR-199b-5p is not a direct effect of IL-4Rα signalling and that the involvement of a secondary extrinsic factor is necessary for the induction of miR-199b-5p expression.

3.2.2 Prediction of a putative functional role of miR-199b-5p in AAMΦ

A key objective of this study was to understand the contribution of miR-199b-5p in the regulation, maintenance and proliferation of AAMΦ. To this end, we utilised target prediction to elucidate the putative functional significance of miR-199b-5p in AAMΦ. As microRNAs have gained importance as regulators of gene expression, several approaches have been developed for identifying their targets. One of the most extensively used techniques involves prediction of targets using algorithm-based software such as TargetScan (www.targetscan.org). TargetScan relies on the identification of potential microRNA targets based on a minimum 7 nucleotide consecutive match/base pairing between the seed site (2-7nt) found at the 5' end of a microRNA and the 3'UTR of the target mRNA. In addition to the seed region, TargetScan extends the analysis to 21-23 nucleotide long fragments representing true interactions. Based on this length of base pairing between the microRNA and target mRNA, the occurrence of an evolutionarily conserved adenine at the first position of the mRNA target site that is thought to act as an anchor for RISC, is also considered. In some cases, the AU content 30nt upstream or downstream of the predicted site may also be taken into account (Witkos et al., 2011). Since miR-199b-5p is an isoform of miR-199a-5p with an identical seed sequence, TargetScan does not differentiate between the two mature microRNAs and they are thus predicted to have the same set of targets. Based on these predicted canonical interactions by TargetScan, a list of 3,267 predicted targets of miR-199a/b-5p irrespective of site conservation amongst species was generated. Of note, a brief pathway analysis of

these predicted targets (data not shown) revealed that the majority of these predicted targets are associated with known proliferative pathways.

As described in Chapter 2, macrophages in the pleural cavity proliferated and alternatively activated during infection with *L. sigmodontis* (Chapter 2, Figure 2.8). Since a significant proportion of the predicted miR-199b-5p targets appeared to be associated with proliferative pathways, the expression of miR-199b-5p during the course of this infection was correlated with the expression of Ki67, a marker of proliferation (Figure 3.2). Interestingly while proliferation started to steadily decline with the progression of infection from day 8 onward, expression of miR-199b-5p also increased. In the introductory chapter, we discussed the dynamics of IL-4 dependent and independent (CSF-1 driven) macrophage proliferation during *L. sigmodontis* infection as shown by Jenkins *et al* (2011). Interestingly, as shown in Figure 3.2, the upregulation of miR-199b-5p expression appeared just as proliferation switches from a CFS-1 dependent phase to IL-4 driven proliferation between day 8 and day 11 with the progression of infection (Jenkins et al., 2011, Jenkins et al., 2013). Furthermore, this was also consistent with the earlier finding that the expression of miR-199b-5p is IL-4Rα dependent (Ruckerl et al., 2012).

The inverse relationship between IL-4 dependent proliferation and miR-199b-5p expression in the *L. sigmodontis* time course led to the hypothesis that IL-4Rα dependent expression of miR-199b-5p acts as a regulator of IL-4 induced proliferation in a negative feedback loop. This was supported by the dependency of miR-199b-5p expression on IL-4Rα signalling and the association of the predicted targets of miR-199b-5p with proliferative pathways. Since we have shown here that miR-199b-5p expression is enhanced in response to IL4/IL-13 only *in vivo* and not *in vitro*, the presence of a secondary extrinsic factor or cell type may also be needed for this negative regulation.

3.2.3 MiR-199b-5p regulates proliferation in RAW 264.7 cells

To address the question of whether or not miR-199b-5p regulates proliferation in macrophages, the effect of overexpression of miR-199b-5p on proliferation was studied in RAW264.7 cells. Significant macrophage proliferation cannot be achieved with primary macrophages in response to IL-4 or IL-13 *in vitro*. Thus, RAW 264.7 cells were chosen based on their capacity to constantly proliferate making them a useful tool to assess the role of miR-199b-5p in regulating macrophage proliferation.

Cells were prestained with CFDA-SE (carboxy fluorescein diacetate - succinimidyl ester); a dye that passively diffuses into cells and forms fluorescent conjugates with intracellular amines upon cleavage by non-specific esterases (Figure 3.3). The dye-protein adducts are retained by the cell throughout division and the fluorescence intensity is reduced by half with each cell division. Following staining with CFDA-SE, cells were transfected with synthetic oligos that are double-stranded RNAs which mimic mature endogenous microRNAs in the cell. Cells were transfected with either miR-199b-5p or the relevant controls. The negative controls were a *C.elegans* microRNA and an siRNA that fails to incorporate into the RISC complex (termed RISC free here on). The positive control was miR-378, which has already been shown to negatively regulate proliferation in RAW 264.7 cells through suppression of AKT-1(Ruckerl et al., 2012).

As mentioned previously, miR-199b-5p is a member of the miR-199 family that is differentially expressed in AAMΦ. Since miR-199a-5p and miR-199b-5p share the same seed sequence and are predicted to bind the same targets, cells were also transfected with miR-199a-5p to study the functional overlap between these microRNAs. As discussed earlier in this chapter, miR-199-3p arises from the same precursor microRNAs as miR-199a/b-5p but with a distinct seed region and hence, a separate repertoire of predicted targets. However, it is known that about 1/3 of mature microRNAs originating from the same precursor are involved in regulation of the same biological pathways (Bartel, 2004). Moreover, miR-199-3p is known to regulate proliferation of other cell types (Shatseva et al., 2011). Thus, cells were also

transfected with miR-199-3p to investigate whether it also regulates proliferation of macrophages.

Cells from each treatment group were harvested at 24 hours and 48 hours post transfection and analysed for fluorescence as a measure of cell division by flow cytometry. 4 hours prior to each harvest, Alamar blue was added to each well and the supernatant harvested just before cells were prepared for FACS analysis. Alamar blue is a cell viability indicator that utilises the metabolic activity of living cells to convert resazurin to a fluorescent molecule, resorufin. Viable cells continuously convert resazurin to resorufin, thereby generating a quantitative measure of cell viability and cytotoxicity (and by inference, replication capacity). In this experiment, cell viability was used as an indirect secondary measure of cell expansion. RNA was also isolated at each time point to measure transfection efficiency.

Analysis of CFSE intensity through flow cytometry revealed that cells transfected with miR-199a-5p, miR-199b-5p and miR-378 showed a significant reduction in the loss of CFSE intensity over time in comparison to cells transfected with miR-199a-3p, RISC free siRNA and the *C. elegans* microRNA (Figure 3.4A). While only 30% of cells transfected with miR-199a-3p, RISC free siRNA and the *C. elegans* microRNAs stained positive for CFSE, ~60-70% of cells transfected with miR-199a-5p, miR-199b-5p and miR-378 still contained CFSE. Similarly, cells transfected with miR-199a/b-5p were significantly brighter (~1.5 fold) in terms of the median fluorescence intensity (Figure 3.4 C). In agreement with this, the rate of conversion of alamar blue was also significantly reduced in cells transfected with miR-199a/b-5p and miR-378, with no change in the conversion rate over a 24 hour period (Figure 3.4 B). In contrast, miR-199a-3p had no significant effect on the rate of alamar blue conversion as indicated by constant breakdown of the reagent and thus, increased fluorescence over time suggesting that the negative regulation of cell expansion is specific to miR-199a/b-5p. These results indicate that miR-199b-5p negatively regulates proliferation in RAW 264.7 cells and also confirms the overlap of function between miR-199a-5p and miR-199b-5p.

3.2.4 MiR-199b-5p also negatively impacts alternative activation in RAW 264.7 cells

Individual microRNAs have the capacity to directly or indirectly regulate the expression levels of hundreds of genes (Krek et al., 2005, Lim et al., 2005, Jackson and Standart, 2007, Fabian et al., 2010).

Although a brief literature search and pathway analysis revealed that predicted targets of miR-199b-5p identified through TargetScan were mostly associated with proliferation, regulation of other pathways is possible and even likely. The main goal of our study is to identify the functional role of microRNAs in the regulation, maintenance and proliferation of AAMΦ. Hence, the impact of miR-199b-5p overexpression on alternative activation was also examined in RAW 264.7 cells. The ability of RAW 264.7 cells to alternatively activate has previously been discussed in Chapter 2. RAW 264.7 cells were transfected under identical conditions to those described in the previous experiment above, however cells in this case were harvested following stimulation with 20ng/ml of IL-4 and IL-13 (Figure 3.5A). Cells were also transfected with miR-199a-5p and miR-199-3p for reasons described previously. MiR-378 was also included in this experiment because it has been shown to target AKT-1, which negatively affects levels of RELM-α, a marker of alternative activation (Ruckerl et al., 2012).

Supernatants were harvested 24 hours post stimulation with IL-4 and IL-13 and subject to ELISAs for YM-1 and RELM-α, markers characteristic of alternative activation. Analysis of YM-1 levels revealed a reduction in secreted protein concentration in cells transfected with members of the miR-199 family and miR-378 compared to cells transfected with either lipid only or cells that received the negative controls, RISC-free siRNA and *C.elegans* microRNA (Figure 3.5B). Among the miR-199 family, cells transfected with miR-199-3p produced essentially no YM-1 compared to miR-199a-5p and miR-199b-5p, which displayed a comparable 50% reduction in protein levels. A similar trend was observed for levels of RELM-α, although it is worth mentioning that RAW 264.7 cells do not secrete significant amounts of RELM-α as reflected in Figure 3.5B. Levels of RELM-α were

significantly reduced in cells transfected with miR-199a-5p, miR-199b-5p and miR-199-3p when compared to RISC free, lipid only and *C. elegans* controls. As predicted, considerable suppression of RELM-α was also observed in cells transfected with the positive control miR-378. These results indicate that miR-199b-5p not only affects proliferation, but also alternative activation in RAW 264.7 cells. Additionally, although miR-199-3p did not affect proliferation of RAW 264.7 cells, it appears to have a substantial effect on alternative activation.

3.2.5 Identification and functional analysis of predicted targets of miR-199b-5p

We have shown that miR-199b-5p has the ability to reduce both proliferation and alternative activation in RAW 264.7 cells. However, RAW 264.7 cells do not secrete copious amounts of YM-1 and RELM-α as shown in Figure 3.5B. Given that miR-199b-5p had a considerable effect on RAW 264.7 cell expansion, we decided to focus on its role in regulating macrophage proliferation. To gain insight into the biology of genes regulated by miR-199b-5p leading to this effect, we sought to identify pathways targeted by this microRNA. As mentioned previously, we initially identified 3,267 predicted targets of miR-199b-5p using the target prediction program TargetScan. These putative targets were identified on the basis of predicted direct binding sites for miR-199b-5p in the 3'UTR of target mRNAs. To help narrow down this number and to select the most promising targets of miR-199b-5p in the context of proliferation, we also utilised additional mRNA array data previously generated in our lab by Graham Thomas. This mRNA array data was generated using MΦ from an *L. sigmodontis* infection time course. Graham Thomas used a generalised linear modelling approach to identify and rank genes that change either positively or negatively in relation to Ki67 expression over the course of infection. In this study, this list of genes was then overlapped with the list of predicted targets of miR-199b-5p to generate a list of 2,440 genes (Figure 3.6). The primary aim of generating this list was to try and tease apart genes and pathways targeted by miR-199b-5p that ultimately result in an effect on macrophage proliferation. To achieve

this, the Ingenuity Pathway Analysis (IPA) program, a web based software, was utilised (http://www.ingenuity.com).

IPA classifies genes based on existing literature and known functions; related sets of genes are then grouped into cellular pathways or biological functions. However, these classifications can be based on both direct and indirect interactions. Given the large number of genes presented in our list of putative targets, the indirect relationships identified by this software posed a possible hindrance in terms of low stringency in selection of pathways targeted by miR-199b-5p. Hence, out of the 2,440 genes identified, we selected for pathway analysis only the top 300 significant genes that change positively in relation to Ki67 and based on P-values obtained from the mRNA array data (P value < 0.005). The significance of the association between these predicted miR-199b-5p targets and pathways identified by IPA were assessed based on two separate conditions:

1. A P-value (right-tailed Fisher's exact test) demonstrating the likelihood that the assembly of genes in a particular dataset within a pathway could be interpreted by random chance alone.
2. A ratio of the number of genes (from our 300 selected genes) that are involved in a given pathway to that of the total number of genes known to be associated with that particular pathway.

Based on the above measures and analysis, the IPA library of canonical pathways identified 11 significantly enriched pathways associated with the 300 genes predicted to be miR-199b-5p targets (P value < 0.001). These included Insulin – like growth factor 1 (IGF-1) signalling, PPARα/RXRα activation, insulin receptor signalling, Type II diabetes mellitus signalling, PI3K/AKT signalling, phosphoinositide biosynthesis and NF- κB signalling among others suggesting that miR-199b-5p may be involved in the modulation of several different pathways (Table 3.1). Various cancer related pathways such as molecular mechanisms of cancer and role of tissue factors in cancer were also presented in the results of this analysis.

To elucidate the role of miR-199b-5p in regulating macrophage proliferation, an examination of existing literature was conducted to determine whether any of the pathways predicted by IPA as being regulated by miR-199b-5p are known to be important in proliferation. Of the 11 pathways identified using IPA, IGF-1 signalling was predicted to be the most significantly regulated by miR-199b-5p (Table 3.1). IGF-1 signalling is crucial for normal embryonic growth and development in mice and this is reflected in the fact that null mutants for the IGF-1 receptor gene (*Igf1r*) die invariably at birth with a severe growth defect, reaching only 45% of the normal size (Liu et al., 1993). Similarly, mice with disrupted *Igf1* gene exhibit a growth deficiency (60% of normal birth weight) and depending on the genetic background these Igf-$1^{-/-}$ dwarfs die shortly after birth (Liu et al., 1993).

IGF-1 signalling has a well-established role in the regulation of proliferation of various cell types including neural progenitor-like and other progenitor cells (Choi et al., 2008, Huat et al., 2014), myoblasts and myocytes (Engert et al., 1996, Yu et al., 2015), skeletal muscle (Schiaffino and Mammucari, 2011) and sertoli cells (Pitetti et al., 2013). Additionally IGF-1 signalling and specifically IGF1R has been implicated in cancer biology, with a reduction in levels of this receptor leading to apoptosis of cancer cells making it an attractive therapeutic target (Yu and Rohan, 2000, Baserga et al., 2003, Werner and Bruchim, 2009, Davison et al., 2011). IGF-1 signalling has also been shown to be essential for proliferation of human fibroblasts and hepatic stellate cells (Sell et al., 1993, Svegliati-Baroni et al., 1999). More importantly, IGF-1 signalling is known to be involved in the proliferation and differentiation of murine BMDM precursors (Long et al., 1998) and has been shown to affect the proliferation rate and morphology of RAW 264.7 cells (Smith et al., 2000).

With the known association of IGF-1 signalling with cancer biology (Baserga et al., 2003, Denduluri et al., 2015), it was interesting to observe that the second most highly regulated pathway predicted to be targeted by miR-199b-5p was “molecular mechanisms of cancer” along with “role of tissue factors in cancer” also featuring in the list of the 11 significant pathways identified (Table 3.1). Of additional interest was insulin receptor signalling, which was also present in this list and predicted to be regulated by miR-199b-5p. The reason being that insulin receptor (IR) and IGF1R

are highly related receptor tyrosine kinases that are capable of forming heterodimers (Treadway et al., 1989, De Meyts and Whittaker, 2002, Cabail et al., 2015). Depending on the IR isoform involved, these hybrid receptors can bind both IGF-1 and insulin (Pandini et al., 2002).

Like IGF1 signalling, IR signalling also plays a role in the proliferation of various cell types (Shawl et al., 2009, Amaya et al., 2014, Escribano et al., 2015). Similar to the IGF1R, IR is also involved in cancer progression and downregulation of IR also results in inhibition of cancer cell proliferation and metastasis (Zhang et al., 2010c, Belfiore and Malaguarnera, 2011). This partial overlap in function may be explained by the well-established roles of the downstream kinases AKT and MEK, through which both the IR and IGF1R function to regulate gene expression as shown in Figure 3.7 (Adams et al., 2004, Cohen, 2006, Taniguchi et al., 2006, Laviola et al., 2007, Siddle, 2011). Activation of these kinases is dependent on phosphorylation of insulin receptor substrates 1 and 2 (IRS-1 and IRS-2), leading to the activation of PI3K and the G-protein Ras respectively (Siddle, 2011). In line with this, IPA analysis also revealed PI3K/AKT signalling as being highly regulated by miR-199b-5p (Table 3.1).

The primary aim of this study is to elucidate the functional role of miR-199b-5p in the proliferation of AAMΦ and the cytokines IL-4 and IL-13 signal through a shared IL-4Rα chain resulting in proliferation and alternative activation of macrophages (Gordon, 2003, Jenkins et al., 2011, Jenkins et al., 2013). IL-4 has previously been shown to directly phosphorylate insulin receptor substrates (IRS-1 and 2) that are downstream of both IR and IGF1R signalling (Wang et al., 1993a, Wang et al., 1993b, Wang et al., 1995, Zamorano et al., 1996, Nelms et al., 1999). A schematic representation of the association of IR, IGFR1 and IL-4 signalling is depicted in Figure 3.7. Given the strong association of the insulin/IGF-1 signalling axis with proliferation and the association of IL-4 with elements common to these pathways, we decided to focus on the regulation of these shared pathways by miR-199b-5p.

3.2.5.1 Validation of predicted targets of miR-199b-5p in the insulin/IGF-1 signalling axis

Having identified insulin/IGF-1 signalling as a pathway potentially regulated by miR-199b-5p that could link to IL-4 induced proliferation, we next sought to identify genes within this pathway that were putative miR-199b-5p targets that could result in the miR-199b-5p directed inhibition of macrophage proliferation. All the predicted targets of miR-199b-5p that form part of this signalling cascade have been depicted in Figure 3.7. The pathway is predicted to be targeted by miR-199b-5p at multiple levels, from the receptors found on the extracellular membrane through to nuclear cell cycle genes. Both the IR (*Insr*) and IGF-1R (*Igf1r*) are putative targets along with IRS-1 (*Irs1*), which forms the core of this signalling cascade. Whilst there are 3 predicted binding sites for miR-199b-5p in the 3'UTR of the *Insr*, both *Igf1r* and *Irs1* have only one predicted site each (based on prediction by TargetScan). Downstream of these molecules, *Pik3r1* and *Pik3cd*, which are the regulatory and catalytic subunits of PI3K respectively, and the kinase AKT (*Akt3*) are also predicted targets of miR-199b-5p with a single binding site in their 3'UTRs. Several other genes that are downstream substrates and involved in the cell cycle were also identified as potential targets. However, since we were interested specifically in macrophage proliferation, we decided to focus on validating the receptors (*Insr* and *Igf1r*), which are known to be expressed on macrophages and their substrate *Irs1* as miR-199b-5p targets. Additionally, downstream molecules in the PI3K/AKT signalling cascade are well established as key components of other canonical pathways and may not be specific to macrophages and were, therefore, not considered for initial validation.

In order to determine whether miR-199b-5p regulates macrophage proliferation by targeting the insulin/IGF-1 signalling cascades, the effect of mir-199b-5p overexpression on the expression levels of its predicted targets (shown in Figure 3.7) was studied. Similar to the experiment described above, RAW 264.7 cells were either left untransfected or transfected with members of the miR-199 family and the appropriate controls, namely miR-378 (positive control), RISC free and a *C. elegans* microRNA (negative controls). Cells were harvested 48 hours post transfection and RNA extracted. The mRNA transcripts of interest were quantified by qRT-PCR. Cell

lysates were also harvested for protein quantification. As can be seen in Figure 3.8A, no effect was observed on the mRNA levels of *Insr* and *Igf1r* following transfection with miR-199b-5p. Unexpectedly, the mRNA levels of *Irs1* were significantly enhanced. This was also observed in cells transfected with miR-199a-5p, which shares the same seed sequence as miR-199b-5p, but not in any of the other conditions. To confirm that this increase in *Irs1* expression was not an artefact of the experiment, levels of *Akt1*, a known target of miR-378 (Ruckerl et al., 2012) were also quantified. As expected, a considerable reduction in *Akt1* expression was observed in cells transfected with miR-378 while expression remained unchanged in cells transfected with all the other mimics (Figure 3.8B).

To investigate whether this increase in expression of the *Irs1* mRNA was also reflected at the protein level, lysates were subjected to Western blot analysis. As is evident in Figure 3.9, IRS1 was not highly expressed in RAW 264.7 cells. However, upon transfection with miR-199a/b-5p, these levels were enhanced, confirming our earlier finding that miR-199b-5p increased *Irs1* expression. As mentioned previously, IL-4 can positively affect levels of IRS1. Moreover, our main goal is to identify the function of miR-199b-5p in the regulation of AAMΦ. During alternative activation, several different factors and signalling cascades downstream of the IL-4Rα can be activated simultaneously. Since IL-4 is not the sole regulator of IRS expression, its levels may be altered by factors other than IL-4. Thus, we also stimulated RAW 264.7 cells with IL-4 following transfection with microRNA mimics to study whether these changes in IRS-1 levels by miR-199b-5p also hold true under conditions of alternative activation. As expected, levels of IRS1 were elevated following stimulation with IL-4 as shown in Figure 3.9. Furthermore, expression of IRS1 was regulated by miR-199a/b-5p in AAMΦ with an increase in protein following transfection (Figure 3.9). This increase was not observed in cells transfected with the other microRNA mimics suggesting that regulation of IRS1 was restricted to miR-199a/b-5p.

The increase in levels of IRS1 was contrary to the known function of microRNAs, which is to regulate gene expression through destabilisation and/or degradation of target mRNA (Bartel, 2009, Guo et al., 2010, Eichhorn et al., 2014). Hence, it was

possible that the reduction in macrophage proliferation may not be IRS-1 mediated. Thus, we also chose to validate other predicted targets of miR-199b-5p downstream of IRS1 that may be downregulated resulting in decreased proliferation. Levels of *Pi3kr1, Pi3kcd, Akt3* and other genes involved in cell cycle regulation including *E2f2, Cdc6, Rbl1, Tk1, Ncapg2, Ccne1* and *Tab1* were quantified (Figure 3.10). Although no significant changes were observed in the expression levels of any of these genes following transfection with miR-199b-5p, it is important to note that microRNAs impose subtle effects and as such it may be difficult to discern these subtle differences that may combinatorially influence proliferation.

3.2.6 *In vivo* delivery of miR-199b-5p

3.2.6.1 Delivery of miR-199b-5p to the peritoneal cavity of mice

We have already shown that miR-199b-5p reduces the rate of proliferation in RAW 264.7 cells. While studies to validate the targets of miR-199b-5p *in vitro* were underway, we attempted to deliver a synthetic mimic of miR-199b-5p *in vivo* to further validate its role in regulating macrophage proliferation. This experiment had 4 separate aims: 1) To establish the conditions for microRNA delivery *in vivo*, 2) To validate that the delivered microRNAs are functional, 3) To investigate whether macrophages were the primary cell type to be transfected and 4) To determine whether miR-199b-5p affected steady state CSF-1 derived proliferation in macrophages. To do this, we utilised microRNA mimics complexed to jetPEI. JetPEI is a lipid-based polymer that forms stable cationic complexes with the mature mimic microRNA, thus facilitating delivery. 20µg of microRNA was complexed to jetPEI (N:P ratio = 6) in 5% glucose and injected intraperitoneally. For efficient transfection of these cationic complexes, the ionic balance within lipid /nucleic acid complexes is crucial. For effective cell entry, these complexes should be cationic. The N:P ratio is a measure of the ionic balance within the complexes and is defined as the number of nitrogen residues of the jetPEI lipid per nucleic acid phosphate. The conditions used in this experiment were based on unpublished transfection data from our lab along with manufacturer suggestions of N:P ratios. Control animals received 5% glucose

only whereas other groups of mice received either miR-199b-5p or a *C. elegans* microRNA as negative control (3.11A). To examine whether the delivered microRNA complexes were functional, an additional group of mice received a microRNA that binds to the 3'UTR of GAPDH resulting in reduction of GAPDH expression (termed siRNA GAPDH here on). Since one of the aims of this experiment was to determine the effect of miR-199b-5p on steady state CSF-1 driven proliferation, animals were injected with bromodeoxyuridine (BrdU) 3 hours prior to culling. BrdU is a thymidine analogue that gets incorporated into newly synthesised DNA and is thus a measure of active proliferation. Animals were culled 48 hours post microRNA delivery and peritoneal exudate cells (PEC) were collected via washing of the peritoneal cavity. Supernatants were collected for ELISAs. PEC cells were divided for FACS analysis and RNA extraction for qRT-PCR. One of the experimental aims was to investigate whether macrophages were the primary cell type to be transfected. To do this, PEC cells were adherence purified to isolate macrophages and the washes collected to harvest other cell types. qRT-PCR analysis revealed that miR-199b-5p and other microRNAs can successfully be delivered *in vivo* (Figure 3.11B). Levels of miR-199b-5p were significantly increased (nearly 3000 fold) in peritoneal macrophages 48 hours post delivery. However, it appears that macrophages may not be the primary cell type that is transfected as other cells in the PEC washes also showed similar increased levels of miR-199b-5p (Figure 3.11B). These other cell types may include other phagocytic cells such as dendritic cells and neutrophils. However, the adherence purification is relatively crude and the washes may still contain macrophages. Similarly, quantification of the *C. elegans* microRNA revealed a significant increase in its expression in the relevant group of mice (Figure 3.11B). Analysis of qRT-PCR results also demonstrated that the microRNAs delivered are indeed functional as represented by the significant reduction in GAPDH expression in the group of mice that received siRNA GAPDH (Figure 3.11B). These results demonstrate that functional microRNAs can be delivered *in vivo*.

The primary aim of this chapter is to elucidate the role of miR-199b-5p in regulating AAMΦ and their responses. Hence, it was important to investigate whether the effect

of miR-199b-5p was specific to IL-4Rα dependent processes. Therefore, having confirmed successful delivery of miR-199b-5p in macrophages, we next investigated whether miR-199b-5p influenced IL-4Rα independent steady state CSF-1 driven proliferation to rule out effects of miR-199b-5p or transfection itself on IL-4Rα independent pathways. To this end, we used flow cytometry to identify peritoneal macrophages based on the expression of CD11b and F4/80. Live cells were identified using Aqua live/dead stain. Lineage negative cells were excluded based on a combined stain that included SiglecF, CD19, TCR-β and Ly6G, which are characteristic markers of eosinophils, B cells, T cells and neutrophils respectively. Next, cells that do not express MHC-II and F4/80 were excluded. Dendritic cells were then identified based on high MHC-II and CD11c expression and also excluded. Macrophages were then identified based on CD11b and F4/80 expression. Response to injection in the peritoneal cavity can result in some blood monocyte derived inflammatory macrophages being recruited to the peritoneal cavity. These were segregated from the tissue resident macrophages based on F4/80 and Tim4 expression. Tissue resident macrophages are F4/80hi and 90% of the tissue resident macrophages also express Tim4 whereas monocyte derived macrophages are F4/80lo and do not express Tim4 (Davies et al., 2013a). Proliferation was quantified using Ki67 and BrdU. In an additional stain panel, Ly6C and Ly6G were used to identify monocytes and neutrophils respectively as markers of inflammatory influx (Soehnlein & Lindbom, 2010).

FACS analysis of the PEC populations revealed that transfection causes an inflammatory influx resulting in tissue resident macrophage disappearance (Barth et al., 1995, Davies et al., 2013b) as shown in Figure 3.12. In a naïve mouse, the majority of the peritoneal macrophage population is tissue resident derived and this was also reflected in the group of mice that received 5% glucose only. The 10% of macrophages that are F4/80lo and monocyte derived were presumably a result of the inflammatory response to the injection itself (Figure 3.12). In contrast, the majority of the macrophage population detected in the mice that received the mimic microRNAs was monocyte derived with low F4/80 expression (~70-80%). This was consistent with the influx of monocytes and to a lesser extent, also neutrophils, which

were not present in the control glucose group. Even though 20-30% of the macrophages in the transfected groups were still tissue resident derived as represented by F4/80hi expression, these numbers were not considered to be enough for further analysis. With a significant disruption to the natural balance of the immune cell populations as represented by the inflammatory influx and resident macrophage disappearance, these results indicated that the peritoneal cavity was an unsuitable site for delivery of miR-199b-5p using this method.

3.2.6.2 Overcoming inflammation – delivery of miR-199b-5p to the lung

Having established previously that inflammatory influx in response to microRNA delivery rendered the peritoneal cavity unsuitable for further use, we next aimed to deliver miR-199b-5p to the lung. We chose to deliver miR-199b-5p to the lung as previous work has shown that it has a higher threshold for mounting an immune response in response to external stimuli compared to the peritoneal cavity (Wissinger et al., 2009, Findlay and Hussell, 2012). As described earlier, 20μg of microRNA was complexed to jetPEI (N:P ratio = 6) in 5% glucose. The microRNAs were delivered to the mice intranasally in this experiment (Figure 3.13A). The experimental aims were similar in terms of confirming microRNA delivery to macrophages in the lung and determining the effect of miR-199b-5p on steady state proliferation. It is important to note that two distinct macrophage populations exist in the lung, namely alveolar and interstitial macrophages (Crowell *et al.*, 1992). Additionally, while peritoneal macrophages are dependent on CSF-1 for their steady state renewal, this is not entirely the case with macrophages in the lung. Self-renewal of alveolar macrophages has been shown to be both CSF-1 and CSF-2 dependent (Guilliams et al., 2013, Hashimoto et al., 2013). 48 hours post transfection the bronchoalveolar lavage (BAL) and whole lung tissue were harvested for FACS analysis and qRT-PCR. Quantification of miR-199b-5p by qRT-PCR revealed a high level of overexpression in both the BAL cells and whole lung tissue, however, to a lesser extent in the lung tissue (Figure 3.13B). This was reflected in the copy numbers with miR-199b-5p transfected mice expressing 10^9 copies/ng RNA

compared to 10^7-10^8 copies/ng in whole lung tissue. Of note, from other research conducted in our lab, it is known that alveolar macrophages comprise approximately 60-70% of the BAL cells. In contrast, macrophages comprise a mere 10% of total lung tissue. This would potentially explain the difference in overexpression of miR-199b-5p between the BAL and lung tissue. BAL cells are limited in number and hence, were prioritised for the quantification of miR-199b-5p by qRT-PCR and could not be FACS analysed. Results from the analysis of different cell populations in the whole lung tissue by FACS were promising with both the alveolar and interstitial macrophage populations intact despite influx of some monocytes and neutrophils in the transfected groups (Figure 3.13C). Alveolar macrophages were classed as being CD11b- CD11c+ SiglecF+ and F4/80+ whereas interstitial macrophages were considered to be CD11b+ CD11c- SiglecF- and F4/80+. These results demonstrate that microRNAs can be delivered to the lung without the consequences of a disruptive inflammatory influx.

A secondary aim of this experiment was to determine the effect of miR-199b-5p on steady state proliferation of macrophages in the lung. This was measured by Ki67 expression. FACS analysis of alveolar macrophages in whole lung tissue showed no difference in Ki67hi levels between mice transfected with miR-199b-5p or the *C. elegans* microRNA *C. el* miR-231. Levels of active proliferation in mice that received glucose only were also comparable (Figure 3.14). Thus, delivery of miR-199b-5p as described above did not alter basal levels of steady state macrophage proliferation in the lung.

3.2.6.2.1 MiR-199b-5p and the regulation of IL-4 induced proliferation in the lung

We have demonstrated that miR-199b-5p can be successfully delivered to the lung without disrupting the macrophage populations. Additionally, the data suggested that miR-199b-5p does not affect steady state proliferation of these macrophage populations. In line with our hypothesis, our next experimental aim was to investigate whether miR-199b-5p regulates IL-4 induced macrophage proliferation in

the lung. Unpublished data previously generated in our lab has shown that two doses of IL-4c are necessary to induce macrophage proliferation in the lung as opposed to a single dose that is sufficient for the peritoneal macrophages. To this end, we delivered either PBS or two doses of IL-4c at 5μg each intraperitoneally on day 0 and day 2 respectively. 20μg of the microRNA complexed to jetPEI was delivered intranasally as already described. However, having established that an N:P ratio of 6 has no adverse effects, the N:P ratio was increased to 8 in this experiment in an effort to improve transfection efficiency in the lung. This was based on existing literature that supports the fact that N/P ratio can significantly influence transfection efficiency (Morimoto et al., 2003, Zhao et al., 2009). Groups of mice injected with either PBS or IL-4c received either miR-199b-5p or the *C. elegans* microRNA while control mice received 5% glucose only (Figure 3.15A). MicroRNAs were delivered on day 1 between the two doses of IL-4c. This rationale is based on the assumption that by the time the second dose of IL-4c provided the necessary boost for macrophage proliferation to occur, the microRNAs would have already suppressed their targets, which may be important for IL-4 induced proliferation. In the peritoneal cavity, macrophage proliferation in response to IL-4c peaks at 42 hours (Jenkins et al., 2011, Jenkins et al., 2013).

However, it is still unknown at which time point the peak of proliferation is observed in the lung. Hence, for this experiment, mice were culled 42 hours post the second dose of IL-4c. 3 hours prior to being culled, mice were injected with BrdU subcutaneously. Having previously identified that miR-199b-5p is the most highly expressed in BAL cells following delivery compared to total lung, BAL cells were harvested for FACS analysis. Lung tissue was also harvested for RNA and protein quantification. We have shown in the previous section that increase in miR-199b-5p levels in BAL cells following intranasal delivery is 10 fold higher than lung tissue. Therefore, lung tissue was used as an indirect measure of transfection efficiency in BAL cells. Quantification of miR-199b-5p and *C.elegans* miR-75 in whole lung tissue revealed significant overexpression of both microRNAs in the relevant groups (Figure 3.15B). Whilst a 6 fold overexpression of miR-199b-5p was observed in total lung, overexpression of *C.elegans* microRNA was significantly higher at ~1000 fold.

This is because the *C.elegans* microRNA is not endogenously expressed resulting in a much greater difference in overexpression. To confirm that IL-4c treatment was successful, RELM-α expression was analysed by flow cytometry as a marker of alternative activation. It is worth mentioning that BAL only contains alveolar macrophages; no interstitial macrophages are found. As shown in Figure 3.15C, expression levels of RELM-α were increased in response to IL-4c treatment in the control mice that received glucose only. However, transfection appeared to have an effect on RELM-α expression with levels significantly enhanced in mice that received both miR-199b-5p and *C. elegans* microRNA, even without IL-4c. In mice that received both a microRNA and two doses of IL-4c, RELM-α levels were the greatest suggesting an additive or possible synergistic effect of transfection with IL-4 (Figure 3.15C). Nevertheless, these results still confirm that IL-4 delivery to the lung was successful resulting in alternative activation of alveolar macrophages.

The main purpose of this experiment was to determine whether miR-199b-5p affects IL-4 induced proliferation in alveolar macrophages. Active proliferation was analysed by measuring both BrdU levels and Ki67hi expression through FACS. As predicted, a significant rise in proliferation was observed based on an increase in the percentage of macrophages staining positive for BrdU (10%) in control mice injected with IL-4c compared to 2% macrophages staining positive for BrdU in glucose only injected mice. (Figure 3.16A & B). Similarly, Ki67hi expression was higher in macrophages isolated from mice injected with IL-4c only (~15%) compared to mice that received glucose only (5%). However, a lower rate of proliferation was observed in mice that received both microRNA complexes (miR-199b-5p or *C. elegans* miR-75) and IL-4c injections, with only 2-5% of macrophages staining positive for BrdU. There was no difference in BrdU levels between these mice and mice that received microRNA complexes only as shown in Figure 3.16A. An increase in the percentage of macrophages expressing Ki67hi was detected in mice that received microRNA complexes and IL-4c (~10-12%) compared to mice that received microRNA complexes without IL-4c (8-10%). However, the median fluorescence intensity (MFI), which is a measure of total protein expression in a cell population, reflected a difference in Ki67hi expression when compared to the percentage of macrophages

expressing the protein. Whilst an increase in Ki67hi was detected in control mice that received IL-4c compared to mice that received glucose only (from 60,000 to ~65000), the same was not true for mice that received microRNA complexes and IL-4c when compared to mice that received microRNAs only. The MFI for these groups remained unchanged at 62000 regardless of IL-4c treatment (Figure 3.16A). The MFI results for BrdU, however, were in agreement with the results obtained when comparing percentage of macrophages positive for BrdU. The control mice treated with IL-4c express higher levels than mice that received glucose only (from 3,500 to ~6000). Although there was no significant difference between the IL-4c treated control group and groups that received the microRNA and IL-4c both (from ~4000 to 5000), the average fold change compared to their relevant control groups was lower (1.7 fold in control mice vs 1.2 fold) (Figure 3.16A). Together, these results would suggest that either miR-199b-5p does not affect IL-4 induced proliferation or that transfection of alveolar macrophages with microRNA complexes hampers IL-4 induced proliferation in general since the control *C.elegans* group also behaves in a similar manner.

3.2.6.2.2 MiR-199b-5p and alternative activation of alveolar macrophages

Although the primary focus of this study was to delineate the role of miR-199b-5p in regulating alveolar macrophage proliferation, we also measured YM-1 and RELM-α levels in the BAL supernatant as we previously saw a minor effect of miR-199b-5p on alternative activation *in vitro*. Protein levels were quantified by ELISA. In agreement with the FACS data (Figure 3.16A), ELISA results showed that transfection alone enhanced RELM-α expression to levels similar to those observed with IL-4c treatment in control mice that receive glucose only (Figure 3.16B). Transfection in combination with IL-4c treatment appeared to have an additive or possibly even a synergistic effect pushing RELM-α levels close to saturation (Figure 3.16B). In contrast, basal YM-1 levels were not affected by transfection. As expected, YM-1 levels were significantly enhanced in response to IL-4c treatment. Interestingly, in line with our *in vitro* data, the levels of secreted YM-1 were

considerably reduced in mice transfected with miR-199b-5p that also received two doses of IL-4c. No such changes were observed in mice that received both *C. elegans* miR-75 and IL-4c. These results show that miR-199b-5p has the capacity to significantly reduce YM-1 expression in alternatively activated alveolar macrophages. Whether this is an effect on protein production or secretion is still unknown.

3.3 Discussion

The primary aim of this chapter was to understand the contribution of miR-199b-5p in regulating AAMΦ and their responses. A role for miR-199a-5p, an isoform of miR-199b-5p, has previously been implicated in inhibiting monocyte/macrophage differentiation (Lin et al., 2014). However, to date the functional significance of this microRNA in regulating macrophage responses has not been reported. Our lab has previously shown that the expression of this microRNA is IL-4Rα dependent (Ruckerl et al., 2012). In this study, we have demonstrated that miR-199b-5p was expressed at high copy numbers *in vivo* but not *in vitro*. Specifically, we found that miR-199b-5p is expressed at 10^3 copies/ng RNA in RAW 264.7 cells and BMDM compared to ~10^5 copies in response to IL-4c delivery to the peritoneal cavity and during *L. sigmodontis* infection. Additionally, the IL-4Rα dependent increase in miR-199b-5p expression appeared to be restricted to *in vivo* models of alternative activation and did not occur *in vitro*. These results suggest that the increase in expression of miR-199b-5p was not a direct effect of IL-4Rα signalling and the involvement of a secondary factor or another cell type expressing IL-4Rα may be necessary for its induction. Indeed, IL-4Rα expression can be found on cells of varying origins including haematopoietic, endothelial, epithelial, muscle, fibroblast and more (Nelms et al., 1999). While *in vivo* conditions of alternative activation would involve the presence of such cell extrinsic factors, the same is not true for *in vitro* situations that involve a homogeneous cell population. This might be the reason why the enhanced expression of miR-199b-5p is limited to AAMΦ isolated from *in vivo* conditions.

With the purpose of identifying the functional significance of miR-199b-5p, we utilised the target prediction software TargetScan to identify predicted targets of this microRNA. The majority of these putative targets were associated with known proliferative pathways. Furthermore, during *L. sigmodontis* infection miR-199b-5p expression negatively correlated with the expression of Ki67, a marker of proliferation. On the basis of these findings, we hypothesised that IL-4Rα dependent expression of miR-199b-5p acts as a regulator of IL-4 induced proliferation in a negative feedback loop. It was also hypothesised that this negative modulation requires the presence of a secondary extrinsic factor or cell type.

In agreement with our hypothesis, overexpression of miR-199b-5p in RAW 264.7 cells resulted in a reduction in proliferation. Additionally, a reduction in the levels of YM-1 and RELM-α was also observed when miR-199b-5p was overexpressed in cells stimulated with IL-4 and IL-13. However, RAW 264.7 cells did not secrete significant amounts of these proteins, especially RELM-α (<1ng/mL), making it difficult to arrive at a concrete conclusion regarding the effect of miR-199b-5p on alternative activation in RAW 264.7 cells. MiR-199a-5p, which shares an identical seed sequence with miR-199b-5p and is predicted to bind the same targets, has been shown to be important in regulating proliferation in various different cell types (Alexander et al., 2013, Song et al., 2014, Hashemi Gheinani et al., 2015).

Hence we further investigated the role of miR-199b-5p in regulating macrophage proliferation. The most promising targets of miR-199b-5p were selected utilising the prediction software TargetScan and previously generated mRNA array data. One caveat to this approach is that TargetScan is known to have a 50-70% rate of false positive predictions besides being unable to predict non-canonical microRNA-target interactions such as bulge and centred sites (Yue et al., 2009, Shin et al., 2010, Witkos et al., 2011, Chi et al., 2012, Martin et al., 2014). This approach would, therefore, result in the exclusion of several "real" targets of miR-199b-5p (greater false negative rate) and inclusion of many genes that are not real targets. Moreover, genes from the mRNA array were selected on the basis of their change in relation to Ki67 during the infection. It is important to note that these changes may have been the result of regulation by several other factors besides microRNAs or a cumulative

effect of different microRNAs operating together. In other words, these changes in gene expression during *L. sigmodontis* infection are not all expected to be specific to miR-199b-5p. Nevertheless, in the absence of additional data from other approaches this was the most reasonable way forward.

Pathway analysis of these shortlisted predicted targets identified 11 significantly enriched pathways including Insulin – like growth factor 1 (IGF-1) signalling, PPARα/RXRα activation, insulin receptor signalling and PI3K/AKT signalling, amongst others suggesting that miR-199b-5p may be involved in the modulation of several different proliferative and other pathways. Various cancer related pathways such as molecular mechanisms of cancer and role of tissue factors in cancer were also present in the results of this analysis. The enrichment of these cancer related pathways in results obtained from IPA analysis is consistent with previous reports that have shown the involvement of miR-199a-5p in the progression of several carcinomas (Sakurai et al., 2011, Xu et al., 2012, Yi et al., 2013, He et al., 2014b, Kim et al., 2015, Kobayashi et al., 2015, Mussnich et al., 2015, Shin et al., 2015). However, the expression of miR-199a-5p has been found to be variable in different cancers; it is enhanced in some whereas reduced in others. This variation in function could be explained by the fact that the genetic expression profiles between different cell types are not identical and hence, the same target gene may have opposing functions in different cell types resulting in a change in the role of this microRNA accordingly.

As a result of this pathway analysis, the finding that miR-199b-5p could potentially regulate the insulin/IGF-1 signalling axis was novel and thus, interesting to pursue further. As discussed previously, there is a high degree of crosstalk between the insulin and IGF-1 signalling cascades as evident from the formation of receptor heterodimers that can bind and signal via both insulin and IGF-1 (Treadway et al., 1989, De Meyts and Whittaker, 2002, Pandini et al., 2002, Cabail et al., 2015). Macrophages are a well-known source of IGF-1, which is necessary for coordinating muscle regeneration and inflammation following injury (Lu et al., 2011, Tidball and Welc, 2015, Tonkin et al., 2015). In fact, AAMΦ are known to produce IGF-1 in response to the T_H2 cytokines IL-4 and IL-13 in a STAT6 dependent manner (Wynes

and Riches, 2003, Forbes and Rosenthal, 2014). In addition, macrophages themselves express large amounts of IGF1R on their surface and the secreted IGF-1 can also modulate macrophage polarisation to a pro-repair phenotype through an autocrine loop (Higashi et al., 2011, Tonkin et al., 2015). Moreover, the role of macrophages in conferring insulin resistance and the effect of insulin on macrophage metabolism and function are already well defined (Costa Rosa et al., 1996, Charo, 2007, Odegaard et al., 2007, Chawla, 2010, Olefsky and Glass, 2010, Wynn et al., 2013).

The existing literature also suggests that there is a strong link between IL-4 signalling and the insulin/IGF-1 axis. Besides being critical for the production of IGF-1, IL-4 plays a crucial role in the regulation of insulin sensitivity in a STAT6 dependent manner (Ricardo-Gonzalez et al., 2010, Chang et al., 2012). Moreover, a common link between IL-4, insulin and IGF-1 pathways has been suggested in haematopoietic cells through the phosphorylation of the central molecule IRS-1 (Wang et al., 1993a). IL-4 can also cooperate with STAT6 and IRS-2 to induce proliferation and differentiation in T cells (Wurster et al., 2002). In macrophages, phosphorylation of IRS-2 by IL-4 is regulated by SOCS1, another molecule important during alternative activation (Losman et al., 1999). IL-4 is also known to protect cells from apoptosis through an IRS-1 mediated mechanism (Zamorano et al., 1996). Furthermore, IRS-1 is also essential for insulin and IL-4 stimulated mitogenesis in haematopoietic cells (Wang et al., 1993b). Additionally, IRS molecules central to the insulin/IGF-1 signalling cascades have also been implicated as being essential for IL-4 induced proliferation through their ability to recruit PI3K (Jiang et al., 2000). Together, the previous literature cited above renders the insulin/IGF-1 signalling as an extremely interesting target for miR-199b-5p and it was hypothesised that miR-199b-5p could exert its effects on IL-4 induced macrophage proliferation by targeting the insulin/IGF-1 signalling axis.

To this end, miR-199b-5p was overexpressed in RAW 264.7 cells and the expression levels of *Insr*, *Igf1r* and *Irs1* quantified. RAW cells were used in this analysis because we had already shown an effect on proliferation of these cells by miR-199b-5p. As detailed in the results section, no effect was observed on the levels of *Insr* and *Igf1r*, despite 3 predicted binding sites for miR-199b-5p in the 3'UTR of *Insr*.

Unexpectedly, the expression of *Irs1* was enhanced several fold upon miR-199b-5p overexpression. It has previously been reported that target mRNAs can be localised to processing bodies (P-bodies), which serve as a site for degradation of untranslated mRNAs (Liu et al., 2005). It was thought that this might be a possibility for the enrichment/increase seen in *Irs1* transcript following miR-199b-5p overexpression. In agreement with the qRT-PCR data, Western blot analysis also revealed a similar increase in the protein levels of IRS1.

Besides localisation to P-bodies, several other factors might contribute to the increase observed in IRS1 expression. In the past, non-canonical binding of microRNAs to their targets has been reported. Conserved microRNA binding sites have been found in the 5'UTR and coding sequence (CDS) regions of a target mRNA (Zhou et al., 2009, Hausser et al., 2013). Moreover, there have been reports of simultaneous 5'UTR and 3'UTR interactions between a microRNA and its target (Lee et al., 2009). MiR-155 has also been shown to enhance TNF-α expression by stabilisation of the transcript by binding to the 3'UTR (Tili et al., 2007, Faraoni et al., 2009). Hence, it is possible that miR-199b-5p exerted its effect on IRS1 through one of these mechanisms. However, upon scanning the 5'UTR and CDS regions of *Irs1*, no such non-canonical binding sites were found. A study by Gokhale & Gadgil (2012) made use of mathematical modelling to formulate a comprehensive model that suggests an explanation for increase in target protein levels based on reversible mRNA-microRNA interactions and selective return of RNA. The authors suggest that in certain cases microRNAs can bind to the target mRNA near degradation signals such as ARE sites (AU rich elements), thereby masking the degradation signal leading to protection of the mRNA (Gokhale and Gadgil, 2012).

From the literature it is expected that an increase in IRS-1 expression would result in an increase in proliferation. However, we observed an increase in IRS-1 expression but an overall reduction in the proliferation of RAW 264.7 cells. It is well established that IRS-1 is the major substrate of IR and IGF1R and essential for normal growth and development. This is reflected in the fact that *Irs1*$^{-/-}$ mice are retarded in embryonic and postnatal growth, reaching only 50% of normal size (Araki et al., 1994, Tamemoto et al., 1994, Dong et al., 2006). Given that IRS1 is

crucial in growth and development and assuming that IRS1 is a target of miR-199b-5p, one explanation for our results would be that a compensatory mechanism exists wherein the cell produces copious amounts of IRS1 to counterweigh the effects of IRS1 downregulation by miR-199b-5p. Having studied the expression of IRS1 48 hours post transfection, it is probable that by this time point, the cell has already recovered from any loss of IRS1. A time course experiment with monitoring of IRS1 levels at regular intervals following overexpression of miR-199b-5p could help answer whether this might be the case.

It is important to note that besides the amount of protein available, the state of activation of IRS1 is important in determining downstream signals for proliferation. This is determined by its phosphorylation and depending on the residue phosphorylated, IRS1 can act as both a positive or negative regulator of proliferation (Gual et al., 2005). For example, phosphorylation of IRS1 at tyrosine residues provides a positive stimulus for proliferation whereas phosphorylation of serine residues may positively or negatively regulate proliferation depending on the kinase involved (Gual et al., 2005). Hence, besides quantification of total protein, it would be useful to examine the active phosphorylated IRS1 sites.

Furthermore, it is highly plausible that the increase in IRS1 levels are in fact indirect rather than a direct effect of miR-199b-5p. In this scenario it would be expected that miR-199b-5p targets a repressor of IRS1. SOCS1 and SOCS3, which are both associated with macrophage activation, are known potent inhibitors of IRS proteins (Ueki et al., 2004). SOCS3 also has a predicted binding site for miR-199b-5p in its 3'UTR. Further experiments are needed to test these hypotheses. Another possibility is that overexpression of miR-199b-5p can potentially saturate RISC complexes and displace other endogenous microRNAs leading to this effect (Khan et al., 2009, Thomson et al., 2011). Although a range of possibilities exist, to explain the up-regulation of IRS1, it seem most likely that miR-199b-5p targets a complex network of genes that cumulatively result in the unexpected increase of IRS1.

While these *in vitro* studies were underway, we next aimed to deliver miR-199b-5p *in vivo* to determine its effect on macrophage proliferation. MiR-199b-5p along with

control microRNA mimics were delivered to the peritoneal cavity of mice. In the absence of an external stimulus, one would not expect IRS substrates to be active and hence most of the macrophage proliferation observed is presumed to be CSF-1 dependent (Hume and MacDonald, 2012, Jenkins et al., 2013). Although functional microRNAs can be delivered to the peritoneal cavity as reflected by reduction in levels of GAPDH following delivery of a microRNA targeting its 3'UTR, this delivery results in an inflammatory influx of monocytes and neutrophils resulting in the disappearance of tissue resident macrophages. Originally characterised by Nelson and Boyden, Barth *et al* have reported that macrophages undergo a physiological response known as the macrophage disappearance reaction (MDR) in response to certain stimuli in the peritoneal compartment, including the recruitment of inflammatory populations such as neutrophils and monocytes (Barth et al., 1995). It was concluded that the remaining tissue resident macrophage numbers are not enough for further analysis. Besides, with the disruption of the natural balance of the immune populations normally found in the peritoneal cavity, any effects observed may not have been significant.

Next, miR-199b-5p was delivered to the lung as this organ is known to have a higher threshold of activation before mounting a strong immune response when compared to the peritoneal cavity (Wissinger et al., 2009, Findlay and Hussell, 2012). Delivery of miR-199b-5p to the lung was successful with no disruption to the two macrophage populations found in the lung, namely alveolar and interstitial. Transfection efficiency in BAL was 10 fold higher than whole lung tissue. It is presumed that most of the microRNAs are delivered to macrophages and this result would fit with the fact that 70% or BAL cells are alveolar macrophages compared to whole lung tissue wherein macrophages make up only 10% of the total cell population. As discussed earlier, homeostatic levels of proliferation are maintained by CSF-1 (Hume and MacDonald, 2012, Jenkins et al., 2013). However, a role for GM-CSF has also been implicated in the self-renewal of alveolar macrophages in the lung (Guilliams et al., 2013, Hashimoto et al., 2013). Nonetheless, in both these situations, insulin/IGF-1 signalling is not expected to be active and hence, it was hypothesised that no effect of miR-199b-5p will be observed on proliferation under steady-state conditions. In

agreement with our hypothesis, it was found that miR-199b-5p does not affect steady state alveolar macrophage proliferation. On the other hand, it was hypothesised that miR-199b-5p would effect IL-4 induced proliferation. This was based on our earlier hypothesis that miR-199b-5p negatively regulates IL-4 induced signalling by targeting the insulin/IGF-1 signalling cascades. This was tested by the delivery of miR-199b-5p or a control *C.elegans* microRNA to the lung either on their own or in combination with IL-4c. Although a reduction was observed in the percentage of alveolar macrophages expressing BrdU (as a measure of active proliferation) when compared to control mice, a similar effect was also observed in mice that received the *C. elegans* microRNA. Similar effects were observed with total Ki67hi protein levels, a secondary measure of proliferation. Hence, it is difficult to confidently conclude any effect of miR-199b-5p on IL-4 induced proliferation. Although the *C. elegans* microRNA utilised in this experiment is species restricted, off target effects of small synthetic RNAs have previously been reported (Jackson and Linsley, 2010). It is possible that the effect observed with this control microRNA was in fact an off target effect, as this microRNA is not present in mice endogenously. A solution to this would be to use several different non-specific controls as a comparison and to determine their effects on IL-4 induced proliferation. A scrambled sequence of miR-199b-5p could also be used as an additional control.

Another aspect to consider with this particular experiment would be the signalling cascade under consideration. Unpublished data from our lab has shown that IR is not very highly expressed in alveolar macrophages. Only ~2-4% of alveolar macrophages stain positive for IR and upon IL-4c injection, this percentage does not change. The same is also true for IRS1 expression in the lung (determined by C_t value >35). In contrast, about 15-20% of peritoneal macrophages express IR in steady state. Following IL-4c delivery, the expression of IR is upregulated with nearly 80% of the macrophages staining positive (unpublished, data not shown). Increasing evidence from data generated in our lab suggests that alveolar and peritoneal macrophages are very distinct populations that behave differently to the same stimuli. Hence, it is possible that the reason we see no difference between miR-199b-5p and the *C. elegans* microRNA in the lung is because miR-199b-5p is not

able to mediate an effect on IL-4 induced proliferation in the absence of significant IR and IRS1 expression. The differences between the glucose and transfected groups in this case may just be a result of transfection in general. In the future, to overcome these inherent differences between macrophage populations and the inflammatory influx in response to transfection in the peritoneal cavity, experiments may be conducted wherein peritoneal or Thio MΦ could be transfected with miR-199b-5p *ex vivo* and injected back into the mouse intraperitoneally. This could be followed by IL-4c injection to determine the effect of miR-199b-5p on IL-4 driven proliferation in the presence of high IR and IRS1 expression.

In the same experiment, we also measured secreted levels of YM-1 and RELM-α in the BAL supernatant. We had previously observed a reduction in the expression of the proteins in RAW 264.7 cells transfected with miR-199b-5p and stimulated with IL-4 and IL-13. However, the RAW 264.7 cells did not secrete significant amounts of protein to have confidence in the conclusions. In the BAL, no significant differences were observed in RELM-α levels between the different groups. Even though no differences were observed in RELM-α protein, it is possible that the additive effect of transfection and IL-4 saturated the system, thereby masking any subtle effects of miR-199b-5p. However, YM-1 was considerably altered in mice that received miR-199b-5p mimic and showed a nearly 50% reduction in secreted protein. With no FACS data for intracellular protein quantification and no RNA for measuring transcript levels, whether this observed reduction is an effect on total protein or a secretion defect still remains unknown. No predicted direct binding sites for miR-199b-5p were found in the 3'UTR of *Chi3l3* (YM-1). The reduction in protein levels observed is therefore likely to be an indirect effect. Mechanisms of YM-1 secretion are still unknown and hence, if this reduction relates to a secretion defect it is not clear how miR-199b-5p might mediate this (for example, which targets of miR-199b-5p would impact YM-1 secretion). Our lab has recently shown that YM-1 is involved in the recruitment of neutrophils during *Nippostrongylus brasiliensis* infection in the lung as a trade-off between nematode killing and host damage (Sutherland et al., 2014). Thus, it would be interesting to deliver miR-199b-

5p to the lung in mice infected with *N. brasiliensis* to examine the effects of miR-199b-5p mediated reduction in YM-1 levels in the context of infection.

Overall, the results in this chapter demonstrate that miR-199b-5p has the ability to regulate proliferation in RAW 264.7 cells. The data in this chapter are the first to represent that miR-199b-5p regulates IRS1, which forms part of the insulin/IGF-1 signalling pathway. Whether this effect translates *in vivo* with an effect on IL-4 induced proliferation is still unclear. We have shown that delivery of microRNAs to the peritoneal cavity results in an inflammatory influx leading to macrophage disappearance. Additionally, we have established that miR-199b-5p can be delivered to the lung without disrupting the balance of the immune populations. It was further shown that miR-199b-5p does not affect steady state proliferation of alveolar macrophages. Besides proliferation, we are the first to show that miR-199b-5p has the ability to regulate alternative activation through downregulation of YM-1 expression. Further experiments are still needed to delineate mechanisms to understand the contribution of miR-199b-5p in the regulation of AAMΦ and their responses. As a starting point, to overcome the lack of IR and IRS-1 expression in the lung and inflammation in response to microRNA delivery in the peritoneal cavity, peritoneal macrophages could be transfected *ex vivo* and injected into mice followed by IL-4c delivery to assess the role of miR-199b-5p in regulating insulin signalling *in vivo*. Additionally, the significance of the regulation of YM-1 by miR-199b-5p in the context of infection still remains to be addressed.

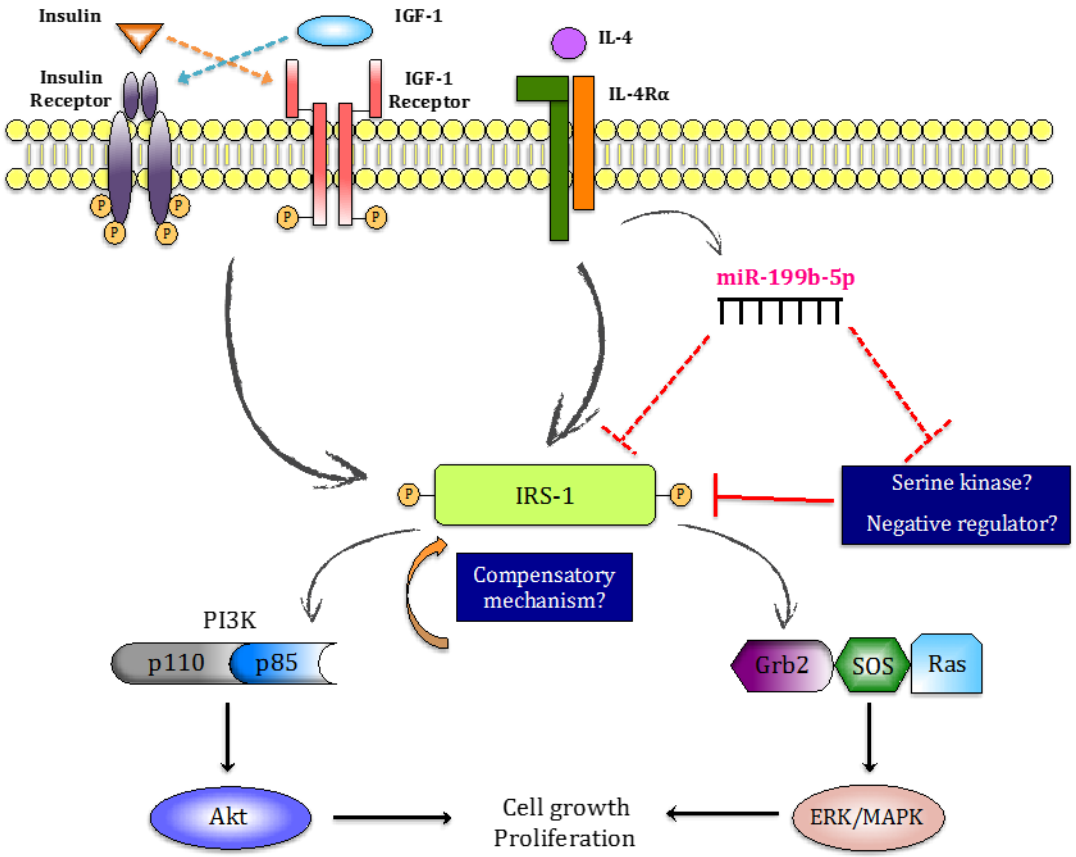

Figure 3. Schematic summary of potential mechanisms resulting in increased IRS-1 levels as a consequence of miR-199b-5p action

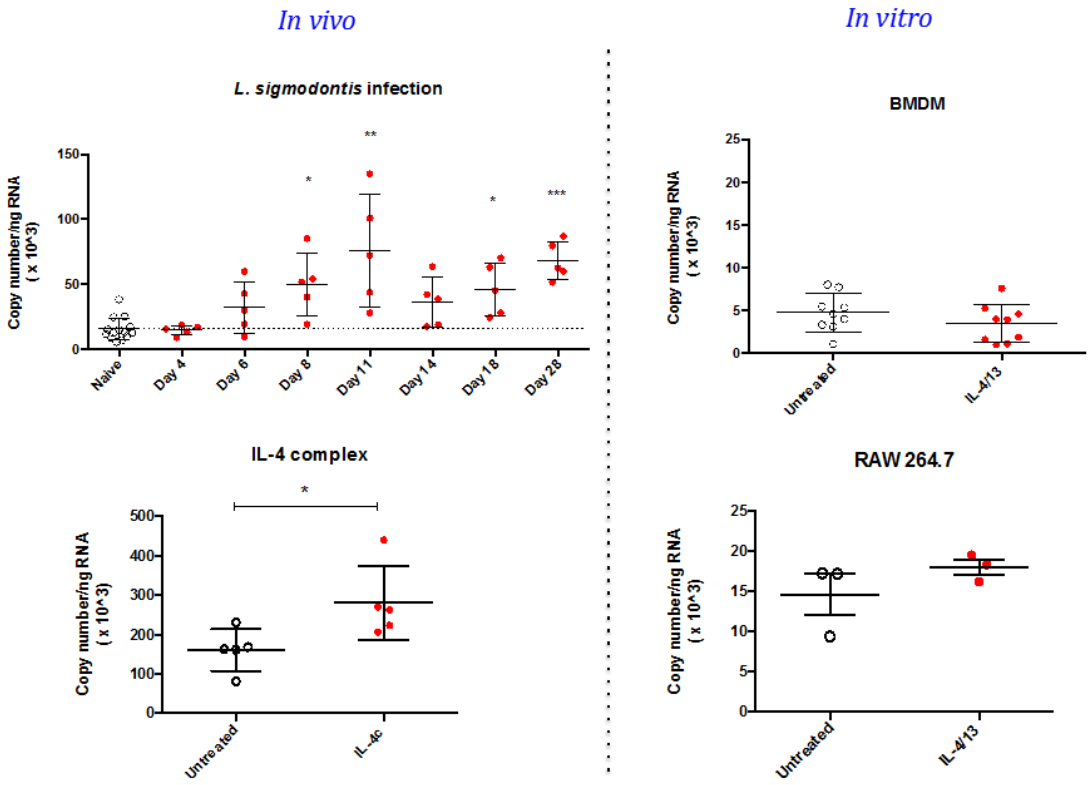

Figure 3.1 MiR-199b-5p is expressed at a higher copy number in AAMΦ *in vivo* compared to AAMΦ *in vitro*.

For the *in vivo* conditions**,** AAMΦ were isolated from the pleural cavity of either WT C57BL/6 mice infected with L3 larvae of the nematode *L. sigmodontis* on various days post infection (n=6) or from the peritoneal cavity of WT C57BL/6 mice injected with 5µg of IL-4c (n=5). For the *in vitro* conditions, BMDM were generated from bone marrow precursors derived from WT C57BL/6 mice cultured in CSF-1 containing medium. Both BMDM and RAW 264.7 cells were stimulated with 20ng/mL of IL-4/IL-13 for 48hr (n=3). In all conditions, cells were lysed and RNA extracted. Data were normalised to *RNU6B* expression. Data are presented as the mean fold change ± SEM and representative of one (*L. sigmodontis* infection) or two separate experiments (RAW 264.7, BMDM and IL-4c). Statistical significance for differences between naïve and treated animals during *L. sigmodontis* infection time course and following IL-4 complex injection was determined using two-way and one-way ANOVA (Kruskal Wallis test) respectively. For BMDM and RAW 264.7 cells, statistical significance was calculated using unpaired two-tailed student's T-test (* P< 0.05, ** P< 0.01, *** P< 0.001).

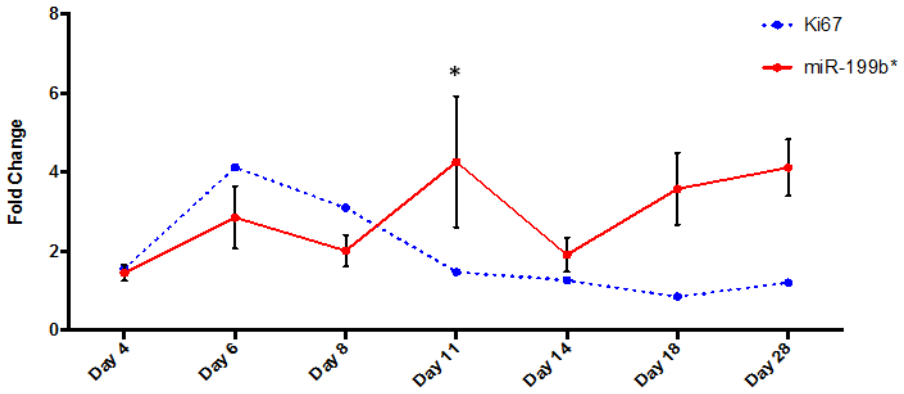

Figure 3.2. Correlation between the expression of miR-199b-5p and Ki67 during *L. sigmodontis* infection in the pleural cavity.

AAMΦ were isolated by adherence purification from the pleural cavity of WT C57BL/6 mice infected with L3 larvae of the nematode *L. sigmodontis* on various days post infection. Cells were lysed and RNA extracted. Data were normalised to *RNU6B* for microRNA expression and *Gapdh* for mRNA expression. Data are presented as the mean fold change ± SEM and representative of a single experiment (n=5).

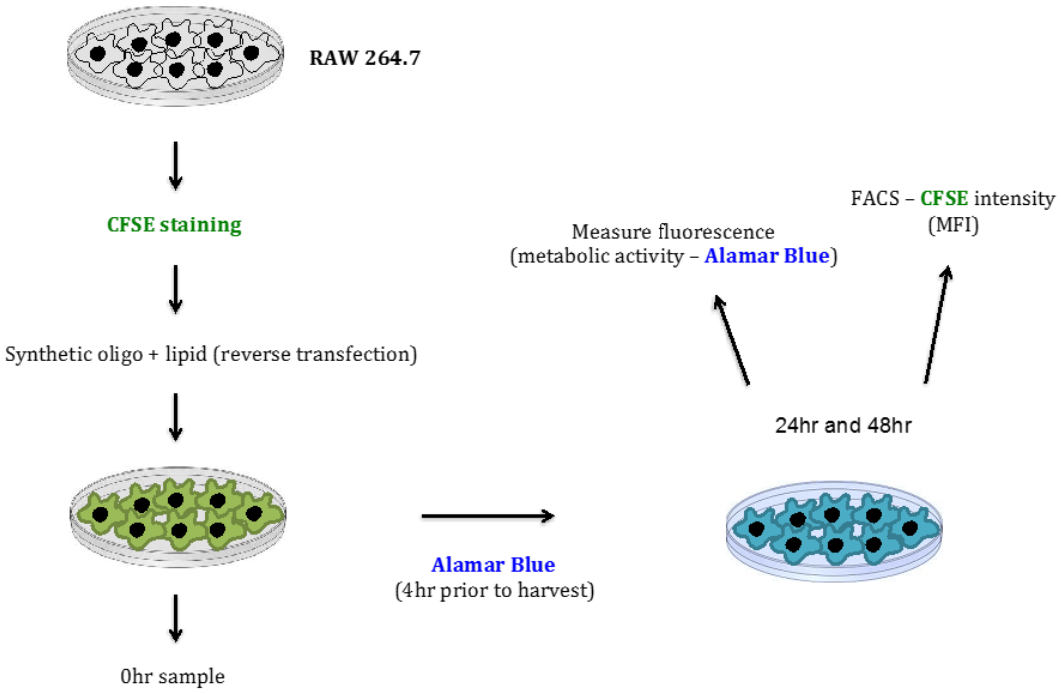

Figure 3.3. Schematic of transfection and analysis of proliferation in RAW 264.7 cells upon transfection of synthetic oligos.

RAW 264.7 cells were pre-stained with CFDA-SE and reverse transfected with synthetic mature microRNA mimics. 4 hours prior to harvest, alamarBlue was added to the supernatant as a measure of metabolic activity. Supernatants and cells were harvested for analyses at 24 and 48 hours post transfection respectively.

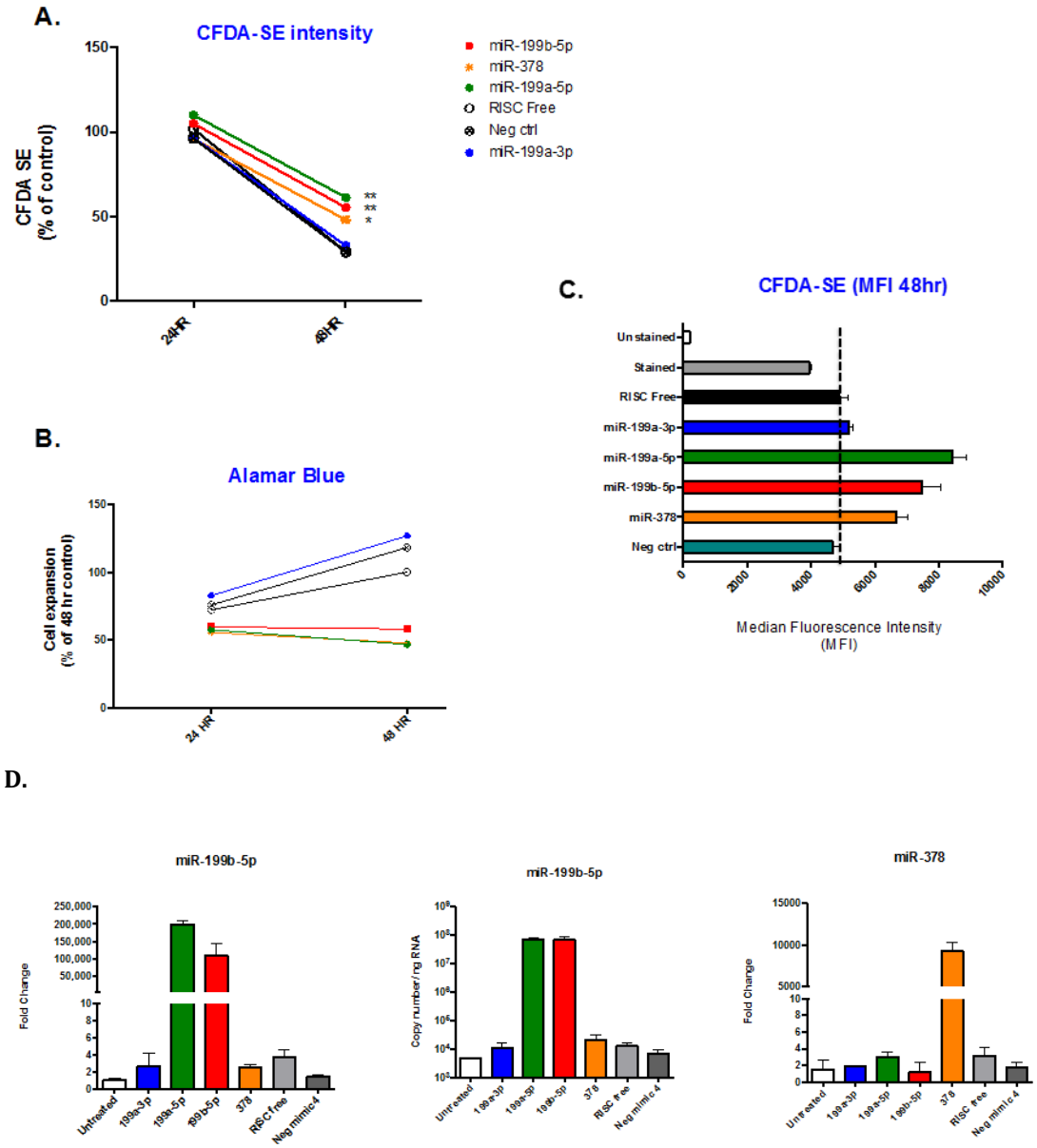

Figure 3.4 Transfection of miR-199a/b-5p suppresses proliferation in RAW 264.7 cells.

RAW 264.7 cells were transfected with 25nM of synthetic miR-199a/b-5p and miR-199-3p along with a positive control (miR-378) and negative controls (RISC Free and *C.elegans* microRNA). **A)** Percentage loss of CFDA-SE intensity and **B)** alamar blue conversion over time compared to RISC Free control were used as indicative measures of proliferation. **C)** Mean fluorescence intensity indicative of CFDA-SE as measured by FACS. CFDA-SE intensity was measured by flow cytometry and alamar blue conversion was measured as a change in fluorescence over time. **D)** Fold change in levels of microRNAs following overexpression in RAW 264.7 cells. Fold changes were calculated as ratios of transfected

samples to RISC Free transfected control samples. Copy numbers of miR-199b-5p following transfection were also calculated using a synthetic standard of known concentration. Statistical significance was determined using one-way or two-way ANOVA where appropriate (* P< 0.05, ** P< 0.01, *** P< 0.001). Data are representative of measures from five separate independent experiments (n=3).

A.

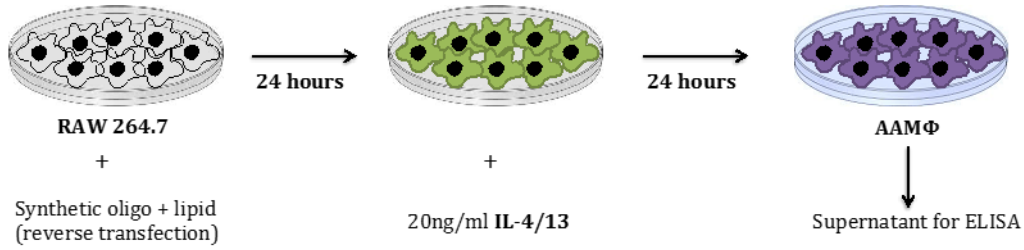

B.

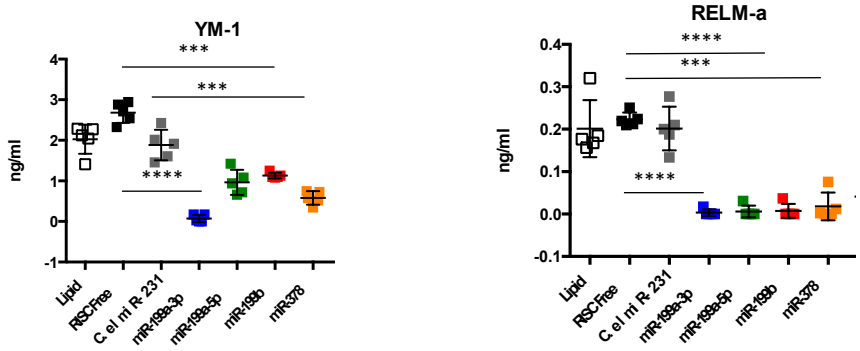

Figure 3.5 Overexpression of miR-199 family members and miR-378 negatively impacts alternative activation in RAW 264.7 cells.

RAW 264.7 cells were transfected with synthetic miR-199a/b-5p, miR-199-3p and positive and negative controls. 24 hours post transfection cells were stimulated with 20ng/mL of IL-4 and IL-13 resulting in their alternative activation. Supernatants were harvested 24 hours post stimulation with IL-4 and IL-13. YM-1 and RELM-α levels were measured by ELISA. Data are representative of a single experiment (n=3) and statistical significance was determined using one-way ANOVA (Kruskal Wallis test) (* P< 0.05, ** P< 0.01, *** P< 0.001).

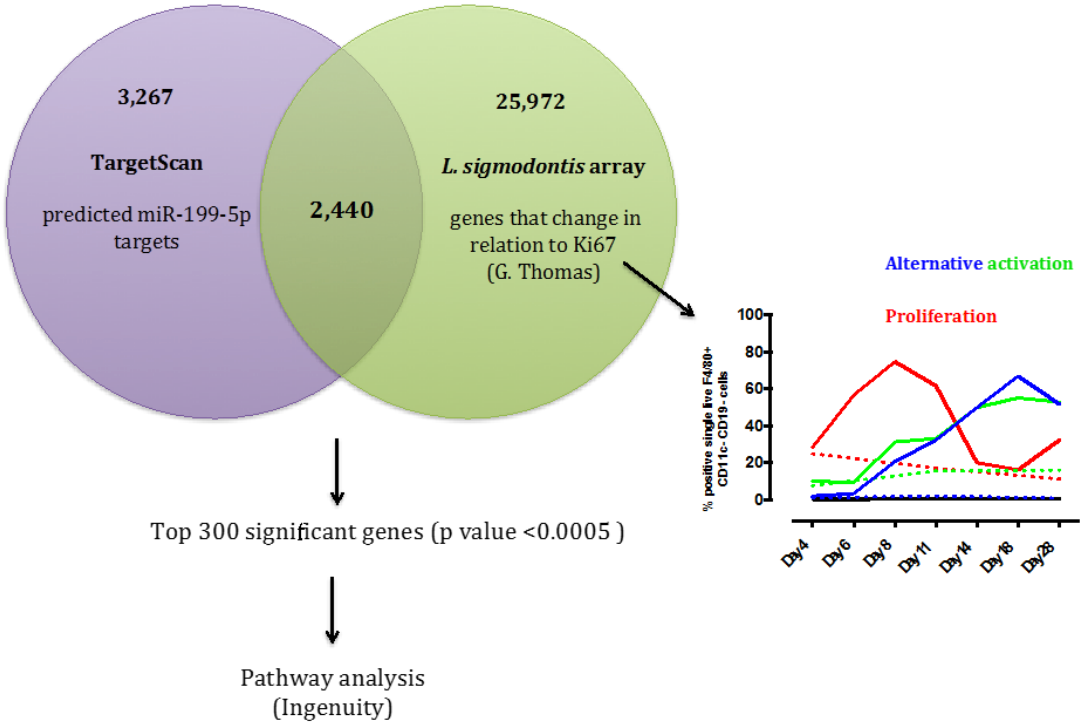

Figure 3.6 Schematic representing the selection of genes for pathway analysis to elucidate the functional role of miR-199b-5p.

Putative targets of miR-199b-5p were identified on the basis of predicted direct binding sites for miR-199b-5p in the 3'UTR of target mRNAs using the prediction software TargetScan. Additional mRNA array data (Graham Thomas) using AAMΦ from an *L. sigmodontis* infection time course was also utilised. In this mRNA array, a generalised linear modelling approach was used to identify genes that change in relation to Ki67, a marker of proliferation, over the course of infection. This list of genes was then overlapped with the list of predicted targets of miR-199b-5p to generate a final list of 2,440 genes. Out of these 2,440 genes, the top 300 significant genes that positively correlate with Ki67 expression based on P-values obtained from the mRNA array data were selected for pathway analysis (P value < 0.005). Pathway analysis was carried out using Ingenuity Pathway Analysis (www.ingenuity.com).

Pathway	Ratio	P value
IGF-1 Signalling	29/97	3.93E-0.7
Molecular Mechanisms of Cancer	70/365	3.38E-0.6
PPARα/RXRα Activation	41/178	4.06E-0.6
Amyloid Processing	18/51	4.65E-0.6
Role of Tissue Factor in Cancer	29/110	6.55E-0.6
NF-κB Signalling	39/172	1.02E-0.5
Superpathway of Inositol Phosphate Compounds	42/193	1.4E-0.5
Insulin Receptor Signalling	32/132	1.49E-0.5
Axonal Guidance Signalling	77/434	2.14E-0.5
AMPK Signalling	39/178	2.36E-0.5
PI3K/AKT Signalling	30/123	2.4E-0.5

TABLE 3.1 Top 11 pathways identified predicted to be miR-199b-5p targets using Ingenuity Pathway Analysis.

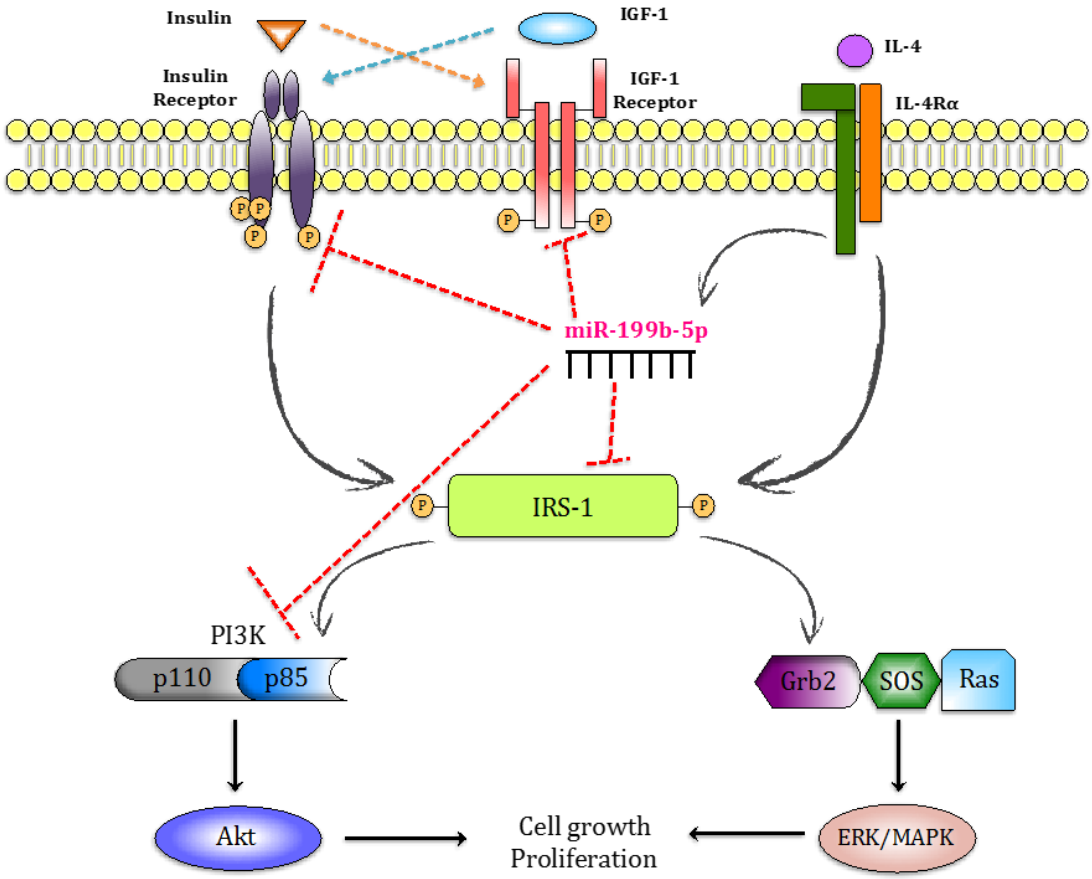

Figure 3.7 Relationship between the IGF-1, Insulin and IL-4Rα signalling pathways and molecules identified as being predicted targets of miR-199b-5p using TargetScan Version 6.2 [available at (http://www.targetscan.org)].

A.

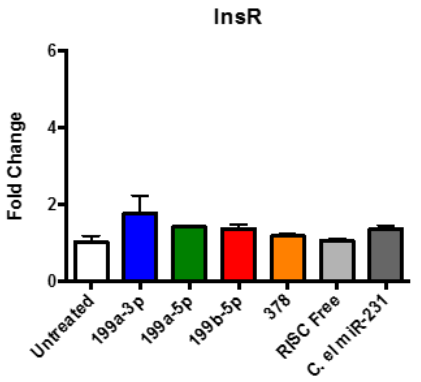

5' ...GAUGUUUCUUGCUUGGAUACACUGGU...3' InsR 3'UTR binding site 1
CUUGUCCAUCAGAUUUGUGACCC miR-199b-5p

5' ...UGAAACCUACCAUAACACUGGC...3' InsR 3'UTR binding site 2
CUUGUCCAUCAGAUUUGUGACCC miR-199b-5p

5' ------AAAGACACACUGGCCA-CCC------ 3' InsR 3'UTR binding site 3
CUUGUCCAUCAGAUUUGUGACCC miR-199b-5p

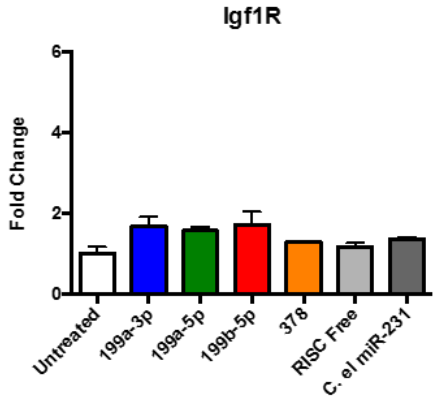

5' AUGGG-AGGGUUUCAGGACACUGGA...3' Igf1r 3'UTR binding site 1
CUUGUCCAUCAGAUUUGUGACCC miR-199b-5p

5' ...AAGCAUCUCCUUUCCUAAACACUGGC...3' Igf1r 3'UTR binding site 2
CUUGUCCAUCAGAUUUGUGACCC miR-199b-5p

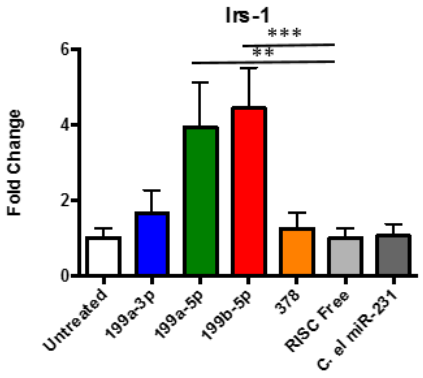

5' ...AGAACCAAGCAUUAAACACUGGG ...3' Irs-1 3'UTR binding site 1
CUUGUCCAUCAGAUUUGUGACCC miR-199b-5p

B.

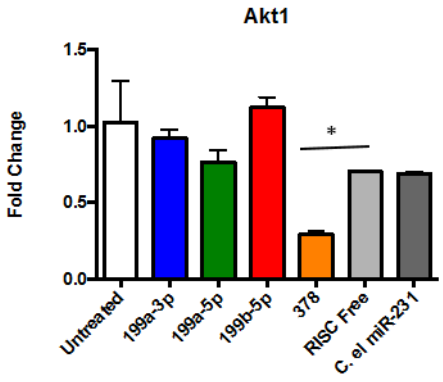

Figure 3.8 Expression of *Insr*, *Igf1r* and *Irs1* in RAW 264.7 cells following transfection with miR-199b-5p.

RAW 264.7 cells were either left untreated or transfected with synthetic microRNAs (25nM) for 48 hours. Total RNA was extracted for quantification by qRT-PCR. Expression of **A)** *Insr*, *Igf1r*, *Irs1* and **B)** *Akt-1* transcripts was quantified. The expression of each gene was normalized to *Gapdh*. Data are presented as mean of fold change ± SEM of three technical replicates (n=3) compared to cells transfected with RISC Free siRNA and representative of three individual experiments. Statistical significance was determined using one-way ANOVA (Kruskal Wallis test) (* P< 0.05, ** P< 0.01, *** P< 0.001) (n=3).

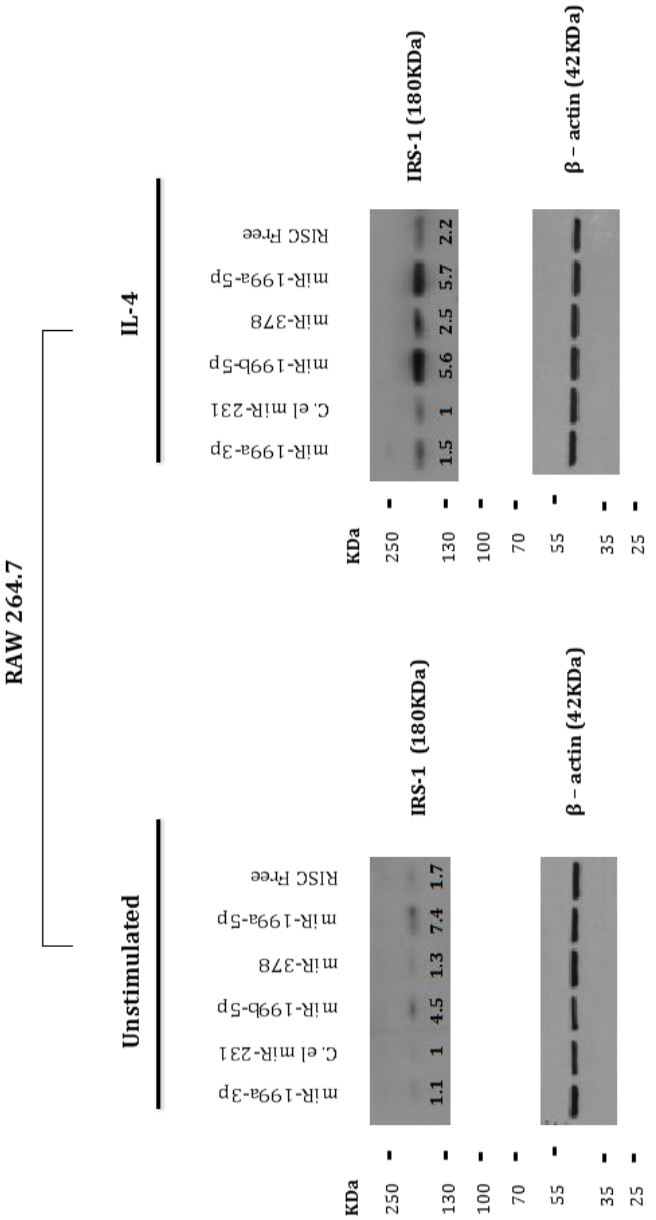

Figure 3.9 Protein expression of IRS-1 in response to miR-199b-5p overexpression in RAW 264.7 cells.

RAW 264.7 cells were either left untreated or transfected with synthetic microRNAs (25nM) for 48 hours. Western blot analysis (ECL-based detection) of IRS-1 was carried out in cells transfected with miR-199b-5p, its isoform miR-199a-5p, miR-199a-3p, miR-378 and negative controls (RISC Free siRNA and *C. elegans* miR-231). Protein levels were quantified using Image Studio Lite software and normalized to β-actin. Results are represented as fold changes relative to cells transfected with *C. elegans* mimic. 50µg lysate was loaded in each lane (pooled n=3). Data are representative of two separate experiments.

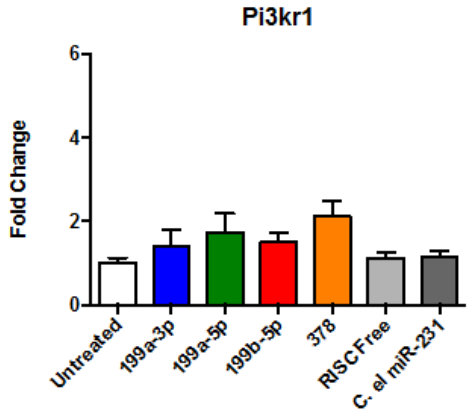
Pi3kr1
Fold Change
0
2
4
6
Untreated
199a-3p
199a-5p
199b-5p
378
RISC Free
C. el miR-231

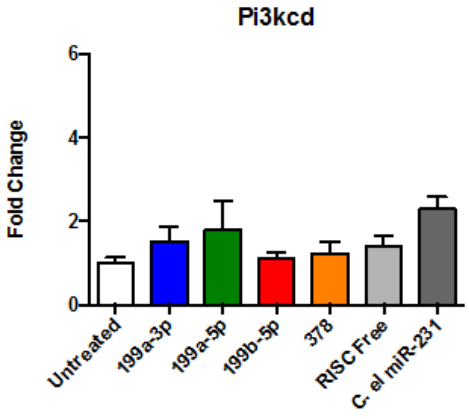
Pi3kcd
Fold Change
0
2
4
6
Untreated
199a-3p
199a-5p
199b-5p
378
RISC Free
C. el miR-231

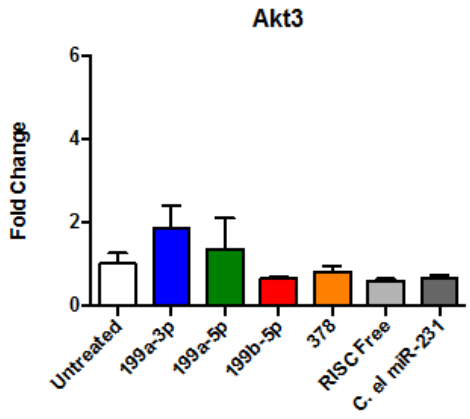
Akt3
Fold Change
0
2
4
6
Untreated
199a-3p
199a-5p
199b-5p
378
RISC Free
C. el miR-231

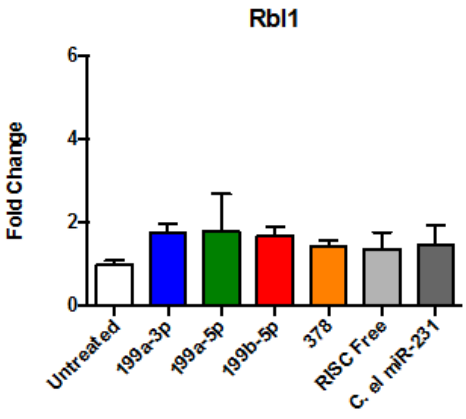
Rbl1
Fold Change
0
2
4
6
Untreated
199a-3p
199a-5p
199b-5p
378
RISC Free
C. el miR-231

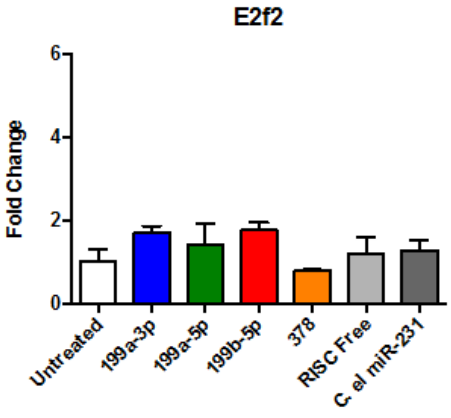
E2f2
Fold Change
0
2
4
6
Untreated
199a-3p
199a-5p
199b-5p
378
RISC Free
C. el miR-231

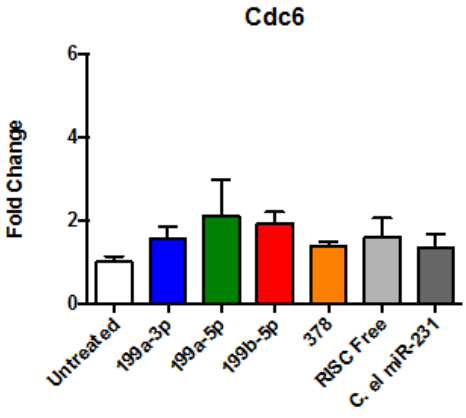
Cdc6
Fold Change
0
2
4
6
Untreated
199a-3p
199a-5p
199b-5p
378
RISC Free
C. el miR-231

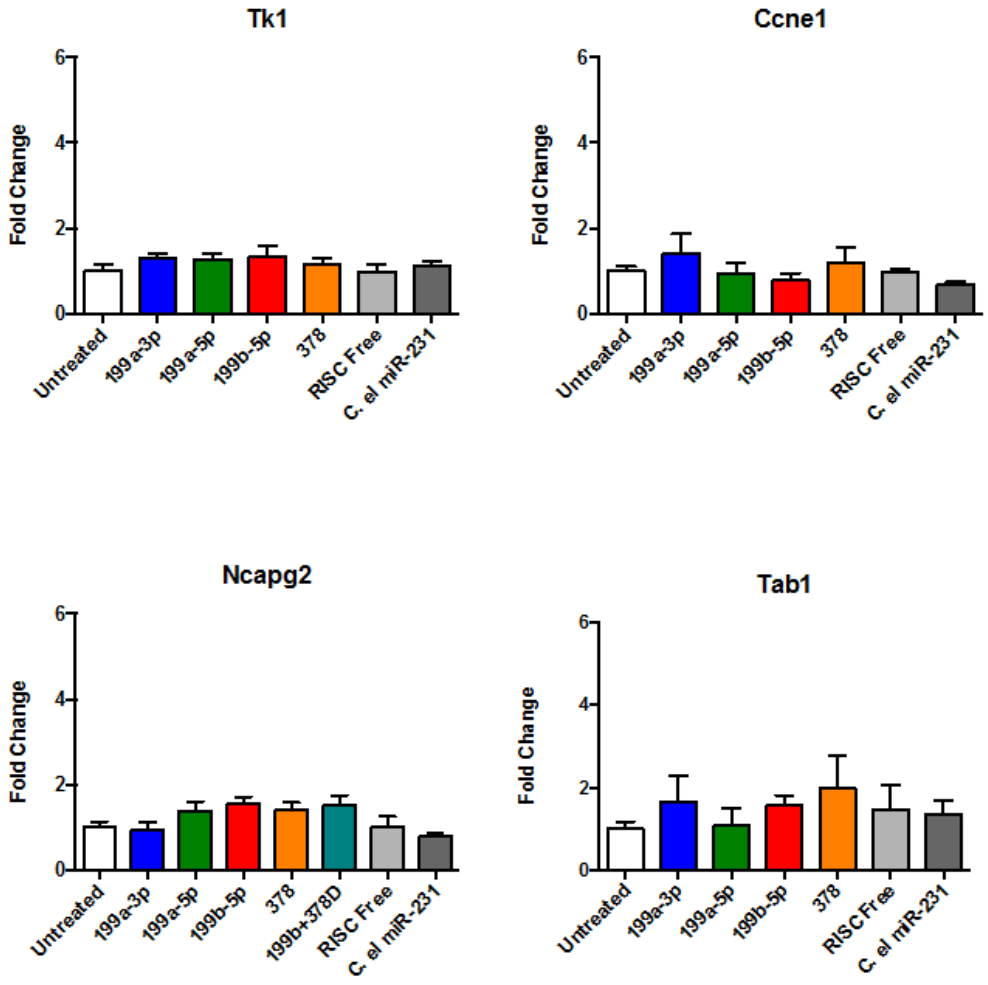

Figure 3.10 Expression of predicted target genes downstream of the insulin/IGF-1 signalling cascade following transfection with miR-199b-5p.

RAW 264.7 cells were either left untreated or transfected with synthetic microRNAs (25nM) for 48 hours. Total RNA was extracted for quantification of expression of transcripts by qRT-PCR. The expression of each gene was normalised to *Gapdh*. Data are presented as mean of fold change ± SEM of three technical replicates compared to cells transfected with RISC Free siRNA and representative of two separate experiments (n=3). Statistical significance was determined using one-way ANOVA (Kruskal Wallis test) (* P< 0.05, ** P< 0.01, *** P< 0.001).

A.

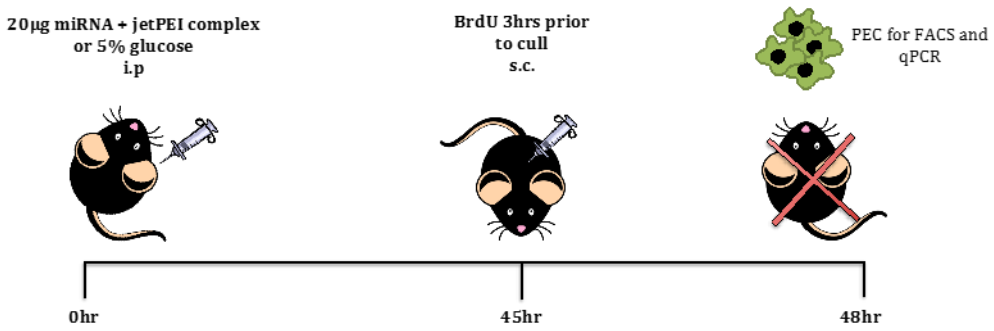
20µg miRNA + jetPEI complex
or 5% glucose
i.p
BrdU 3hrs prior
to cull
s.c.
PEC for FACS and
qPCR
0hr
45hr
48hr

B.

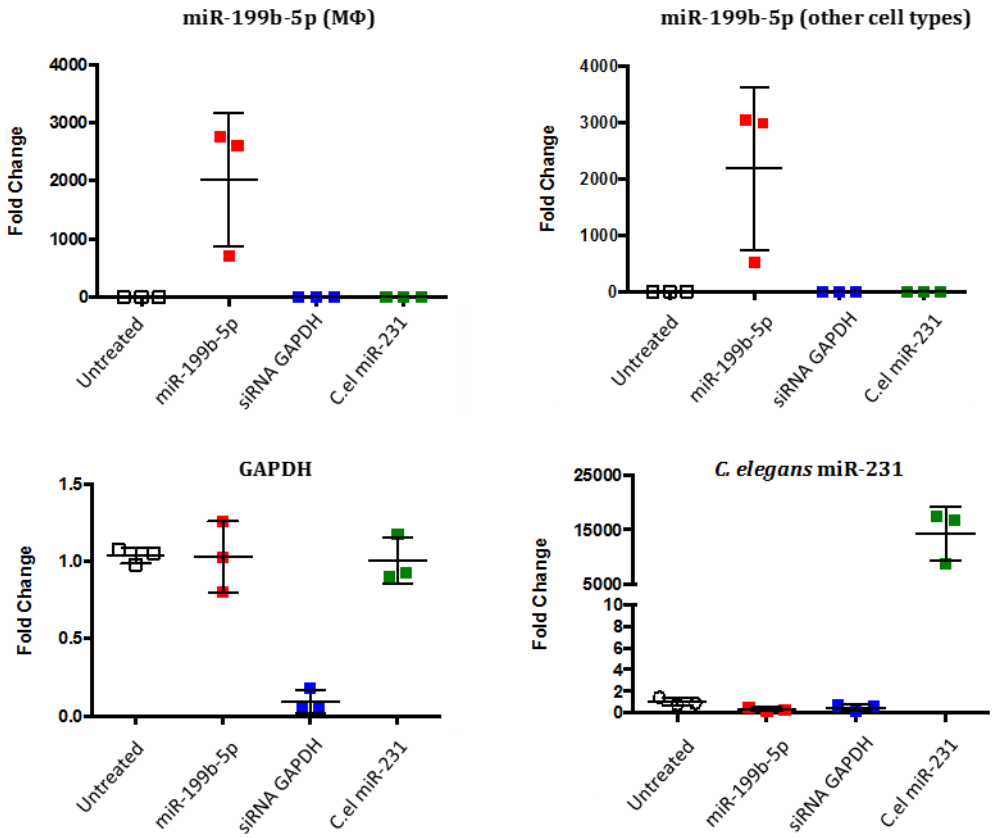
miR-199b-5p (MΦ)
miR-199b-5p (other cell types)
Fold Change
4000
3000
2000
1000
0
Untreated
miR-199b-5p
siRNA GAPDH
C.el miR-231
GAPDH
1.5
1.0
0.5
0.0
C. elegans miR-231
25000
15000
5000
10
8
6
4
2
0

Figure 3.11 Delivery of miR-199b-5p to the peritoneal cavity of mice.

A) WT C57BL/6 mice were injected intraperitoneally with 20µg of microRNA complexed to jetPEI (N:P ratio = 6) in 5% glucose. Control animals received 5% glucose only whereas other groups of mice received either miR-199b-5p or *C. elegans* microRNA as negative control. A microRNA targeting the 3'UTR of GAPDH (siRNA GAPDH) was used as a positive control. Animals were injected with BrdU 3 hours prior to culling. Animals were culled 48 hours post microRNA delivery and peritoneal exudate cells (PEC) were collected via washing of the peritoneal cavity.

B) Quantification of delivered microRNAs in PEC cells. PEC cells were adherence purified for 4 hours to obtain macrophages that were lysed to obtain RNA for qRT-PCR. Cells from the washes of adherence purification were also lysed to collect RNA. The expression of microRNAs was normalized to *RNU6B.* Copy number for miR-199b-5p was determined using a synthetic miR-199b-5p standard of known concentration. Expression of *Gapdh* was normalised to *18s RNA.* Data are presented as mean of fold change ± SEM (n=3) and representative of a single experiment. Statistical significance was determined using one-way ANOVA (Kruskal Wallis test) (* $P< 0.05$, ** $P< 0.01$, *** $P< 0.001$) (n=3).

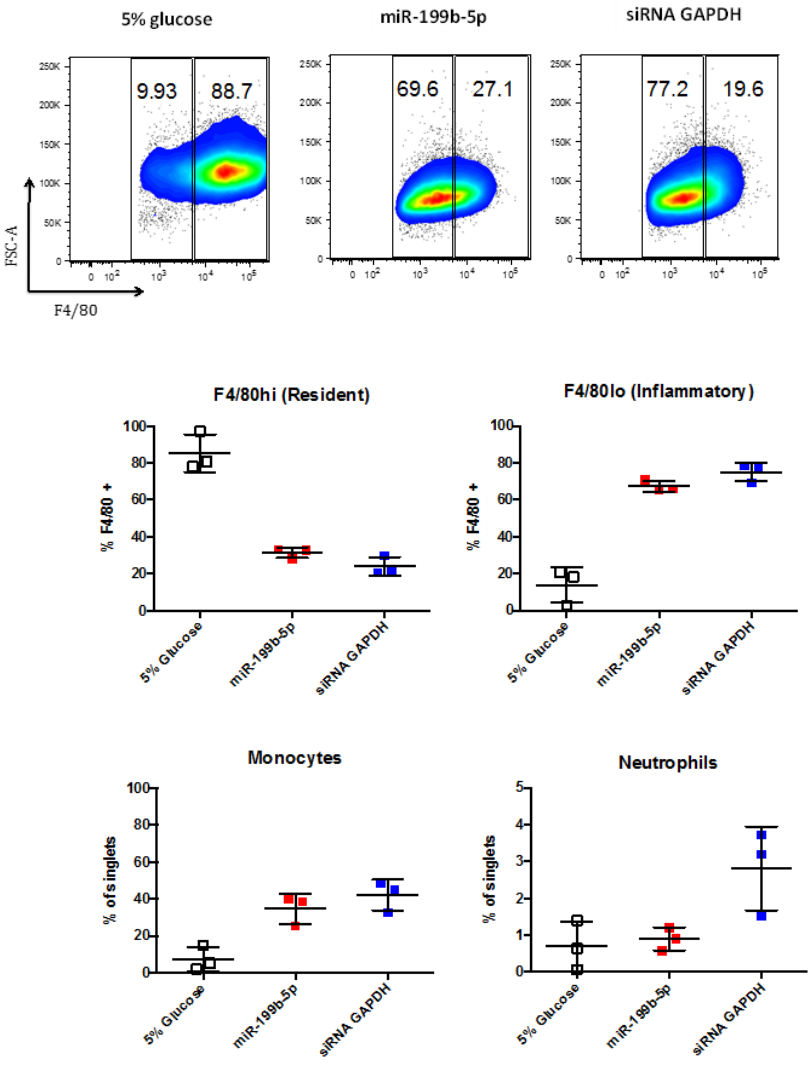

Figure 3.12 Delivery of microRNAs to the peritoneal cavity causes an inflammatory influx resulting in macrophage disappearance.

PEC cells isolated from mice in Figure 3.11A were FACS analysed for identification of immune cell populations. In a naïve mouse, majority of the peritoneal macrophage population is tissue resident derived and expresses high levels of F4/80. This was reflected in the group of mice that received 5% glucose. In contrast, majority of the macrophage population detected in the mice that received the mimic microRNAs was monocyte derived with low F4/80 expression (~70-80%). This was consistent with the influx of monocytes and to a lesser extent neutrophils, which were not present in the control glucose group. Inflammatory influx of these cells resulted in disappearance of the tissue resident macrophages in mice that received miR-199b-5p or siRNA GAPDH. Data are representative of a single experiment (n=3).

A.


0hr
48hr
20µg miRNA + jetPEI complex
or 5% glucose
Intranasal delivery
BAL and lung for
FACS and
qPCR

B.

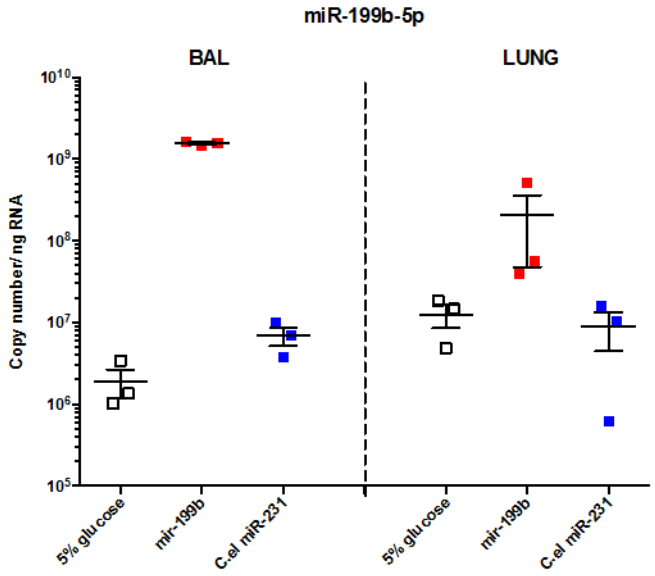
miR-199b-5p
BAL
LUNG
Copy number/ ng RNA
5% glucose
mir-199b
C.el miR-231
5% glucose
mir-199b
C.el miR-231

C.

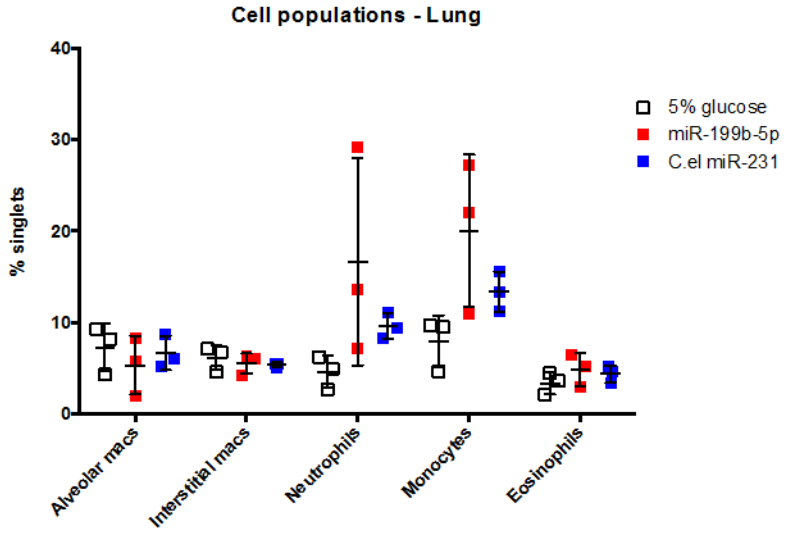

Figure 3.13 A) Delivery of miR-199b-5p to the lung.

WT C57BL/6 mice were administered 20µg of microRNA complexed to jetPEI (N:P ratio = 6) in 5% glucose intranasally. Control animals received 5% glucose only whereas other groups of mice received either miR-199b-5p or a *C. elegans* microRNA as negative control. Animals were culled 48 hours post microRNA delivery and bronchoalveolar lavage (BAL) fluid and whole lung tissue were harvested for FACS analysis and qRT-PCR.

B) Quantification of miR-199b-5p following intranasal delivery in BAL cells and whole lung tissue. BAL cells were lysed to obtain RNA for qRT-PCR whereas whole lung tissue was digested prior to being lysed using a tissue lyser for extraction of RNA. Copy numbers for miR-199b-5p were determined using a synthetic miR-199b-5p standard of known concentration. Data are presented as mean of fold change ± SEM (n=3) and representative of a single experiment.

C) Delivery of microRNAs to the lung does not significantly disrupt the macrophage populations. Whole lung tissue was digested into a single cell suspension. Subsequently, cells were stained with antibodies conjugated to the relevant fluorophores and FACS analysed. Data are representative of a single experiment (n=3).

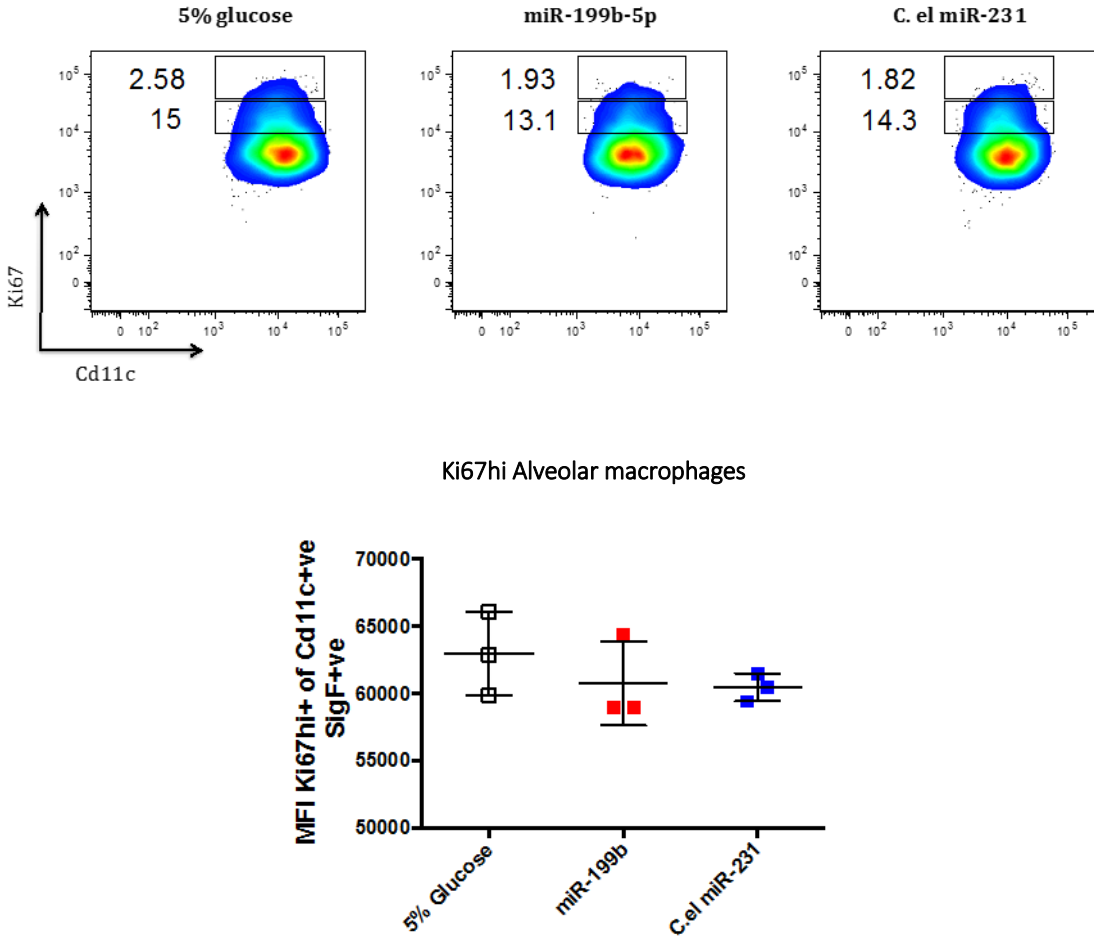

Figure 3.14 miR-199b-5p does not affect basal levels of steady state macrophage proliferation in alveolar macrophages.

Whole lung tissue was digested into a single cell suspension. Cells were stained with antibodies conjugated to the relevant fluorophores and FACS analysed. FACS analysis of alveolar macrophages in whole lung tissue showed no difference in Ki67hi* levels between mice transfected with miR-199b-5p or the *C. elegans* microRNA. Levels of active proliferation in mice that received glucose only were also comparable. *Ki67hi measures active proliferation and is only expressed in cells in the S-phase of the cell cycle. Data are presented are representative of a single experiment (n=3).

A.

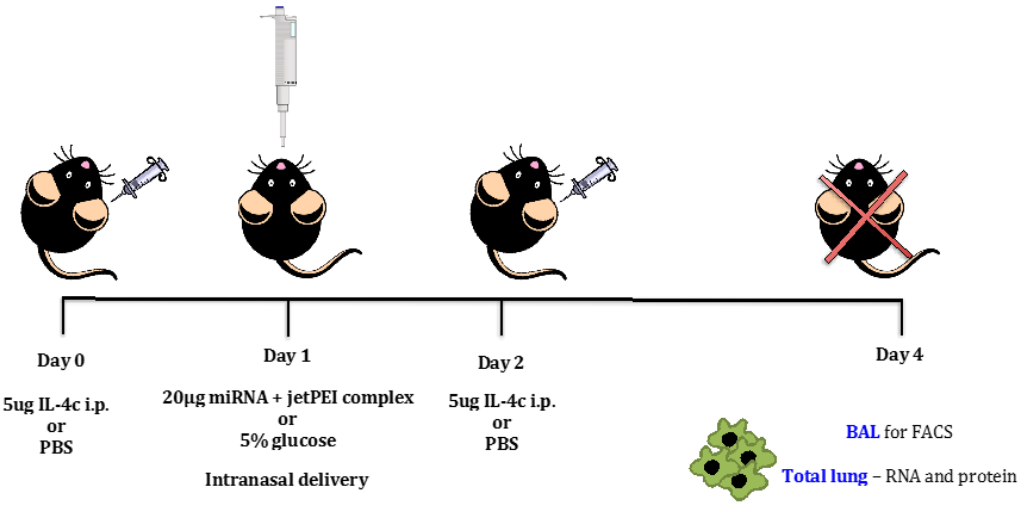
Day 0
5ug IL-4c i.p.
or
PBS
Day 1
20µg miRNA + jetPEI complex
or
5% glucose
Intranasal delivery
Day 2
5ug IL-4c i.p.
or
PBS
Day 4
BAL for FACS
Total lung – RNA and protein

B.

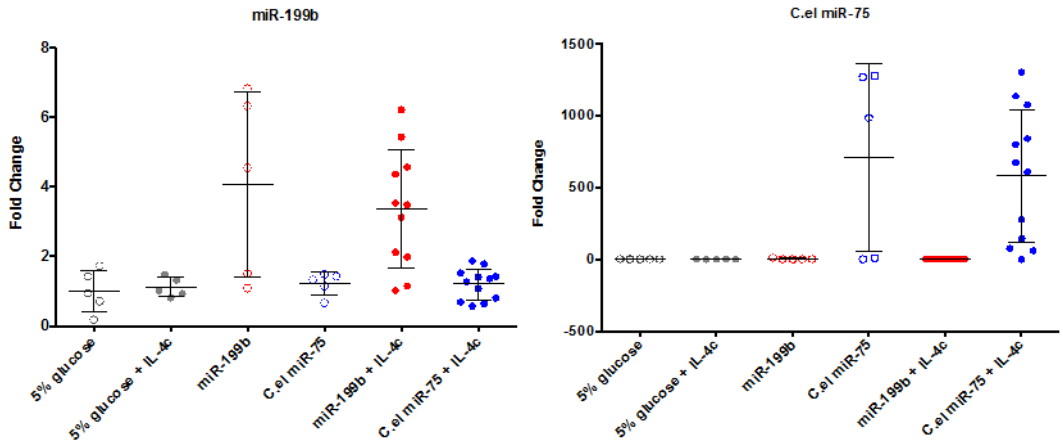
miR-199b
Fold Change
8
6
4
2
0
5% glucose
5% glucose + IL-4c
miR-199b
C.el miR-75
miR-199b + IL-4c
C.el miR-75 + IL-4c
C.el miR-75
Fold Change
1500
1000
500
0
-500
5% glucose
5% glucose + IL-4c
miR-199b
C.el miR-75
miR-199b + IL-4c
C.el miR-75 + IL-4c

C.

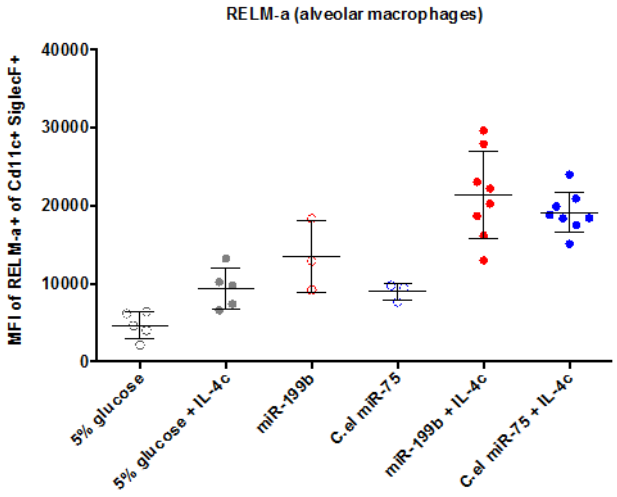

Figure 3.15 A) Experimental design to deliver miR-199b-5p and induce IL-4 driven proliferation in the lung.

WT C57BL/6 mice received two doses of IL-4c at 5µg each on day 0 and day 2 respectively. Mice were administered with 20µg of microRNA complexed to jetPEI (N:P ratio = 8) in 5% glucose intranasally on day 1. Control animals received 5% glucose only whereas other groups of mice received either miR-199b-5p or the *C. elegans* microRNA as a negative control. Animals received 10µg of BrdU subcutaneously 3 hours before they were culled. Animals were culled 48 hours after the final dose of IL-4c. BAL fluid and whole lung tissue were harvested for FACS analysis and qRT-PCR.

B) Quantification of miR-199b-5p following intranasal delivery in whole lung tissue. Whole lung tissue was digested and RNA extracted for qRT-PCR. MicroRNA expression was normalised to *RNU6B.* Fold change was calculated relative to the 5% glucose group.

C) Confirmation of alternative activation in alveolar macrophages following IL-4c delivery. BAL cells were harvested from the mice described in Figure 3.15A and stained with antibodies conjugated to the relevant fluorophores and FACS analysed. RELM-α expression is depicted as median fluorescence intensity in CD11c+ SiglecF+ CD11b$^{lo/-}$ cells classified as alveolar macrophages. Data presented in A, B & C are representative of a single experiment (n=5-12).

A.

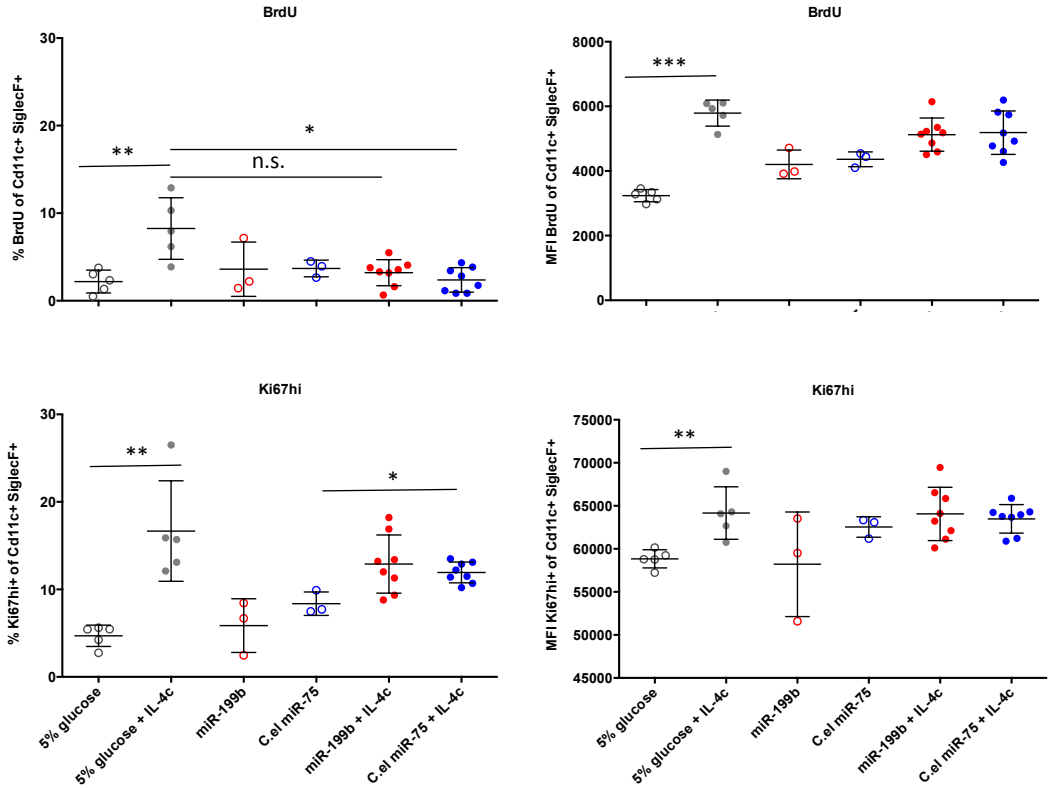
BrdU
% BrdU of Cd11c+ SiglecF+
**
*
n.s.
BrdU
MFI BrdU of Cd11c+ SiglecF+
***
Ki67hi
% Ki67hi+ of Cd11c+ SiglecF+
**
*
Ki67hi
MFI Ki67hi+ of Cd11c+ SiglecF+
**
5% glucose
5% glucose + IL-4c
miR-199b
C.el miR-75
miR-199b + IL-4c
C.el miR-75 + IL-4c

B.

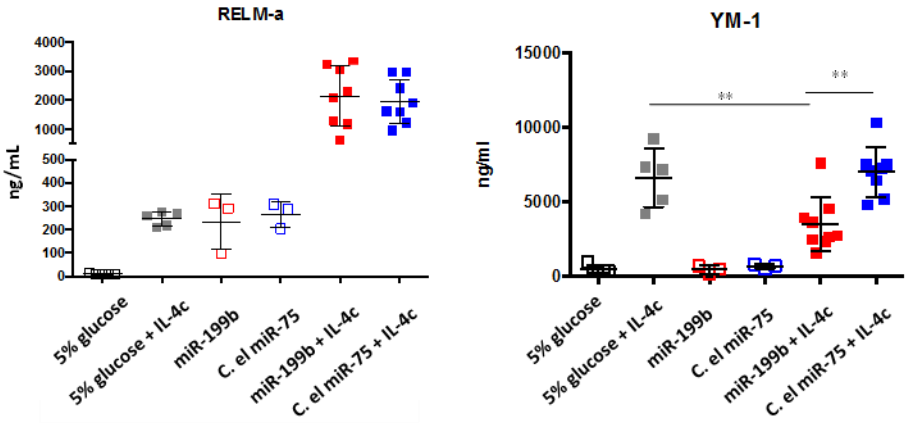
RELM-a
ng/mL
YM-1
ng/ml
**
**
5% glucose
5% glucose + IL-4c
miR-199b
C. el miR-75
miR-199b + IL-4c
C. el miR-75 + IL-4c

Figure 3.16 A) BrdU and Ki67hi levels in alveolar macrophages as measures of active cell proliferation by flow cytometry.

BAL cells were harvested from mice injected with PBS or IL-4c along with administration of synthetic microRNAs as described in Figure 3.15A. BAL cells were stained for Ki67 and BrdU incorporation and FACS analysed. Data are presented as percentage positivity within alveolar macrophage populations and representative of a single experiment (n=5-12). Statistical significance was determined using one-way ANOVA (Kruskal Wallis test) (* P< 0.05, ** P< 0.01, *** P< 0.001)

B) Quantification of alternative activation proteins in BAL supernatant following microRNA and PBS or IL-4c delivery. BAL cells were harvested from the mice described in Figure 3.15A and centrifuged to obtain supernatants, which were subsequently subject to quantification by ELISA. Statistical significance was determined using one-way ANOVA (Kruskal Wallis test) (* P< 0.05, ** P< 0.01, *** P< 0.001). Data are presented as percentage positivity within alveolar macrophage populations and representative of a single experiment (n=5-12).

Chapter 4: Alternative activation and proliferation of macrophages in the absence of miR-378

SUMMARY:

The Allen lab has previously shown that miR-378-3p expression is associated with AAMΦ through targeting of AKT-1. Intact AKT-1 signalling is an essential component for IL-4 driven macrophage proliferation and despite the knowledge that AKT-1 is a direct target of miR-378-3p, the direct influence of this microRNA on the regulation of AAMΦ is still unknown. In this chapter, the consequences of the deficiency of the microRNAs miR-378-3p and miR-378-5p on AAMΦ in mice have been addressed. Various AAMΦ conditions, both *in vitro* and *in vivo*, were studied to elucidate the ability of macrophages isolated from WT, heterozygous and KO animals to alternatively activate. The influence of miR-378 deficiency on IL-4 induced proliferation was also addressed *in vivo*. Although the lack of miR-378 had no significant effect on IL-4 driven macrophage proliferation, results from this chapter support a role for miR-378 in the regulation of alternative activation through an impact on YM-1 and RELM-α expression. Lastly, we also utilised *Litomosoides sigmodontis*, a murine model of filarial infection, to determine whether this regulation by miR-378 had functional consequences.

4.1 Introduction

Tumour associated macrophages, which display an M2 phenotype and some characteristics of AAMΦ, are known to contribute to angiogenesis and play a dual role during development, tissue injury and regeneration (Sunderkotter et al., 1994, Lamagna et al., 2006, Ribatti et al., 2007, Nucera et al., 2011). The importance of microRNAs in angiogenesis and endothelial function has previously been shown through the disruption of Dicer and Drosha – two key enzymes for microRNA biogenesis (Kuehbacher et al., 2007). Endothelial specific deletion of Dicer in mice has provided evidence that microRNAs are required for postnatal angiogenesis in response to angiogenic stimuli (Suarez et al., 2008). MiR-378 is a well-known angiomiR with an established role in tumour angiogenesis (Urbich et al., 2008, Chen et al., 2012b, Chan et al., 2014). In mice, four isoforms of miR-378 (a-d) have been reported, with miR-378a being the only isoform that gives rise to both miR-378-5p (or miR-378*) and 3p. Whilst miR-378b gives rise to mature miR-378-3p only, both miR-378c/d give rise to miR-378-5p only. MiR-378 is enriched in CD34+ haematopoeitic progenitor cells and increases cell survival whilst reducing cell death (Wang and Olson, 2009). Vascular endothelial growth factor (VEGF) plays a fundamental role as a key regulator of angiogenesis (Ferrara, 2001, Ferrara and Gerber, 2001). MiR-378-5p and miR-125a share the same seed region and miR-378 promotes VEGF expression by competing with miR-125a for binding sites in the VEGF 3'UTR (Hua et al., 2006). MiR-378 also enhances angiogenesis in tumour progression by targeting Suppressor of fused (Sufu) and Fus-1, which are both tumour suppressors (Lee et al., 2007). Sufu is a negative regulator of Shh signalling. Vessels induced by Shh are characterised by expression of angiogenic cytokines, including VEGF and angiopoietin-1 and 2, and have large diameters (Wang and Olson, 2009).

As reviewed already in the introductory chapter, AAMΦ are key orchestrators of metabolism (Odegaard and Chawla, 2011, Biswas and Mantovani, 2012). MiR-378 has previously been reported to control glucose and lipid homeostasis (Fernandez-Hernando et al., 2011, Liu et al., 2014). Peroxisome proliferator-activated receptors (PPARs) transcriptionally regulate alternative macrophage activation and hence, lipid

metabolism (Chawla et al., 2001, Odegaard et al., 2007, Chawla, 2010). Interestingly, miR-378 is embedded within the parent gene *Ppargc1b*, which encodes PGC-1β, a transcriptional regulator of oxidative energy metabolism. MiR-378 is known to counterbalance these metabolic actions of PGC-1β through the control of mitochondrial metabolism and systemic energy homeostasis (Eichner et al., 2010, Carrer et al., 2012).

The major objective of this thesis is to identify microRNAs associated with alternative activation in macrophages and to understand their contribution in the regulation of this phenotype. As described in chapter 2, the expression profiles of ten microRNAs highly regulated by IL-4 were studied under various conditions of alternative activation. From these studies, the expression of miR-378 was identified as being strongly associated with AAMΦ (Figure 2.9, Chapter 2). Our lab has previously shown that miR-378-3p has the capacity to negatively modulate AKT-1 expression, thereby potentially regulating IL-4 induced proliferation of AAMΦ (Ruckerl et al., 2012). However, a caveat in this study was the inability to demonstrate a direct effect of miR-378-3p on IL-4 driven proliferation of macrophages. Instead, following its validation as a direct target of miR-378-3p, AKT-1 expression was blocked with triciribine treatment *in vivo*. This resulted in a reduction in IL-4 induced proliferation as well as alternative activation (Ruckerl et al., 2012).

Work in this chapter, therefore, aims to study the direct effects of miR-378 on IL-4 driven activation and proliferation of macrophages that may in turn contribute to the various effector functions of AAMΦ. To this end, mice genetically lacking miR-378 (miR-378-3p) and miR-378* (miR-378-5p) (obtained from the Olson lab) were utilised. The contribution of miR-378 to the activation, maintenance and proliferation of AAMΦ was investigated both *in vitro* and *in vivo* under varying conditions of alternative activation.

4.2 Results

4.2.1 Validation of mice genetically lacking miR-378/378*

MiR-378 knockout (miR-378 KO) mice were obtained from the Olson lab. The null allele of miR-378/miR-378* was generated using a targeting vector containing a neomycin resistance gene. This neomycin resistance gene was flanked by loxP sites and a diphtheria toxin gene cassette and its expression driven by the pGK promoter. The miR-378/378* targeting strategy was designed to replace the premiR sequence with the neomycin resistance cassette flanked by loxP sites. The targeting vectors were electroporated into 129SvEv-derived ES cells and analysed for homologous recombination. Selected clones were injected into C57BL/6 blastocysts. High-percentage chimeric male mice were crossed to C57BL/6 females to achieve germline transmission of the targeted allele. Mice heterozygous for neomycin were crossed with CAG-Cre-transgenic mice to remove the cassette (Carrer et al., 2012).

Prior to conducting any experiments on mice deficient in miR-378, an initial validation was carried out to confirm the expression levels of known miR-378 targets described in the literature. Carrer *et al.* from the Olson lab previously reported miR-378 and miR-378* as integral components of a regulatory circuit that functions under conditions of metabolic stress to control systemic energy homeostasis. They have shown that carnitine O-acetyltransferase (CRAT), a mitochondrial enzyme involved in fatty acid metabolism, and MED13, a component of the Mediator complex that controls nuclear hormone receptor activity, are repressed by miR-378 and miR-378*, respectively (Carrer et al., 2012). CRAT and MED13 were, therefore, chosen as validated targets to confirm the functionality of miR-378/378* deficiency in these genetically altered mice in our husbandry conditions.

Peritoneal exudate cells were harvested from the peritoneal cavity of naïve wild type (WT), heterozygous (Het) and knockout (KO) mice. Peritoneal tissue resident macrophages were then adherence purified for 4 hours before being subject to RNA extraction. As expected, qRT-PCR analysis of this macrophage population revealed significantly higher levels of miR-378 in WT mice in comparison to the

heterozygous animals (Figure 4.1A). Essentially no expression of miR-378 was found in macrophages harvested from the KO animals. Levels of CRAT and MED13 were also measured in the same samples. Significantly elevated levels of both CRAT and MED13 were observed in both heterozygous and KO mice when compared to the WT animals (Figure 4.1B). Even though significant differences were observed between the WT and heterozygous animals with a 2 fold and ~5 fold change for CRAT and MED13 respectively, the disparity between the WT and KO mice was much greater with CRAT levels being 4 fold higher and MED13 levels being nearly 15 fold higher in macrophages isolated from the KO mice.

4.2.2 Alternative activation of bone marrow derived macrophages in the absence of miR-378

Having validated the absence of miR-378 and modulation of known targets in these mice, the next aim of this study was to address the kinetics of alternative activation in the absence of this microRNA. Bone marrow derived macrophages (BMDM) were chosen for the initial study as they present a homogeneous primary macrophage population that is relatively simple to generate *in vitro* and possesses all the characteristics of AAMΦ, except proliferation, when stimulated with IL-4 and IL-13. Bone marrow precursors were isolated from WT, heterozygous and KO mice and cultured in L929 conditioned medium containing CSF-1 for 7 days to generate BMDMs. These BMDMs were seeded and stimulated with 20ng/mL of IL-4 and IL-13 to obtain AAMΦ. Of note, no differences were observed in cell viability and total cell numbers between the different genotypes. Cells were harvested at 24 and 48 hours post stimulation and subject to intracellular staining for FACS analysis and supernatants were collected for measuring secreted protein levels by ELISA (Figure 4.2A).

Due to lack of sufficient mouse numbers from each genotype at the time, experiments between heterozygous and KO mice and WT and KO mice were carried out separately as shown in Figure 4.2B and 4.2C. For FACS analysis, macrophages

were gated based on CD11b and F4/80 expression. Intracellular staining for both RELM-α and YM-1 revealed differences in expression between heterozygous and KO mice, with expression levels being higher in the KO mice as indicated by the percentage of macrophages expressing these proteins in Figure 4.2B. Approximately 40-45% of macrophages isolated from heterozygous mice were positive for RELM-α. In comparison, around 60% of the macrophages harvested from KO mice expressed RELM-α. These differences were also reflected in the levels of secreted protein, with the heterozygous BMDMs producing 1.5 fold lower levels of RELM-α (~150ng/mL) when compared to macrophages isolated from the KO animals (250ng/mL) as shown in Figure 4.2B. Similar to RELM-α, YM-1 was also expressed by ~40% macrophages isolated from heterozygous animals. In the KO animals, the expression of YM-1 was comparatively higher, with approximately 45% of the BMDMs positive for this protein. Reflecting the intracellular staining results, significant differences were also observed in levels of secreted YM-1 as measured by ELISA. BMDMs from the KO mice produced twice as much YM-1 as that produced by macrophages from heterozygous mice (Figure 4.2B). Similar results were obtained for samples harvested 48 hours post stimulation (data not shown).

An identical comparison was also carried out between BMDMs generated from either WT or KO mice. However, as reflected in Figure 4.2C, expression levels of RELM-α and YM-1 observed were much lower, possibly due to staining and/or other experimental conditions. Nonetheless, results suggested a similar trend for increased RELM-α and YM-1 expression in BMDMs from KO mice when compared to WT (Figure 4.2C). Macrophages derived from KO animals showed a 3 fold increase in the percentage of cells positive for RELM-α expression when compared to the WT controls. Similarly, a nearly 2 fold increase in secreted RELM-α levels was also observed. Contrastingly but in agreement with previous findings from the last experiment, no significant differences were observed in the percentage of macrophages expressing intracellular YM-1, but secreted YM-1 levels were 2 fold greater in BMDMs from KO mice. (Figure 4.2C).

The experiment described above was then repeated with BMDMs derived from WT, heterozygous and KO mice in a single experiment. Intracellular staining of macrophages for RELM-α at 24 hours revealed a similar pattern of expression as observed previously. In particular ~20% of macrophages from WT mice were positive for RELM-α expression in comparison to approximately 40% and 55-60% of macrophages derived from heterozygous and KO animals, as depicted in Figure 4.2D. Quantification of secreted RELM-α protein also displayed a similar trend with significantly higher RELM-α expression in BMDMs isolated from heterozygous and KO mice (~2 and 3 fold respectively). Additionally, a greater percentage of macrophages derived from mice lacking miR-378 were positive for YM-1 expression (Figure 4.2D) whereas no differences were observed in the number of macrophages expressing YM-1 from WT and heterozygous mice. In agreement with this, the amount of YM-1 detected in the supernatant harvested from KO BMDMs was twice as much as the amount detected in samples from the WT and heterozygous BMDMs (Figure 4.2D). As represented in Figure 4.2E, samples harvested 48 hours post stimulation with IL-4 and IL-13 also exhibited similar expression profiles for both RELM-α and YM-1 when stained intracellularly. Although the levels of secreted RELM-α were still significantly higher in the supernatants harvested from miR-378 KO BMDMs at 48 hours, contrary to the differences observed at 24 hours, levels of YM-1 observed at 48 hours were indistinguishable between samples (Figure 4.2E). Taken together, these results suggest that in the absence of miR-378, the kinetics of alternative activation in BMDMs appear to be disrupted. This was reflected by the fact that levels of both YM-1 and RELM-α were significantly higher in mice lacking miR-378 at 24 hours post IL-4/13 stimulation. However, although these differences in RELM-α expression are still distinguishable after 48 hours, the effect of miR-378 deficiency on YM-1 expression was much less evident. In addition, the lack of miR-378 was also assessed in alternatively activated Thio MΦ. The results from these experiments involving Thio MΦ confirmed and supported the findings from BMDMs above (data not shown). A detailed discussion of the kinetics of alternative activation in Thio MΦ is covered later in this chapter.

4.2.3 IL-4 induced proliferation in the absence of miR-378

From the above experiments it is clear that there are differences in the kinetics of alternative activation in BMDMs derived from mice deficient in miR-378 compared to WT or heterozygous controls. Until now, the conditions of alternative activation utilised were restricted to stimulation of primary macrophages *in vitro* that do not proliferate in response to IL-4. As mentioned earlier, miR-378 suppresses AKT-1; a factor important for enhancement of alternative activation and essential for IL-4 induced macrophage proliferation (Ruckerl et al., 2012). Hence, the next goal of this study was to address the effect of miR-378 deficiency on IL-4 driven proliferation *in vivo*. To this end, WT or miR-378 KO mice were injected with a single dose of PBS or 5µg IL-4c intraperitoneally (Figure 4.3A). Heterozygous mice were not used in this experiment as a sufficient number of these mice were not available. However, experimental repeats including mice heterozygous for miR-378 are described in the next section. Tissue resident peritoneal macrophages alternatively activate and proliferate in response to IL-4c injection. Proliferation peaks at 42 hours post delivery and begins to decline around 72 hours. Thus, mice were sacrificed at 42 hours and 72 hours post IL-4c delivery. Mice were also injected with BrdU subcutaneously as a measure for active proliferation 3 hours prior to being culled. Peritoneal exudate cells (PEC) were harvested through washing of the peritoneal cavity. The PEC was divided and cells were either stained directly for FACS analysis or adherence purified at 37°C for 4 hours and lysed for RNA extraction. Supernatants were also harvested for protein quantification by ELISA (Figure 4.3A).

With the dependency of IL-4 driven proliferation on AKT-1 and the negative modulation of AKT-1 expression by miR-378, it was hypothesised that in the absence of miR-378, IL-4 induced proliferation would be enhanced. Active proliferation following IL-4c delivery was measured through the expression of BrdU and Ki67hi by peritoneal macrophages. Macrophages were identified based on CD11b and F4/80 expression by FACS. At 42 hours post injection, no changes were observed in the percentage of macrophages expressing BrdU or Ki67hi. Approximately 40% of peritoneal macrophages isolated from both WT and miR-378 KO mice stained positive for BrdU whereas ~ 20% of the F4/80+ population was

positive for Ki67hi expression (Figure 4.3B). Contrary to our hypothesis, the percentage of miR-378 KO macrophages expressing BrdU at 72 hours post IL-4c delivery was in fact lower than the percentage of WT macrophages expressing BrdU (10% versus ~5%). Compared to the PBS injected controls, a sub population of WT macrophages was still actively proliferating at this time point, whereas no differences were observed between the PBS and IL-4c injected groups in miR-378 KO mice (Figure 4.3B). A similar trend was observed with percentage positivity for Ki67hi, with ~ 20% of the macrophages still actively proliferating whilst the macrophages isolated from miR-378 KO mice had stopped proliferating at 72 hours as shown in Figure 4.3B.

In the same experiment, the levels of RELM-α and YM-1 proteins were also measured. No significant differences were observed in the percentage of macrophages expressing RELM-α between the WT and KO groups at both 42 and 72 hours post IL-4c delivery (Figure 4.3B). We observed very high levels of RELM-α expression in miR-378 KO mice in the absence of IL-4c at the 42 hour time point. However, the lack of RELM-α protein in the supernatants isolated from the peritoneal washes of these PBS injected control mice (as measured by ELISA) suggested this was an artefact of FACS staining. In agreement with the FACS results, no changes were observed in RELM-α protein between the WT and KO groups injected with IL-4c. Similarly, YM-1 expression was quantified in the supernatants and no noticeable differences were observed between samples obtained from mice regardless of a deficiency in miR-378.

The experiment described above was repeated with mice that were either WT, heterozygous or deficient in miR-378 (Figure 4.4A). Mice were injected with either PBS or 5μg IL-4c intraperitoneally and samples harvested at 42 and 72 hours post injection. In agreement with the previous experiment, a trend towards a lower rate of proliferation in macrophages isolated from mice lacking miR-378 was observed. However, no differences were observed in proliferation between macrophages obtained from WT or heterozygous mice (Figure 4.4B). Analysis of expression of YM-1 and RELM-α revealed no difference between the three groups at 42 hours post delivery, however, once again a slight trend towards increased number of

macrophages expressing YM-1 and RELM-α was observed at 72 hours. With only 3 mice at this time point in the KO group, these differences were not statistically significant (Figure 4.4B). Contrary to the results obtained for the intracellular staining of YM-1 and RELM-α wherein no differences were observed at 42 hours, secreted levels of YM-1 were significantly higher in miR-378 KO mice compared to the WT and heterozygous groups (Figure 4.4C). This difference in YM-1 expression at 42 hours was lost by 72 hours. Contrastingly no significant differences were found in the expression of RELM-α at 42 hours, but samples harvested from heterozygous and KO mice displayed significantly elevated levels at 72 hours when compared to the WT mice. It is important to note that the statistical analysis was underpowered due to limitations in animal numbers, thereby making it difficult to assess subtle effects that microRNAs are usually associated with.

When IL-4c is injected into the peritoneal cavity, a small proportion of the recombinant IL-4 is also transported to the pleural cavity. The tissue resident populations in both the peritoneal and pleural cavity respond similarly to IL-4 resulting in the alternative activation, proliferation and accumulation of the local macrophage population. Thus, in a separate experiment, pleural exudate cells (PLEC) were harvested, along with peritoneal macrophages to compare the activation and proliferation states of the resident macrophage populations in these cavities in the absence of miR-378 (Figure 4.5A). Because no significant differences were observed between the WT and heterozygous mice in the last two experiments involving peritoneal macrophages, only heterozygous and KO mice were used in this experiment. First, the peritoneal macrophage population was analysed. As shown in Figure 4.5B, consistent with the previous results in peritoneal macrophages, no significant differences were found in the intracellular levels of Ki67hi, RELM-α or YM-1 in peritoneal macrophages at both 42 and 72 hours following IL-4c delivery. However, once again, differences were observed in the amount of secreted RELM-α and YM-1 with the miR-378 KO mice producing greater quantities of both proteins, notably at 72 hours post IL-4c injection (Figure 4.5C).

Next, the macrophage population isolated from the pleural cavity was analysed. Mirroring the results obtained from the tissue resident population in the peritoneal

cavity, no differences were observed in the percentage of macrophages positive for Ki67hi, RELM-α and YM-1 in the pleural cavity at both 42 and 72 hours following IL-4c treatment (Figure 4.5D). Consistent with the results from the peritoneal cavity, macrophages from the pleural cavity of mice lacking miR-378 also produced higher quantities of secreted RELM-α and YM-1 proteins compared to the heterozygous group of mice as represented in Figure 4.5E.

Cumulatively, data from these three independent experiments suggest that the differences observed between mice deficient in miR-378 and those with miR-378 partially or completely intact, particularly in case of characteristic markers of alternative activation, appear to be transient and time dependent. Whilst a time dependent increase in alternative activation was observed, the lack of miR-378 had no significant effect on IL-4 driven proliferation but a possible unexpected suppression in some experiments instead.

4.2.4 Kinetics of alternative activation in thioglycollate elicited macrophages in miR-378 deficient mice

Having verified that some differences exist in the alternative activation of macrophages in the absence of miR-378, we next sought to investigate whether these differences were the result of accumulation of small differences over time or an initial defect in activation. To this end, we utilised inflammatory Thio MΦ to perform a time course experiment. Besides their ability to alternatively activate *in vitro,* injection of thioglycollate into the peritoneal cavity results in the rapid recruitment of a large number of inflammatory macrophages sufficient to fill the need for a substantial number of cells in this experiment. WT, heterozygous or KO mice were injected with 4% thioglycollate intraperitoneally as depicted in the schematic in Figure 4.6A. Three days following injection, PEC was harvested and Thio MΦ adherence purified for 4 hours. These Thio MΦ were then stimulated with 20ng/mL of IL-4/IL-13. Supernatants were harvested at 2hr, 4hr, 6hr, 8hr, 10hr, 12hr, 16hr and 24hr post stimulation. Quantification of both YM-1 and RELM-α by

ELISA revealed that the differences observed previously between the KO and WT mice were due to an accumulation of minor differences in expression/secretion over time. As detailed further in Chapter 5, we have shown that expression of RELM-α and YM-1 at the transcript level is initiated at 6-8 hours post stimulation with IL-4 and IL-13. Thus, it is expected that protein will be produced at about 8-10 hours post stimulation. Consistent with this assumption, both RELM-α and YM-1 proteins were readily detectable by 12 hours post stimulation as shown in Figure 4.6B. Overall, the findings from this time course support both the *in vitro* and *in vivo* data discussed in the previous sections of this chapter.

4.2.5 Functional significance of miR-378 in a murine model of filarial infection

So far, this study has shown that the normal kinetics of alternative activation are altered in the absence of miR-378. To address the function of miR-378 as a regulator of alternative activation, a murine model of filarial infection was utilised. Mice either WT, heterozygous or KO for miR-378 were infected with 30 infective L3 larvae of *Litomosoides sigmodontis* (Figure 4.7A). As described previously in the introductory chapter and Chapter 2, *L. sigmodontis* is a nematode that migrates to the pleural cavity and induces a T_H2 response. AAMΦ are a distinguishing feature of inflammation driven by helminth infections. As the larvae enter the pleural cavity, the tissue resident pleural macrophages undergo alternative activation and also proliferate in response to IL-4 (Chapter 2, Figure 2.7). Due to limitations in mouse numbers, a single time point of day 8 was chosen for harvest. The main aim of this study was to delineate the functional significance of miR-378 during an infection. At day 8-post infection, macrophages in the cavity are alternatively activated and beginning to switch from CSF-1 dependent steady state proliferation to IL-4 driven proliferation (Jenkins et al., 2011, Jenkins et al., 2013). We reasoned that at day 8, the subtle differences in activation and/or proliferation between the control mice and mice lacking miR-378 would be most evident. Since the effects observed both *in*

vitro and *in vivo* appeared to be transient and time dependent, the small differences may not be discernable at later time points.

Mice were culled on day 8 and PLEC isolated from all three groups of mice, namely WT, heterozygous and KOs. Cells were stained and subject to FACS analysis whilst supernatants were used for quantification of secreted YM-1 and RELM-α. FACS analysis of pleural macrophages characterised by CD11b and F4/80 expression revealed no differences between the three groups of mice in terms of percentage positivity for Ki67, RELM-α or YM-1. Consistent with the intracellular expression of RELM-α and YM-1, no significant differences were observed between mice lacking miR-378 and control WT or heterozygous mice. In conclusion, these results suggest that miR-378 is not crucial for the activation and proliferation dynamics of pleural macrophages during *L. sigmodontis* infection, at least at day 8 post infection.

4.3 Discussion

Our lab has previously indicated that miR-378 may potentially negatively regulate IL-4 driven proliferation and to an extent also alternative activation of macrophages through the modulation of its direct target AKT-1 (Ruckerl et al., 2012). To date, this is the only study linking miR-378 to the regulation of AAMΦ responses. However, the effects of miR-378 shown through the use of an AKT-1 inhibitor were indirect evidence to support this hypothesis. Just like a single microRNA has the ability to regulate several hundred genes, an mRNA may also be targeted by many microRNAs, making fine-tuning of targets a complex relationship. Hence, the phenotype observed by Ruckerl *et al.* upon inhibition of AKT-1 could potentially have been the result of abrogation of regulation by additional microRNAs and mechanisms beyond miR-378. In this chapter, we have shown for the first time the direct effects of miR-378 deficiency on the regulation of AAMΦ and their responses.

The effects of miR-378 deficiency on alternative activation were first examined *in vitro*. BMDMs derived from WT, heterozygous or miR-378 KO mice were stimulated with IL-4/IL-13 for up to 48 hours. Levels of both intracellular and secreted RELM-α and YM-1 were enhanced in the KO mice when compared to the WT and heterozygous controls. Although no significant changes were observed in YM-1 expression between the WT and heterozygous animals, changes in RELM-α levels were evident between these two groups. This in line with the findings of Ruckerl *et al.* wherein *in vitro* inhibition of AKT-1 with triciribine in alternatively activated Thio MΦ results in abrogation of *Retnla* (RELM-α) expression but only partial inhibition of *Chi3l3* (YM-1) (Ruckerl et al., 2012). Additionally, although alternative activation is a STAT6 dependent process (Gordon and Martinez, 2010), the regulation of RELM-α and YM-1 may differ downstream with greater dependency of molecular regulation on miR-378 resulting in a more profound effect on expression of one over the other in miR-378 deficient mice.

In the previous study, Ruckerl *et al.* showed that the most prominent effect of AKT-1 inhibition (as an indirect measure of the effect of miR-378) is on IL-4 driven proliferation of macrophages. In their experiment, mice received vehicle control or

triciribine, an AKT-1 specific inhibitor, intraperitoneally 1 hour prior to the injection of IL-4c. This pre-treatment with triciribine completely abrogated IL-4 induced proliferation. Simultaneously, protein levels of RELM-α were partially reduced whereas YM-1 expression remained unaffected. Thus, in our study, to address whether miR-378 has a direct primary function in the regulation of IL-4 driven proliferation, mice were injected with IL-4c intraperitoneally to induce alternative activation and proliferation of tissue resident peritoneal macrophages. As expected, delivery of recombinant IL-4 resulted in expansion of the local macrophage population (Jenkins et al., 2011, Jenkins et al., 2013). It was predicted that in the absence of miR-378, full repression of AKT-1 would not occur as it would in the WT mice leading to a higher rate of AAMΦ proliferation in the KO mice. However, no difference was observed in the extent of active macrophage proliferation between WT, heterozygous or KO animals as measured by BrdU and Ki67hi levels. It is not surprising that triciribine treatment did not directly mimic miR-378 deficiency. MicroRNAs are well established as key players in the regulation of cell cycle and proliferation (Hwang and Mendell, 2006, Zhang et al., 2007, Bueno and Malumbres, 2011, Wang and Blelloch, 2011). Combinatorial targeting (Hon and Zhang, 2007) and microRNA synergistic networks (Xu et al., 2011) are a key feature in microRNA repression of gene expression. Often microRNAs (or a single microRNA) do not induce complete knockdown of their targets (Xiao and Rajewsky, 2009) and act in families targeting an entire signalling pathway rather than individual members leading to a general suppression (Guo et al., 2010). Furthermore, competition between microRNAs for target sites also shapes post-transcriptional gene regulation (Jens and Rajewsky, 2015). Hence, it is highly plausible that the lack of miR-378 is compensated for by other microRNAs involved in the regulation of macrophage proliferation. This may also be reflected in the fact that a trend towards reduced proliferation was noticeable in the KO mice when compared to controls.

In addition to its effects on proliferation, AKT-1 also influences alternative activation. Therefore, the levels of RELM-α and YM-1 were also measured following IL-4c injection. RELM-α expression was significantly higher in the KO mice compared to both WT and heterozygous animals. Samples obtained from the

heterozygous mice also exhibited greater levels of secreted RELM-α compared to WT controls. However, these differences were only apparent through quantification by ELISA and no changes were seen at the intracellular level in the percentage of macrophages expressing RELM-α (Figure 4.4). This can be potentially explained by the fact that upon delivery of active rIL-4 at a single dose of 5μg, >80% macrophages stain positive for RELM-α. At this dose, intracellular protein expression is likely saturated. A dose titration study involving delivery of recombinant IL-4 at varying concentrations may help elucidate the role of miR-378 in intracellular RELM-α protein levels in AAMΦ *in vivo*. Similarly, the levels of secreted YM-1 were also higher in mice lacking miR-378 when compared to control animals, although subtle differences were also noticeable at the intracellular level in some cases. It is also worth noting that between experimental repeats, the results varied with time suggesting that the effect of miR-378 on alternative activation is transient and time dependent.

The next question addressed was whether these subtle changes were a result of an initial defect in activation due to improper AKT-1 (and other) responses or a slow accumulation of small differences over time. A time course study of the kinetics of alternative activation in thioglycollate-elicited macrophages over a course of 24 hours was conducted. Quantification of secreted RELM-α and YM-1 proteins revealed significant differences between the amounts of protein produced by KO mice compared to WT controls at 24hr post stimulation with IL-4/IL-13. Expression of RELM-α and YM-1 was consistently lower over time, with subtle differences in protein quantity apparent from 12-16 hours post stimulation. It still remains to be determined if these differences are also reflected at the transcript level and whether they are a direct result of miR-378 being absent. To determine whether these differences are AKT-1 mediated, and hence, a direct or indirect effect of miR-378, AKT-1 expression or activity needs to be quantified and correlated with the changes in RELM-α and YM-1 expression over time.

Lastly, to determine whether the deficiency of miR-378 and the differences observed in alternative activation in the KO mice had functional consequences, mice were infected with *Litomosoides sigmodontis.* At day 8 post infection, no differences were

observed in macrophage responses between the WT, heterozygous and KO mice. The rate of proliferation and the amounts of RELM-α and YM-1 produced, both intracellular and secreted, were indistinguishable between the three infected groups. Previously in this chapter, we showed differences in alternative activation of pleural macrophages upon peritoneal IL-4c injection in mice, with elevated levels of both RELM-α and YM-1 in the KO mice in comparison to the WT animals. This is in contrast to the lack of differences between the different genotypes during *L. sigmodontis* infection. Infection is much more complex than IL-4c delivery wherein other cell types and factors have a much greater influence on the overall response generated against the nematode. During *L. sigmodontis* infection, a robust T_H2 response ensues, marked by leukocyte infiltration and increased levels of IL-5 and IL-13 (Babayan et al., 2003b). Early on during infection, ILC2s also expand in the pleural cavity and produce IL-5 and IL-13 (Boyd et al., 2015). Secretion of IL-5 results in the recruitment of eosinophils, which also produce IL-4 besides T_H2 cells as infection progresses (Al-Qaoud et al., 1997, Babayan et al., 2003b). The presence of IL-4 and IL-13 in the cavity results in the alternative activation and proliferation of pleural tissue resident macrophages. In parallel, the nematode also elicits a strong systemic T_H2 response characterised by elevated levels of IgG1, IgE and IL-5 in the blood plasma (Babayan et al., 2003b). Exposure to infective L3 larvae also results in the rapid recruitment and increase in T_{reg} cells (Taylor et al., 2009) besides other immune cell types. Moreover, products such as microRNAs and exosomes containing immunomodulatory molecules are also secreted by the parasite (Buck et al., 2014). In contrast, delivery of recombinant IL-4 to the peritoneal cavity is relatively less complex as the main populations residing in the peritoneal cavity comprise mainly B cells and macrophages as evidenced by FACS data (data not shown).

Since microRNAs often act as fine tuners and not master regulators of responses (Selbach et al., 2008), it would not be surprising if subtle effects of microRNAs induced by IL-4 alone were diluted out with infection. Furthermore, many signalling cascades are activated simultaneously in response to infection or insult. With the knowledge that microRNAs exert subtle effects on gene expression (Mourelatos,

2008, Hon and Zhang, 2007) along with the fact that several microRNAs are co-induced during immune responses (Lindsay, 2008, Zhou et al., 2011, Lu and Liston, 2009, Chen et al., 2013), the probability of compensation for the lack of a single microRNA is also high. In this chapter, we have also shown that the effects of miR-378 on alternative activation were the result of a build up of subtle differences over time. Day 8 is a relatively early time point in the course of *L. sigmodontis* infection. It is possible that differences may become more evident at later time points during infection, especially when activation and proliferation are at their peak at day 11. An infection with incorporation of several time points would help to answer these questions.

In addition to the experiments described in this chapter, additional experiments could be envisioned with the miR-378 KO mice to pin down the role of microRNAs in regulating macrophage function. Firstly, it is yet to be determined if miR-378 plays a concrete role in the regulation of IL-4 driven macrophage proliferation through the direct suppression of AKT-1. Through the results described in this study, it is evident that miR-378 alone is not responsible for the regulation of AAMΦ proliferation. However, the lack of miR-378 does have an effect on alternative activation. In chapter 3, we have reported a role for miR-199b-5p in the regulation of macrophage proliferation. Additionally, we have shown that microRNA mimics can be delivered *in vivo* and that overexpression of miR-199b-5p significantly affects YM-1 expression. With microRNAs working in synergy with one another to regulate signalling cascades, it would be extremely interesting to inhibit miR-199b-5p in mice lacking miR-378 to study their additive contribution in regulating AAMΦ activation and proliferation.

Secondly, besides its role in regulating AAMΦ responses, miR-378 is a known regulator of metabolic pathways, including insulin signalling and mitochondrial metabolism (Carrer et al., 2012, Liu et al., 2014). We have demonstrated in Chapter 3 that miR-199b-5p regulates IRS-1 expression; a key component of insulin signalling that is also regulated by IL-4. AAMΦ have key functions in regulating metabolism and utilise oxidative phosphorylation to fuel their functions (Odegaard and Chawla, 2011, Galvan-Pena and O'Neill, 2014, Vats et al., 2006, Schug and Li,

2009). Thus, it would be intriguing to address the cumulative effect of these microRNAs in regulating AAMΦ responses outwith proliferation and characteristic hallmarks of activation.

Thirdly, a role for miR-378 has been implicated in adipogenesis (Kulyte et al., 2014, Gerin et al., 2010, Ortega et al., 2010). AAMΦ are key players during thermogenesis and macrophages found in the adipose tissue also display the M2 phenotype (Kang et al., 2008, Suganami and Ogawa, 2010, Nguyen et al., 2011). FAT-associated lymphoid clusters (FALCs) are a type of lymphoid tissue associated with visceral fat that expand in response to inflammation. This FALC formation in response to inflammation is IL-4Rα dependent and a role for FALCs has been implicated as a centre for differentiation of B cells into plasma cells and germinal centre like B cells, indicative of an important function during immune responses (Benezech et al., 2015). Thus, it may be interesting to address the role of miR-378 towards FALC development during infection in the different miR-378 genotypes. In resting conditions, FALCs are composed mainly of IgM^+ B cells (Benezech et al., 2015). Therefore, as a starting point, IgM levels could be measured in the supernatants harvested from the pleural cavity at day 8 post *L. sigmodontis* infection as an indirect indication of any FALC developmental defects.

In conclusion, the results from this chapter support a role for miR-378 in the regulation of alternative activation, with a greater contribution in regulating RELM-α expression than YM-1. Of note, only the levels of RELM-α and YM-1 were evaluated as characteristic markers of alternative activation. The effects of miR-378 deficiency on other molecules that are also upregulated during alternative activation still remain to be assessed. However, no effect was observed on IL-4 driven macrophage proliferation, despite AKT-1 being a direct target of this microRNA. Further work to identify whether these differences in RELM-α and YM-1 occur at the transcript level underpinning its impact on IL-4R α signalling would provide a better understanding of the regulation of the AAMΦ phenotype by miR-378. In the context of infection, no significant role for miR-378 could be established. However, due to experimental limitations, it is too early to conclusively rule out a role for miR-378 in helminth infection.

A.

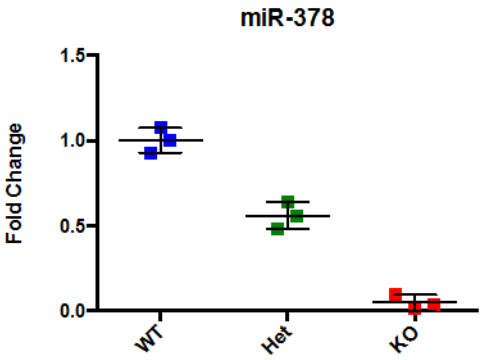

B.

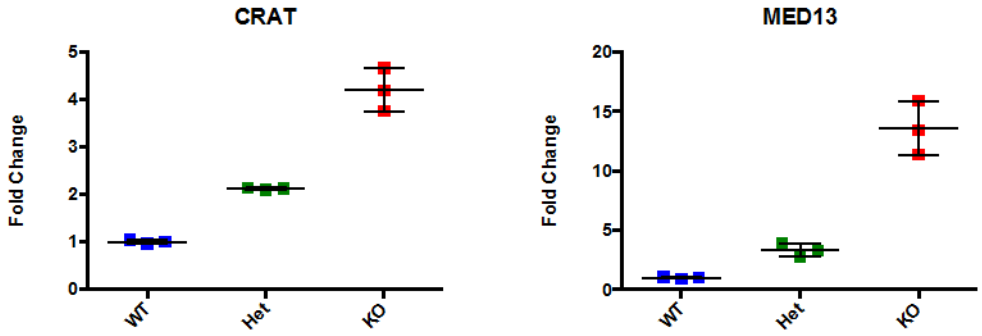

Figure 4.1 Literature validation of mice genetically lacking miR-378/378*

Peritoneal exudate cells (PEC) were harvested from WT, heterozygous and KO mice. Peritoneal macrophages were then adherence purified after incubation at 37C for 4 hours. Cells were lysed and RNA extracted. **A.** MiR-378 levels were quantified by qRT-PCR and normalised to RNU6B expression **B.** *CRAT* and *MED13* transcripts were also quantified by qRT-PCR and expression normalised to 18S. Fold changes were calculated relative to the WT animals. Data represented are the mean fold change ± SEM and determined using one-way ANOVA (Kruskal Wallis test) (* P< 0.05, ** P< 0.01, *** P< 0.001). Data are representative of measures from three separate independent experiments (n=3).

A.

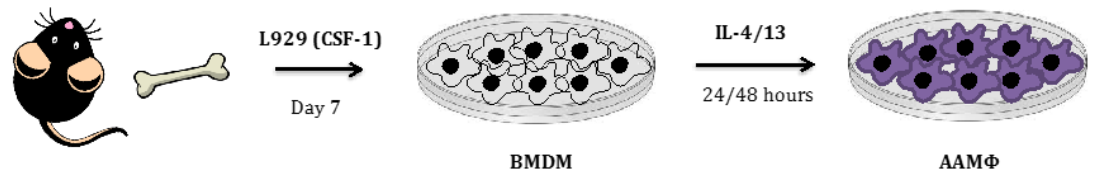

B.

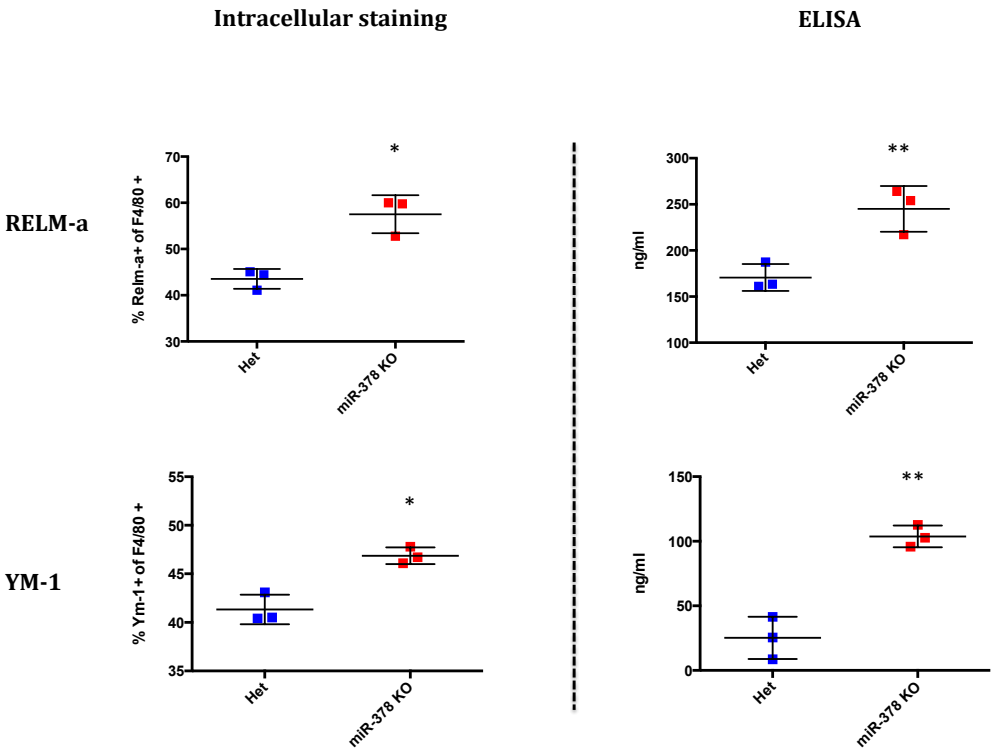

Figure 4.2 Alternative activation in BMDMs derived from WT, heterozygous or miR-378 KO mice 24 and 48 hours post IL-4/IL-13 stimulation.

A) Total bone marrow was isolated from mice and cultured in media containing CSF-1 for 7 days. Cells were harvested on day 7 and seeded overnight before stimulation with 20ng/mL of IL-4 and IL-13. Supernatants were harvested at 24 and 48 hours post stimulation and cells were stained for FACS analysis. **B)** Intracellular and secreted RELM-α and YM-1 expression in BMDM derived from heterozygous and KO mice. Data are representative of a single experiment (n=3). **Only IL-4/IL-13 treated samples are shown**

C.

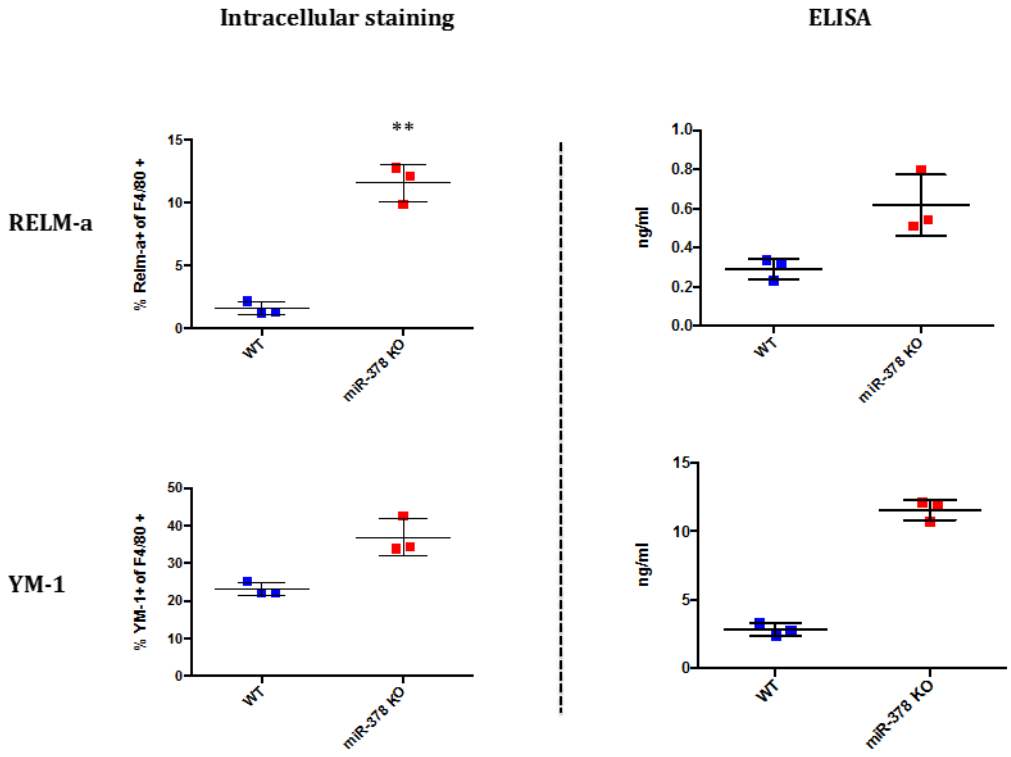

Figure 4.2 Alternative activation in BMDMs derived from WT, heterozygous or miR-378 KO mice 24 and 48 hours post IL-4/IL-13 stimulation.

C) Levels of intracellular and secreted RELM-α and YM-1 in BMDM isolated from WT and KO animals at 24 hours post stimulation. Data are representative of a single experiment (n=3). **Only IL-4/IL-13 treated samples are shown**

D.

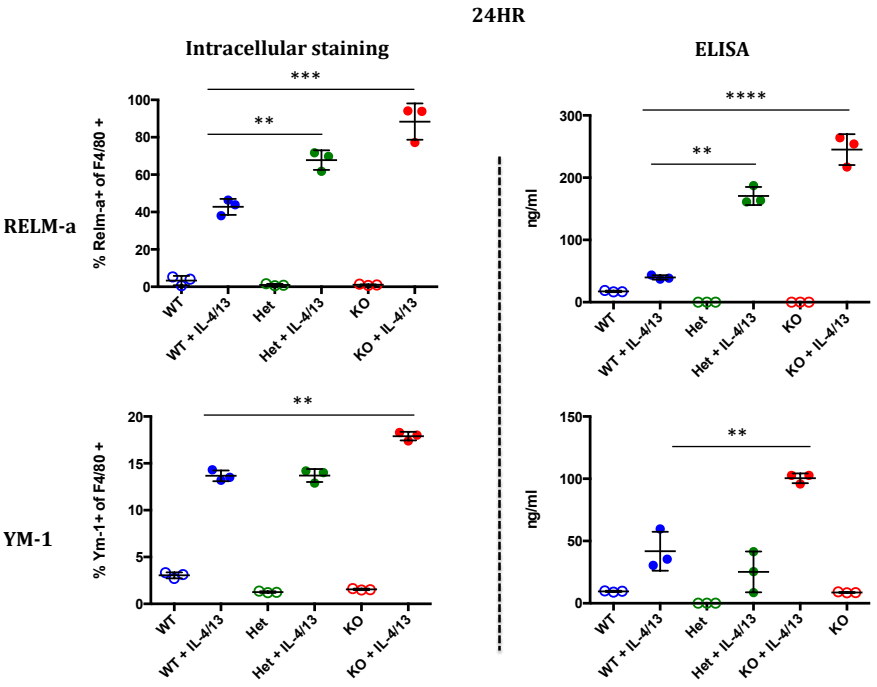
24HR
Intracellular staining
ELISA
RELM-a
YM-1
% Relm-a+ of F4/80 +
% Ym-1+ of F4/80 +
ng/ml
WT
WT + IL-4/13
Het
Het + IL-4/13
KO
KO + IL-4/13

E.

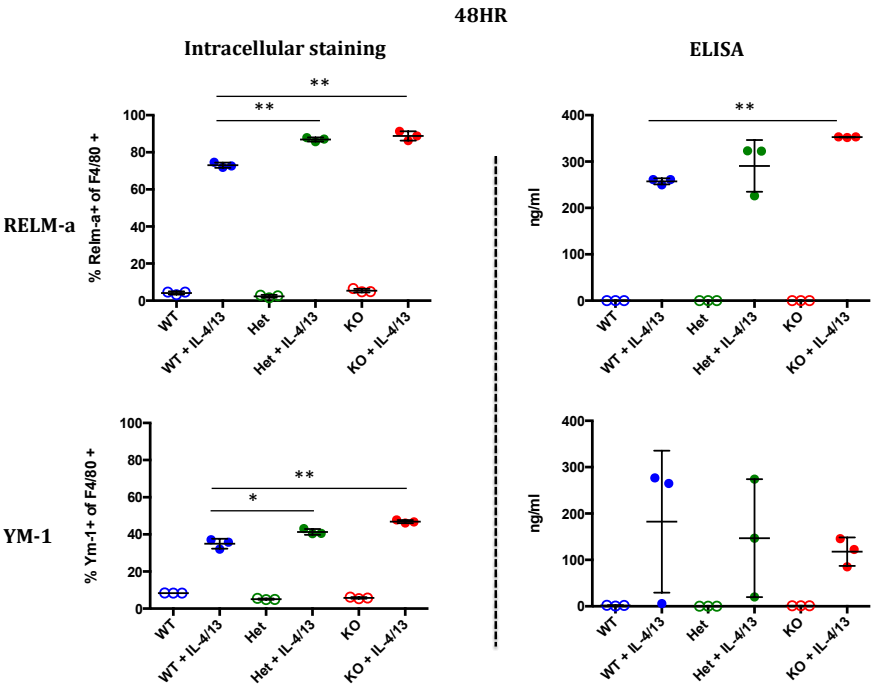
48HR
Intracellular staining
ELISA
RELM-a
YM-1
% Relm-a+ of F4/80 +
% Ym-1+ of F4/80 +
ng/ml
WT
WT + IL-4/13
Het
Het + IL-4/13
KO
KO + IL-4/13

Figure 4.2 Alternative activation in BMDMs derived from WT, heterozygous or miR-378 KO mice 24 and 48 hours post IL-4/IL-13 stimulation. D & E) Experimental repeat of BMDMs inclusive of all three miR-378 genotypes, namely WT, heterozygous and KO. Intracellular and secreted levels of RELM-α and YM-1 were measured by flow cytometry and ELISA at **D)** 24 hours and **E)** 48 hours post stimulation respectively**.** Data are represented as mean ± SEM and determined using one-way ANOVA (Kruskal Wallis test) (* P< 0.05, ** P< 0.01, *** P< 0.001). Data are representative of measures from two separate independent experiments (n=3).

A.

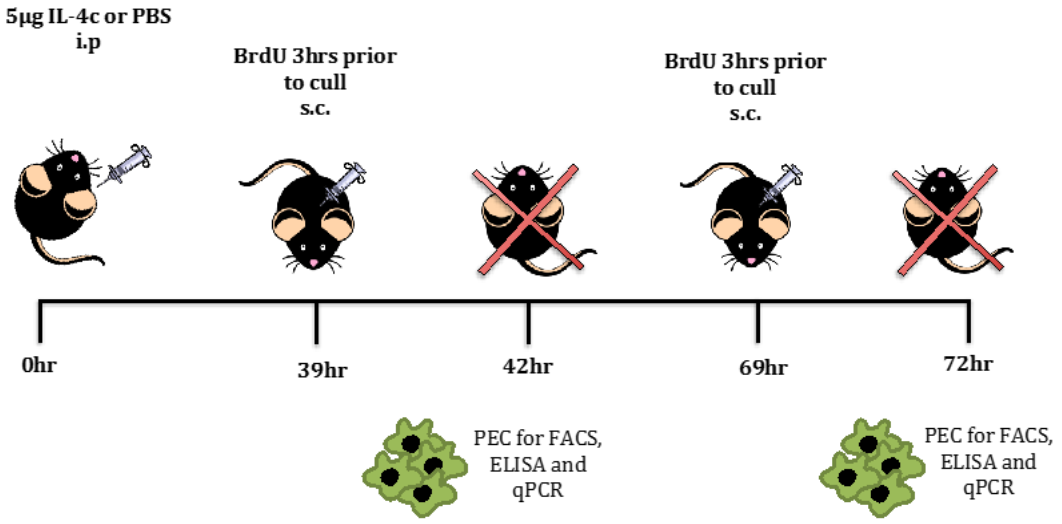
5µg IL-4c or PBS
i.p
BrdU 3hrs prior
to cull
s.c.
BrdU 3hrs prior
to cull
s.c.
0hr
39hr
42hr
69hr
72hr
PEC for FACS,
ELISA and
qPCR
PEC for FACS,
ELISA and
qPCR

B.

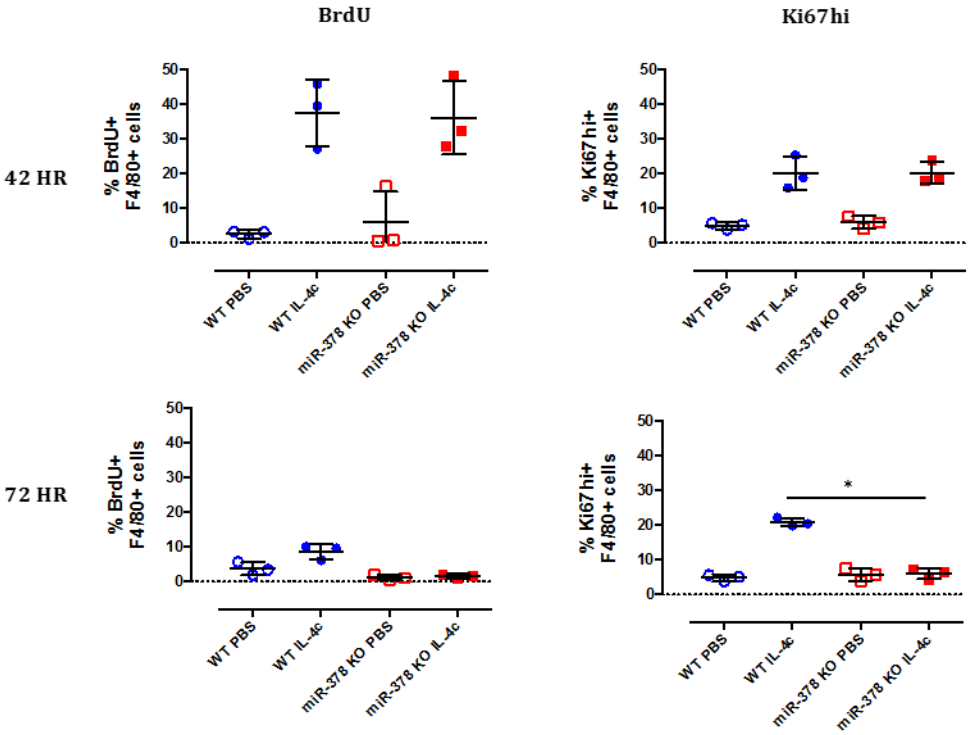
BrdU
Ki67hi
42 HR
72 HR
% BrdU+ F4/80+ cells
% Ki67hi+ F4/80+ cells
WT PBS
WT IL-4c
miR-378 KO PBS
miR-378 KO IL-4c
*

B.

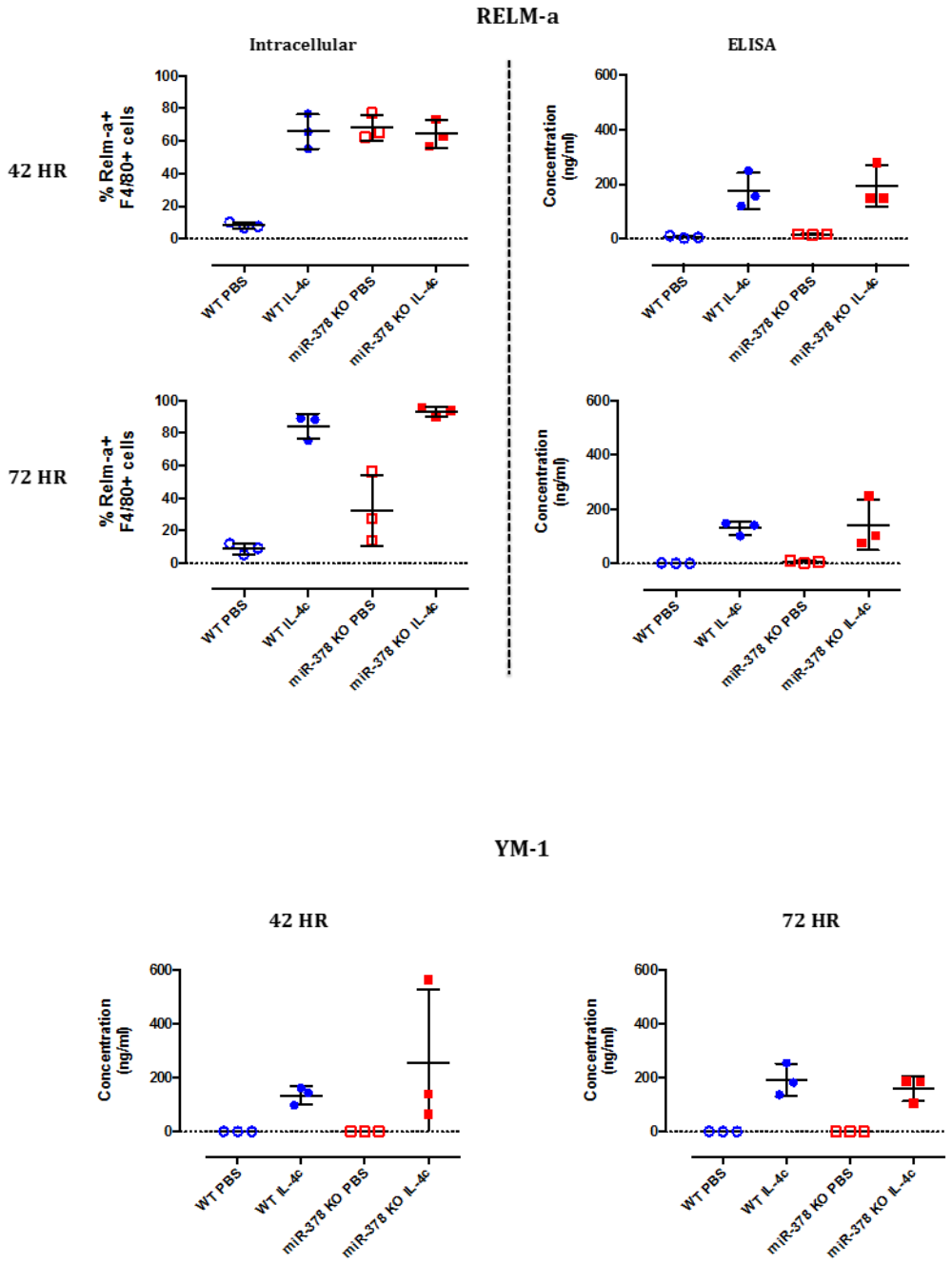

Figure 4.3 IL-4 driven proliferation and alternative activation in the peritoneal cavity in the absence of miR-378.

A) WT mice or miR-378 KO mice were injected with either PBS or IL-4c intraperitoneally. BrdU was also injected subcutaneously 3 hours prior to culling. Pleural exudate cells (PEC)

were harvested at 42 and 72 hours post injection. Cells were utilised either for FACS analysis or qRT-PCR and supernatants harvested for protein quantification by ELISA.

B) Graphs represent FACS analysis of intracellular staining of peritoneal macrophages for BrdU, Ki67hi and RELM-α at 42 and 72 hour time points. Results from quantification of secreted RELM-α and YM-1 by ELISA at 42 and 72 hours post injection are also displayed. Data are represented as mean ± SEM and determined using one-way ANOVA (Kruskal Wallis test) (* $P< 0.05$, ** $P< 0.01$, *** $P< 0.001$). Data are representative of a single experiment (n=3).

A.

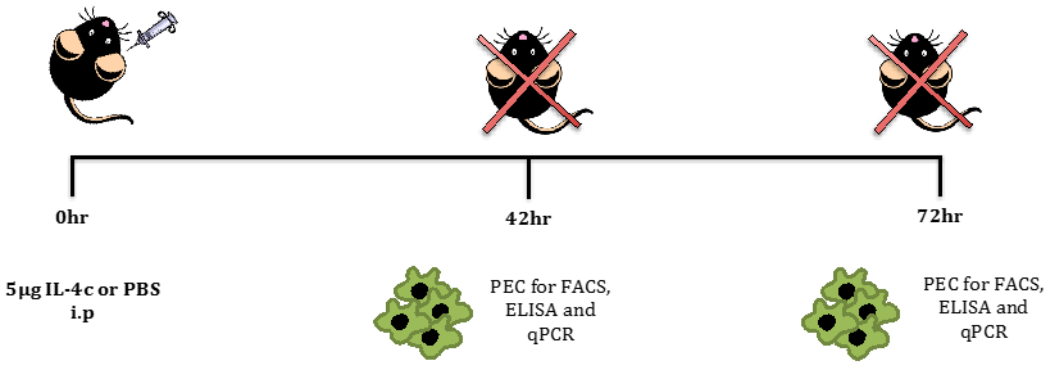
0hr
42hr
72hr
5µg IL-4c or PBS
i.p
PEC for FACS,
ELISA and
qPCR
PEC for FACS,
ELISA and
qPCR

B.

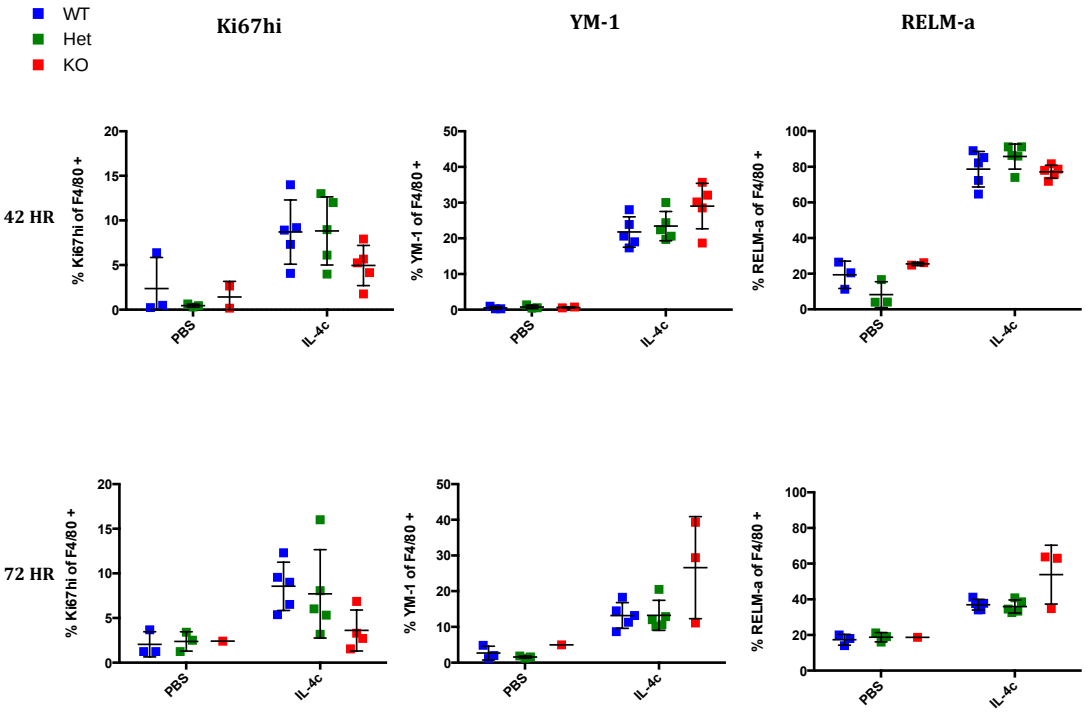
WT
Het
KO
Ki67hi
YM-1
RELM-a
42 HR
72 HR
% Ki67hi of F4/80 +
% YM-1 of F4/80 +
% RELM-a of F4/80 +
PBS
IL-4c

C.

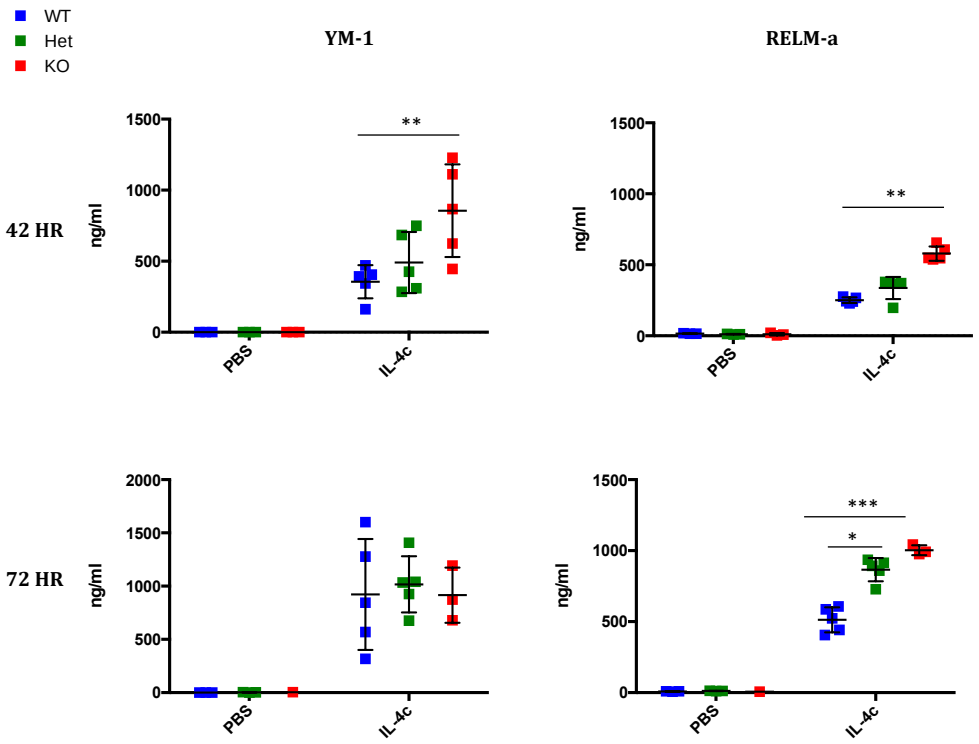

Figure 4.4 Comparison of IL-4 induced proliferation and alternative activation in the peritoneal cavity of WT, heterozygous and miR-378 KO mice.

A) WT mice, heterozygous mice or miR-378 null mice were injected with either PBS or IL-4c intraperitoneally. PEC was harvested at 42 and 72 hours and cells were subject to FACS analysis and supernatants harvested for ELISA. **B)** Graphs represent FACS analysis of intracellular staining of peritoneal macrophages for Ki67hi, YM-1 and RELM-α at 42 and 72 hours. **C)** Results from quantification of secreted RELM-α and YM-1 by ELISA at 42 and 72 hours post treatment. Data are represented as mean ± SEM and determined using one-way ANOVA (Kruskal Wallis test) (* P< 0.05, ** P< 0.01, *** P< 0.001). Data are representative of a single experiment (n=5).

A.

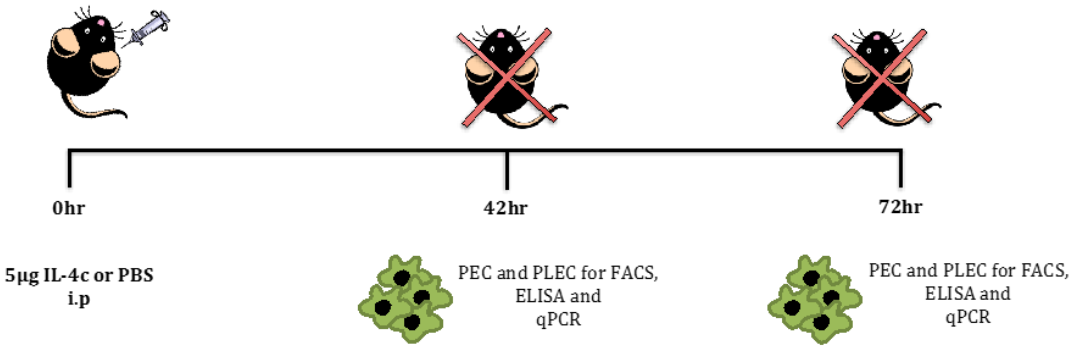

B.

Peritoneal Cavity

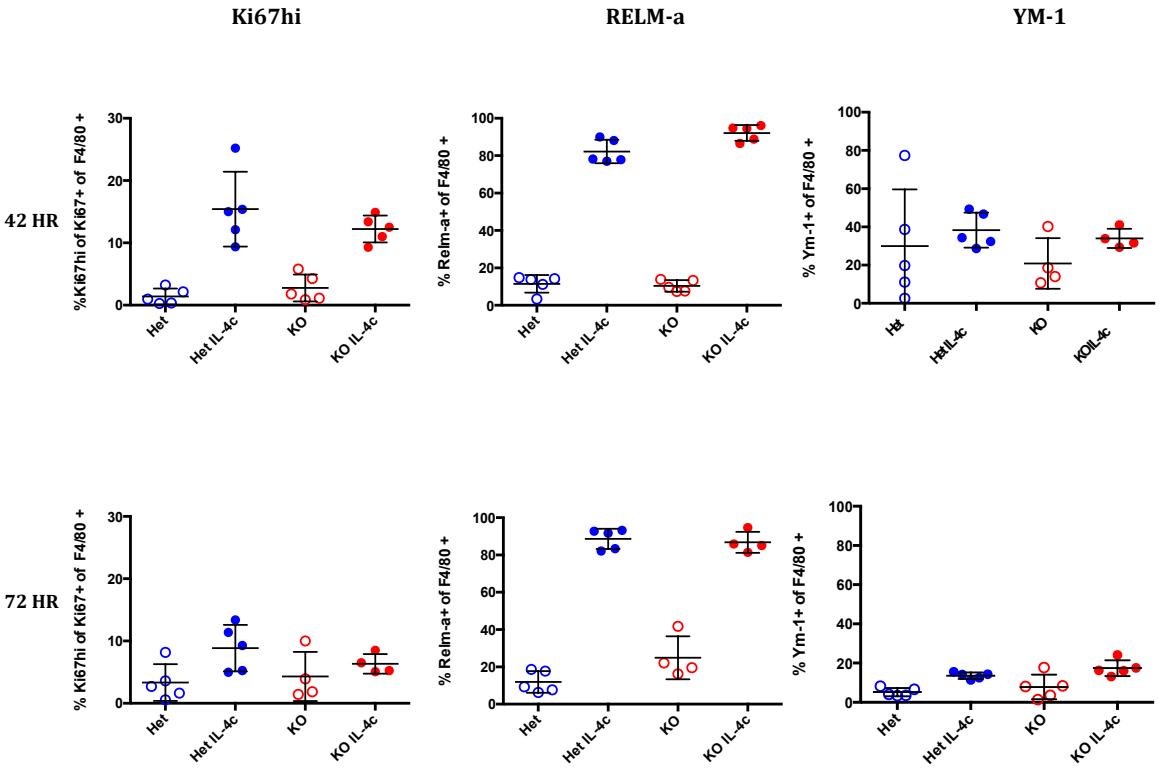

C.

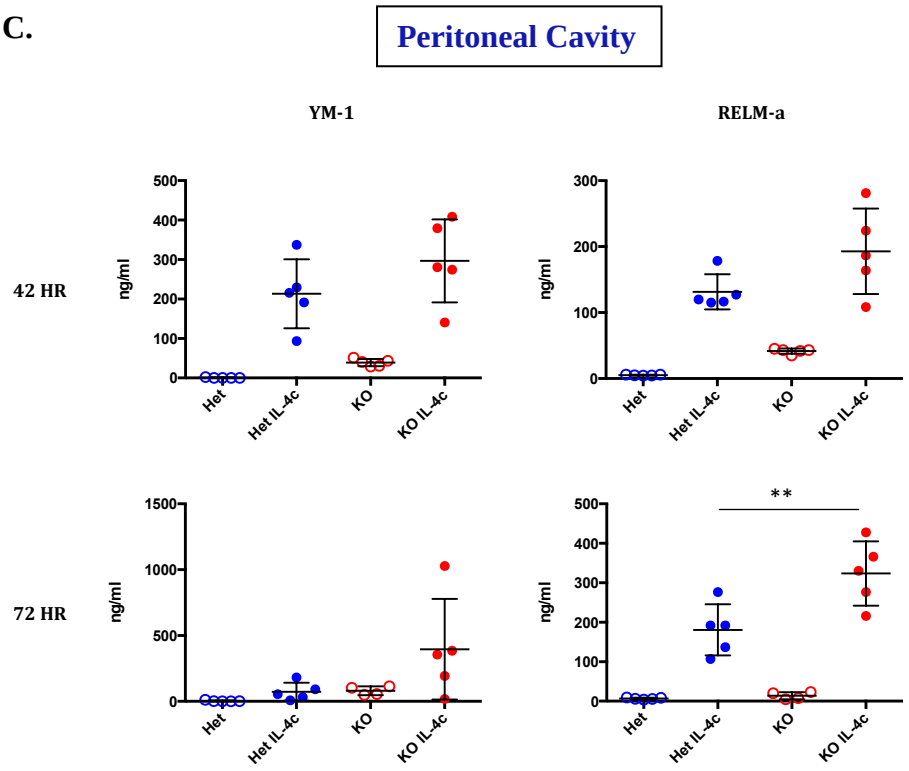
Peritoneal Cavity
YM-1
RELM-a
42 HR
72 HR
ng/ml
Het
Het IL-4c
KO
KO IL-4c
**

D.

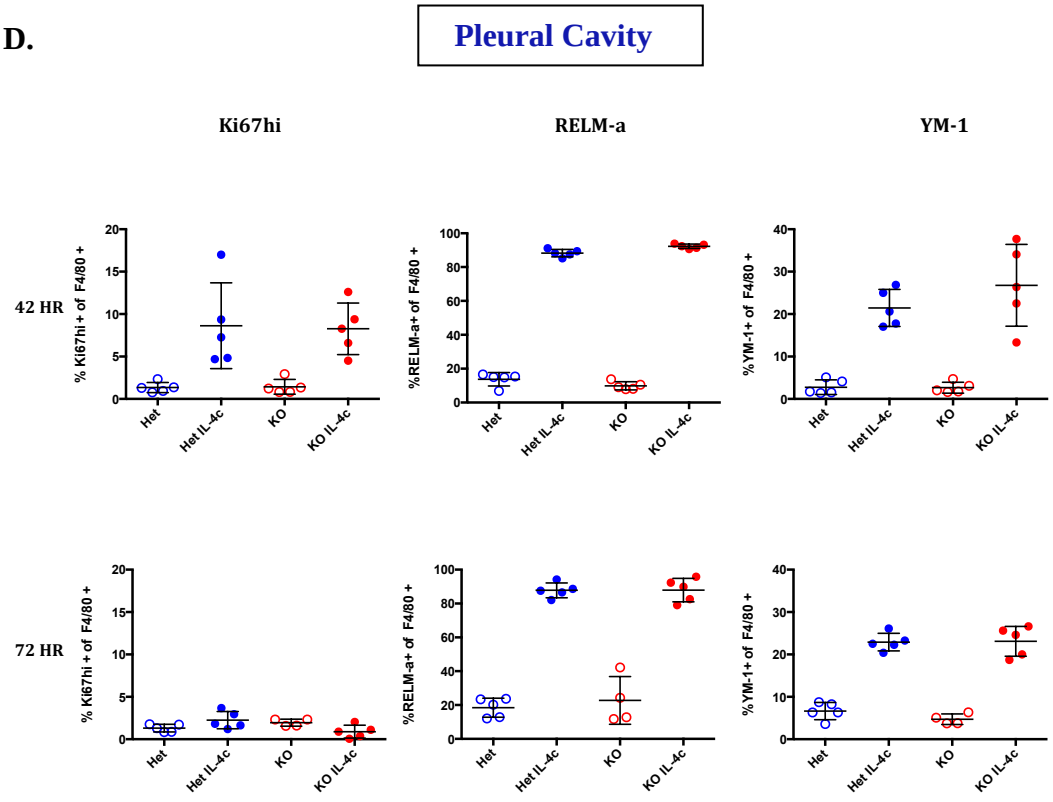
Pleural Cavity
Ki67hi
RELM-a
YM-1
42 HR
72 HR
% Ki67hi+ of F4/80 +
%RELM-a+ of F4/80 +
%YM-1+ of F4/80 +
Het
Het IL-4c
KO
KO IL-4c

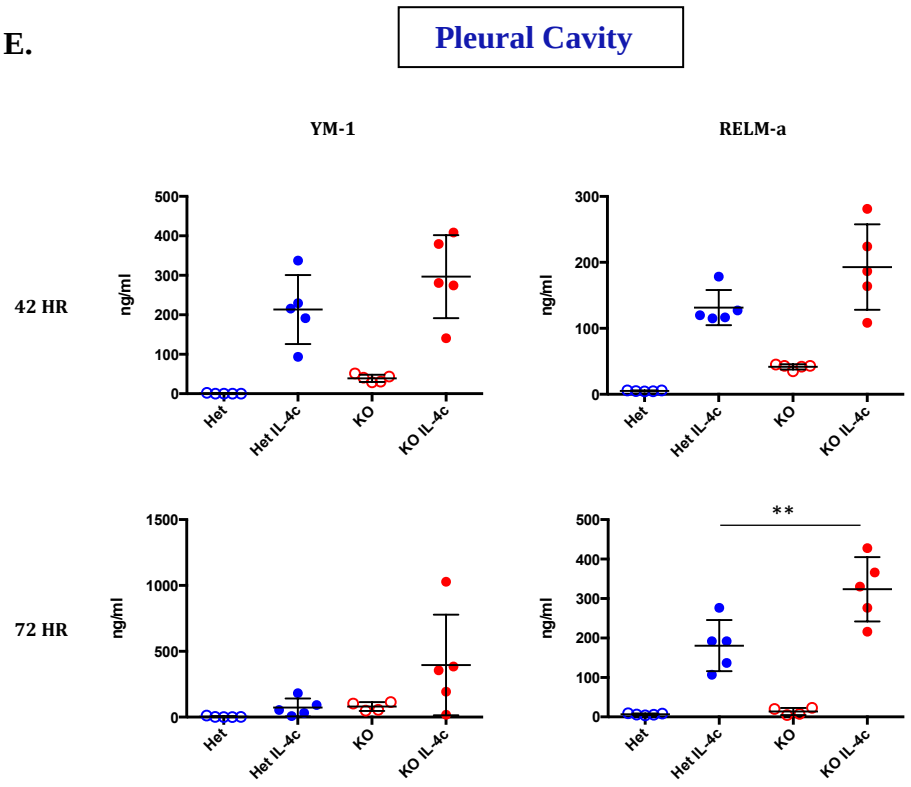

Figure 4.5 Comparison of IL-4 driven proliferation and alternative activation in the peritoneal and pleural cavities of heterozygous and KO mice.

A) Heterozygous mice or miR-378 deficient mice were injected with either PBS or IL-4c intraperitoneally. PEC and PLEC were harvested at 42 and 72 hours. **B & D)** FACS analysis of intracellular staining of peritoneal and pleural macrophages for Ki67hi, RELM-α and YM-1 expression at 42 and 72 hours. **C & E)** Results from quantification of secreted RELM-α and YM-1 by ELISA from the peritoneal and pleural cavities at 42 and 72 hours post treatment. Data are represented as mean ± SEM and determined using one-way ANOVA (Kruskal Wallis test) (* P< 0.05, ** P< 0.01, *** P< 0.001). Data are representative of a single experiment (n=5).

A.

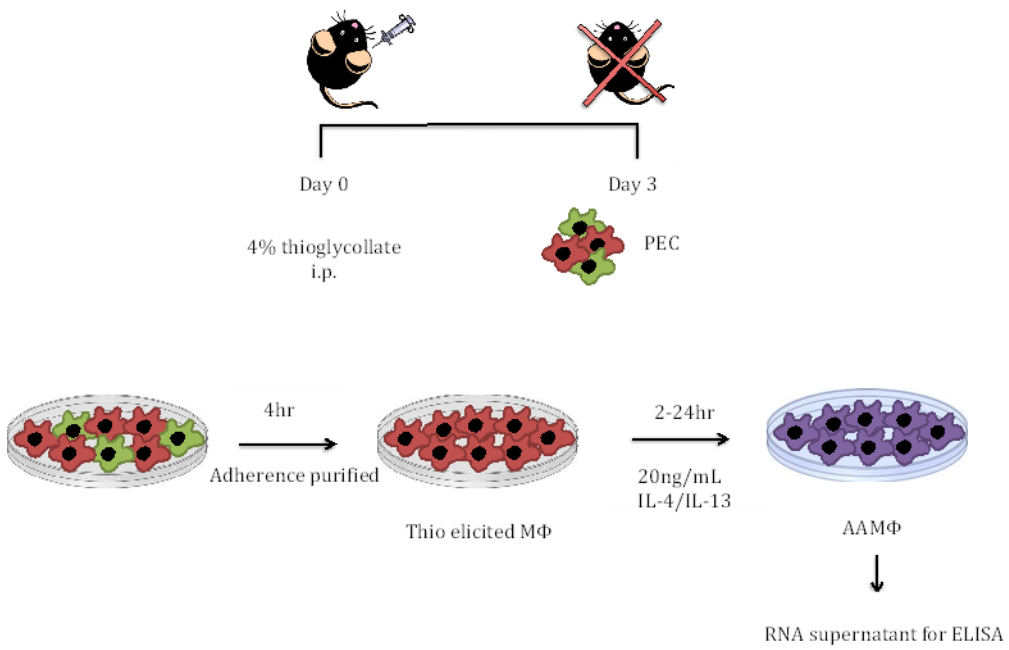
Day 0
Day 3
4% thioglycollate
i.p.
PEC
4hr
Adherence purified
Thio elicited MΦ
2-24hr
20ng/mL
IL-4/IL-13
AAMΦ
RNA supernatant for ELISA

B.

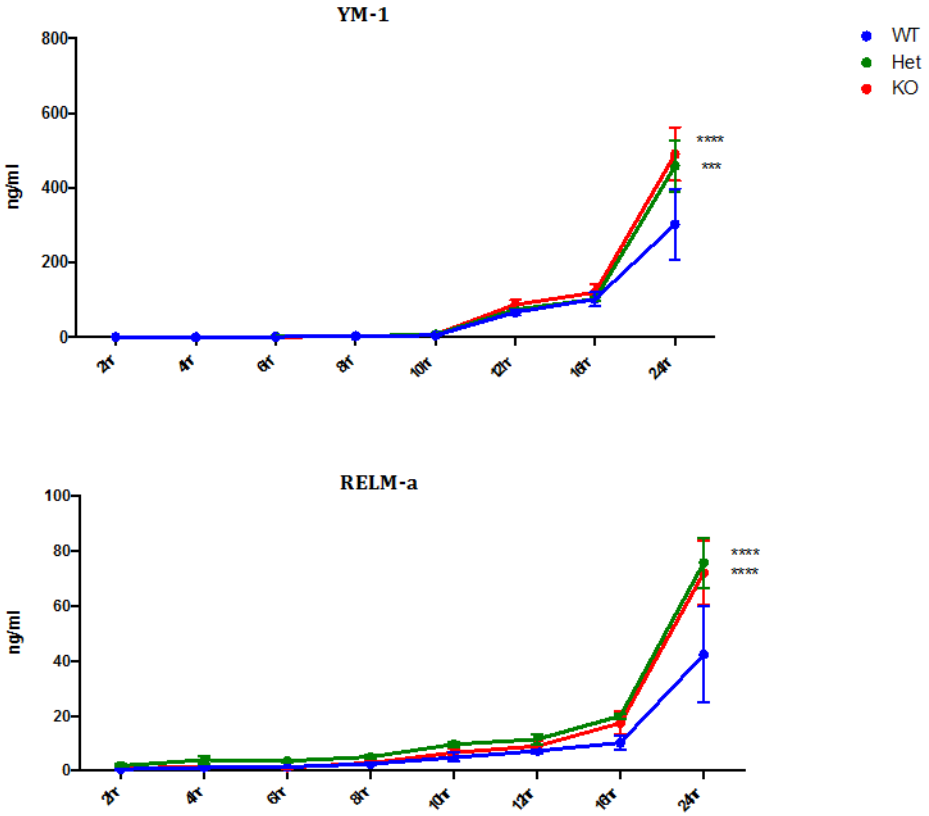
YM-1
ng/ml
800
600
400
200
0
2hr
4hr
6hr
8hr
10hr
12hr
16hr
24hr
****
***
WT
Het
KO
RELM-a
ng/ml
100
80
60
40
20
0
****
****

Figure 4.6 Kinetics of alternative activation in thioglycollate elicited macrophages.

A) Schematic for isolation of thioglycollate elicited macrophages. WT, heterozygous or KO mice were injected with 4% thioglycollate intraperitoneally. PEC was harvested 3 days post injection and macrophages adherence purified for 4 hours at 37C. Purified macrophages were stimulated with 20ng/mL of IL-4 and IL-13. Samples were harvested at various time points ranging from 2hr to 24hr. **B)** The levels of secreted YM-1 and RELM-α proteins were quantified in the PEC supernatant by ELISA. Data are represented as mean ± SEM and determined using one-way ANOVA (Kruskal Wallis test) (* P< 0.05, ** P< 0.01, *** P< 0.001). Data are representative of a single experiment (n=5).

A.


Day 0
Day 8
30 L3
s.c.
PLEC for FACS,
ELISA and
qPCR

B.

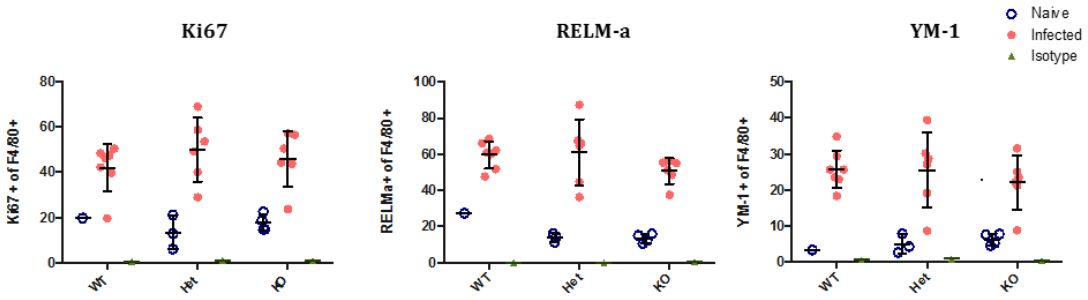
Ki67
RELM-a
YM-1
Naive
Infected
Isotype
K67 + of F4/80+
RELMa+ of F4/80+
YM-1+ of F4/80+
Wt
Het
KO
WT
Het
KO

C.

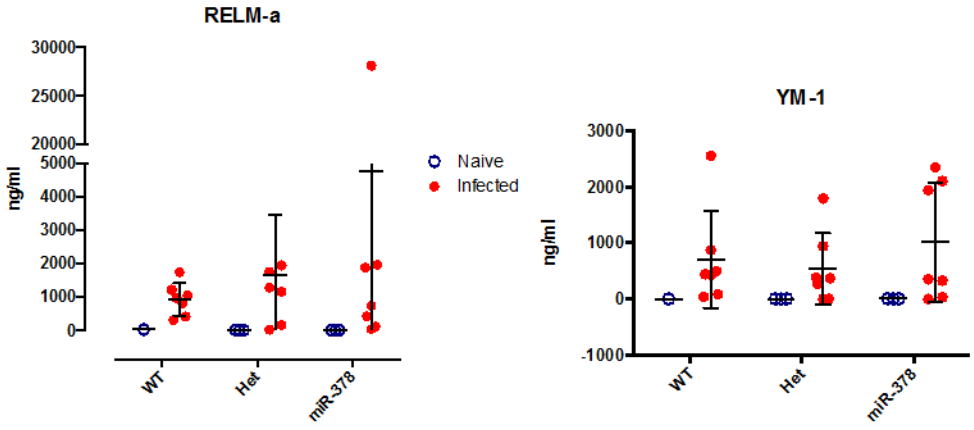
RELM-a
YM-1
ng/ml
Naive
Infected
WT
Het
miR-378

Figure 4.7 Alternative activation and macrophage proliferation during *L. sigmodontis* infection in WT mice, heterozygous mice and miR-378 KO mice.

A) Mice were infected with infective larvae subcutaneously and culled at day 8 post infection. Pleural lavage (PLEC) was harvested for analysis. **B)** Analysis of intracellular staining for Ki67, RELM-α and YM-1 expression in F4/80+ pleural macrophages. **C)** Quantification of secreted YM-1 and RELM-α proteins in the PLEC supernatant was carried out by ELISA. Data are represented as mean ± SEM and determined using one-way ANOVA (Kruskal Wallis test) (* $P< 0.05$, ** $P< 0.01$, *** $P< 0.001$). Data are representative of a single experiment (n=6).

Chapter 5: Analysis of miR-146 levels in AAMΦ and generation of a stable cell line towards the biochemical identification of microRNA targets

SUMMARY:

MiR-146a is a highly studied microRNA that has previously been linked strongly to T_H1 immune responses, especially classical activation of macrophages. However, a role for this microRNA in regulating AAMΦ is yet to be determined. In Chapter 2, we have showed that expression of miR-146 is central to a range of alternative activation conditions *in vitro* and *in vivo*. The central focus of this chapter is to examine the role of miR-146 in the regulation of AAMΦ. Expression of miR-146a and miR-146b, the two isoforms of miR-146, was found to be opposite in AAMΦ, with a decrease in miR-146a and increase in miR-146b expression in response to IL-4 both *in vitro* and *in vivo*. Based on this difference in expression and their known functions in suppressing excessive proinflammatory responses, it was hypothesised that miR-146a/b serve to regulate proinflammatory molecules (and signals) in a fine balance to allow efficient alternative activation to occur. However, a difference of just two nucleotides between the sequences of these two miR-146 isoforms proved to be a hindrance to test this hypothesis in terms of shared targets. Therefore, the latter half of this chapter was devoted to the generation and optimisation of a stable cell line for the identification of microRNA targets using CLASH (cross-linking, ligation and sequencing of hybrids).

5.1 Introduction

The primary aim of this thesis is to identify microRNAs differentially expressed in AAMΦ and to study their functional roles in regulating this phenotype. We have shown previously in Chapter 2 that the mature forms of miR-146a and miR-146b, originating from the 5' arms of their respective precursor microRNAs, are differentially regulated in response to IL-4. MiR-146a and miR-146b are two isoforms of miR-146 that are derived from two separate genes located on different chromosomes. These mature forms share identical seed regions and differ in their sequences by just two nucleotides in the 3' region. Of these, miR-146a is one of the most widely studied microRNAs in the context of immune responses (Pedersen and David, 2008, Rusca and Monticelli, 2011). A role for miR-146a has been proposed in the regulation of both innate and adaptive immunity (Boldin et al., 2011, Labbaye and Testa, 2012).

The functional properties of miR-146a have been particularly well characterised in monocytes and macrophages. The miR-146a promoter contains several binding sites for NF-κB and induction of miR-146a is NF-κB dependent (Taganov et al., 2006). MiR-146a has been shown to target Interleukin-1 receptor-associated kinase 1 (IRAK1) and TNF receptor associated factor 6 (TRAF6) both *in vitro* and *in vivo* (Taganov et al., 2006, Hou et al., 2009) and is involved in a negative feedback loop suppressing the expression of genes such as IL-6 (He et al., 2014c), IL-8 (Bhaumik et al., 2009), IL-1β (Perry et al., 2008) and TNF-α (Sheedy and O'Neill, 2008). Moreover, infection of murine macrophages with vesicular stomatitis virus (VSV) induces miR-146a, which negatively regulates the RIG-I antiviral pathway by targeting IRAK, IRAK2 and TRAF6, thereby suppressing the production of interferons (Hou et al., 2009). In addition to its role in regulating innate immune responses, miR-146a is also known to be essential in adaptive immunity. T cells deficient in miR-146a are hyperactive in both antigenic and chronic inflammatory autoimmune responses, whereas the deficiency of miR-146a in T_{reg} cells results in a breakdown of immunological tolerance due to enhanced expression of signal transducer and activator transcription 1 (STAT1), otherwise suppressed by miR-146a

(Lu et al., 2010, Yang et al., 2012). MiR-146a is also one of the few microRNAs to be differentially expressed in T_H1 and T_H2 cells, suggesting that miR-146a could potentially be involved in fate determination (Curtale et al., 2010, Labbaye and Testa, 2012). Furthermore, miR-146a-deficient mice, in addition to autoimmunity, develop an exaggerated pro-inflammatory response when exposed to LPS (Boldin et al., 2011). The aged knockout mice also develop tumours in secondary lymphoid organs and undergo myeloproliferation, suggesting the involvement of miR-146a in regulating development and activation of immune cells (Boldin et al., 2011, O'Neill et al., 2011, Sonkoly and Pivarcsi, 2011). More recently, a role for miR-146a has been implicated in the modulation of inflammatory responses through its transfer between cells through exosomes (Alexander et al., 2015, Okoye et al., 2014).

In contrast to miR-146a, the other isoform of miR-146 i.e. miR-146b, has not been as extensively studied. Although both microRNAs are predicted to bind the same targets due to identical seed sequences, their transcriptional regulation has been shown to be different. Whilst miR-146a expression is NF-κB dependent (Taganov et al., 2006), expression of miR-146b is dependent on GATA-1 (Zhai et al., 2014) and STAT3 (Xiang et al., 2014). The induction of both microRNAs has been reported during proinflammatory responses. However, production of miR-146a has been shown to be dependent on IL-1β whereas miR-146b expression is reliant on IFN-γ (Kutty et al., 2013). Additionally, induction of miR-146a is regulated intracellularly via NF-κB and JNK-1/2 whilst miR-146b expression is thought to be MEK-1/2 and JNK1/2 mediated (Perry et al., 2009). Like miR-146a, a role for miR-146b has also been implicated in regulating proinflammatory responses (Taganov et al., 2006, Xiang et al., 2014). A survey of current literature reveals that the function of miR-146b is largely associated with several cancers and tumour metastasis, particularly in gliomas (Xia et al., 2009, Katakowski et al., 2010, Garcia et al., 2011, Katakowski et al., 2013). Dysregulation of miR-146b has also been linked to regulation during thyroid carcinomas (Chou et al., 2010, Deng et al., 2015) and a role for miR-146b has been implicated in the modulation of Transforming Growth Factor-β (TGF- β) signalling via suppression of SMAD4 in thyroid tumorigenesis (Geraldo et al., 2012). MiR-146b expression is also altered during obesity (Chen et al., 2014c).

Besides the negative regulation of TLR signalling through IRAK1 and TRAF6, miR-146b is also induced by IL-10 and can display anti-inflammatory properties in monocytes through targeting multiple components of the TLR4 pathway (Curtale et al., 2012, Renzi et al., 2012). Other than that, the role of miR-146b in immune responses still remains largely unknown.

Based on the existing literature reviewed above, miR-146 has a well-defined role in the regulation of CAMΦ and limiting their responses. However, a role for miR-146 in the regulation of AAMΦ is yet to be determined. A previous study carried out by our lab identified miR-146a as being differentially expressed in AAMΦ isolated from *B. malayi* implant in mice (Ruckerl et al., 2012). In this chapter, the expression profiles of both miR-146a and miR-146b were explored in detail under different conditions of alternative activation to infer potential roles of miR-146 in regulating AAMΦ. However, the extent of similarity between the mature sequences of miR-146a and miR-146b limits the ability to delineate their targets and functions using synthetic inhibitors, which are likely to bind to both forms.

To overcome this hurdle, a part of this chapter focused on setting up the tools required to biochemically identify targets using the "cross-linking, ligation and sequencing of hybrids (CLASH)" technique (Helwak et al., 2013). MicroRNA binding sites are generally situated in the 3'UTR of mRNAs and target recognition is largely mediated through complementarity to the seed region of the microRNA (position 2-8nt in the mature microRNA sequence). However, non-canonical binding of targets via bulged or centred interactions has gained importance over the past years (Shin et al., 2010, Chi et al., 2012, Martin et al., 2014, Cloonan, 2015) but these interactions are still difficult to identify. Identification of microRNA targets involves a balance between computational and experimental approaches (Thomson et al., 2011, Hausser and Zavolan, 2014). As discussed previously in Chapter 3 the false positive rate relating to target prediction is relatively high (50-70%) (Thomson et al., 2011), largely due to the reliance on canonical binding and exclusion of other factors that could affect binding affinities such as RNA structures and RNA-binding proteins that might affect binding site accessibility (Ameres et al., 2007, Kedde and Agami,

2008). A common method to identify direct microRNA targets involves the immunoprecipitation of Argonaute (AGO) proteins followed by sequencing of the isolated AGO-bound RNAs (Hausser and Zavolan, 2014). CLASH (Helwak et al., 2013) is a variation of one such high throughput sequencing technique involving AGO cross-linking and immunoprecipitation (HITS-CLIP) that can be utilised for the identification of direct microRNA targets (Ule et al., 2003, Licatalosi et al., 2008, Konig et al., 2011). In CLASH, like other CLIP techniques, following cross linking tagged AGO protein bound to microRNAs and their target mRNAs contained within the RISC complexes is immunoprecipitated. However, , in an additional step that distinguishes CLASH from other similar techniques as shown in Figure 5 below, the microRNA is then ligated to its target mRNA, thereby providing physical evidence of direct target binding without relying on the assumption of canonical binding site interactions (Helwak et al., 2013, Helwak and Tollervey, 2014).

A secondary aim of this chapter, therefore, was to generate a suitable stable macrophage cell line expressing the tagged AGO protein for the identification of miR-146 targets using CLASH. In the second half of this chapter, a RAW 264.7 macrophage cell line expressing tagged murine Argonaute 2 (mAGO2) was generated.

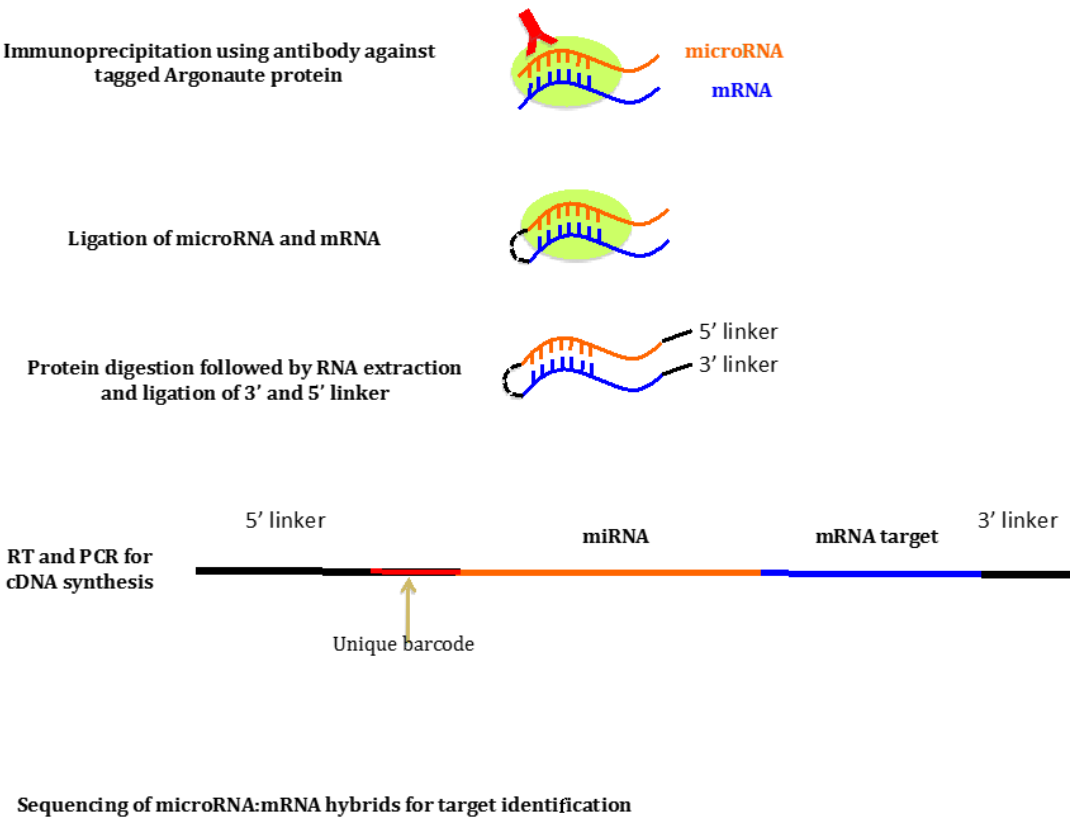

Figure 5. A brief simplified overview of the Cross Linking And Sequencing of Hybrids (CLASH) protocol.

5.2 Results

5.2.1 Contrasting regulation of miR-146a and miR-146b during alternative activation in macrophages across different cell types

As discussed in chapter 2, microarray data identified both miR-146a and miR-146b as being differentially regulated in bone marrow derived macrophages in response to IL-4. In this section, the expression profiles of these isoforms have been examined in detail under varying conditions of alternative activation.

5.2.2 Macrophage cell lines

RAW 264.7 and J774A.1 cells were treated with IL-4 and IL-13 for 24 and 48 hours. Contrasting expression of miR-146a and miR-146b was observed in both macrophage cell lines (Figure 5.1A and 5.1B). Whilst miR-146a levels were reduced, expression of miR-146b was enhanced. It has previously been reported that LPS induces the expression of both miR-146a and miR-146b (Taganov et al., 2006, Curtale et al., 2012, Chen et al., 2014b). Hence, in a repeat experiment, both RAW 264.7 and J774A.1 cells were also stimulated with 10ng/mL LPS. In agreement with the existing literature, qRT-PCR analysis revealed that expression levels of both miR-146a and miR-146b were up-regulated nearly 2-3 fold in response to LPS treatment compared to untreated controls in both RAW 264.7 (Figure 5.2A) and J774A.1 (Figure 5.2B) cells. In line with our previous findings, there was a 2-fold reduction in the expression of miR-146a in both the cell lines at 24 and 48 hours post stimulation with IL-4/IL-13 (Figure 5.2A and Figure 5.2B). In contrast, miR-146b was upregulated in RAW 264.7 cells by 1.5 fold (Figure 5.2A) compared to untreated controls in response to IL-4/IL-13. Although a 1.5 fold increase in its expression was also observed in J774A.1 cells at 48 hours, no significant change was observed at 24 hours (Figure 5.2B). Together, these results from two different macrophage cell lines confirm that miR-146a and miR-146b levels are differentially altered in macrophages in response to IL-4 and IL-13.

Having confirmed that the expression of both these microRNAs was altered in RAW 264.7 cells in response to a combination of IL-4 and IL-13, we next sought to identify the relative contribution of these two cytokines towards altered miR-146a/b expression. To this end, cells were left untreated or stimulated with either 20ng/mL of IL-4 or IL-13 or a combination of both IL-4 and IL-13. RNA was extracted from lysed cells at 24 and 48 hours for qRT-PCR analysis. The altered expression of both miR-146a and miR-146b was induced equally by IL-4 or IL-13 alone and the effect combining the two cytokines on expression of these microRNAs was not additive (Figure 5.3). This is in contrast to results in chapter 2 that showed alternative activation of RAW 264.7 cells was mainly driven by IL-4.

5.2.3 Primary macrophages

Having determined the response of both miR-146 isoforms to classical and alternative activation of the cell lines, the differences in their expression in primary AAMΦ and CAMΦ were determined. BMDMs were generated from bone marrow precursors derived from WT C57BL/6 mice and stimulated with either 10ng/mL of LPS or 20ng/mL of IL-4/IL-13. Cells were harvested at 24 and 48 hours post stimulation. As was observed in the cell lines, both miR-146a and miR-146b were significantly up regulated in BMDMs in response to LPS treatment at 24 hours (Figure 5.4A). There was a gradual decline in expression of miR-146a in response to IL-4/IL-13 treatment over time, with levels being reduced by nearly 2 fold at 48 hours as shown in Figure 5.4B. In contrast, expression of miR-146b was enhanced with time with a 2 fold increase at 48 hours post IL-4/IL-13 stimulation (Figure 5.4B). These alterations in expressions of both miR-146a and miR-146b were also reflected in the copy numbers determined using synthetic standards at 24 and 48 hours post treatment with IL-4 and IL-13 (Figure 5.4C and 5D). Analysis of the copy numbers also revealed that BMDMs that miR-146a levels are 100 fold higher than miR-146b levels in these cells: 10^7 copies/ng of RNA versus 10^5 copies/ng of RNA respectively.

To extend the analysis to other *in vitro* conditions of alternative activation, the expression of both miR-146 isoforms was investigated in Thio elicited MΦ

adherence purified from PEC populations obtained from WT C57BL/6 mice. The Thio elicited MΦ were stimulated with 10ng/mL of LPS or 20ng/mL of IL-4 and IL-13 *in vitro* for up to 48 hours before RNA was harvested for qRT-PCR. Consistent with the previous findings, levels of both miR-146a and miR-146b were significantly increased (average of 3 fold) in response to LPS treatment (Figures 5.5A and 5.5B). Also consistent with earlier experiments, expression of miR-146a was downregulated by >2 fold at 48 hours post stimulation with IL-4/IL-13, whereas expression of miR-146b was upregulated (Figures 5.5A and 5.5B). Taken together these findings suggest similar changes in miR-146a/b expression levels in response to IL-4/13 treatment of a range of macrophages *in vitro*.

5.2.4 IL-4c treatment in the peritoneal cavity of mice

Having examined the expression profiles of these microRNAs under conditions of alternative activation *in vitro*, we next sought to determine if these changes in miR-146a and miR-146b expression also occurred *in vivo*. Peritoneal macrophages sorted from PEC cells isolated from WT C57BL/6 mice injected with a single dose of 5μg of recombinant IL-4 (24 hours post injection) express significantly lower amounts of miR-146a (~2 fold reduction) and higher amounts of miR-146b (~1.5 fold increase) when compared to macrophages isolated from mice injected with PBS only (Figure 5.6A). These changes in the relative expression levels of miR-146a/b were also reflected in the copy numbers as measured using synthetic microRNA standards (Figure 5.6B). In agreement with the *in vitro* data obtained from BMDMs, miR-146a is expressed at significantly higher copy numbers/ng RNA in macrophages isolated from the peritoneal cavity (10^6-10^7 copies) when compared to miR-146b expression in the same population (10^5 copies/ng RNA) as shown in Figure 5.6B.

5.2.5 Litomosoides sigmodontis infection in mice

Until now we have shown a consistent downregulation in the expression of miR-146a during alternative activation whilst at the same time showing that levels of miR-146b are increased across different conditions. To investigate whether the contrasting expression of miR-146a and miR-146b also occurred in an environment

with potential functional consequences, we next examined the expression levels these microRNA isoforms over the course of *L. sigmodontis* infection. With the progression of infection over time, a statistically non-significant trend towards downregulation of miR-146a expression was observed. In contrast, the expression of miR-146b was significantly increased over the course of infection (Figure 5.7A).

Since the transcriptional regulation of miR-146a and miR-146b in response to IL-4/IL-13 is in opposition, we hypothesised that miR-146b is up-regulated during alternative activation to compensate for the reduction in levels of miR-146a through suppression of shared targets. Therefore, in the same study, we also analysed the change in copy numbers of these microRNAs over the course of infection progression as represented in Figure 5.7B. There was a significant difference in the levels of miR-146a and miR-146b that are expressed by pleural macrophages during infection with *L. sigmodontis*.. Macrophages isolated from naïve mice expressed ~ 10^6 copies of miR-146a per ng of RNA whereas miR-146b was only expressed at around 10^4 copies/ng RNA. Whilst there was significant up-regulation of miR-146b by approximately 10 fold with the progression of infection, the levels of miR-146a appeared to remain unchanged at ~10^6 copies/ng RNA (Figure 5.7B). Although this lack of altered miR-146a expression was in agreement with the fold change in its expression during *L. sigmodontis* infection (Figure 5.7A), it is in contrast to the consistent downregulation in its expression during other conditions of alternative activation. Therefore, with a lack in reduction of miR-146a copy number over the course of infection, it seems that a compensatory mechanism may not exist between miR-146a/b, at least in this model of infection. Furthermore it is not clear what effect a 10 fold increase in miR-146b would have on the regulation of shared targets, since miR-146a was still expressed at ~10 fold higher copy numbers.

5.2.6 MiR-146a/b expression profiles over the course of alternative activation

Because miR-146a and miR-146b are isoforms with identical seed sequences that differ in their 3' region by just 2 nucleotides, they are predicted to share targets and indeed have been shown to bind some of the same mRNA targets. For example, both miR-146a/b are negative regulators of TLR signalling and target the same molecules in this pathway (Taganov et al., 2006). Hence, based on their differential regulation in AAMΦ along with their known functions in suppressing excessive proinflammatory responses, it was hypothesised that miR-146a/b serve to regulate proinflammatory molecules (and signals) in a fine balance to allow efficient alternative activation to occur.

To help formulate a hypothesis related to whether miR-146 is important for the initiation and/or maintenance of alternative activation, the expression profiles of miR-146a/b were studied during a time course of alternative activation in RAW 264.7 cells. The rationale behind this experiment was to examine the onset of changes in miR-146a/b expression in relation to the expression of *Chi3l3* (YM-1), a characteristic marker of alternative activation. With the known role of miR-146 in regulating proinflammatory responses (TLR signalling), classical activation was used as a control in this experiment. RAW 264.7 cells were left untreated or stimulated with 10ng/mL of LPS or 20ng/mL of IL-4 and IL-13. Cells were harvested at 0hr, 2hr, 4hr, 6hr, 8hr, 12hr, 18hr, 24hr, 36hr and 48hr post stimulation. Quantification by qRT-PCR revealed a gradual increase in *Chi3l3* (YM-1) expression over time (Figure 5.8A). A significant increase in mRNA expression was observed at 4-6hr post IL-4/IL-13 stimulation and this continued to rise steadily until peak expression at 18-24hr hours post treatment (Figure 5.8A). On the other hand, mRNA levels of TNF-α (*Tnfa*) and iNOS (*Nos2*) were used as a measure of classical activation (Figure 5.8B). As expected, both TNF-α and iNOS mRNAs were induced fairly quickly following exposure to LPS, with expression significantly increased at 2 hours post treatment. Their expression levels peaked at 4 hours with a gradual decline over time as shown in Figure 5.8B. Consistent with existing literature, both miR-146a and miR-146b

were significantly up-regulated in response to LPS treatment (Nahid et al., 2009, Nahid et al., 2011) as is reflected in Figure 5.8C. Expression escalated quickly by 6 hours post stimulation and continued to rise until 24-48hr. This increase correlated with the decrease in TNF-α and iNOS. There was a decline in their expression as levels of miR-146a/b continued to rise and this is in agreement with their role as regulators of endotoxin tolerance in a negative feedback loop (Nahid et al., 2009, Nahid et al., 2011). Following confirmation of miR-146a/b expression during classical activation, their expression profiles over the course of alternative activation were next examined (Figure 5.8C). Consistent with the previous data obtained from RAW 264.7 cells, expression of miR-146a was reduced upon exposure to IL-4 /IL-13 over time. This reduction was observed from 8 hours post treatment but wasn't significant until 12 hours. This reduction in expression was maintained until 48 hours (Figure 5.8C & Appendix 4). In contrast, miR-146b expression was enhanced from 18 hours post treatment until 48 hours (Figure 5.8C & Appendix 4).

The primary aim of this experiment was to examine potential correlation between the expression of miR-146a/b to *Chi3l3* (YM-1) expression. We have shown that miR-146a expression declined in response to IL-4/IL-13 while expression of *Chi3l3* was greatly enhanced over the course of alternative activation (Figures 5.8A and 5.8C). Correlation of miR-146a expression over time to *Chi3l3* mRNA levels revealed a moderate negative correlation with a Pearson's *r* value of -0.59. However, this correlation was not statistically significant with a P value of 0.09 as shown in Figure 5.8D. Similarly, a correlation was calculated between miR-146b expression and *Chi3l3* mRNA levels (Figure 5.8E). There was a strong overlap in the induction of both miR-146b and YM-1 upon exposure to the cytokines IL-4 and IL-13, with expression of both being significantly up-regulated over time. This was reflected in a moderately positive correlation of 0.59 as determined by Pearson's *r* coefficient. This positive correlation was statistically significant with a P value of 0.01 (Figure 5.8E).

During this time course, levels of miR-146a began to decline at 12 hours post stimulation with IL-4/IL-13 whereas expression of miR-146b was significantly enhanced from 18 hours onwards. Both miR-146a and miR-146b had moderate

negative and positive correlations with alternative activation respectively as measured through *Chi3l3* (YM-1) levels. Taken together, these results indicate that there may be a fine balance between the switching off of miR-146a and induction of miR-146b expression, which also coincides with the onset of the peak of alternative activation. This would suggest that a compensatory mechanism might exist between miR-146a and miR-146b with the suppression of shared proinflammatory targets, which would otherwise hinder efficient alternative activation. To further validate this hypothesis, experiments involving inhibition of either miR-146a or miR-146b or both would help determine whether miR-146 was involved in the regulation of alternative activation and if this regulation was based on suppression of shared targets by miR-146a/b in a compensatory mechanism through differential transcriptional regulation. However, due to the high sequence similarity between these two isoforms, with a difference of just two nucleotides, synthetic inhibitors would not be specific to one form (at least when targeting the mature microRNA). Although this specific inhibition was not necessary to study the overall role of miR-146 in regulating AAMΦ, it was important to delineate the role of the two miR-146 isoforms and testing our specific hypothesis. To overcome this hurdle and to determine whether miR-146a/b bind the same targets under conditions of alternative activation, the use of the technique cross-linking, ligation and sequencing of hybrids (CLASH) was considered. We thus decided to generate a stable RAW 264.7 cell line expressing tagged mAGO2 for the identification of microRNA targets

5.2.7 Generation of a stable RAW 264.7 cell line expressing tagged mAGO2 for the identification of microRNA targets

CLASH relies on the co-immunoprecipitation of UV cross-linked complexes containing microRNAs and their target mRNAs bound to tagged AGO protein (Helwak and Tollervey, 2014). Making use of endogenous AGO protein to immunoprecipitate protein-RNA complexes is not an efficient process as the binding affinity of the anti-AGO antibody is not strong enough to survive the stringent

purification conditions utilised during the process. Therefore, it is essential to have a system that is capable of stable expression of the tagged AGO protein. There are four Argonaute proteins found in humans and mice (AGO 1-4) that are thought to be functionally redundant (Su et al., 2009). However, out of the four only AGO2 is known to have slicer activity essential for cleavage of target mRNAs based on near perfect complementarity to microRNAs (Karginov et al., 2010, Bracken et al., 2011). Furthermore, a role for AGO2 has been implicated in development. *Ago2*$^{-/-}$ mice are embryonic lethal whereas other AGO proteins are dispensable suggesting a crucial role for AGO2 in development (Liu et al., 2004a). Therefore, mAGO2 was selected for this study. In order to create such a stable macrophage cell line for the identification of miR-146a/b (and other microRNA) targets, a lentiviral system of transduction was utilised. RAW 264.7 cells were chosen based on their ability to both classically and alternatively activate (Chapter 2). We have also shown that successful synthetic microRNA transfection can be achieved in RAW 264.7 cells enabling microRNA levels to be manipulated in subsequent experiments. A lentivirus is a retroviral vector system that has the ability to infect both dividing and non-dividing cells and can efficiently drive gene expression both *in vitro* and *in vivo* (Naldini et al., 1996, Lois et al., 2001, Ailles et al., 2002, Scherr et al., 2002). It is an advantageous system to use in terms of its low immunogenicity and long-term stable expression of the gene of interest.

Lentiviral expression vectors generally contain large regions of repeated DNA sequences from the long terminal repeats (LTRs) of retroviruses from which they are derived. These LTRs are the basis for homologous recombination and incorporation of the gene of interest, which is cloned in between two LTR regions. For the generation of lentiviruses, three different plasmid constructs were utilised. Two of these encoded essential packaging genes encoding the envelope protein (pMD2.5-VSV-G) and the other packaging protein required for replication (psPAX2). The third vector was the transfer vector pLVX-EF1α-IRES-ZsGreen1 containing the LTR regions. It is a bicistronic vector that contains an internal ribosomal entry site (IRES) that allows the gene of interest and the ZsGreen1 fluorescent protein to be simultaneously co-expressed. This vector consists of an EF-1α promoter, derived

from the human EEF1A1 gene that expresses the alpha subunit of eukaryotic elongation factor 1. This promoter allows robust and constitutive expression of the gene of interest in cell types in which CMV promoters are often silenced, such as hematopoietic and stem cells (Teschendorf et al., 2002). Additionally, the vector allows efficient flow cytometric detection of stably or transiently transfected cells through the ZsGreen1 fluorescent protein without the need for other time consuming selection processes such as drug and clonal selection.

A tagged protein construct using the vector pCDNA3 with murine AGO2 (mAGO2) fused to a Protein A-TEV protease-Histidine (HTP) tag was available in the lab (Figure 5.9A). It was decided that a new tag should be designed for these studies in order to eliminate potential issues with specific binding of IgG to Protein A. This affinity could be a potential hindrance for performing CLASH *in vivo* to confirm the results obtained *in vitro* as well as for factoring in processes such as IL-4 induced macrophage proliferation that cannot be utilised *in vitro*. Furthermore previous work in the lab suggested that the TEV cleavage site was not functional. Therefore, the PTH tag was replaced with a new tag consisting of 3xFLAG residues, a PreScission protease site and 6x Histidine residues (FPH). The new tag was cloned into the pLVX-EF1α-ZsGreen1 vector as shown in Figures 5.9B and 5.9C. The HTP tag DNA sequence was first excised from the pCDNA3 vector by restriction digestion with BamHI and EcoRV (Figure 5.9A). The FPH tag was generated through annealing and elongation of two overlapping oligos using the Klenow fragment DNA polymerase. BamHI and ExoRV restriction sites were designed at the end of these oligos, which were then used to digest and clone the tag into pCDNA3 upstream of mAGO2 (Figure 5.9B). For cloning the FPH-mAGO2 into the pLVX-EF1α lentiviral construct, the BamHI site in pCDNA3 was replaced with an SpeI digestion site through PCR amplification (Figure 5.9C). This amplified PCR product was then digested with SpeI and NotI and cloned into the lentiviral vector (Figure 5.9D).

Prior to lentiviral packaging, the expression of the tagged protein was examined based on $CaCl_2$ transfection. RAW 264.7 cells were left untreated or transfected with pLVX-EF1α-ZsGreen1 empty vector or the pLVX-EF1 α-ZsGreen1 vector

containing the FPH-mAGO2 sequence. Protein lysates were harvested at 48 hours post transfection and analysed by Western blot using antibodies against the FLAG tag and mAGO2 protein. As shown in Figure 5.10A and 5.10B, cells transfected with pLVX-EF1α-ZsGreen1-FPH-mAGO2 and the control vector pCDNA3-FPH-mAGO2 expressed high levels of FLAG tag and mAGO2 whereas the tagged protein was absent in untreated cells or cells transfected with the control empty vectors pLVX-EF1α-ZsGreen1 and pCDNA3. Cells transfected with the vectors containing FPH-mAGO2 also expressed high levels of mAGO2 and no bands were observed for endogenous mAGO2 in the control wells. This may be attributed to the fact that the exposure for the blots shown was a mere 10 seconds which may not have been enough for quantification of endogenous levels. This would indicate that upon transfection there was a substantial over-expression of the protein compared to the endogenous level.

Following verification of tagged mAGO2 expression, the pLVX-EF1α-ZsGreen1-FPH-mAGO2 construct was co-transfected with pMD2.5-VSV-G and psPAX2 into HEK293T cells to generate lentiviral particles. The viral supernatant was harvested and concentrated by ultracentrifugation (~100 fold) before being used for transduction of RAW264.7 cells. The protocol has previously been established in the lab and it was determined that the viral supernatant contains ~10^8 particles/mL prior to ultracentrifugation (Dr. Shatakshi Sood). This was determined based on lentiviral titering of the freshly harvested supernatant using HEK293T cells. Following concentration of the lentiviral stock, a previously determined optimal volume of 25μL for 3T3 and HEK293T cells (unpublished data) was used for the generation of a stable cell line. To do this, RAW 264.7 cells were left untreated or transduced with the concentrated viral supernatant. 48 hours post transduction, cells were harvested for analysis of ZsGreen1 expression by flow cytometry. FACS analysis of ZsGreen1 expression revealed successful transduction of a very small percentage of RAW 264.7 cells (8.2%) with the empty pLVX-EF1α-ZsGreen1 vector and the percentage of cells transduced with the pLVX-EF1α-ZsGreen1-FPH-mAGO2 construct was only 6% as shown in Figure 5.11. Although the actual percentage of transduced cells was minute, these results suggested that the lentiviral generation, transduction and

the analysis of transduction through ZsGreen1 expression worked as a system overall.

It is well established that macrophages are a difficult cell type to transfect or transduce. To ensure the lentiviruses are capable of efficient transduction NIH-3T3 cells were transduced with lentivirus containing either the empty vector pLVX-EF1α-ZsGreen1 or the pLVX-EF1α-ZsGreen1-FPH-mAGO2 construct. NIH-3T3 cells were chosen because a high level of lentiviral transduction efficiency has previously been achieved with this cell line in our lab. Similar to the previous experiment described above, cells were transduced with 25μL of concentrated lentiviral stock and harvested at 48 hours for FACS analysis. Analysis of ZsGreen1 expression showed that 97.7% of NIH-3T3 cells transduced with the empty pLVX-EF1α-ZsGreen1 vector were positive for ZsGreen1 expression. Cells transduced with pLVX-EF1α-ZsGreen1-FPH-mAGO2 also showed high percentage positivity for ZsGreen1 (90.9%) as shown in Figure 5.12. In comparison, untreated cells did not express any ZsGreen1 protein as expected (Figure 5.12). Thus, these results confirm that the lentiviral system works well for transduction and that the poor transduction efficiency seen in RAW 264.7 cells (Figure 5.11) is related to the cell type rather than the protocol involved.

Following concentration by ultracentrifugation, the lentivirus stock is usually frozen at -80C. For transduction, this stock is then thawed for use. It has been suggested that each freeze thaw cycle might reduce the viability and activity of the virus by as much as 30%. Therefore, in an effort to improve transduction efficiency of RAW 264.7 cells, the supernatant harvested from HEK293T cells following lentiviral packaging was centrifuged to remove any HEK293T cells and cellular debris and transferred directly to RAW 264.7 cells for 48 hours. Cells were then analysed for ZsGreen1 expression by FACS. Analysis showed a marked improvement in the percentage of cells successfully transduced as measured by ZsGreen1 expression (Figure 5.13). 37.2% cells transduced with pLVX-EF1α-ZsGreen1 empty vector lentivirus were positive for ZsGreen1 whereas 24.8% cells transduced with pLVX-EF1α-ZsGreen1-FPH-mAGO2 containing lentivirus expressed ZsGreen1 (Figure 5.13). These results

suggest that direct transfer of freshly harvested supernatant containing lentiviruses results in greater transduction efficiency in RAW 264.7 cells than virus that has been frozen after concentration by ultracentrifugation.

Although freshly harvested supernatant resulted in a better transduction efficiency of the RAW cells, only ~30% of the cells were successfully transduced. Therefore, in an effort to improve the transduction efficiency in RAW cells, the transduction protocol was further optimised. Using HEK293T cells and serial dilutions of the lentiviral stock, the lentiviral titre was determined through percentage positivity of cells for ZsGreen1 using flow cytometry (data not shown). Based on the viral titre, RAW 264.7 cells were either left untreated or transduced with lentivirus containing the empty pLVX-EF1α-ZsGreen1 construct at various MOIs ranging from 10.8 to 172.8 (Figure 5.14). Additionally, existing literature states that an MOI of 10-25 is ideal for macrophage transduction with lentiviruses (Leyva et al., 2011). Therefore, RAW264.7 cells were also transduced with pLVX-EF1α-ZsGreen1-FPH-mAGO2 containing lentivirus at an MOI of 16.2 (Figure 5.14). Due to limited amounts of lentivirus containing the tagged mAGO2 construct and the involvement of a longer procedure to generate this construct, the empty pLVX-EF1α-ZsGreen1 construct was utilised in this experiment for optimisation of transduction at different MOIs. As shown in Figure 5.14, increased transduction efficiency was observed with increasing MOIs (MOI-10.8-86.4) ranging from 4.3% to 34.9% of ZsGreen1 expression in cells transduced with the empty vector containing lentivirus. Cells transduced with pLVX-EF1α-ZsGreen1-FPH-mAGO2 containing lentivirus at MOI 16.2 showed a comparable 7.2% positivity for ZsGreen1 in comparison to the empty vector (Figure 5.14).

Although an increase in ZsGreen1 expression was observed with increasing MOIs of lentivirus (Figure 5.15A), the percentage viability of cells was also profoundly affected with higher lentivirus doses as shown in Figure 5.15B. Maximal transduction was observed at MOI 43.2 as reflected in the mean fluorescence intensity of ZsGreen1 (Figure 5.15A) but at the same time, only ~ 10% of the cells were intact following transduction. Similar trends were observed with an inverse

correlation between transduction efficiency and cell viability at the higher MOIs of 86.4 and 172.8. Although transduction was the lowest at MOI 10.8 and MOI 16.2, the cells in these samples were in fact the healthiest with nearly 50% of the population intact (Figures 5.15A and 5.15B).

Although lentiviral vectors are non infectious, the envelope proteins may still be recognised by pathogen recognition receptors and induce a proinflammatory response. Besides Type-1 interferons, TNF-α production is induced relatively quickly in macrophages upon viral contact and can result in cell death depending on the accumulated concentrations (Willeaume et al., 1995). To investigate this inverse correlation between MOI and cell viability, the levels of TNF-α were quantified (range 0.001-2ng/mL) in the supernatants harvested from RAW 264.7 cells transduced at varying MOIs for 24hr, 48hr and 72hr respectively. As represented in Figure 5.16A, TNF-α levels were indeed elevated in cells transduced at MOIs greater than 21.6 at 24 hours following transduction. Interestingly, the viability of cells transduced with the lentivirus containing the FPH-mAGO2 construct was the lowest (<5%) and TNF-α expression was the highest (beyond the detection limit) in this sample (Figure 5.16A and 5.16B) at 24 hours post transduction. The elevated TNF-α levels returned to baseline levels from untreated cells by 48 hours (Figure 5.16A). Overall these results suggest that the loss of cell viability with increased transduction is associated with the production of proinflammatory molecules in response to viral recognition.

To address this issue and to improve cell viability as well as transduction efficiency, RAW 264.7 cells were transduced with freshly harvested viral supernatant and centrifuged for 1 hour at an increased temperature of 32C to enhance viral entry. Thereafter, the supernatant was aspirated and the culture medium replaced every hour for 10-12 hours post transduction. Cells were then harvested 48 hours post transduction and FACS analysed for ZsGreen1 expression. Cell viability was improved from <10% to greater than 30% for cells transduced with both empty vector and FPH-mAGO2 containing lentiviruses (Figure 5.17). At the same time, transduction efficiency was also profoundly increased to >50% as shown in Figure

5.17. These cells positive for ZsGreen1 were then sorted using flow cytometry and cultured for 48 hours to repopulate numbers. After 48 hours, a small proportion of the cells was reanalysed by FACS to confirm percentage positivity for ZsGreen1 before further analyses. FACS analysis revealed an enrichment in cells positive for ZsGreen1 from 56.5% to 74.6% in cells transduced with pLVX-EF1α-ZsGreen1 containing lentivirus. The cell viability was also improved from 30% to 60.7% as predicted due to cell recovery in the absence of any external stimuli (Figure 5.18). In contrast, the percentage positivity for ZsGreen1 in cells transduced with pLVX-EF1α-ZsGreen1-FPH-mAGO2 lentivirus was decreased to 38.7% compared to an earlier 50%. However, cell viability was improved from 30% to 57.5% (Figure 5.18). The cells were incubated for a further 5 days to allow maximal growth and recovery before being FACS analysed again to resort the populations and exclude any ZsGreen1 negative cells. As shown in Figure 5.19, cells transduced with pLVX-EF1α-ZsGreen1 lentivirus that expressed ZsGreen1 was significantly lower at at day 7 compared to day 2 (30.6% versus 74.6%) although the viability had further increased to 69%. Similarly, cells transduced with pLVX-EF1α-ZsGreen1-FPH-mAGO2 lentivirus had completely lost ZsGreen1 expression but viability was greatly improved at 75.5% (Figure 5.19). Taken together, these results imply that either transduction of RAW 264.7 cells is transient with expression being lost by day 7 or the cells lose the integrated copy of the gene of interest over time through unknown mechanisms.

5.3 Discussion

MicroRNAs tend to be highly redundant, with multiple individual microRNAs converging upon the same target mRNAs. Some of this redundancy owes to different microRNAs sharing identical or highly similar seed sequences. The focus of this chapter was two such microRNA isoforms that share the same seed sequence but differ by two nucleotides in their 3' regions: miR-146a and miR-146b. MiR-146 has a well-established role in regulating CAMΦ and their responses (Taganov et al., 2006, Curtale et al., 2012, He et al., 2014c). However, a functional role for miR-146 in regulating alternative activation is yet to be determined and the relationship between the two isoforms in this context is unknown. Thus, in conjunction with Chapter 2, the expression profiles of these two isoforms were studied in AAMΦ in detail. It was found that both miR-146a and miR-146b are differentially expressed during alternative activation; however, their expression patterns differed: there was a reduction in miR-146a levels and an enhancement of miR-146b expression. This differential regulation was observed under various conditions of alternative activation including cell lines, BMDMs, Thio elicited MΦ and following IL-4c delivery *in vivo* suggesting a consistent alteration of miR-146 expression in AAMΦ. Based on their contrasting expression during alternative activation and their known role for negatively regulating proinflammatory responses, it was hypothesised that miR-146a/b contribute to efficient alternative activation through the suppression of shared proinflammatory targets in a compensatory mechanism.

Although a significant increase was observed in miR-146b expression in AAMΦ isolated from *L. sigmodontis* infection at various time points, no significant changes were observed in miR-146a expression over the course of infection. This could be attributed to two reasons -1) All quantification was carried out by qRT-PCR. With high sequence similarity between the two isoforms and a difference of just two nucleotides, it was probable that the primer specificity was not sensitive enough to differentiate between miR-146a and miR-146b. To investigate this further, synthetic microRNA standards of known concentrations for both miR-146a and miR-146b were tested at various dilutions for primer specificity (Appendix 5). A high degree of

cross talk was observed with primers binding efficiently to both isoforms implying that the changes in expression quantified by qRT-PCR may not be valid. However, besides fold changes, copy numbers of miR-146a/b were quantified per ng of RNA for each of the alternative activation conditions that were studied. These also reflected significant differences in miR-146a and miR-146b expression with miR-146a expressed at a much higher copy number (10^6-10^7 copies/ng RNA) compared to miR-146b (10^5 copies/ng RNA). These results would suggest that although primer specificity may be a concern, the large difference between miR-146a and miR-146b expression levels in macrophages reduced our concern. 2) During *L. sigmodontis* infection, macrophages were isolated by adherence purification. In all the other conditions of alternative activation that were studied, the populations were relatively homogeneous, either cell lines or BMDMs, or FACS sorted after IL-4c injection. Although adherence purification is an efficient technique to distinguish macrophages from other cell types, it does not result in a population that consists purely of macrophages. We found that these populations were 60-80% pure as analysed by FACS (data not shown). Thus, there are likely other cell types within the well that do not get washed away and may contribute to the quantification of miR-146 in the samples. MiR-146a especially is differentially expressed in different T helper cell subsets and is involved in fate determination (Monticelli et al., 2005, Rusca and Monticelli, 2011). Significant differences in miR-146b expression during the infection were only detectable day 11 onwards. By this time, other immune cell types are already present in the cavity and the adaptive immune responses are well initiated (Babayan et al., 2003a, Graham et al., 2005b). Thus, it is plausible that some of these cell types might have contributed to the levels of miR-146 detected and the reason why a reduction in miR-146a was not observed. It is also worth mentioning that besides IL-4Rα signalling, infection with a nematode creates a complex environment with simultaneous cues and external stimuli that may also affect microRNA expression. In all the other conditions studied, especially the *in vitro* models of alternative activation, this complex network of signals did not exist. Furthermore, changes in microRNA expression are subtle. Hence, it is possible that significant changes at the individual cell level may get masked in an infection environment and, therefore, cannot be detected.

Finally, the expression of miR-146a/b was correlated to the expression of YM-1, a marker characteristic of alternative activation. Whilst a non-significant negative correlation was observed for miR-146a, a moderately positive and significant correlation existed between miR-146b and YM-1 expression. Additionally, as levels of miR-146a began to decline, a rise in miR-146b expression was observed suggesting there may exist a compensatory mechanism to suppress shared targets. Expression of miR-146a is NF-κB dependent (Taganov et al., 2006) whereas miR-146b expression is STAT3 induced (Xiang et al., 2014). NF-κB is a nuclear factor considered to be a prototypical signal for the expression of several proinflammatory molecules and a well-known regulator of classical activation (Lawrence, 2009, Martinez, 2011). Although IL-4 can induce NF-κB processing, it is able to do so only in B cells and not in T cells or macrophages (Thieu et al., 2007). Contrastingly, both IL-4 and IL-13 are potent activators of STAT3 (Wery-Zennaro et al., 1999, Umeshita-Suyama et al., 2000, Bhattacharjee et al., 2013). Thus, the downregulation of miR-146a expression and induction of miR-146b with the progression of/during alternative activation may be explained through differential regulation at the transcriptional levels.

With the predicted/hypothesised role of miR-146a/b in regulating alternative activation through the suppression of shared proinflammatory targets, the next obvious step was to inhibit these microRNAs together and individually to assess their effect on alternative activation and to identify shared targets. The most commonly used microRNA inhibitors are chemically modified antisense oligonucleotides that sequester mature endogenous microRNA (Stenvang et al., 2012). Due to the high sequence similarity between miR-146a/b, it is likely not possible to inhibit one microRNA alone – the key to delineating functions and shared targets of miR-146a vs. miR-146b during alternative activation as a compensatory mechanism. In Chapter 3 synthetic microRNA delivery *in vivo* was achieved. MiR-146a KO mice exist and it may be possible to inhibit miR-146b in these mice to study their targets and effect on activation. However, delivery *in vivo* is not restricted to macrophages and thus, in the absence of two important microRNAs may result in outcomes not related to macrophage activation.

Another common approach used for the identification of microRNA targets involves the cross-linking of RNA-protein complexes followed by immunoprecipitation of tagged AGO protein and sequencing of associated RNAs (Ule et al., 2003, Licatalosi et al., 2008, Hausser and Zavolan, 2014). Several modifications of this method exist. One such modification termed CLASH (Helwak et al., 2013, Helwak and Tollervey, 2014) has been established for use in our lab. CLASH differs from other cross linking and immunoprecipitation (CLIP) techniques in that it involves an additional ligation step to join microRNAs to their mRNA targets, thus providing evidence for direct physical interaction. The latter half of this chapter focused on the generation of a stable cell line expressing tagged mAGO2 protein for the identification of miR-146 (and other microRNA) targets using CLASH.

For the generation of the tagged mAGO2 cell line, RAW 264.7 cells and a lentiviral system of transduction were utilised. FPH tagged mAGO2 was successfully cloned into an EF-1α promoter driven bicistronic vector containing an IRES site that allows the gene of interest and the ZsGreen1 fluorescent protein to be simultaneously co-expressed. RAW 264.7 cells were then transfected with this vector and overexpression of FPH tagged mAGO2 was confirmed. Next, RAW 264.7 cells were transduced with lentiviral particles containing this vector with and without FPH-mAGO2. Transduction of RAW 264.7 cells resulted in a very low level of ZsGreen1 expression (~8-10%) compared to control NIH-3T3 cells, which showed a near perfect 100% transduction efficiency. It was thought that low transduction efficiency in macrophages might be due to too low of a MOI, as this parameter was optimised for NIH-3T3 and HEK293T cells, both with different cell origins. The requirements for efficient transduction may vary with different cell types. An existing study that evaluated transduction efficiency in primary macrophages using lentiviral vectors states that an MOI of 10-50 depending on the vector used is ideal (Leyva et al., 2011). Thus, the lentivirus was titred using HEK293T cells and RAW 2647 cells were transduced with varying MOIs ranging from 10 to 175. Although increased transduction up to 30% was observed with increasing MOIs, this also led to a significant decrease in cell viability. This was attributed to the production of TNF-α by the macrophages in response to the lentivirus. TNF-α is one of the first molecules

to be produced by macrophages in response to viruses besides interferons (Malmgaard, 2004, Malmgaard et al., 2004, Paludan et al., 2001, Paludan and Mogensen, 2001). TNF-α signalling is a key player in inducing cell death (Nagata and Golstein, 1995, Boldin et al., 1996, Wajant et al., 2003). Hence, it was not surprising that transduction with increasing MOIs of lentivirus resulted in rapidly rising TNF-α production that correlated with increased cell death. Of note, TNF-α levels were particularly elevated in response to lentivirus containing the FPH-mAGO2 protein compared to the empty vector without the protein, even when the cells were transduced at comparable MOIs. The cause of this difference is unclear as the lentiviral particles are identical except for the presence of FPH-mAGO2. The mAGO2 sequence is unlikely to be the cause of the elevated TNF-α levels as the sequence is identical to endogenous mAGO2 protein. Thus, it is possible that the FPH tag may be responsible for this difference, potentially due to a conformational change that might increase endogenous recognition resulting in inflammation. However, it may very well be an artefact of the experiment and needs to be repeated to confirm the variations between the empty vector and protein containing lentivirus. It is also worth mentioning that macrophages compared to other cell types are highly autofluorescent when analysed by FACS. When cell death occurs or cells are stressed, the autofluorescence increases many-fold. Hence, it is also possible that the increasing ZsGreen1 expression observed with increasing MOIs may have been the result of increased autofluorescence.

Studies in this chapter have also provided evidence that utilisation of frozen concentrated lentiviral stock may negatively affect transduction efficiency. However, whether this is due to loss of viral activity would require measurement of viral recovery in fresh vs. frozen samples. The use of freshly harvested supernatant along with replacement of culture media every hour to remove proinflammatory molecules such as TNF-α resulted in a RAW 264.7-FPH-mAGO2 cell line expressing ZsGreen1 with improved viability. Unfortunately, expression was reduced 48 hours after sorting of the ZsGreen1 positive population and completely lost after 7 days. The cause and mechanisms behind this loss are still unknown. As professional phagocytes, macrophages are endowed with many potent degradation enzymes that

can disrupt nucleic acid integrity and make gene transfer into these cells an inefficient process. This is especially true of activated macrophages, which undergo a dramatic change in their physiology following exposure to immune or inflammatory stimuli (Zhang et al., 2009). Thus, it is probable that the transduction did not result in integration of FPH-mAGO2 in the genome and was in fact, only transient.

Several possibilities exist to overcome problems associated with a transiently transfected cell line for CLASH. Utilising FACS, single cells expressing ZsGreen1 could be sorted into individual wells and cultured in an effort to obtain a clone that may have a successfully integrated copy of FPH-mAGO2 and could give rise to a healthy population expressing the tagged protein. Another option would be to utilise large numbers of these transiently transfected cells for CLASH 48 hours after sorting as 30% of the cells are still positive for ZsGreen1 at this stage. However, this would utilise expensive reagents and be extremely time consuming. An easier solution would be to change the lentiviral construct (pLVX-EF1α-ZsGreen1) to one specifically designed for macrophage expression. A macrophage restricted expression system involving the use of *Csf1r* and the highly conserved Fms-intronic regulatory element (FIRE) has previously been used for the expression of transgenes (Pridans et al., 2014). Pridans et al. have developed a lentiviral construct comprising mouse FIRE and *Csf1r* promoter elements that are capable of directing macrophage restricted gene expression in several species. *Csf1r* promoter is constitutively and uniquely expressed in macrophages. This construct is readily available and may be an extremely useful tool to overcome the problems faced in this chapter. Lastly, our lab has very recently generated a transgenic mouse expressing FPH tagged mAGO2 in all cells, thus, overcoming the problems associated with successful and efficient transduction of macrophages. This mouse will be a tremendously advantageous tool to identify microRNA targets with physiological levels of endogenously tagged AGO protein using CLASH for studies conducted both *in vitro* and *in vivo*. It will be particularly interesting for microRNAs such as miR-199b-5p discussed in Chapter 3 that are not expressed highly or induced *in vitro*.

In summary, we cannot yet draw conclusions about the role of miR-146 in the regulation of AAMΦ from the results generated from the studies in this chapter.

Although it is clear that miR-146a/b are differentially and regulated during alternative activation, further experiments and optimisation need to be carried out to successfully identify whether they share the same targets or different ones and how this fits with regulation of the AAMΦ phenotype. Thus, as a starting point a stable cell line expressing tagged mAGO2 should be generated utilising the *Csf1r*-FIRE to progress with the identification of miR-146a/b targets using CLASH. Critically because both microRNAs and targets are sequenced during CLASH and any differences between these microRNAs will be elucidated.

A.

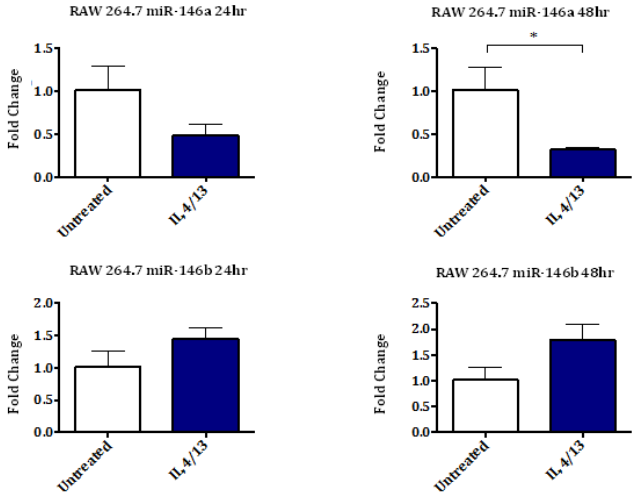

B.

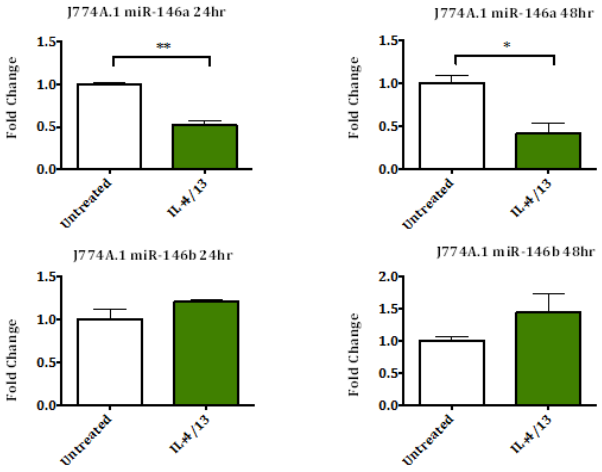

Figure 5.1 Contrasting changes in miR-146a and miR-146b levels in response to alternative activation A) RAW 264.7 cells and B) J774A.1 cells.

Cells were left untreated or stimulated with 20ng/mL of IL-4 and IL-13 for 24hr and 48hr respectively. Quantification was carried out by qRT-PCR and transcripts were normalised to *RNU6B*. Data represented are the mean fold change ± SEM and representative of two separate experiments (n=3). Statistical significance for differences between treated and untreated samples were calculated based on unpaired two-tailed Student's t-test (* P< 0.05, ** P< 0.01, *** P< 0.001, ****P<0.0001).

A.

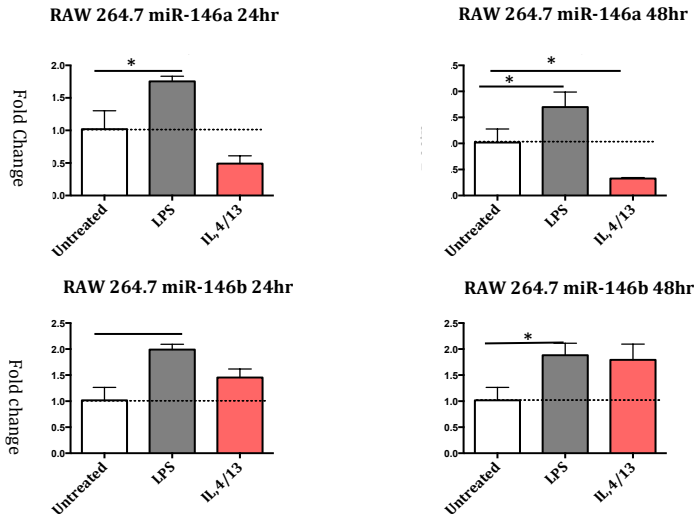

B.

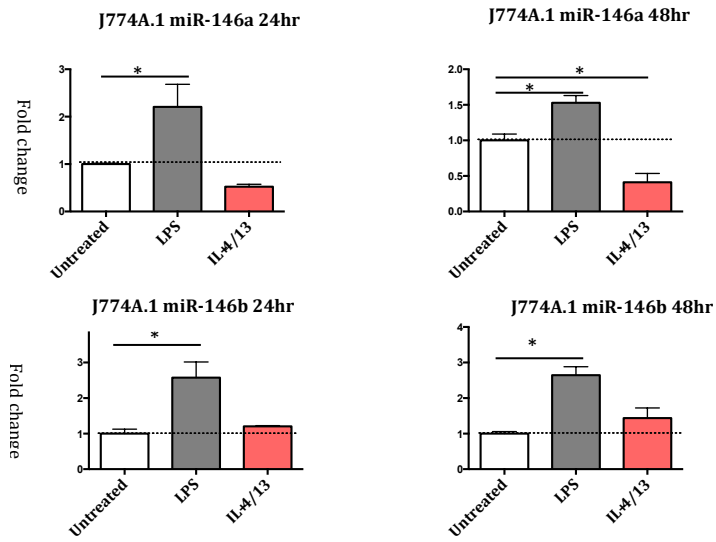

Figure 5.2 Expression profiles of miR-146a and miR-146b in classically and alternatively activated A) RAW 264.7 cells and B) J774A.1 cells.

Cells were left untreated or stimulated with either 10ng/mL of LPS or 20ng/mL of IL-4 and IL-13 for 24hr and 48hr respectively. Quantification was carried out by qRT-PCR and transcripts were normalised to *RNU6B*. Data represented are the mean fold change ± SEM and representative of a single experiment (n=3). Statistical significance for differences between treated and untreated samples were calculated based on one-way ANOVA (* P< 0.05, ** P< 0.01, *** P< 0.001, ****P<0.0001).

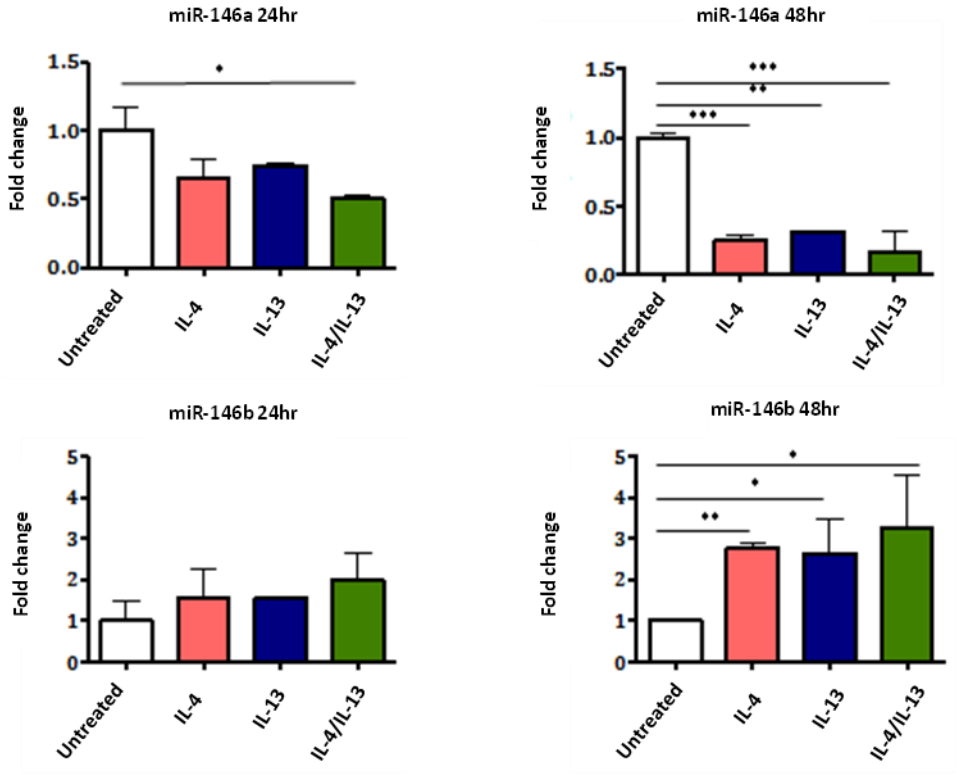

Figure 5.3 MiR-146a and miR-146b expression in RAW 264.7 cells following stimulation with IL-4 or IL-13 alone or in combination.

Cells were left untreated or stimulated with either 20ng/mL of IL-4 or IL-13 alone or IL-4 & IL-13 for 24hr and 48hr respectively. Quantification was carried out by qRT-PCR and transcripts were normalised to *RNU6B*. Data represented are the mean fold change ± SEM and representative of two separate experiments (n=3). Statistical significance for differences between treated and untreated samples were calculated based on one-way ANOVA (* P< 0.05, ** P< 0.01, *** P< 0.001, ****P<0.0001).

A.

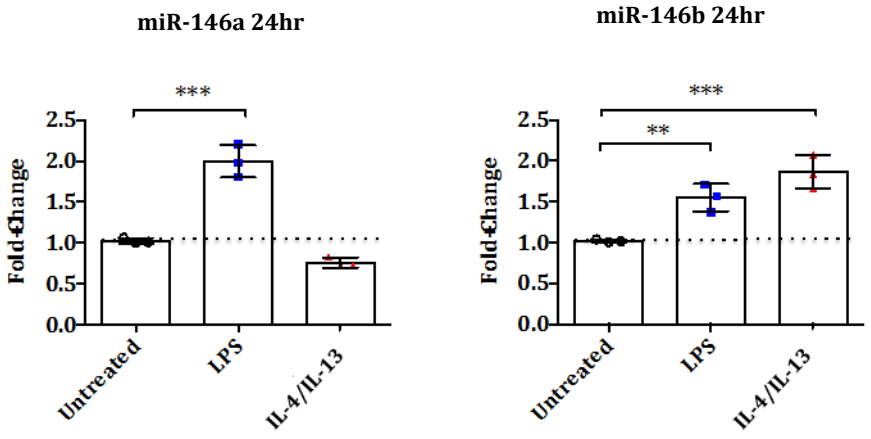

B.

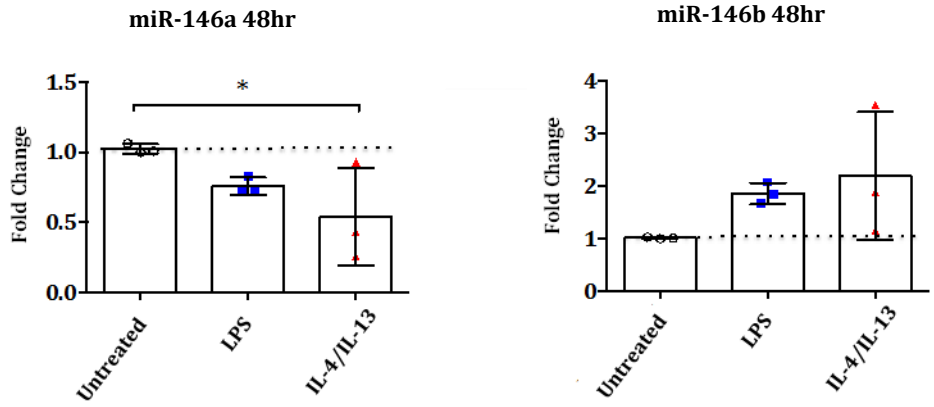

Figure 5.4 Quantification of miR-146a and miR-146b expression in classically and alternatively activated BMDM.

Bone marrow precursors derived from WT C57BL/6 mice were cultured in CSF-1 containing medium for 7 days to generate BMDMs. Cells were left untreated or stimulated with either 10ng/mL of LPS or 20ng/mL of IL-4 and IL-13 for **A)** 24hr and **B)** 48hr respectively. Quantification was carried out by qRT-PCR and transcripts were normalised to *RNU6B*. Data represented are the mean fold change ± SEM and representative of two separate experiments (n=3).

C.

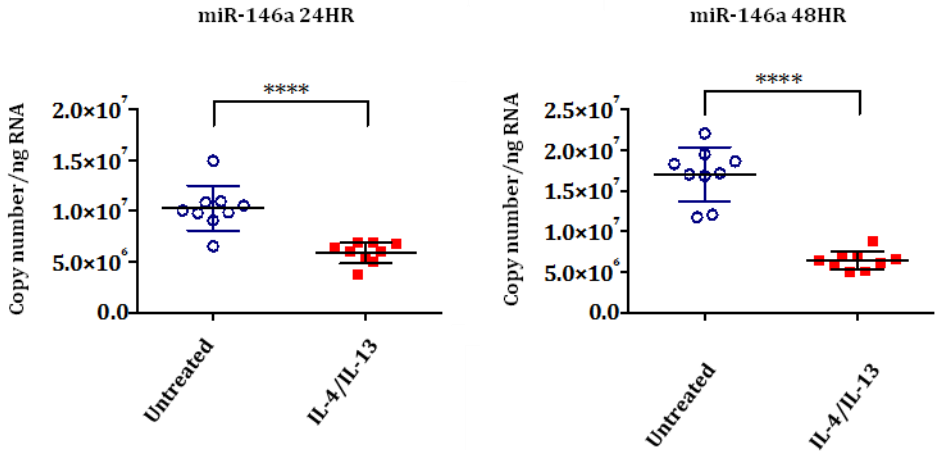

D.

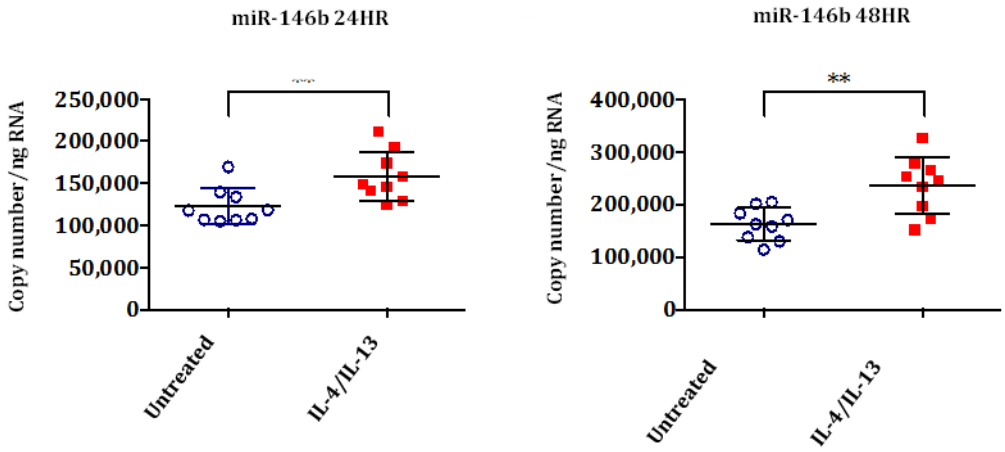

Figure 5.4 Quantification of miR-146a and miR-146b expression in classically and alternatively activated BMDM.

Copy number per ng of RNA of **C)** miR-146a and **D)** miR-146b in untreated or IL-4/IL-13 stimulated BMDMs as determined using synthetic microRNA standards. Statistical significance for differences between treated and untreated samples were calculated based on one-way ANOVA or unpaired two tailed Student's t-test where appropriate (* P< 0.05, ** P< 0.01, *** P< 0.001, ****P<0.0001) and representative of two pooled experiments (n=5).

A.

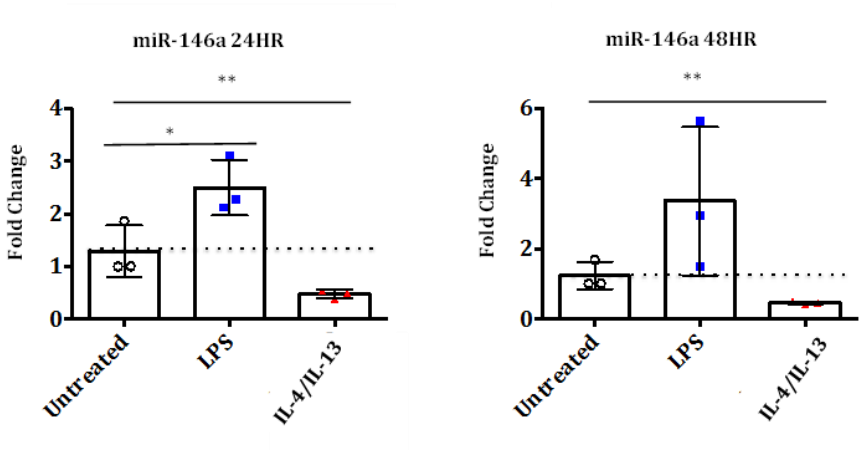

B.

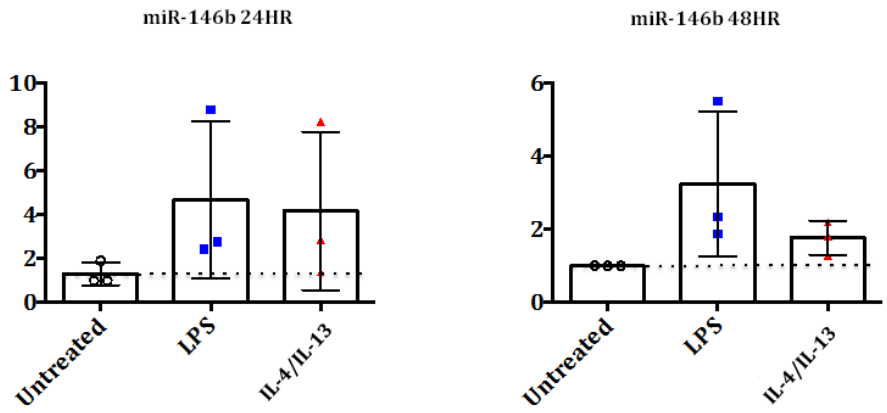

Figure 5.5 Changes in expression of miR-146a and miR-146b in Thio elicited MΦ stimulated with LPS or IL-4/IL-13.

WT C57BL/6 mice were injected with 4% thioglycollate intraperitoneally. On day 3, PEC populations were harvested and adherence purified for 4 hours at 37C to obtain Thio elicited MΦ. Cells were left untreated or stimulated with either 10ng/mL of LPS or 20ng/mL of IL-4 and IL-13 for 24hr and 48hr. Expression of **A)** miR-146a and **B)** miR-146b was quantified by qRT-PCR and transcripts were normalised to *RNU6B*. Data represented are the mean fold change ± SEM compared to untreated controls and representative of two separate experiments (n=3). Statistical significance for differences between treated and untreated samples were calculated based on one-way ANOVA (* P< 0.05, ** P< 0.01, *** P< 0.001, ****P<0.0001).

A.

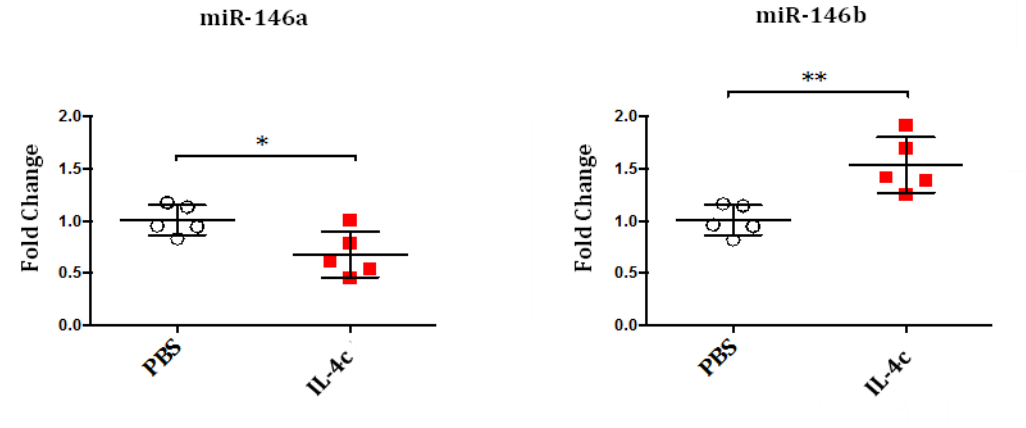

B.

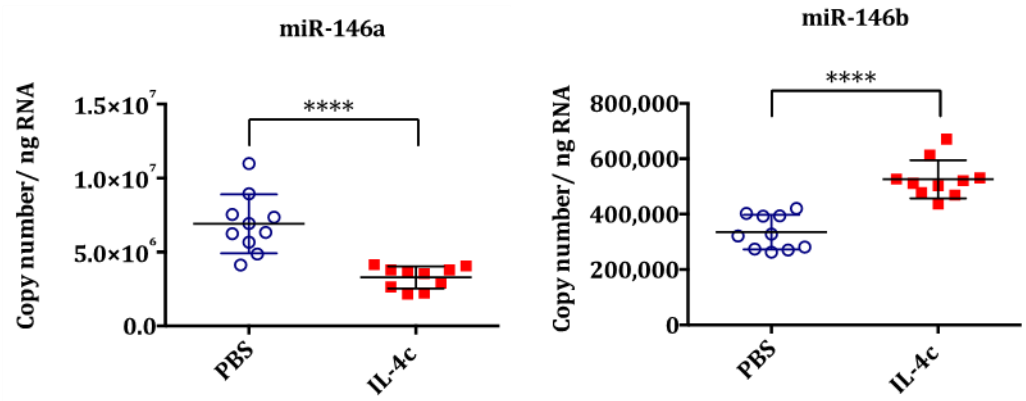

Figure 5.6 Expression profiles and quantification of miR-146a/b following IL-4c delivery in the peritoneal cavity.

WT C57BL/6 mice were injected with either PBS or 5µg of IL-4c intraperitoneally. PEC cells were harvested 24 hours post injection and macrophages sorted by FACS. **A)** MiR-146a and miR-146b levels as measured by qRT-PCR. Sorted macrophages were lysed and RNA extracted. Transcripts were normalised to *RNU6B* and fold changes calculated in comparison to PBS injected samples. **B)** Copy number/ng RNA of miR-146a and miR-146b in macrophages following IL-4c delivery. Data represented are the mean fold change ± SEM compared to untreated controls and representative of two separate experiments (n=5). Statistical significance for differences between treated and untreated samples were calculated based on two tailed unpaired Student's t-test (* P< 0.05, ** P< 0.01, *** P< 0.001, ****P<0.0001).

A.

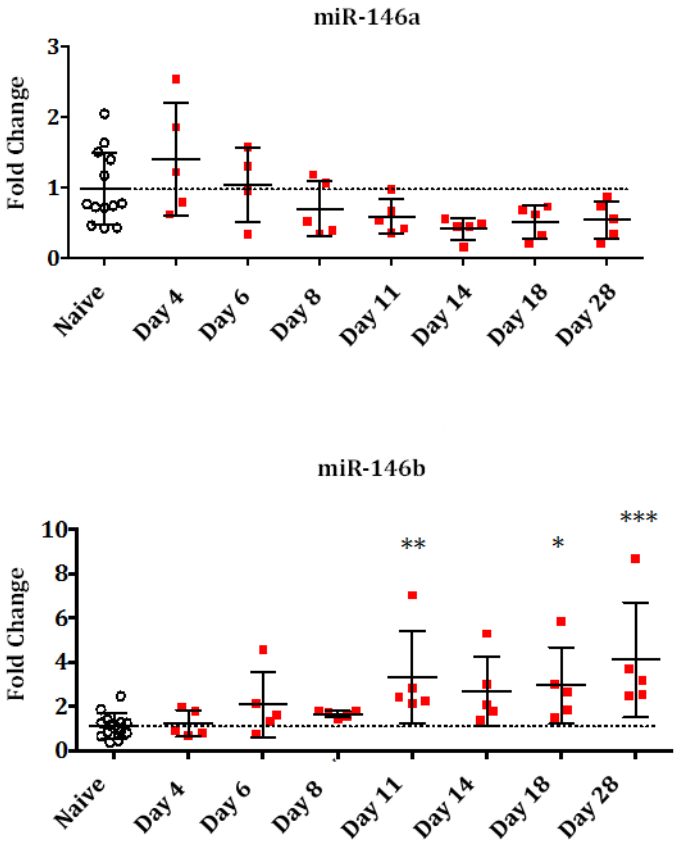
miR-146a
Fold Change
3
2
1
0
Naive
Day 4
Day 6
Day 8
Day 11
Day 14
Day 18
Day 28
miR-146b
Fold Change
10
8
6
4
2
0
**
*
***
Naive
Day 4
Day 6
Day 8
Day 11
Day 14
Day 18
Day 28

B.

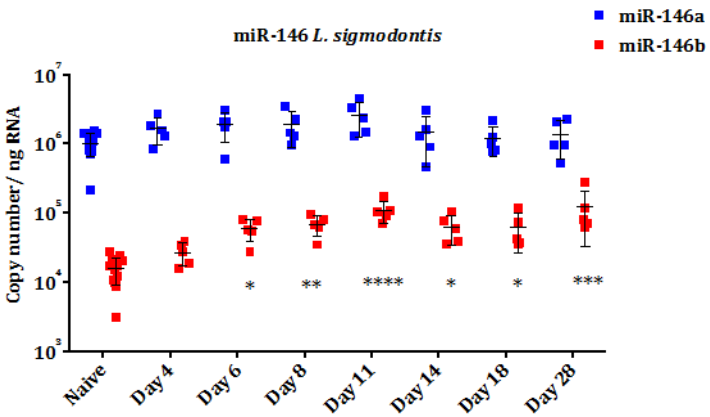
miR-146 L. sigmodontis
miR-146a
miR-146b
Copy number / ng RNA
10^7
10^6
10^5
10^4
10^3
*
**
****
*
*
***
Naive
Day 4
Day 6
Day 8
Day 11
Day 14
Day 18
Day 28

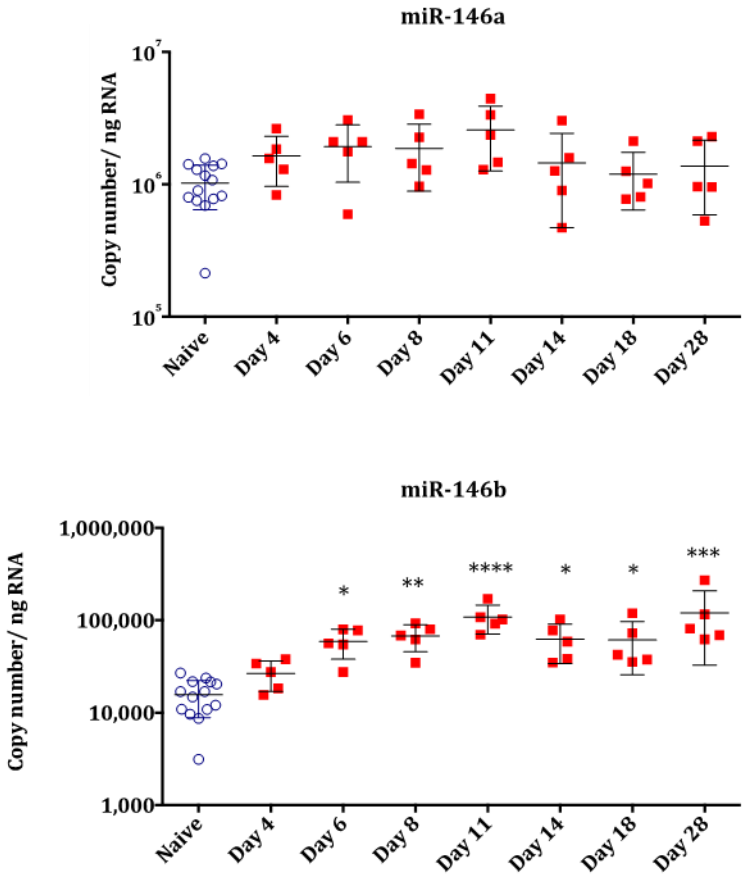

Figure 5.7 Relative expression levels and copy numbers of miR-146a and miR-146b during *L. sigmodontis* infection.

Pleural macrophages were isolated from pleural exudate cells through adherence purification on days 4, 6, 8, 11, 14, 18 and 28 post infection. RNA was extracted and **A)** microRNA expression quantified by qRT-PCR, normalised to *RNU6B* and fold changes calculated in comparison to a pool of naïve animals (day 4, 11 and day 28) from various time points. **B)** In the same samples, copy number/ng of RNA was determined using synthetic microRNA standards. Data represented are the mean fold change ± SEM compared to untreated controls and representative a single experiment (n=5). Statistical significance for differences between treated and untreated samples were determined using one way or two-way ANOVA where appropriate (* P< 0.05, ** P< 0.01, *** P< 0.001).

A.

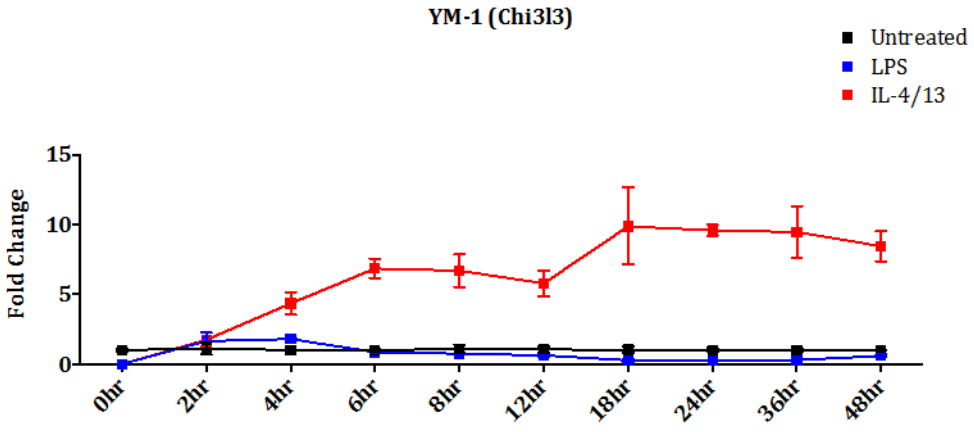
YM-1 (Chi3l3)
Untreated
LPS
IL-4/13
Fold Change
15
10
5
0
0hr
2hr
4hr
6hr
8hr
12hr
18hr
24hr
36hr
48hr

B.

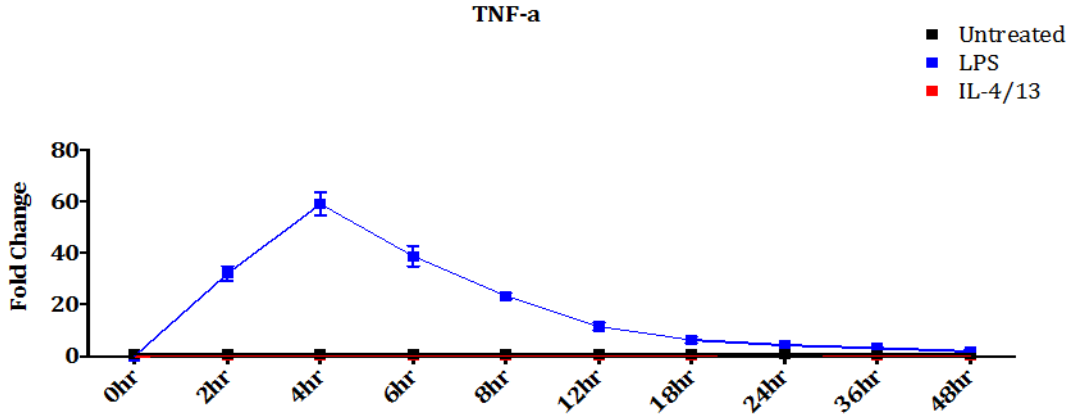
TNF-a
Untreated
LPS
IL-4/13
Fold Change
80
60
40
20
0
0hr
2hr
4hr
6hr
8hr
12hr
18hr
24hr
36hr
48hr

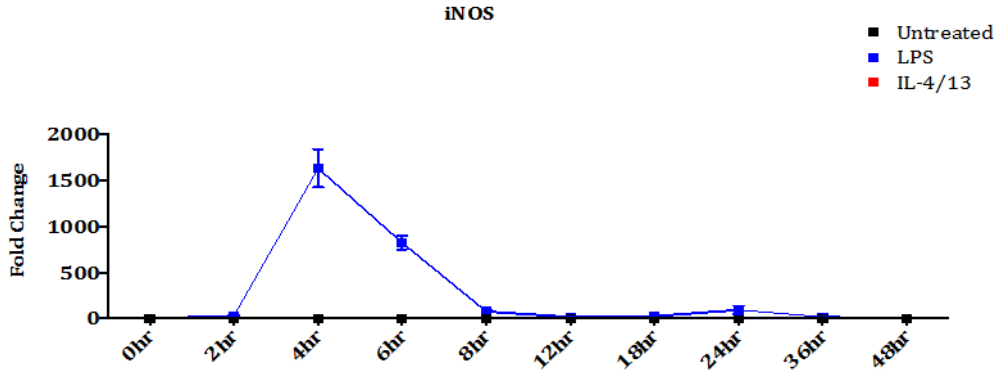
iNOS
Untreated
LPS
IL-4/13
Fold Change
2000
1500
1000
500
0
0hr
2hr
4hr
6hr
8hr
12hr
18hr
24hr
36hr
48hr

C.

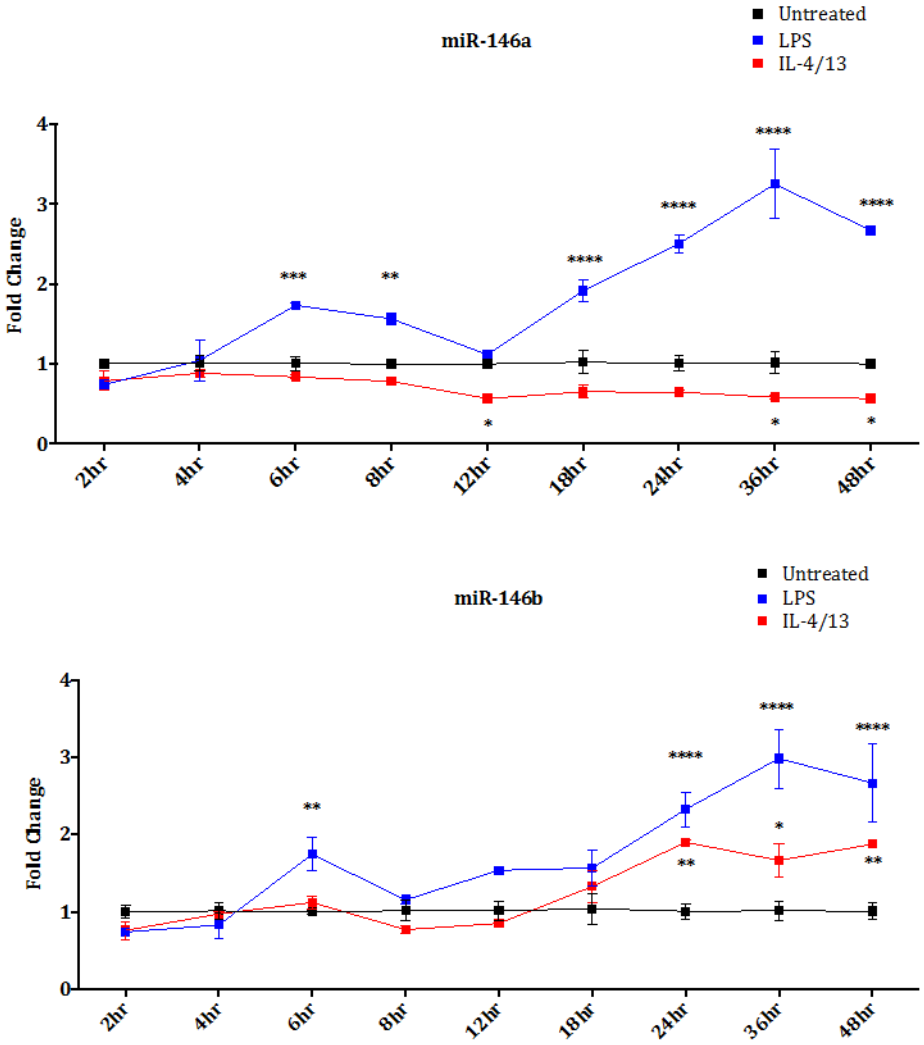
miR-146a
Untreated
LPS
IL-4/13
Fold Change
0
1
2
3
4
2hr
4hr
6hr
8hr
12hr
18hr
24hr
36hr
48hr
***
**
****
****
****
****
*
*
*
miR-146b
Untreated
LPS
IL-4/13
Fold Change
0
1
2
3
4
2hr
4hr
6hr
8hr
12hr
18hr
24hr
36hr
48hr
**
****
****
****
*
**
**

D.

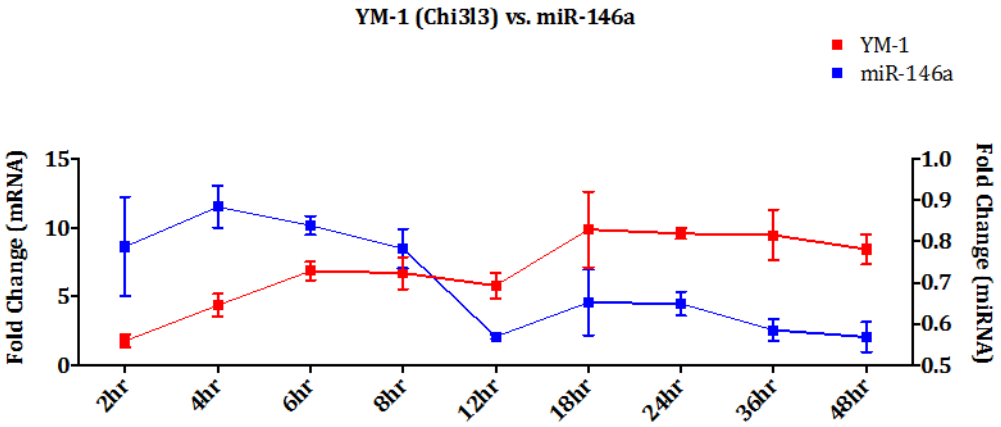

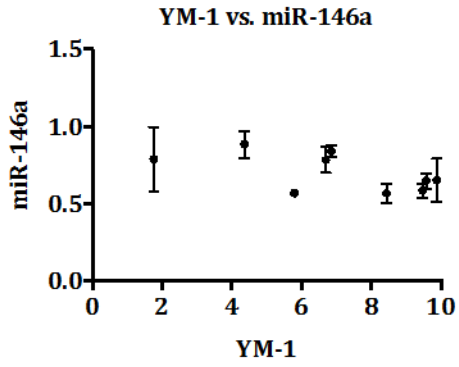

Pearson *r* = -0.59
P value = 0.094

E.

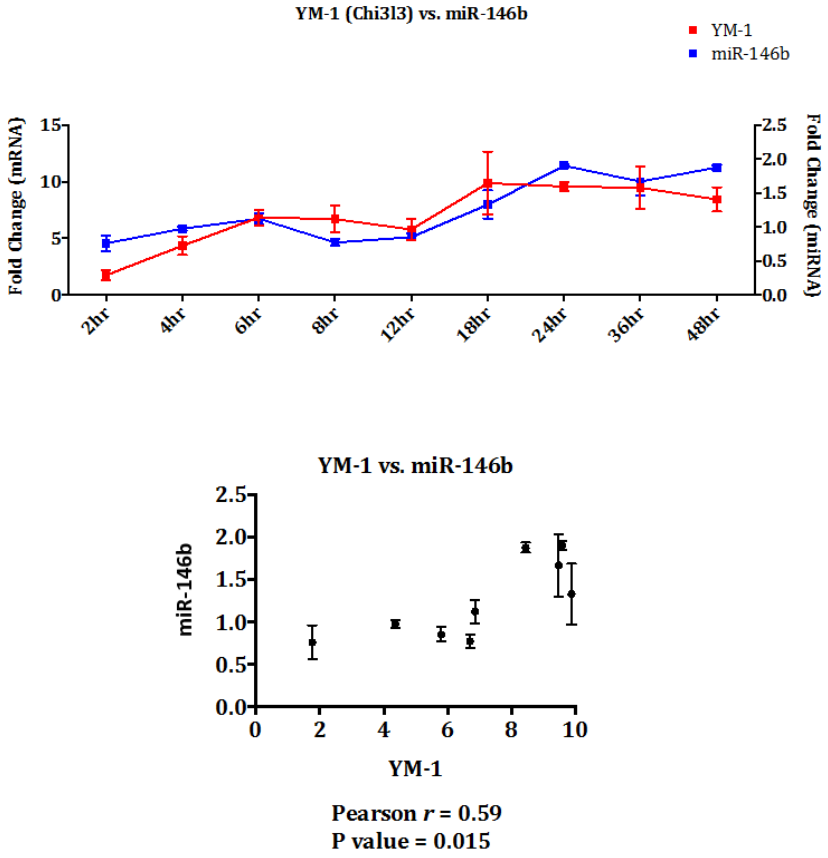

Figure 5.8. Expression kinetics of miR-146a and miR-146b during alternative activation time course in RAW 264.7 cells.

Cells were left untreated or stimulated with either 10ng/mL of LPS or 20ng/mL of IL-4/IL-13 for various time points ranging from 0hr to 48hr. RNA was extracted and microRNA or mRNA expression was quantified by qRT-PCR **A & B)** YM-1, **TNF**-a and iNOS expression was normalised to *Gapdh* and fold changes calculated in comparison to untreated samples at respective time points stated. **C)** MiR-146a and miR-146b expression was normalised to *RNU6b* and fold changes calculated in comparison to untreated samples at respective time points stated. **D & E)** miR-146a and miR-146b expression was correlated to YM-1 expression using Pearson's correlation and *r-value*.. Data represented are the mean fold change ± SEM compared to untreated controls and representative an individual experiment (n=3). Statistical significance for differences between treated and untreated samples were determined using two-way ANOVA where appropriate (* P< 0.05, ** P< 0.01, *** P< 0.001).

A.

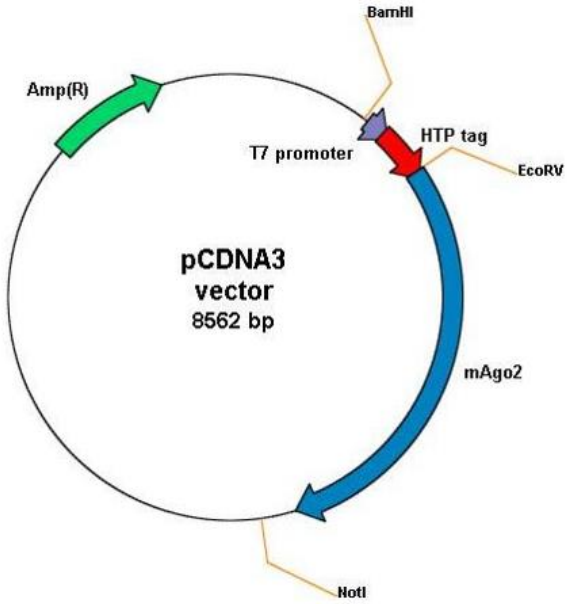
BamHI
Amp(R)
HTP tag
T7 promoter
EcoRV
pCDNA3
vector
8562 bp
mAgo2
NotI

B.

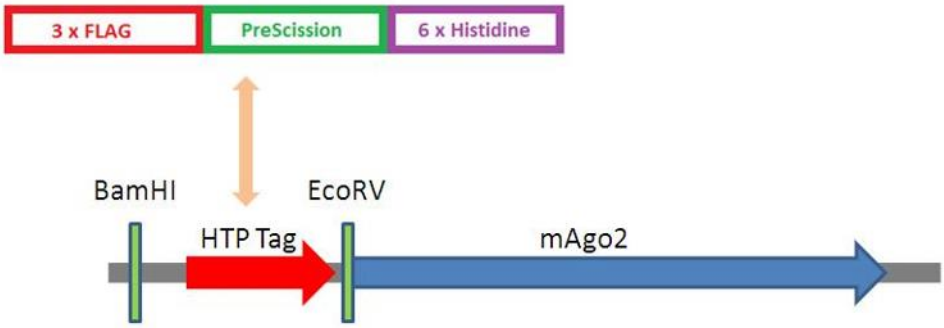
3 x FLAG
PreScission
6 x Histidine
BamHI
EcoRV
HTP Tag
mAgo2

C.

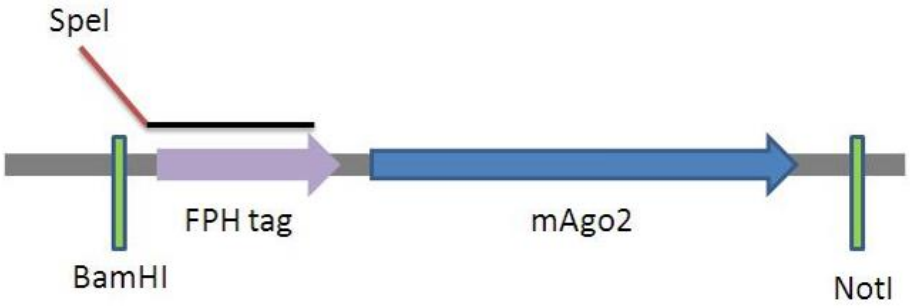

D.

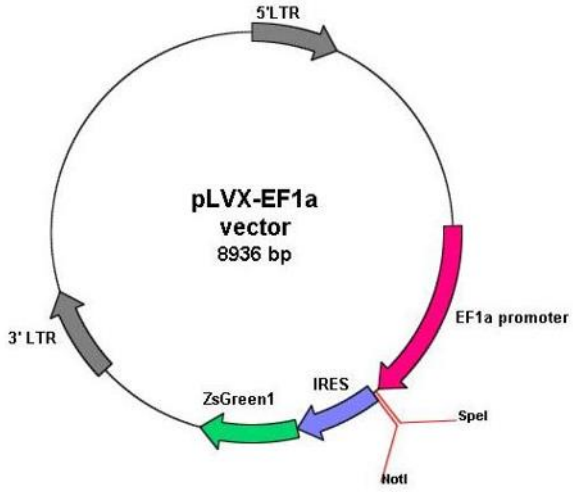

Figure 5.9 Generation of pLVX-EF1α-ZsGreen1-FPH-mAGO2 construct for lentiviral transduction of RAW 264.7 cells.

A) Map of pCDNA3 plasmid containing mAGO2 fused to ProteinA-TEV-Histidine (HTP) tag **B)** HTP tag in pCDNA3 was cleaved through restriction digestion with BamHI and EvoRV and replaced with the FPH tag. **C)** FPH-mAGO2 was amplified by PCR and SpeI site introduced to replace the BamHI site at the N terminus. The PCR product was digested with SpeI and NotI and inserted in pLVX-EF1α-ZsGreen1 lentiviral vector containing LTR regions for recombination. **D)** Map of the pLVX-EF1α-ZsGreen1 lentiviral vector. The vector was digested with SpeI and NotI for the introduction of FPH-mAGO2 downstream of the EF-1α promoter.

A.

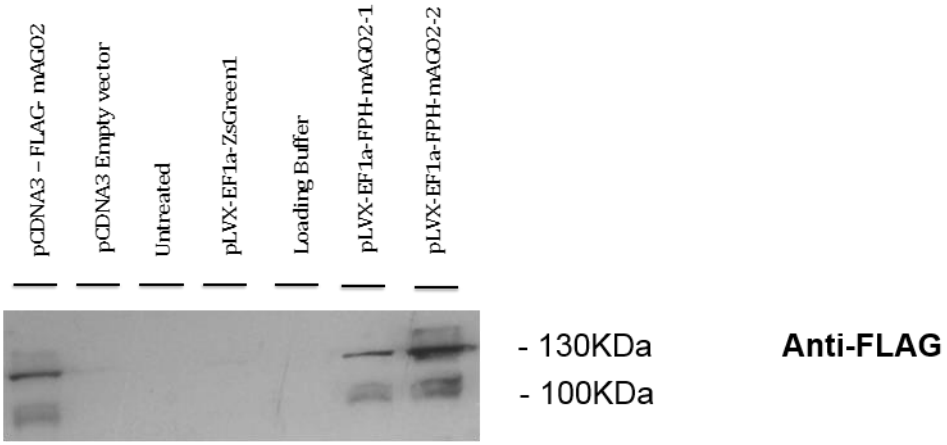

B.

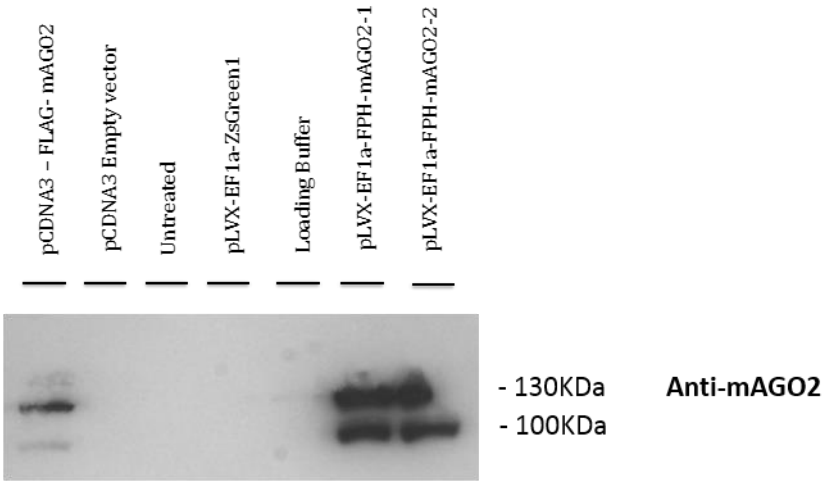

Figure 5.10 Expression of FLAG-PreScission-Histidine tagged mAGO2 in RAW 264.7 cells transfected with pLVX-EF1α-ZsGreen1-FPH-mAGO2 lentiviral vector.

RAW 264.7 cells were seeded at a density of $1x10^6$ cells/well in a 6 well plate. Cells were left untreated or transfected with either pLVX-EF1α-ZsGreen1 empty vector or pLVX-EF1α-ZsGreen1-FPH-mAGO2 lentiviral plasmid construct using Lipofectamine-2000 and incubated for 48 hours. Cells were also transfected with pCDNA3 empty vector or pCDNA3 containing FPH-mAGO2. 25µg of total protein was loaded onto 12% SDS-PAGE gels. Western blot analysis (ECL detection) was carried out using **A)** Anti-FLAG M2 antibody and **B)** anti-mAGO2 antibody. Data are representative of two separate experiments (n=3 pooled).

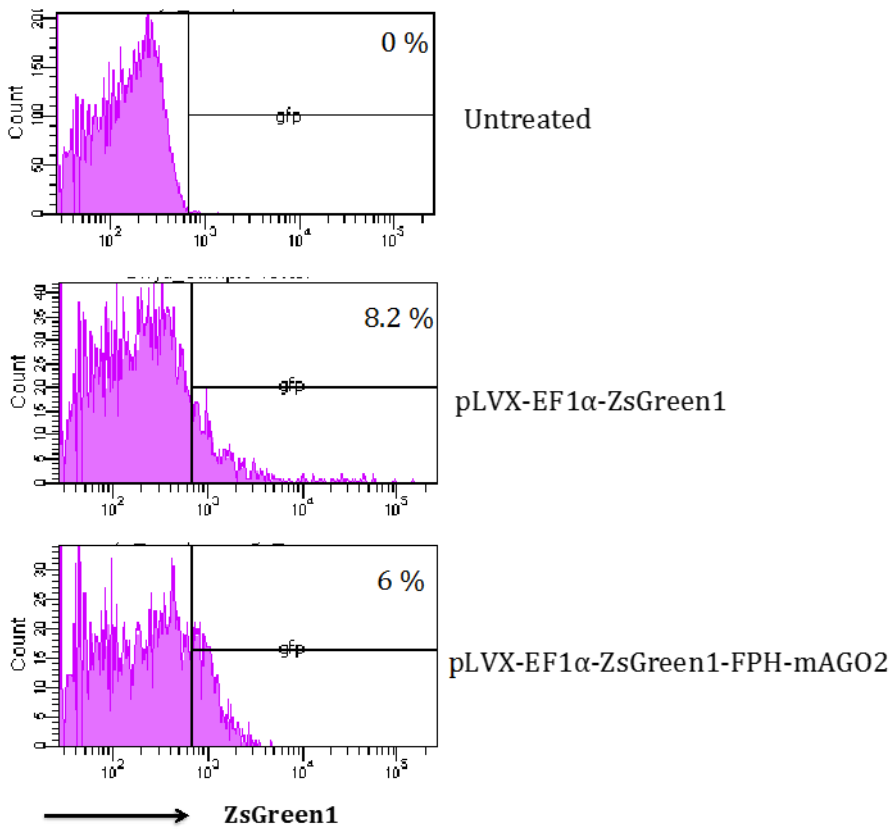

Figure 5.11. ZsGreen1 expression in RAW 264.7 cells following lentiviral transduction.

RAW 264.7 cells were left untreated or transduced with 25µl of concentrated lentivirus containing either pLVX-EF1α-ZsGreen1 empty vector or pLVX-EF1α-ZsGreen1-FPH-mAGO2 construct for 48 hours before being FACS analysed. Histograms display percentage positive cells for ZsGreen1 expression based on gating using the untreated sample. Data were analysed using FlowJo software and are representative of two separate experiments (n=3 pooled).

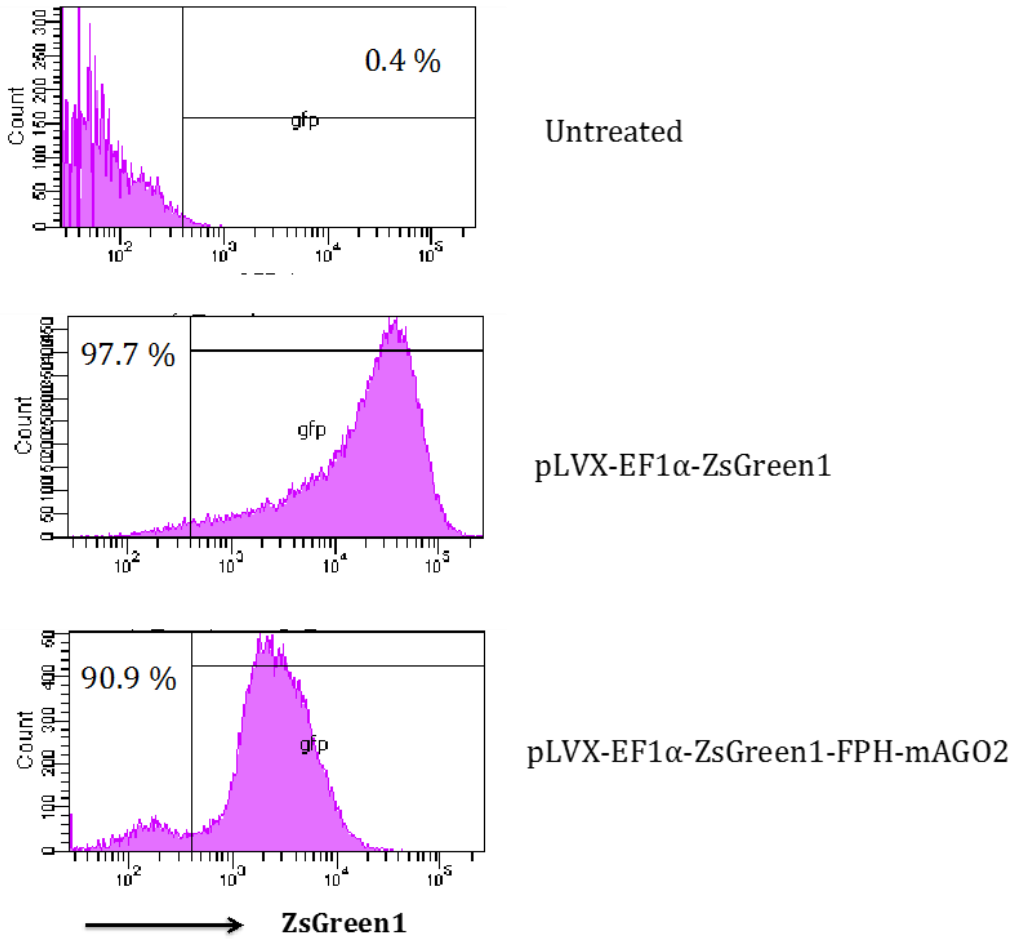

Figure 5.12 ZsGreen1 expression in NIH-3T3 cells following lentiviral transduction.

NIH-3T3 cells were left untreated or transduced with lentivirus containing either pLVX-EF1α-ZsGreen1 empty vector or pLVX-EF1α-ZsGreen1-FPH-mAGO2 construct for 48 hours. Histograms display percentage positive cells for ZsGreen1 expression based on gating using the untreated sample. Data were analysed using FlowJo software and are representative of two separate experiments (n=3 pooled).

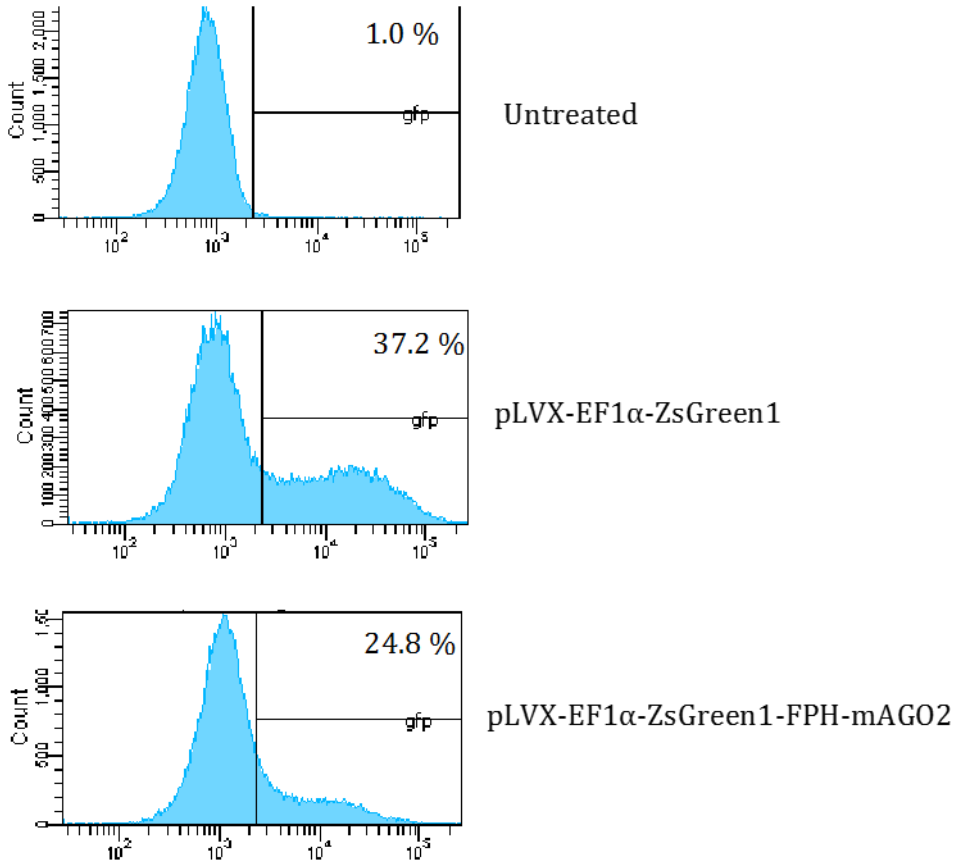

Figure 5.13 ZsGreen1 expression in RAW 264.7 cells following lentiviral transduction with freshly harvested supernatant.

RAW 264.7 cells were left untreated or transduced with freshly harvested supernatant from HEK293T cells containing lentivirus without ultracentrifugation. Cells were transduced with either pLVX-EF1α-ZsGreen1 empty vector or pLVX-EF1α-ZsGreen1-FPH-mAGO2 construct lentiviruses for 48 hours. Histograms display percentage positive cells for ZsGreen1 expression based on gating using the untreated sample. Data were analysed using FlowJo software and are representative of two separate experiments (n=3 pooled).

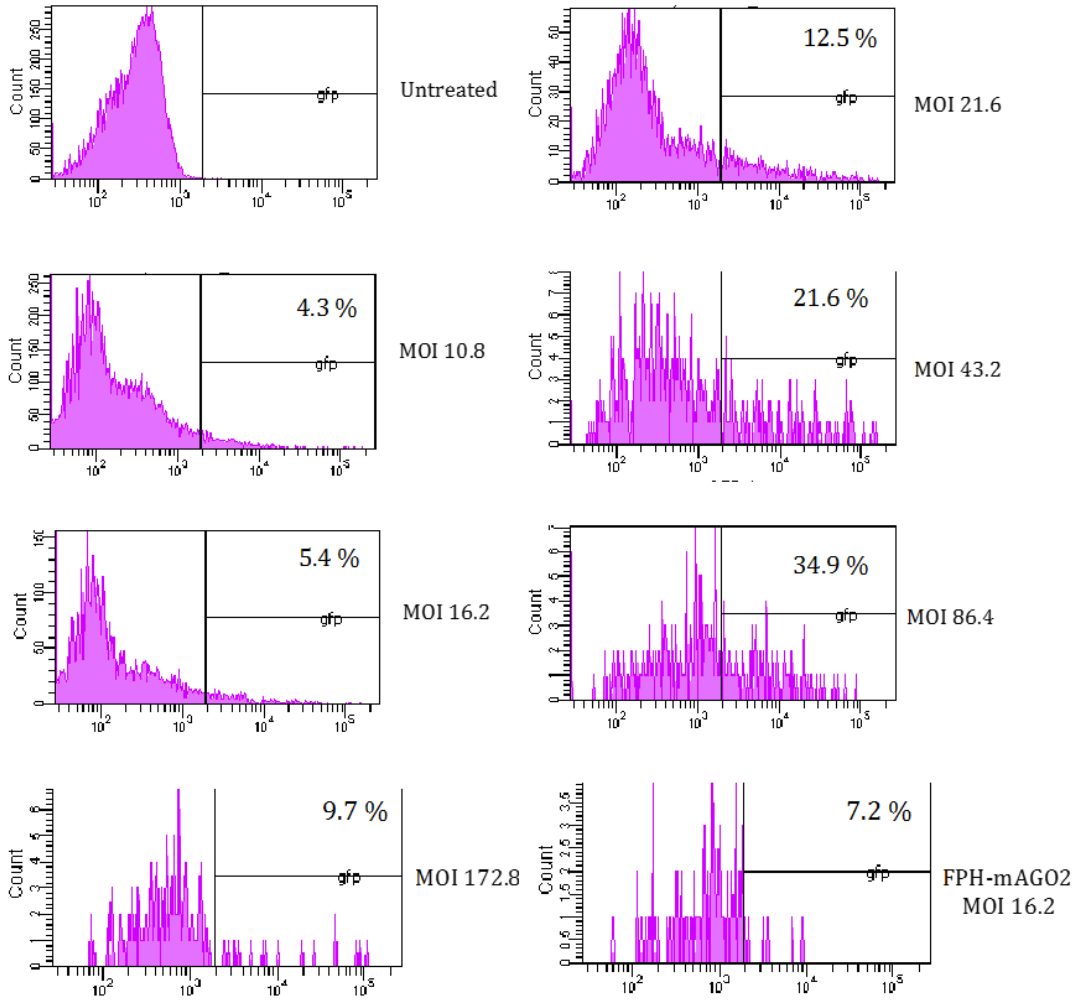

Figure 5.14. ZsGreen1 expression following transduction of RAW 264.7 cells with increasing MOIs of lentivirus.

RAW 264.7 cells were left untreated or transduced with pLVX-EF1α-ZsGreen1 empty vector lentivirus at varying MOIs of 10.8, 16.2, 21.6, 43.2, 86.4 or 172.8 for 48 hours. Cells were also transduced with lentivirus containing pLVX-EF1α-ZsGreen1-FPH-mAGO2 construct for 48 hours at MOI 16.2. Histograms display percentage positive cells for ZsGreen1 expression based on gating using the untreated sample. Data were analysed using FlowJo software and are representative of an individual experiment (n=3 pooled).

A.

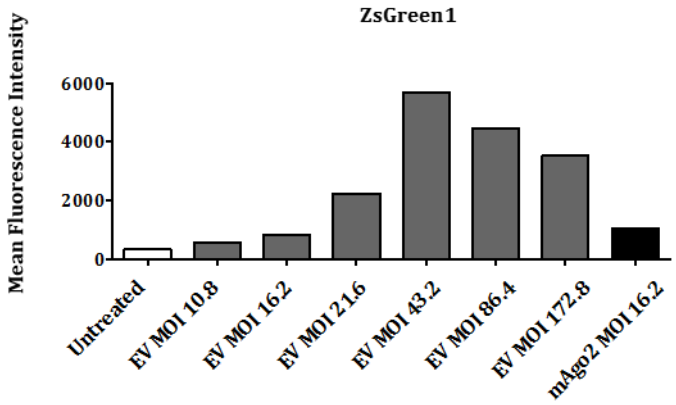

B.

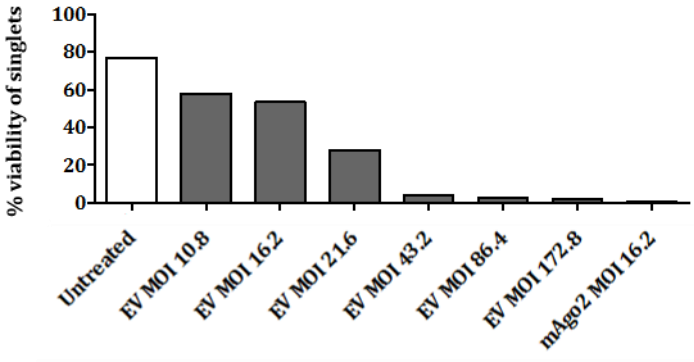

Figure 5.15 ZsGreen1 expression and percentage cell viability following transduction of RAW 264.7 cells with increasing MOIs of lentivirus.

RAW 264.7 cells were left untreated or transduced with pLVX-EF1α-ZsGreen1 empty vector lentivirus at varying MOIs of 10.8, 16.2, 21.6, 43.2, 86.4 or 172.8 for 48 hours. Cells were also transduced with lentivirus containing pLVX-EF1α-ZsGreen1-FPH-mAGO2 construct at MOI 16.2. Graphs represent **A)** mean fluorescence intensity for ZsGreen1 expression based on gating using the untreated sample and **B)** percentage viability of singlets based on propidium iodide staining Data were analysed using FlowJo software and are representative of an individual experiment (n=3 pooled).

A.

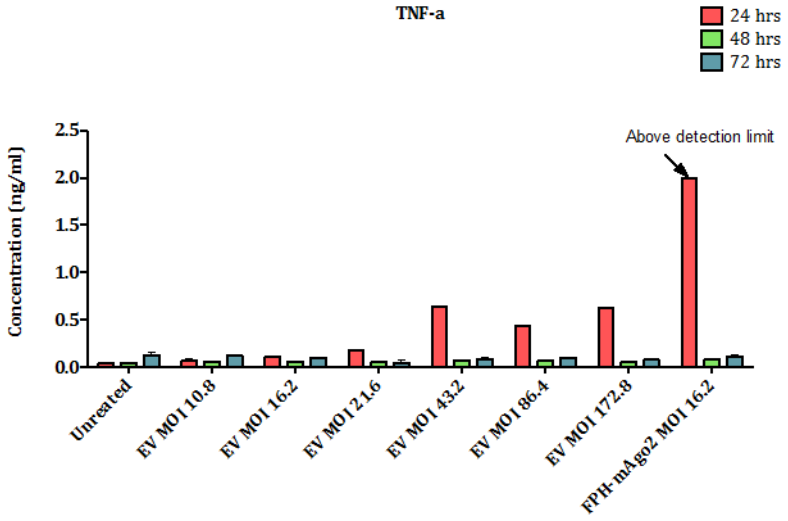

B.

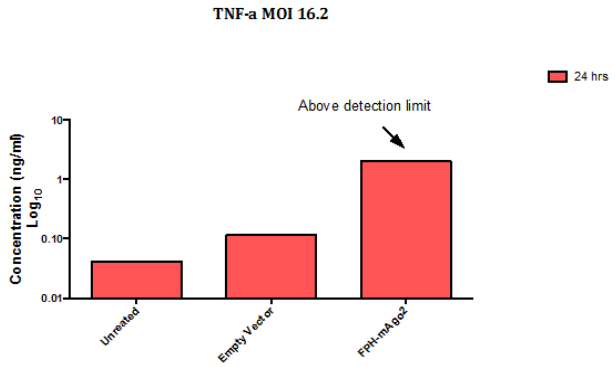

Figure 5.16 Expression levels of secreted TNF-a following transduction of RAW 264.7 cells with increasing MOIs of lentivirus.

RAW 264.7 cells were left untreated or transduced with pLVX-EF1α-ZsGreen1 empty vector lentivirus at varying MOIs of 10.8, 16.2, 21.6, 43.2, 86.4 or 172.8 up to 72 hours. Cells were also transduced with lentivirus containing pLVX-EF1α-ZsGreen1-FPH-mAGO2 construct at MOI 16.2. Supernatants were harvested at 24hr, 48hr and 72hr post transduction. Graphs represent **A)** TNF-a levels as measured by ELISA at 24hr, 48hr and 72hr after transduction and **B)** Comparison of TNF-a levels as measured by ELISA 24hr post transduction in untreated cells or cells transduced with lentivirus containing empty vector or FPH tagged mAGO2 at MOI 16.2. Data were analysed using FlowJo software and are representative of an individual experiment (n=3 pooled).

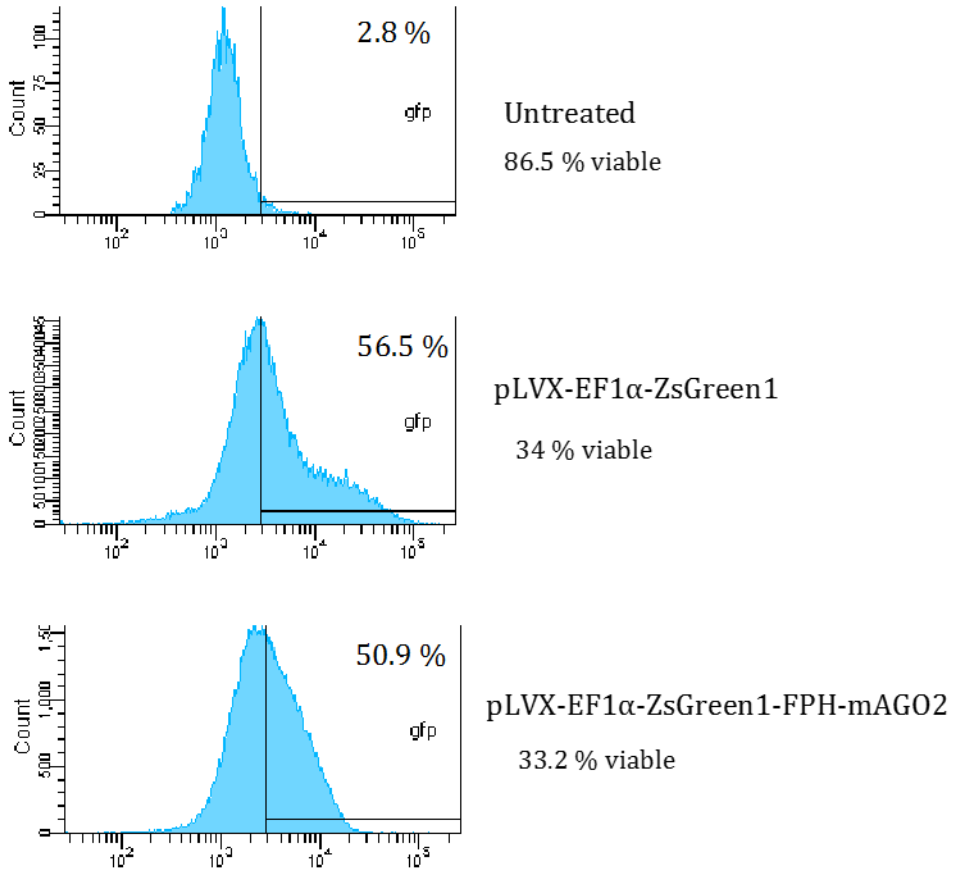

Figure 5.17 ZsGreen1 expression in RAW 264.7 cells following lentiviral transduction with freshly harvested supernatant.

RAW 264.7 cells were left untreated or transduced with freshly harvested supernatant from HEK293T cells containing lentivirus without ultracentrifuation. Cells were transduced with either pLVX-EF1α-ZsGreen1 empty vector or pLVX-EF1α-ZsGreen1-FPH-mAGO2 lentiviruses for 1 hour with centrifugation at 500xg. The medium was aspirated and replaced with fresh culture medium every hour for 10-12 hours. Histograms display percentage positive cells for ZsGreen1 expression based on gating using the untreated sample. Data were analysed using FlowJo software and are representative of an individual experiment (n=3 pooled).

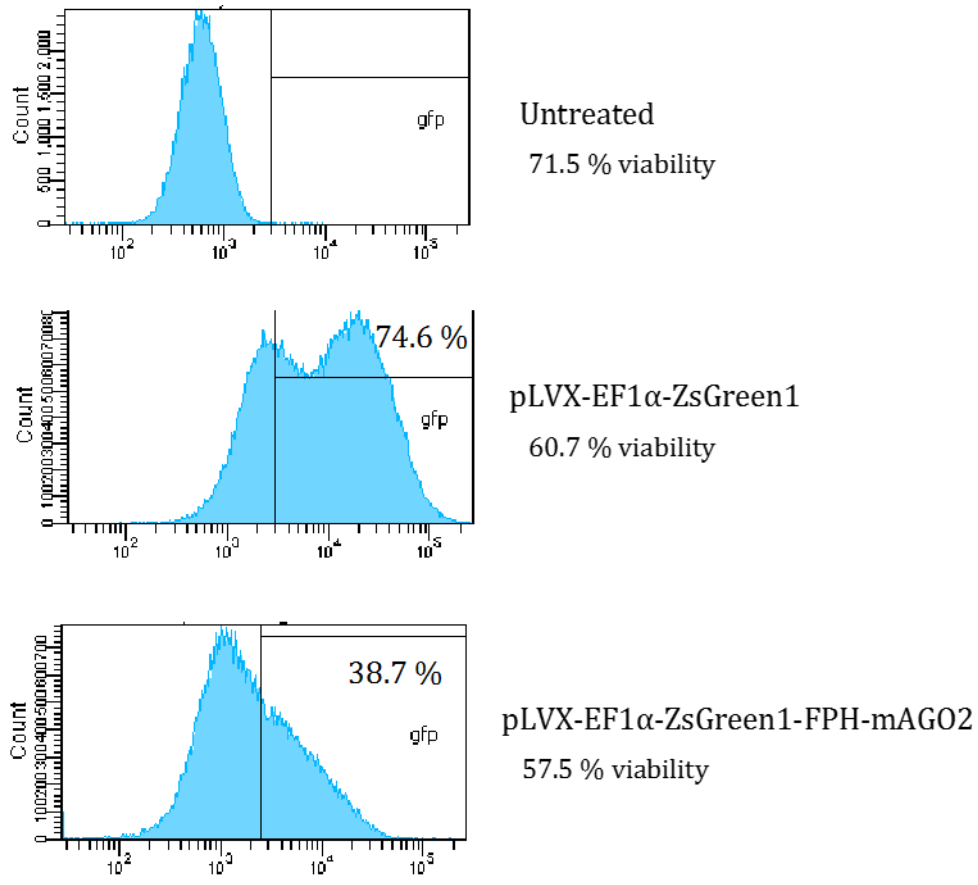

Figure 5.18 ZsGreen1 expression in RAW 264.7 cells 48 hours after FACS sorting.

RAW 264.7 cells were left untreated or transduced with freshly harvested supernatant from HEK293T cells containing lentivirus without ultracentrifuation. Cells were transduced with either pLVX-EF1α-ZsGreen1 empty vector or pLVX-EF1α-ZsGreen1-FPH-mAGO2 construct lentiviruses for 1 hour with centrifugation at 500xg. Medium was aspirated and replaced with fresh culture medium every hour for 10-12 hours. 24 hours post transduction, cells were FACS sorted based on ZsGreen1 expression and cultured for a further 48 hours before being FACS analysed. Histograms display percentage positive cells for ZsGreen1 expression based on gating using the untreated sample. Data were analysed using FlowJo software and are representative of an individual experiment (n=5 pooled).

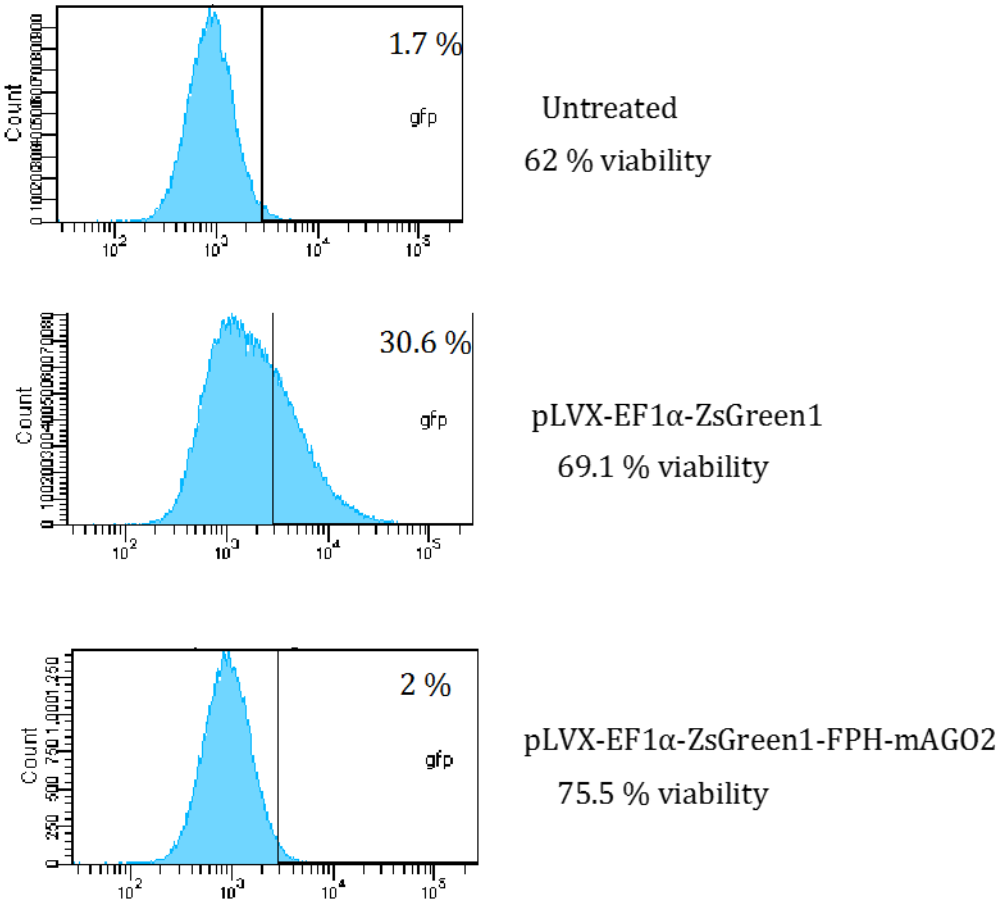

Figure 5.19. FACS analysis of ZsGreen1 expression in RAW 264.7 one week (7 days) after FACS sorting.

RAW 264.7 cells were either left untreated or transduced with freshly harvested supernatant from HEK293T cells containing lentivirus without ultracentrifuation. Cells were transduced with either pLVX-EF1α-ZsGreen1 empty vector or pLVX-EF1α-ZsGreen1-FPH-mAGO2 construct lentiviruses for 1 hour with centrifugation at 500xg. Medium was aspirated and replaced with fresh culture medium every hour for 10-12 hours. 24 hours post transduction, cells were FACS sorted based on ZsGreen1 expression and cultured for a further 7 days before being FACS analysed. Histograms display percentage positive cells for ZsGreen1 expression based on gating using the untreated sample. Data were analysed using FlowJo software and are representative of an individual experiment (n=3 pooled).

Chapter 6: Concluding remarks and future direction

6.1 Rationale and objectives of thesis

Diversity and plasticity are hallmarks of macrophages, which display a wide range of phenotypes dictated by environmental cues they encounter. Amongst this broad spectrum of highly distinct functional phenotypes, macrophages have been usefully classified as being classically or alternatively activated depending on their exposure to T_H1 or T_H2 stimuli respectively (Mosser and Edwards, 2008, Martinez and Gordon, 2014). Specifically, the concept of a distinct state of alternative macrophage activation induced by T_H2 cytokines IL-4 and IL-13 has gained considerable ground in recent years. AAMΦ have been implicated in a range of physiological and pathological processes including homeostasis, helminth infections, chronic diseases & inflammation, wound healing, metabolic functions and tumour progression (Gordon, 2003, Gordon and Martinez, 2010, Martinez and Gordon, 2014). Thus, to avoid functional dysregulation and to maintain the balance and efficiency of the immune response, it is crucial that AAMΦ responses are tightly regulated. Furthermore, with great diversity in their function, macrophages are an attractive therapeutic target, but this requires a greater understanding of the systemic, cellular and molecular processes involved in the regulation of the different phenotypes.

The substantial progress of microRNAs as therapeutics has been demonstrated by the development of a miR-122 inhibitor as an anti-viral agent – the first microRNA targeted drug currently in clinical trials (Janssen et al., 2013). Over the past decade, cellular microRNAs have also gained importance as immunomodulatory regulators and have been reported to be involved in regulating macrophage function (Graff et al., 2012a, Liu and Abraham, 2013a, Squadrito et al., 2013). Although microRNAs are well-established fine tuners of macrophage responses, the majority of the existing literature focuses on CAMΦ (Alam and O'Neill, 2011, O'Neill et al., 2011, Quinn and O'Neill, 2011, He et al., 2014a). Previously, research in the Allen lab demonstrated that microRNAs are also differentially expressed and involved in the

regulation of AAMΦ (Ruckerl et al., 2012). Besides work from our lab, studies delineating the involvement of microRNAs in alternative activation are sparse, thereby necessitating further investigation in the regulation of this phenotype. Thus, the central hypothesis of this thesis focused on the functional role of microRNAs in the induction, maintenance and proliferation of AAMΦ.

The studies presented in this thesis aimed to:

1. Identify and validate differential expression of microRNAs during alternative activation.
2. Examine specific targets and cellular pathways regulated by these microRNAs.
3. Generate a stable macrophage cell line for the biochemical identification of direct microRNA targets.

6.2 Conclusions

At the time of carrying out the work presented in this thesis, no published data suggesting a role for microRNA regulation of AAMΦ existed beyond the study carried out by Ruckerl *et al.* (2012) from our lab. Thus, the first aim of this thesis was to utilise existing microarray datasets (provided by D. Ruckerl and A.Buck, involving a collaboration with Thermofisher) to identify and validate ten microRNAs differentially expressed during alternative activation. We demonstrated that these microRNAs were highly regulated in response to IL-4 (and also IL-13 in some cases) both in *in vitro* and *in vivo* models of alternative activation. The validation of the expression profiles of these microRNAs as being associated with alternative activation provided a framework for the selection of three microRNA candidates for further studies presented in the later chapters of this thesis. Additionally, some of the microRNAs examined in our study, for example, miR-223 and miR-125a-5p, have subsequently been identified as regulators of AAMΦ (Zhuang et al., 2012, Banerjee et al., 2013b, Squadrito et al., 2014, Ying et al., 2015). Due to time constraints, the roles of only a select few microRNAs were investigated further in this study. However, these new findings linking some of our shortlisted microRNAs to

alternative activation validate our approach and open up exciting new avenues to further investigate the roles of microRNAs not addressed in this thesis.

The second aim of this thesis was to examine the potential of selected microRNA candidates as regulators of AAMΦ responses. These included miR-199b-5p, miR-378-3p and miR-146a/b on the basis of the consistency in their expression under a range of conditions of alternative activation. Two of the microRNAs that we selected for further study, miR-199b-5p and miR-378-3p, have previously been identified as being IL-4Rα dependent (Ruckerl et al., 2012). Roles for both miR-146 and miR-199b-5p have previously been proposed in macrophages as regulators of TLR signalling (Taganov et al., 2006, Lin et al., 2014) and monocyte/macrophage differentiation (Lin et al., 2014) respectively. However, no reports of their association with alternative activation have been published. Although miR-378-3p is known to directly target AKT-1, which is essential for IL-4 induced macrophage proliferation (Ruckerl et al., 2012), the direct impact of this microRNA on AAMΦ was previously unknown.

In Chapter 3, we showed that miR-199b-5p was expressed at high copy numbers and induced in response to IL-4 *in vivo* and that these numbers and changes were not reflected *in vitro*. MiR-199a-5p, an isoform of miR-199b-5p that is generated from another chromosomal locus but is identical in the mature sequence, is a well-known regulator of proliferation in other cell types (Alexander et al., 2013, Song et al., 2014, Hashemi Gheinani et al., 2015, Zhang et al., 2015). Macrophages, on the other hand, are known to proliferate in response to IL-4, for example, during infection with the nematodes *Litomosoides sigmodontis* and *Heligomosoides polygyrus* (Jenkins et al., 2011, Jenkins et al., 2013) and are key contributors to the progression of fibrosis (Murray and Wynn, 2011, Wynn and Barron, 2010) and tumours (Gordon and Martinez, 2010) during resolution phases. Thus, it is plausible that this IL-4 induced proliferation may be important in conferring these pathologies. We, therefore, investigated the effect of overexpression of this microRNA on macrophage proliferation both *in vitro* and *in vivo*. We showed that miR-199b-5p reduced macrophage proliferation *in vitro* but its effect *in vivo* was inconclusive. This can potentially be attributed to different macrophage origins and the lack of consistency

in the expression of miR-199b-5p targets in these populations. For example, miR-199b-5p was shown to affect IRS-1 expression, a critical molecule in the insulin/IGF-1 signalling axis. Peritoneal macrophages highly upregulate IR and IGF-1 signalling in response to IL-4 treatment, however, the same is not true for alveolar macrophages. Since miR-199b-5p could only be delivered to the lung without disrupting the natural immune population balance and macrophage disappearance, no concrete conclusions could be drawn regarding the *in vivo* action of this microRNA. Thus, it is still necessary to confirm if the effect of miR-199b-5p on macrophage proliferation is restricted to macrophages of specific origins and whether this effect is mediated via insulin signalling or other targeted pathways.

Successful delivery of the microRNA *in vivo* without disruption of the natural immune balance, however, is advantageous to examine the functionality of not just this microRNA, but also others and especially in the context of disease models. At the same time, a caveat to this approach is restricted delivery to specific organs and not knowing which cell types take up the microRNA containing lipid complexes other than macrophages in the absence of cell sorting. Even though Chapter 3 was focused on the role of miR-199b-5p in regulating macrophage proliferation, we have also shown that introduction of a miR-199b-5p synthetic mimic in combination with IL-4 results in the reduction of YM-1, a marker characteristic of alternative activation. Although the functions of CLPs still remain largely unknown, our lab has recently shown that YM-1 promotes IL-17 induced neutrophilia, which is important for limiting parasite survival in a nematode infection model (Sutherland et al., 2014). Whilst it is yet to be determined if this effect on YM-1 expression is at the transcriptional level or a secretion defect, these data provide a starting point for further research on the potential of miR-199b-5p as a mediator of negative feedback loops for both macrophage proliferation and activation.

In this thesis (Chapter 4), we have also provided new and direct evidence of the impact of miR-378-3p deficiency on the regulation of AAMΦ. The ability of macrophages isolated from WT and miR-378 KO mice to alternatively activate was studied in various systems both *in vitro* and *in vivo*. The influence of miR-378 deficiency on IL-4 induced proliferation was also addressed *in vivo*. Although AKT-

1 is a direct target of miR-378-3p and essential for IL-4 induced proliferation (Ruckerl et al., 2012), data from these studies demonstrated that miR-378 did not solely impact macrophage proliferation. Instead, a greater effect was observed on RELM-α and YM-1 expression as measures of alternative activation, with an increase in protein expression in miR-378 KO mice. These experiments reflect the complexity and interdependency of biological networks that exist *in vivo*. It would be of great interest to understand the functional consequences of the miR-378 mediated regulation of alternative activation over the course of an entire infection time course using a T_H2-inducing pathogen like *Litomosoides sigmodontis*. MicroRNAs can regulate a large number of genes involved in diverse or similar cellular pathways and therefore, it is logical to speculate that other microRNAs might also be involved in the regulation of AAMΦ in the absence of miR-378. Hence, it would be of interest to inhibit other IL-4Rα dependent microRNAs such as miR-199b-5p in the miR-378 KO mice. Multiple targeting of microRNAs may reveal microRNA combinations that determine macrophage proliferation and activation dynamics.

In chapter 5 we characterised the opposing expression profiles of the miR-146 isoforms, miR-146a and miR-146b, during alternative activation and hypothesised a role for miR-146a and miR-146b in promoting efficient AAMΦ responses through shared targets. However, a difference of just 2 nucleotides in the sequences of these mature microRNAs proved to be a hindrance in delineating their specific roles during alternative activation. This involved overcoming the challenges of specific individual inhibition of these microRNA isoforms and the consequent generation of a stable macrophage cell line expressing tagged mAGO2 for the biochemical identification of miR-146a/b (and other microRNA) targets. Using a lentiviral transduction system, we were able to generate a cell line expressing tagged protein, however, this expression was only transient. The issue of transient transduction may potentially be resolved through the use of a different lentiviral construct comprising a *Csf1r* promoter region that is constitutively expressed by macrophages. However, the existence of the recently developed FLAG tagged-AGO2 mouse is an extremely useful tool to overcome these challenges and for characterisation of microRNAs and their direct targets in different *in vivo* models of alternative activation.

6.3 Future directions

The findings presented in this thesis provide a strong foundation for further studies of the functional role of microRNAs in regulating AAMΦ and their responses. The data presented provide insight into the complex regulatory microRNA networks that exist and can result in similar outcomes through targeting of different pathways by different microRNAs. Nevertheless, a number of questions based on the data obtained from this thesis merit further investigation.

Chapter 2:

- What is the functional significance of other shortlisted microRNAs that are altered in response to IL-4 such as miR-99 and miR-223?
- Do certain microRNAs such as miR-125b-5p, miR-221 and miR-222 play significant roles that are specific to the origin of macrophages i.e. tissue resident vs. blood monocyte derived?
- Does dependency on IL-4Rα for induction of microRNA expression define a stronger link for microRNAs to regulate AAMΦ and their responses?

Chapter 3:

- The expression of miR-199b-5p was induced in response to IL-4 only *in vivo* and not *in vitro.* Besides IL-4Rα signalling, which other factor or cell type is necessary for the induction of miR-199b-5p?

- Given that miR-199b-5p enhances IRS-1 expression, does it contribute to the regulation of proliferation in peritoneal macrophages that express InsR and IRS-1 in response to IL-4? Would this suggest that macrophages employ varying mechanisms of proliferation depending on origin and location?

- Is the reduction of YM-1 expression by miR-199b-5p specific to alveolar macrophages? Does this effect on YM-1 expression have functional consequences?

Chapter 4:

- Does the regulation of alternative activation markers RELM- α and YM-1 by miR-378 have functional consequences in the context of infection?
- Does this increase in RELM- α and YM-1 expression also translate at the transcriptional level?
- Do miR-199b-5p and miR-378 have an additive or synergistic function in regulating macrophage proliferation and activation?
- If so, is there a functional outcome of miR-199b-5p inhibition in miR-378 KO mice?

Chapter 5:

- Do miR-146a/b play a significant role in promoting alternative activation through suppression of shared proinflammatory molecules?
- Do these two miRNAs target the same genes because of sequence identity or do they target different genes since their transcriptional regulation appears to be highly distinct?
- Will the utilisation of a constitutively expressed *Csf1r*-FIRE lentiviral construct overcome challenges of transient macrophage transduction?
- Will the FLAG tagged mAGO2 expressing mouse overcome all the technical hurdles and provide both microRNA and target information during alternative macrophage activation and proliferation?

Chapter 7: Materials and methods

7.1 Mice

All mouse strains used were maintained and bred under specific pathogen-free conditions at the University of Edinburgh animal facilities, in accordance with the U.K. Home Office and local ethically approved guidelines. Wild type BALB/c and C57BL/6 mice were bred in house.

For the microarray datasets generated by D. Ruckerl (described in Chapter 2), WT or IL-4Rα $^{-/-}$ animals on a BALB/c background bred in house were utilised for the *B. malayi* implants and thioglycollate treatment. For the bone marrow derived macrophage (BMDM) microarray, bone marrow precursors were obtained from 6-10 week old WT BALB/c mice. For all other experiments, the mice were 6-8 weeks old and were sex matched at the start of each experiment.

7.1.1 MiR-378/378* KO mice

MiR-378/378* KO animals described and utilised in Chapter 4 were obtained from the Olson lab. The targeting vector used to generate the null allele of miR-378 and miR-378* contained a neomycin resistance gene driven by the pGK promoter and flanked by loxP sites. The plasmid also contained a diphtheria toxin gene cassette. The neomycin resistance cassette flanked by loxP sites was designed to replace the pre-miR miR-378/378* sequence. To this end, the 5' and 3' arms of homology were generated using Taq PCR amplification from 129SvEv genomic DNA. The targeting vector was electroporated into 129SvEv embryonic stem cells. Five hundred ES clones were analysed for homologous recombination by Southern blot. Three successful clones targeting the miR-378/378* allele were injected into 3.5 days old C57BL/6 blastocysts. High percentage chimeric male mice were crossed with C57BL/6 female mice to achieve germline transmission of the targeted allele. Subsequently, heterozygous mice containing the neomycin cassette were crossed with CAG-Cre transgenic mice to remove the neomycin cassette. These mice were

initially on a mixed C57BL/6 and SV129 background and backcrossed with WT C57BL/6 mice for several generations before all the experiments were performed in Chapter 4, unless otherwise stated.

7.2 *In vivo* procedures

7.2.1 *Litomosoides sigmodontis* infection

L. sigmodontis life cycle was maintained and infective third stage larvae (L3) were obtained from infected gerbils as described by Le Goff et al (2002). Female C57BL/6 mice aged 6-8 weeks were infected with 25-30 L3 larvae suspended in 100µl Roswell Park Memorial Institute-1640 (RPMI) medium by subcutaneous injection. Naïve controls received no treatment. Mice were sacrificed by terminal anaesthesia by administration of 100µL of 1:1 Domitor/Vetalar, injected subcutaneously. Mice were bled by brachial bleeding and pleural exudate cells (PLEC) were harvested as described later under macrophage purification.

7.2.2 IL-4 complex injection

IL-4 anti-IL-4 murine antibody complex (IL-4c) was prepared by mixing 5µg of recombinant IL-4 (13.5kDa; Peprotech) with 25µg of anti-IL-4 antibody [clone 11B11 (Bio X Cell)]. The complex was incubated on ice for 15 minutes and made up to a final desired volume of 100µl per mouse with Phosphate Buffered Saline (PBS). To assess peritoneal and pleural macrophage proliferation, mice were injected intraperitoneally with a single dose of either PBS only control or IL-4c, followed by 100µL subcutaneous injection of 10mg/mL BrdU 3 hours prior to sacrifice. Mice were culled and Peritoneal Exudate Cells (PEC) or PLEC were harvested at 42 hours and 72 hours post injection. For obtaining proliferation of alveolar macrophages, mice were injected with either PBS or IL-4c on day 0 and day 2 and macrophages were isolated 4 days post injection.

7.2.3 MicroRNA delivery

Synthetic microRNA mimic (Dharmacon; 20µg per mouse) was complexed with *in vivo* JetPEI (Polyplus) at an appropriate N:P ratio (6 or 8 as described in Chapter 3) in 5% glucose. Calculations were based on a final volume of 40µl or 100µl per mouse for intranasal or intraperitoneal delivery respectively. The mixture was incubated for 15 minutes at room temperature. For intranasal delivery, mice were anaesthetised briefly with 3-5% isoflurane and the complex was delivered using a micropipette. The control mice were administered with 5% glucose only. PEC cells were harvested 48 hours after intraperitoneal injection. For intranasal microRNAs delivered to the lung, Bronchoalveolar lavage (BAL) fluid and lungs were harvested either 48 hours post delivery. In experiments wherein two doses of IL-4c were injected, harvests were carried out 72 hours post microRNA delivery.

7.2.4 Thioglycollate elicited macrophages

Mice were injected intraperitoneally with 400µl of thioglycollate matured for 3 months at room temperature in the dark. 72 hours post injection, PEC cells were harvested and processed for analysis either by flow cytometry or adherence purified for assessing *in vitro* activation and/or RNA extraction.

7.2.5 Bone marrow derived macrophages (BMDM)

The tibia and femur were retrieved from the hind legs of mice (WT C57BL/6 or miR-378/378* genotypes). The marrow was flushed using Dulbecco's Modified Eagle's Medium (DMEM) containing 10% foetal calf serum and 2mM L-glutamine, 0.25 U/mL penicillin and 100mg/mL streptomycin using a 26G needle. Clumps were disrupted by aspiration and dispensing through a 19G needle. Cells were centrifuged at 1200RPM for 10 minutes at 4°C. The medium was discarded and the cell pellet was resuspended in 2-3mL of Red Blood Cell (RBC) lysis buffer (Sigma) and incubated on ice for 5 minutes. Consequently, the solution was made isotonic by addition of 20mL complete DMEM. Cells were centrifuged at 1200RPM for 10

minutes at 4°C and the cell pellet resuspended in Plutznik medium (DMEM, 25% FCS, 25% L-929-conditioned-medium as a source of CSF-1/M-CSF, 1% L-Glutamine, 1% P/S, 0.1% b-Mercaptoethanol). Cells were counted and seeded at 7.5 x 10^6 cells in 10mL media in 10cm^2 bacterial grade petridishes. The cells were incubated at 37°C with 5% CO_2 for 7-9 days. The medium was changed on days 2, 4 and 6 (and 8 if necessary). On day 7 (or 9), the culture medium was removed and cells were washed with pre-warmed PBS. 10mL detachment buffer [1xPBS + 0.144g glucose + 4.8ml EDTA (0.5M); 800mL final volume, filter sterilised before use] was added to each petridish and cells were incubated at 37°C with 5% CO_2 for 10-15 minutes. Detached cells were collected, FACS stained for confirmation of differentiation as assessed by their surface expression of F4/80 and CD11b markers, and utilised for further experiments.

7.3 Macrophage isolation and purification

7.3.1 Peritoneal exudate cells (PEC)

PEC cells were obtained by washing the peritoneal cavity of euthanised mice first with 3mL of RPMI containing 1% penicillin and streptomycin and 0.2% neonatal mouse serum (NMS) followed by two subsequent washes with 5mL media, which was collected in a separate tube. The first 3mL of PEC wash, the cells were centrifuged and 1mL of supernatant was transferred to eppendorfs for quantification of proteins by ELISA. The remaining 10mL of liquid obtained from the peritoneal washes was mixed with the cell pellet and centrifuged at 1200RPM for 5 minutes at 4°C and resuspended in 2mL fresh medium. The cells were counted with an automated Cellometer T4 (Peqlab) and 5 x 10^5 cells (or 2 x 10^5 cells for naïve samples) were used for FACS analysis. For experiments involving adherence purification, PECs were seeded at 5 x 10^6 cells/well in 6 well cell culture plates (NUNC) in RPMI media containing 5% FCS and 2mM L-glutamine, 0.25 U/mL penicillin, and 100mg/mL streptomycin. For naïve mice, cells were seeded at 1 x 10^6 cells/well in 12 well plates. Following incubation at 37°C with 5% CO_2 for 4 hours, non-adherent cells were washed off and the adherent cell population detached with a

rubber policeman. In some experiments where indicated, following IL-4c injection, peritoneal macrophages were purified (>90%) by sorting on a FACS Aria cell sorter (BD Biosciences) based on their expression of surface molecules ($F4/80^{+,}$ $CD11b^{+}$, $SiglecF^{-}$, $CD11c^{-}$, $CD19^{-}$, $CD3^{-}$, $Ly6G^{-}$; all antibodies were purchased from BioLegend or eBioscience). The remaining cells were lysed for RNA extraction and qRT-PCR.

7.3.2 Pleural exudate cells (PLEC)

PLECs were obtained by washing the pleural cavity of euthanised mice 9 times with 1mL of RPMI containing 1% penicillin and streptomycin and 0.5% neonatal mouse serum (NMS) for each wash. The first two 1mL washes were collected separately in a 15 mL Falcon tube (Greiner). The first 2mL obtained from the washes were centrifuged at 1200RPM for 5 minutes at 4°C and the supernatant was harvested for ELISAs. Like PECs, the remaining cells were either counted and stained directly for FACS analysis or seeded in 6 or 12 well plates for adherence purification and lysed for RNA extraction and qRT-PCR.

7.3.3 Alveolar macrophages

Alveolar macrophages were analysed by flow cytometry or qRT-PCR as part of the BAL fluid or total lung. The BAL fluid was obtained by cannulation of the trachea with plastic tubing and washing of the alveolar spaces four times with 400µL of PBS containing 1% BSA. Cells were centrifuged at 1200RPM for 5 minutes at 4°C and the supernatant was harvested for ELISAs. Cells were resuspended in 200µL PBS containing 1% BSA and used directly for FACS analysis according to the protocol described later. For the lung, whole lung tissue was immersed in RNA Later solution (Ambion). Single-cell suspensions of the right lung lobe were prepared by digestion for 25 minutes at 37°C with 0.2 U/mL Liberase TL (Roche) and 80 U/mL DNase (Life Tech) in Hank's balanced-salt solution, followed by forcing of tissue suspensions through a 70µM filter. Cells were centrifuged at 1200RPM for 5 minutes

at 4°C and red blood cells were lysed in 3mL of RBC buffer (Sigma) for 5 minutes on ice. Total cells were counted with an automated Cellometer T4 (Peqlab) and 5 x 10^5 cells/sample were used for FACS. The remaining cells were lysed for RNA extraction and qRT-PCR.

7.4 Cell culture

Two macrophage cell lines, RAW 264.7 (ATCC-TIB71) and J774A.1 were used. RAW 264.7 cells were obtained from American Type Culture Collection (Manassas, VA). J774A.1 cells were obtained from liquid nitrogen stocks of the Allen lab. The source and passage of these cells was unknown. Both RAW 264.7 and J774A.1 cells were cultured in DMEM (Sigma) containing 10% heat-inactivated FCS (Sigma), 2mM L-glutamine, 0.25 U/mL penicillin, and 100mg/mL streptomycin (Gibco, Life Tech).

NIH 3T3 fibroblasts (ATCC CRL1658) are mouse cells generated from a NIH Swiss mouse embryo. The cells were obtained from American Type Culture Collection (Manassas, VA). The cells were grown in DMEM (Sigma) containing 10% heat-inactivated calf serum [HI-CS (Sigma)], 2mM L-glutamine, 0.25 U/mL penicillin, and 100mg/mL streptomycin (Gibco, Life Tech).

Human embryonic kidney 293T cells, HEK293T (ATCC CRC 3216) were maintained in complete Iscove's Modified Eagle Medium [IMEM (Sigma)] containing 10% HI-FBS, 2mM L-glutamine, 0.25 U/mL penicillin, 100mg/mL streptomycin and 25mM 4-(2-hydroxyethyl)-1-piperazineethanesulfonic acid [HEPES (Invitrogen)].

All cells were grown at 37°C with 5% CO_2 and 95% humidity.

7.5 Macrophage activation

Cells were cultured in either DMEM (for BMDMs, RAW 264.7 and J774A.1 cells) or RPMI (for thioglycollate elicited macrophages) supplemented with 5% FCS, 2mM L-glutamine, 0.25 U/mL penicillin and 100mg/mL streptomycin overnight prior to activation with external stimuli in 96 or 24 well plates. Cells were either left untreated or stimulated with 20ng/mL of recombinant IL-4 and IL-13 (Peprotech) and incubated for various periods of time as appropriate at 37°C with 5% CO_2. For classical activation, cells were exposed to 100ng/mL of LPS (*Escherichia coli* 0111:B4; Sigma Aldrich) or medium alone for the desired time period. Following treatment, supernatants were harvested for ELISA and cells washed with cold PBS before being processed for FACS analysis and/or lysed for RNA extraction.

7.6 Flow Cytometry

Cells were seeded at a density of $5x10^5$ cells/well in V bottomed 96 well plates (Greiner) and centrifuged at 1200RPM for 5 minutes at 4°C. Cells were washed twice with 200µL of D-PBS with centrifugation at 1200RPM for 5 minutes at 4°C. The cells were incubated with Aqua live/dead stain (Thermofisher) made up in D-PBS for 10 minutes at room temperature. Subsequently, cells were incubated on ice for 15 minutes with Fc block (CD16/CD32 and neonatal mouse serum) made in FACS buffer (PBS supplemented with 2mM EDTA and 0.5% BSA). Cells were then stained on ice for 30 minutes with fluorescence-conjugated antibodies (in FACS buffer) of interest that bind to surface markers. The lab has previously determined the optimal dilutions of these antibodies. Details of staining panels and antibodies utilised to identify different macrophage populations of interest are detailed below. For permeabilisation and intracellular staining, cells were washed with 200µL of FACS buffer prior to overnight fixation with 2% paraformaldehyde (eBioscience) at 4°C. Cells were stained with antibodies of interest conjugated to the relevant fluorophore in permeabilisation buffer for 45 minutes at room temperature. When using biotinylated antibodies, an additional step involving the incubation of cells with fluorochrome conjugated streptavidin beads was performed. The cells were then

washed twice with permeabilisation buffer wash (eBioscience) followed by a final wash in FACS buffer. Finally the samples were resuspended in 50-300µL of FACS buffer and acquired on either LSR II (BD Biosciences, USA), Canto II (BD Biosciences, USA) or MacsQuant (Miltenyi, Germany) flow cytometers using BD FACS Diva software. All data was analysed using the FlowJo software.

Table 7.1 Macrophage populations and surface markers utilised for gating on FlowJo software:

Population	Surface Markers
Peritoneal macrophages:	
Tissue resident	$CD11b^{hi/+}$ $F4/80^{hi}$ $Tim4^{+}$ $CD11c^{lo/-}$ $MHCII^{lo/-}$
Inflammatory	$CD11b^{hi/+}$ $F4/80^{lo}$ $Tim4^{-}$ $CD11c^{lo/-}$ $MHCII^{hi/+}$
Pleural macrophages:	
Tissue resident	$CD11b^{hi/+}$ $F4/80^{+}$ $Tim4^{+}$ $CD11c^{lo/-}$ $MHCII^{lo/-}$
Inflammatory	$CD11b^{hi/+}$ $F4/80^{+}$ $Tim4^{-}$ $CD11c^{lo/-}$ $MHCII^{hi/+}$
Alveolar macrophages	$CD11b^{lo/-}$ $F4/80^{+}$ $CD11c^{hi/+}$ $SiglecF^{+}$
Interstitial macrophages	$CD11b^{hi/+}$ $F4/80^{+}$ $CD11c^{-}$ $SiglecF^{-}$

Table 7.2 Details of antibodies utilised for FACS staining:

Antigen	Conjugate	Supplier	Clone
BrdU	PE	Biolegend	BU20a
CD11b	AF780	eBiosciences	M1/70
CD11b	AF488	BioLegend	M1/70
CD11b	Pacific Blue	BioLegend	M1/70
CD11b	PECy7	BioLegend	M1/70
CD11c	APC	BioLegend	N418
CD11c	APC	eBiosciences	N418
CD11c	APCCy7	BioLegend	N418
CD11c	BV421	BioLegend	N418
CD11c	FITC	BioLegend	N418
CD11c	PE	BioLegend	N418
CD11c	PECy7	eBiosciences	N418
CD19	PE	Biolegend	6D5
CD19	BV421	Biolegend	6D5
CD19	PE	Biolegend	6D5
CD4	FITC	BioLegend	GK1.5
CD4	PB	BioLegend	GK1.5
CD4	PercP	BioLegend	GK1.5
CD45.2	PerCP	BioLegend	104
F4/80	PE	eBiosciences	BM8
F4/80	PECy7	BioLegend	BM8
F4/80	PECy7	eBiosciences	BM8
Gr1	FITC	eBiosciences	RB6-8C5

Gr1	PercP	BioLegend	RB6-8C5
Ki67	AF488	BioLegend	Ki-67
Ki67	FITC	BD Pharm	B56
Ki67	PE	BD Pharm	BV56
Ly6C	Biotin	BioLegend	HK1.4
Ly6C	FITC	BioLegend	HK1.4
Ly6G	AF647	BioLegend	1A8
Ly6G	APC/Cy7	BioLegend	1A8
Ly6G	BV421	BioLegend	1A8
Ly6G	PE	BD Pharm	1A8
Ly6G	PercP/Cy5.5	BioLegend	1A8
MHC class II (I-A/I-E)	BV421	BioLegend	M5/114.15.2
MHCII	AF780	eBiosciences	M5/114.15.2
MHCII	PercP	BioLegend	M5/114.15.2
MHCII (I-A/I-E)	Pacific Blue	Biolegend	M5/114.15.2
Streptavidin	AF780	eBiosciences	x
Streptavidin	APC	BioLegend	x
Streptavidin	PercP	BioLegend	x
TCR beta	Pacific Blue	Biolegend	H57-597
Tim4	PE	BioLegend	RMT4-54
Zenon Rabbit IgG	AF488	Molecular Probes	x
Zenon Rabbit IgG	AF647	Molecular Probes	x
Zenon Rabbit IgG	Pacific Blue	Molecular Probes	x
Zenon Rabbit IgG	PE	Molecular Probes	x
Ym1	Biotin	RnD Labs	x

7.7 Extraction of RNA

For whole lung tissue stored in RNA Later, tissue was transferred to a 2mL eppendorf containing a stainless steel bead (Qiagen) and 500µL of TRIzol (Thermofisher)/Qiazol (Qiagen). The lung tissue was subsequently homogenised using a TissueLyser (Qiagen) followed by addition of 500µL of TRIzol/Qiazol. For *in vitro* cell culture and PEC, PLEC and BAL, cells were washed twice with ice cold PBS before the addition of 500µL of TRIzol/Qiazol. Cells were incubated with the lysing reagent for 10 minutes at room temperature and transferred to 1.5mL eppendorfs. Subsequently, 100µL of chloroform was added to the tube and the samples were mixed by inversion followed by incubation at room temperature for 2-3 minutes. Samples were then centrifuged at 11,400RPM for 20 minutes at 4°C. Next, the aqueous phase was transferred into fresh eppendorf tubes containing 300µL of isopropanol and 2µL of 15mg/mL of GlycoBlue (Ambion). The samples were mixed by inversion and incubated at room temperature for 15 minutes followed by centrifugation at 11,200RPM for 10 minutes at 4°C. The supernatant was discarded and the pellet was washed twice with 70% ethanol. Following the final wash, the pellet was air dried at room temperature for 15-20 minutes and finally resuspended in 30-50µL of RNase and DNase free water (Gibco, Invitrogen). The tubes were incubated at 56°C for 10 minutes for the pellet to completely dissolve. The extracted RNA was placed on ice immediately or stored at -70°C. RNA was quantified and assessed for purity and quality using NanoDrop ND-1000 (ThermoScientific). In some instances, RNA integrity was also determined by urea based polyacrylamide gel electrophoresis (PAGE).

7.8 Reverse transcription (RT) and quantitative Real-Time Polymerase Chain Reaction (qRT-PCR)

For experiments involving comparison of RAW 264.7 and J774A.1 cell line activation (detailed in Chapter 2), 200ng of total RNA was treated with 50 U Tetro reverse transcriptase (Bioline), 40 mM dNTPs (Promega), 0.5µg primers (Roche) and RNasin inhibitor (Promega) for synthesis of cDNA for qRT-PCR. This method was

used for cDNA synthesis from mRNAs only. The completed reaction was stored at 4°C to prevent cDNA degradation. Prior to quantification by qRT-PCR, the newly synthesised cDNA was diluted 1:5 with RNase and DNase free water.

For all other experiments, reverse transcription was carried out using miScript II RT kit (Qiagen). 200ng of RNA in a volume of 6µL (in H_2O) from each sample was added to a final reaction volume of 10µL containing 2µL of 5x miScript HiFlex buffer, 1µL of 10x miScript Nucleics mix and 1µL of miScript Reverse Transcriptase enzyme. This method synthesised cDNA from both mRNAs and microRNAs. The RT reaction was incubated at 37°C for 1 hour followed by inactivation of the RT enzyme at 95°C for 5 minutes. The completed reaction was stored at 4°C to prevent cDNA degradation. Prior to quantification by qRT-PCR, the newly synthesised cDNA was diluted 1:10 with RNase and DNase free water.

The abundance of transcripts from the genes of interest was measured by real-time PCR with the Lightcycler 480 II system (Roche) with a SYBR Green I Master kit (Roche) or Brilliant III SYBR Master Mix kit (Agilent) for mRNAs. Kits were used according to manufacturer's instructions. For microRNAs, the miScript SYBR Green PCR kit (Qiagen) was utilised. A total reaction volume of 5µL containing 2µL of 2x QuantiTect SYBR Green PCR Master mix, 0.5µL of 10x miScript universal primer, 0.5 µL of 10x miScript specific primer and 0.5 µL of cDNA template and 1.5µL of RNase/DNase-free water was used in 384 well plates (Roche). Specific primer pairs that were utilised for quantification of microRNAs and mRNAs are described in the Table 7.3 below. Primer pairs for mRNA quantification were generated using the online Roche Universal Probe Library primer design tool (http://www.roche-applied-science.com) and purchased from Invitrogen. For microRNAs, custom-made primers available at Qiagen were purchased as forward primers. A universal reverse primer (Qiagen) for microRNA quantification was used for all reactions.

The temperature profile used for quantification of mRNAs comprised a pre-denaturation step for 5 minutes at 95°C followed by 45 cycles consisting of denaturation for 10 seconds at 95°C, annealing for 10 seconds at 60°C and

elongation for 10 seconds at 72°C. For microRNA quantification, a standard protocol designed by Qiagen with a longer annealing time of 30 seconds and 55 cycles was used. Fluorescence data collection was performed at the end of each elongation step. All samples were tested in duplicates and nuclease free water was used as a non-template control.

Table 7.3. List of primers used for qRT-PCR

Primer	**Sequence**
AKT1_F	TCGTGTGGCAGGATGTGTAT
AKT1_R	ACCTGGTGTCAGTCTCAGAGG
AKT3_F	TGGACCACTGTTATAGAGAGAACATTT
AKT3_R	TGGATAGCTTCCGTCCACTC
ARG-1_F	GTCTGTGGGGAAAGCCAAT
ARG-1_R	GCTTCCAACTGCCAGACTGT
CCNE1_F	TTTCTGCAGCGTCATCCTC
CCNE1_R	TGGAGCTTATAGACTTCGCACA
CDC6_F	CTACCTTTCTGGCGCTCCT
CDC6_R	GGATTTAAAGCCTTTTACTTCCTTC
CHI3L3_F	TCACAGGTCTGGCAATTCTTCTG
CHI3L3_R	TTGTCCTTAGGAGGGCTTCCTC
E2F2_F	CCAAATTGTGCGATGTGC
E2F2_R	GAATTCAGGGACCGTAGGC
GAPDH_F	ATGACATCAAGAAGGTGGTG
GAPDH_R	CATACCAGGAAATGAGCTTG
IGF1R_F	GAGAATTTCCTTCACAATTCCATC

IGF1R_R	CACTTGCATGACGTCTCTCC
INSR_F	TCTTTCTTCAGGAAGCTACATCTG
INSR_R	TGTCCAAGGCATAAAAAGAATAGTT
IRS-1_F	CTATGCCAGCATCAGCTTCC
IRS-1_R	TTGCTGAGGTCATTTAGGTCTTC
NCAPG2_F	GTCTTCGGATGTGGTCAGGT
NCAPG2_R	ACAGCTGTGAGGCACACAAT
NOS2_F	GCATTTGGGAATGTAGACTG
NOS2_R	GTTGCATTGGAAGTGAAGCGTTT
PIK3CD_F	AGCTGCTCCAAAGATATCCAGT
PIK3CD_R	TGCTTTAGCGCCTCTTCCT
PIK3R1_F	GACGGCACTTTCCTTGTCC
PIK3R1_R	TGACTTCGCCGTCTACCAC
RBL1_F	ATGACTTCACGGCCATCC
RBL1_R	TAAAGAGCATGCCAGCCAGT
RETNLA_F	TATGAACAGATGGGCCTCCT
RETNLA_R	GGCAGTTGCAAGTATCTCCAC
TAB1_F	GTCAGAGGGGCTGTACAAGG
TAB1_R	AATCATCGCGGCAATCTC
TK1_F	TCGATGAGGGGCAGTTTT
TK1_R	CGAAAGCCTTCCTCTGGA
TNFA_F	GGAAATAGCTCCCAGAAAAGCAAG
TNFA_R	TAGCAAATCGGCTGACGGTGTG

7.8.1 qRT-PCR data analysis

PCR amplification was analysed using the second-derivative maximum algorithm $2^{-\Delta\Delta Ct}$ method (Livak and Schmittgen, 2001). Fold change was calculated as the ratio of the relative change between a treated sample and the average of the relative change values of naïve/untreated samples. For quantification of mRNAs in some instances, relative expression was calculated using a standard curve generated through serial dilutions of a pool of all samples. In each instance, expression of the gene of interest was normalised to housekeeping genes described in the relevant sections for mRNAs and *RNU6B* for microRNAs.

Absolute quantification of microRNAs was carried out using synthetic single stranded RNA oligonucleotides corresponding to the exact mature microRNA sequence under consideration (IDT). Synthetic microRNAs were reverse transcribed using the Qiagen miScript II RT kit in a manner similar to that described above. A standard curve was generated for each microRNA using a dilution series of known input amount of the synthetic oligonucleotide. C_t values obtained using a SYBR Green based detection system were then plotted against the known logarithmic copy numbers of the synthetic microRNA and a standard curve linear equation was generated, where C_t = a (Log copy number) + b. An example of the standard curves generated is shown in Appendix 6.

Statistical analysis for qRT-PCR (and other) data was carried out using GraphPad Prism (Version 6) software. Depending on the group sizes and number of parameters in question, the relevant statistical tests such as one-way or two-way ANOVA, unpaired two-tailed Student's t-Test were applied and P-values <0.05 were considered to be statistically significant.

7.9 Protein Quantification

7.9.1 Enzyme Linked Immunosorbent Assay (ELISA)

ELISA kits were utilised for the measurement of RELM-α (Peprotech) and YM-1 (DuoSet; R&D Systems) proteins in the supernatants.

7.9.1.1 RELM-α

Carbonate Buffer:

Solution A: 8.5g NaH_2CO_3 (or $NaHCO_3$) in 100ml distilled water (1M)

Solution B: 10.6g Na_2CO_3 in 100ml distilled water (1M)

Add 45.3ml of A and 18.2ml of B to 936.5ml distilled water = Carbonate Buffer.

Check pH and adjust to pH 9.6 if required

Wash Buffer:

1x PBS / 0.05% Tween-20 (500 µL tween / litre PBS)

96 well flat bottomed plates (NUNC Maxisorp) were coated with 50µL/well of 1µg/mL rabbit anti-mouse RELM-α capture antibody (Peprotech) diluted in carbonate buffer and incubated overnight at 4°C. The plates were then washed thrice with the wash buffer and blocked with 200µL/well of blocking buffer (PBS containing 10% FCS) for 2 hours at room temperature. Plates were inverted to remove the blocking buffer and samples at appropriate dilutions and standard (0.1-100ng/mL; Peprotech) were added to the relevant wells. The plates were then incubated overnight at 4°C. Subsequently, the plates were emptied and washed thrice with wash buffer and 50µL/well of 0.25 µg/mL of rabbit anti-mouse RELM-α biotin antibody was added followed by an incubation at room temperature for 2 hours. Next, the plates were emptied and washed 6 times with the wash buffer before the addition of 50µL/well of 0.5mg/mL streptavidin-peroxidase (KPL) to each well and incubation at 37°C for 30 minutes. The plates were then washed 8 times with the wash buffer prior to addition of 50µL TMB MicroWell Peroxidase substrate system (KPL). Once the reaction developed, it was stopped by the addition of 50µL of

0.18M H_2SO_4. The plate was then read at 450nm using a spectrophotometer (Varioskan).

7.9.1.2 YM-1

96 well flat bottomed plates (NUNC Maxisorp) were coated with 50µL/well of 1µg/mL rat anti-mouse ECL-F capture antibody diluted in PBS (DuoSet; R&D Sytems) and incubated overnight at 4°C. The plates were then washed thrice with the wash buffer and blocked with 200µL/well of blocking buffer (PBS containing 10% FCS) for 2 hours at room temperature. Plates were inverted to remove the blocking buffer and samples at appropriate dilutions and standard (0.01-20ng/mL; Allen lab) were added to the relevant wells. The plates were then incubated overnight at 4°C. Subsequently, the plates were emptied and washed thrice with wash buffer and 50µL/well of 0.1µg/mL of goat anti-mouse ECL-F biotin antibody was added followed by an incubation at room temperature for 2 hours. Next, the plates were emptied and washed 6 times with the wash buffer before the addition of 50µL/well of 0.5mg/mL streptavidin-peroxidase (KPL) to each well and incubation at 37°C for 30 minutes. The plates were then washed 8 times with the wash buffer prior to addition of 50µL TMB MicroWell Peroxidase substrate system (KPL). Once the reaction developed, it was stopped by the addition of 50µL of 0.18M H_2SO_4. The plate was then read at 450nm using a spectrophotometer (Varioskan).

7.9.1.3 Arginase assay

50µL sample was combined with 50µL 25mM Tris-HCl and 10µL of $MnCl_2$ and incubated at 56°C for 10 minutes. Samples were transferred on ice and 100µL of L-Arginine (pH 9.7) was added before incubating at either 4°C or 37°C for 2 hours. Urea was used as the standard (0-20mM). Following incubation, samples and standard were placed on ice and 40µl from each transferred to a tube containing 160µL stop solution (10% H_2SO_4, 30% H_3PO_4) and 8µl of Isonitrosopropiophenone (ISPF) dye. Samples were boiled at 97°C for 30 minutes and cooled down to 10°C.

200µL of each sample was transferred to a 96 well plate and the absorbance measured at 540nm using spectrophotometer (Varioskan).

7.9.2 Western Blot

4x SDS-PAGE loading buffer:
50mM Tris-Cl (pH 6.8), 12.5mM EDTA, 2% SDS, 10% glycerol, 1% β-mercaptoethanol and 0.02% bromophenol blue

NP-40 lysis buffer:
50mM Tris-Cl (pH 7.5), 100mM NaCl, 1% NP40 (IGEPAL), protease inhibitors and phosphatase inhibitors (Roche)

10% Ammonium Persulfate (APS): 1gm of APS in 10mL dH_2O

Laemmli running buffer (10x), pH 8.3:
30.3gm Tris, 144.2gm Glycine, 10gm SDS in 1 litre of dH_2O

Transfer buffer (10x):
29gm Tris, 144gm Glycine, 3.7gm SDS in 1 litre of dH_2O
1X buffer prepared with 10% transfer buffer (10X), 20% methanol and 70% dH_2O

1M Tris-HCl, pH 6.8: 120gm of Tris dissolved in total volume of 1 litre with dH_2O

1.5M Tris- HCl, pH 8.8: 181gm of Tris dissolved in total volume of 1 litre with dH_2O

Tris-buffered saline-Tween (TBS-T): 10mM Tris-HCl, 100mM NaCl, 0.2% Tween-20

Blocking buffer: 5% skimmed milk powder in TBS-T

Protein lysates were prepared on ice by washing cells once with cold PBS followed by cell lysis using NP-40 lysis buffer containing protease and phosphatase inhibitors (Roche). Cell lysates were transferred into eppendorf tubes and placed on ice for 30 minutes with intermittent mixing by inverting. Cell debris was removed by centrifugation at 12,000 x g at 4°C for 15 minutes and transfer of supernatant to new tubes. The protein was quantified by BCA assay (Thermofisher) following the manufacturer's protocol. Briefly, a standard curve was generated using bovine serum albumin (BSA) with concentrations ranging from 0 to 2,000ng/µL and the protein concentrations of samples were calculated using the standard curve as the reference. The protein lysates (25-50µg) were mixed with 4x SDS loading buffer and boiled at 95°C for 5 minutes followed by loading onto a sodium dodecyl sulfate polyacrylamide (SDS-PAGE) gel comprising a 12% resolving gel and 5% stacking gel. To prepare 30 mL of the resolving gel, 9.9 mL of dH_2O was mixed with 12mL of 30% polyacrylamide, 7.5mL of 1.5M Tris (pH 8.8), 300µL of 10% SDS, 300µL of 10% APS and 12µL of TEMED. The gel mixture was poured between the glass slabs and immediately overlaid with isopropanol for an even surface. Once the gel solidified, the isopropanol was removed and the gel was washed with dH_2O. 10mL of the stacking gel was prepared with 6.8mL of d dH_2O, 1.7ml of 30% polyacrylamide, 1.25mL of 1M Tris (pH 6.8), 100µL of 10% SDS, 300µl of 10% APS and 10µL of TEMED and poured on top of the resolving gel.

Samples were loaded onto the polyacrylamide gel along with a marker [Fermentas PageRuler Plus Prestained Protein Ladder (ThermoScientific)]. The gel was run at 120 Volts for 2 hours at room temperature. The separated proteins on the gel were transferred onto a nitrocellulose Hybond EC membrane (Biorad) by wet blot procedure. This transfer was carried out at 35 Volts at 4°C overnight. Following protein transfer, the membrane was incubated with 5% skimmed milk in TBS-T at room temperature to block the membrane. After 2 hours, the blocking buffer was replaced with primary antibody diluted in 5% skimmed milk (or 5% BSA where relevant) in TBS-T and incubated at 4°C overnight. The membrane was washed three times with TBS-T for 10 minutes each and incubated with the secondary antibody conjugated to HRP (Horseradish Peroxidase) and diluted in blocking buffer at room

temperature for 2 hours. The unbound antibody was removed by washing the membrane three times with TBS-T for 10 minutes each. The protein was detected using an ECL (Enhanced Chemiluminescent Substrate) based western blotting detection system (Pierce, ThermoScientific), X-ray films (Fuji) and a film developer (Konica Minolta) in a dark room.

7.10 Transfection with synthetic oligonucleotides

All procedures carried out involved the reverse transfection of cells wherein cells were mixed with the transfection complex prior to seeding in plates designed for tissue culture at densities detailed in Table 7.4. RAW 264.7 cells were transfected with synthetic mature microRNA mimics or control oligonucleotides (Dharmacon) using Lipofectamine-2000 (ThermoFisher). The constituents of the transfection mixture were based on different well sizes and are described in Table 7.4. Briefly, 4% lipid mixture was prepared by diluting Lipofectamine-2000 with Opti-MEM (ThermoFisher) followed by incubation at room temperature for 5 minutes. This lipid mixture was subsequently added drop wise to a new tube containing the microRNA/Opti-MEM mixture (1:1). The mixture was incubated at room temperature for a further 20 minutes to allow complexing before the addition of cells at a desired concentration in antiobiotic-free culture medium to the same tube. This mixture containing the synthetic oligos at a final concentration of 25nM was then pipetted into each well at a desired volume and concentration in accordance with 3before being incubated at 37°C with 5% CO_2 for 24 hours. The medium was then replaced with complete culture medium containing antibiotics for a further 24 hours before harvesting cells for the relevant analysis.

Plate format (wells)	**Volume of 500nM microRNA** (μL)	**Opti-MEM** (μL)	**4% Lipofectamine-2000 in Opti-MEM** (μL)	**Cell Density**	**Total volume in well** (μL)
6	50	50	100	1 x 10^6 cells in 800μL	1000
24	12.5	12.5	25	3 x 10^5 cells in 450μL	500

Table 7.4. Volumes of different reagents utilised (per well) for transfection of RAW264.7 cells with synthetic microRNAs depending on plate formats.

7.11 Measurement of cell expansion with Carboxyfluorescein diacetate succinimidyl ester (CFDA-SE) and alamarBlue

RAW264.7 cells were stained with 5μM of Vybrant CFDA-SE cell tracer dye (Invitrogen) according to manufacturer's guidelines followed by reverse transfection with synthetic oligonucleotides (25nM) as described previously. Cells were incubated at 37°C with 5% CO_2 and analysed for proliferation at 24 hours and 48 hours post transfection. 4 hours before the end of the incubation period, alamarBlue (ThermoFisher) was added to the culture medium (1:10 dilution). Cell expansion was analysed by measuring alamarBlue conversion in a FluoStar (BMG Labtech) fluorescence plate reader and Vybrant CFDA-SE dilution as a measure of cell proliferation by FACS analysis. Data are presented as percentage of control (RISC-Free) to account for inter-experimental variations in staining intensity.

7.12 3xFLAG-PreScission-6xHistidine (FPH) tag generation

The FPH tag was generated utilising the annealing and extension of two partially overlapping oligonucleotides of ~100nt each. The sequences of these oligonucleotides are as follow:

Table 7.5 Oligonucleotides used for the generation of 3xFLAG-PreScission-Histidine tag

Forward Oligo 1 (100nt):	**BamHI – Kozak – Start codon - 3xFLAG** **cttaGGATCCGCCACCATGGACTACAAAGATGACGAC GATAAAGACTACAAAGATGACGACGATAAAGACTA CAAAGATGACGACGATAAAgcactcttg**
Oligo 2:	**3xFLAG – PreScission – 6 x Histidine – S-G-G-G-G-S alpha helical linker –EcoRV** **CGACGATAAAgcactcTTGGAGGTACTCTTTCAGGGAC CCgcttcaggaCACCATCACCATCACCATAGTGGTGGCG GGGGCTCAGATATC**
Reverse Complement Oligo 2 (95nt):	**cttaGATATCTGAGCCCCCGCCACCACTATGGTGATG GTGATGGTGtcctgaagcGGGTCCCTGAAAGAGTACCT CCAAgagtgcTTTATCGTCG**
Final FPH tag sequence:	**BamHI – Kozak – Start codon - 3xFLAG-PreScission – 6 x Histidine – S-G-G-G-G-S alpha helical linker –EcoRV** **cttaGGATCCGCCACCATGGACTACAAAGATGACGAC GATAAAGACTACAAAGATGACGACGATAAAGACTA CAAAGATGACGACGATAAAgcactcTTGGAGGTACTCT TTCAGGGACCCGCTTCAGGACACCATCACCATCAC CATAGTGGTGGCGGGGGCTCAGATATCtaag**

The oligonucleotides were reconstituted in nuclease free water at a stock concentration of 100μM. The oligonucleotides were then mixed with New England Biolabs Buffer 4 and nuclease free water to achieve a final working concentration of 25μM in 87μL reaction volume. The mix was incubated at 94°C for 5 minutes and gradually cooled down to 65°C and incubated at this temperature for 5 minutes to anneal the oligonucleotides. Subsequently, the mixture was cooled to a final temperature of 37°C and 2μL Klenow fragment 3'-5' DNA exo-polymerase (New England Biolabs) was added to the tube. 11μL of dNTPs (0.25mM each) were then added to the tube, mixed by inversion and incubated at 37°C for 1 hour. After 1 hour, the polymerase was inactivated by heating the mixture to 75°C for 20 minutes.

7.13 Generation of plasmid constructs

Restriction sites for BamHI and EcoRV were designed within the oligonucleotides and the tag was successively digested with a purification step in between using filter columns as outlined by the manufacturer (New England Biolabs). Simultaneously, a pCDNA3 construct containing mAgo2 fused with a ProteinA-TEV protease-Histidine (HTP) tag was digested with the same restriction enzymes and the HTP tag was replaced with the new FPH tag with overnight ligation at a molar ratio of 3:1 (insert:vector) with T4 ligase (New England Biolabs) at 16°C.

Successful clones were sequenced and subsequently for cloning the FPH-mAgo2 sequence into the pLVX-EF1α lentiviral construct, the BamHI site upstream of the FPH tag in the pCDNA3 plasmid was replaced with an SpeI site through PCR amplification. The cycling conditions consisted of the initial denaturation at 95°C for 2 minutes followed by amplification for 30 cycles comprising 95°C for 30 seconds, 65°C for 30 seconds and elongation at 72°C for 3 minutes. A final extension step consisted of elongation at 72°C for 5 minutes. The PCR product was held at 4°C. This was followed by digestion of both the PCR amplified tag containing the SpeI site and the pLVX-EF1α vector with SpeI and NotI. The digested fragment was then cloned into pLVX-EF1α tag with overnight ligation at a molar ratio of 3:1

(insert:vector) with T4 ligase (New England Biolabs) at 16°C. Successful clones were sequenced and transformed into DH5α competent cells to generate glycerol stocks.

7.14 Generation of lentivirus

HEK293T cells were transfected with the pLVX-EF1α-FPH-mAGO2 vector or the control pLVX-EF1α vector using calcium chloride transfection. The reagents used for this method are as follow:

2x HBS [Hexadimethrine Bromide (Polybrene)] Stock (for 50 ml):
281mM NaCl (2.81mL from 5M)
100mM HEPES (1.19 gm)
1.5 mM Na2HPO4 (weigh 0.1065 gm dissolve in 1 mL and add 100μL)
Adjust final pH to 7.12, filter sterilize through a 0.22μm filter and store at -20°C.

2.5M $CaCl_2$ (50 ml):
13.875gm of anhydrous tissue culture grade, 0.22μm filtered and stored at -20°C.

1x TE buffer:
10 mM Tris (pH 8.0, 0.5 mL from 1 M Tris)
1 mM EDTA (pH 8.0, 0.1 mL from 0.5 M EDTA)
Dilute 1:10 with dH_2O (0.1x TE buffer), 0.22μm filtered and stored at 4°C.

Na Butyrate: make a 1000x stock solution (10mM, 0.011gm in 10mL of dH_2O)
0.22μm filter aliquot and store at -20°C.

pMD2.G-VSV-G (http://www.addgene.org/12259/) envelope vector
psPAX2 (http://www.addgene.org/12260/) packaging vector

Table 7.6 Reference table for volumes and concentrations used for $CaCl_2$ transfection:

	Media (mL)	0.1x TE (µL)	$CaCl_2$ 2.5M (µL)	2x HBS (µL)	Cell number	DNA (µg)
p150	22	1125	125	1250	9000000	63
p100	11	562.5	62.5	625	4500000	31.5
p60	5.5	281.2	31.25	312.5	2250000	15.75
p30	2.75	140.6	15.62	156.25	1125000	7.875
6 well	2.75	140.6	15.62	156.25	1125000	7.875
12 well	1.375	70.31	7.81	78.12	562500	3.937
24 well	0.687	35.15	3.90	39.06	281250	1.968
48 well	0.344	17.58	1.95	19.53	140625	0.984
96 well	0.172	8.79	0.98	9.76	70312.5	0.492

HEK293T cells were seeded in $10cm^2$ petridishes at a density of $4.5x10^6$ cells/dish 24 hours prior to transfection with 16µg of pLVX-EF1α-FPH-mAGO2 vector, 4.5 µg of pMD2.GVSV-G (envelope plasmid) and 11.5 µg of psPAX2 (packaging plasmid) using the calcium chloride transfection method. The cells were ~90% confluent before proceeding with transfection. The plasmid solution was made up to a final volume of 562.5µL with 0.1x TE/dH_2O in a 2:1 ratio in accordance with the reference table above. 62.5µL of 2.5M $CaCl_2$ was then added to this mixture followed by drop wise addition of 625µL of 2x HBS solution to the DNA-TE-CaCl2 mixture while vortexing at full speed under sterile conditions. The petridishes were then incubated at 37°C with 5% CO_2. 18 hours post transfection, the culture medium was replaced with 11mL complete medium [IMDM supplemented with 2mM L-Glutamine, 25mM of HEPES, 10% FBS, Penicillin (25 U/mL) and Streptomycin (25 U/mL)] containing 10µM sodium butyrate. The supernatant was harvested 30 hours after media changing (48 hours post transfection) and filtered through 0.22µm filter followed by ultracentrifugation at 19,500 rpm at 4°C for 2 hours to concentrate the generated lentiviruses. Pellets were resuspended in complete IMEM and stored at -70°C.

7.15 Lentiviral transduction

Polybrene (1000x solution): Polybrene is a polycation that neutralises charge interaction to increase binding between pseudoviral capsid and cellular membrane.

For initial experiments, RAW264.7 cells were seeded $3x10^5$ cells per well in a 6 well plate 24 hours prior to transduction. The culture medium was aspirated and cells were infected with 1mL of complete DMEM medium containing 4μg/mL polybrene (1:1000) and 25μL of the concentrated lentivirus. Alternatively, the lentivirus was tittered and cells were transduced with the desired MOI. Where indicated, RAW 264.7 cells were seeded in 10cm2 petridishes at $5x10^6$ cells/dish and freshly harvested supernatant from HEK293T cells containing the lentivirus was centrifuged at 4000 RPM for 10 minutes to remove cellular debris and transferred onto RAW 264.7 cells following addition of polybrene. The petridishes/plates were centrifuged at 500xg for 1 hour at 32°C to enhance transduction. Cells were incubated at 37°C with 5% CO_2. The media was changed following centrifugation and fresh culture medium (complete DMEM) was added. Where appropriate, cells were washed and fresh medium was added every hour for 9-12 hours post transduction to remove pro-inflammatory death inducing molecules. Cells were analysed for ZsGreen1 expression 24 hours and 48 hours post transduction by flow cytometry.

7.16 Genotyping of miR-378/378* mice

The REDExtract-N-Amp PCR ReadyMix (Sigma-Aldrich) was utilised for genotyping of mice. Ear clips were immersed in 100μL of the Extraction Buffer followed by the addition of 25μL Tissue Preparation solution. Samples were mixed by inversion and incubated at room temperature for 10 minutes and subsequently heated at 95°C for 3 minutes and cooled down to 10°C. 100μL of the Neutralisation B solution was added to each sample and mixed by inversion. Samples (DNA template) were stored at 4°C or used straightaway for PCR amplification. In a fresh tube, 5μL of the REDExtract-N-Amp PCR reaction mix was mixed with 2μL of DNA template, 0.5μL each of the forward and reverse primers (listed in Table 7.3)

and 2µL of nuclease free water. The samples were then subject to a PCR comprising an initial denaturation step at 96°C for 3 minutes followed by 30 cycles of denaturation at 95°C for 30 seconds, annealing at 56°C for 30 seconds and elongation at 72°C for 30 seconds. This was followed by a final extension at 72°C for 4 minutes and samples were stored at 4°C or run on a 2% agarose gel. The following banding patterns were observed for the different genotypes:

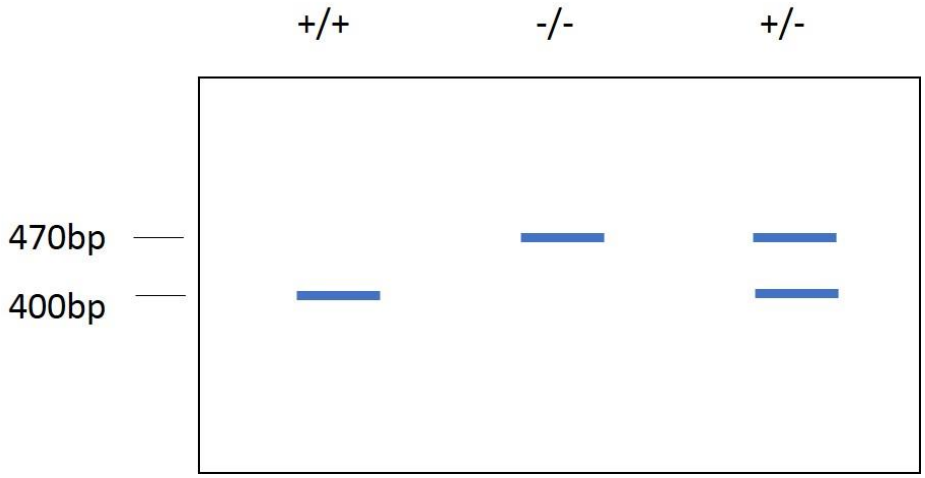

7.17 Statistical data analysis

The statistical approach utilised for individual experiments was dependent on the parameters under consideration. All statistical analysis was carried out using GraphPad Prism (Versions 5 and 6) software.

For a simple comparison between two groups involving a single parameter such as treatment or time, a two-tailed unpaired Student's T-test was utilised (Mann-Whitney test for non-parametric data).

For analysis involving three or more groups and a single parameter such as treatment or time, a one-way ANOVA using means of replicates (biological or technical) was utilised (Kruskal-Wallis H test for non-parametric data).

For analysis involving multiple groups and parameters such as treatment and time, a two-way ANOVA using means of replicates (biological or technical) was utilised.

Chapter 8: Appendices

8.1 Appendix 1: Expression profiles of other markers associated with alternative activation in RAW 264.7 cells

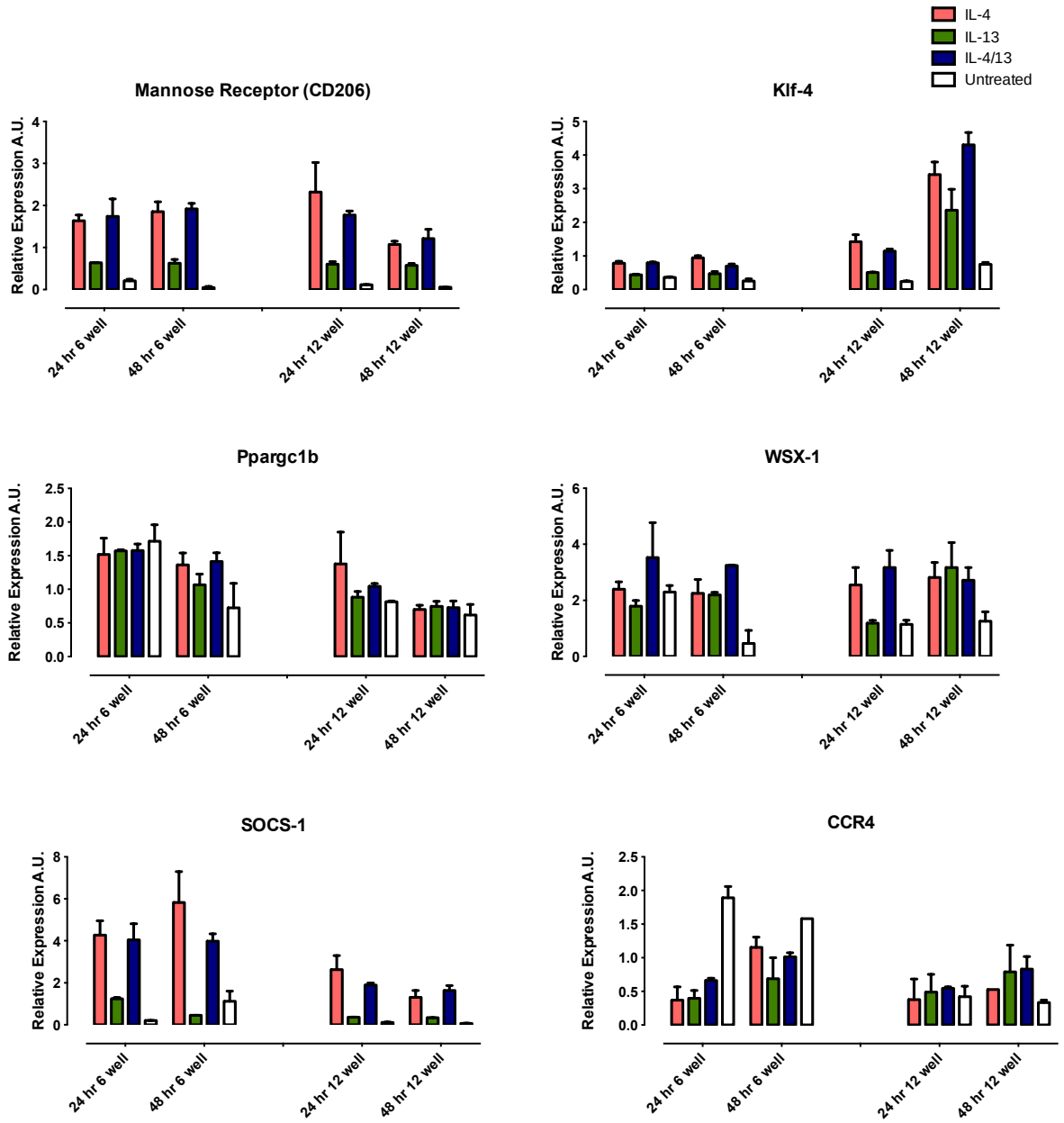

8.2 Appendix 2: Alternative activation in RAW264.7 cells is mainly IL-4 driven

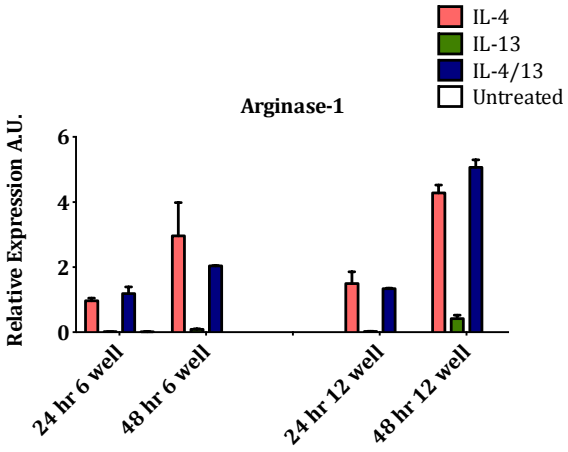

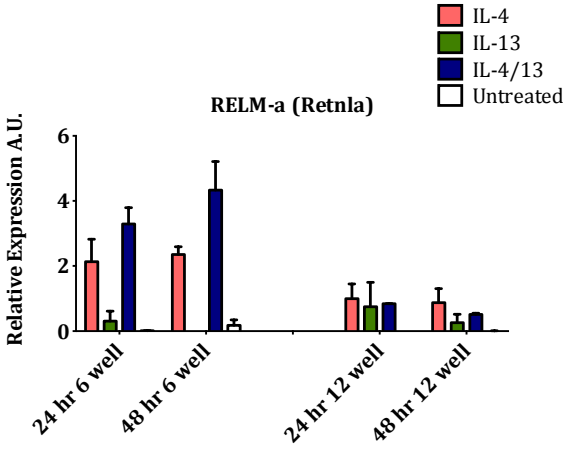

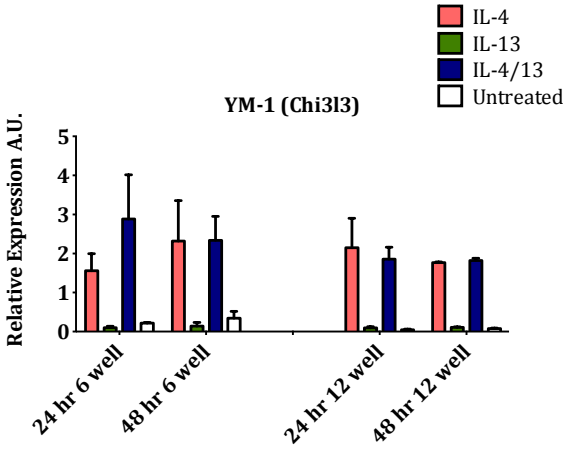

8.3 Appendix 3: Expression profiles of ten shortlisted microRNAs in Thioglycollate elicited macrophages

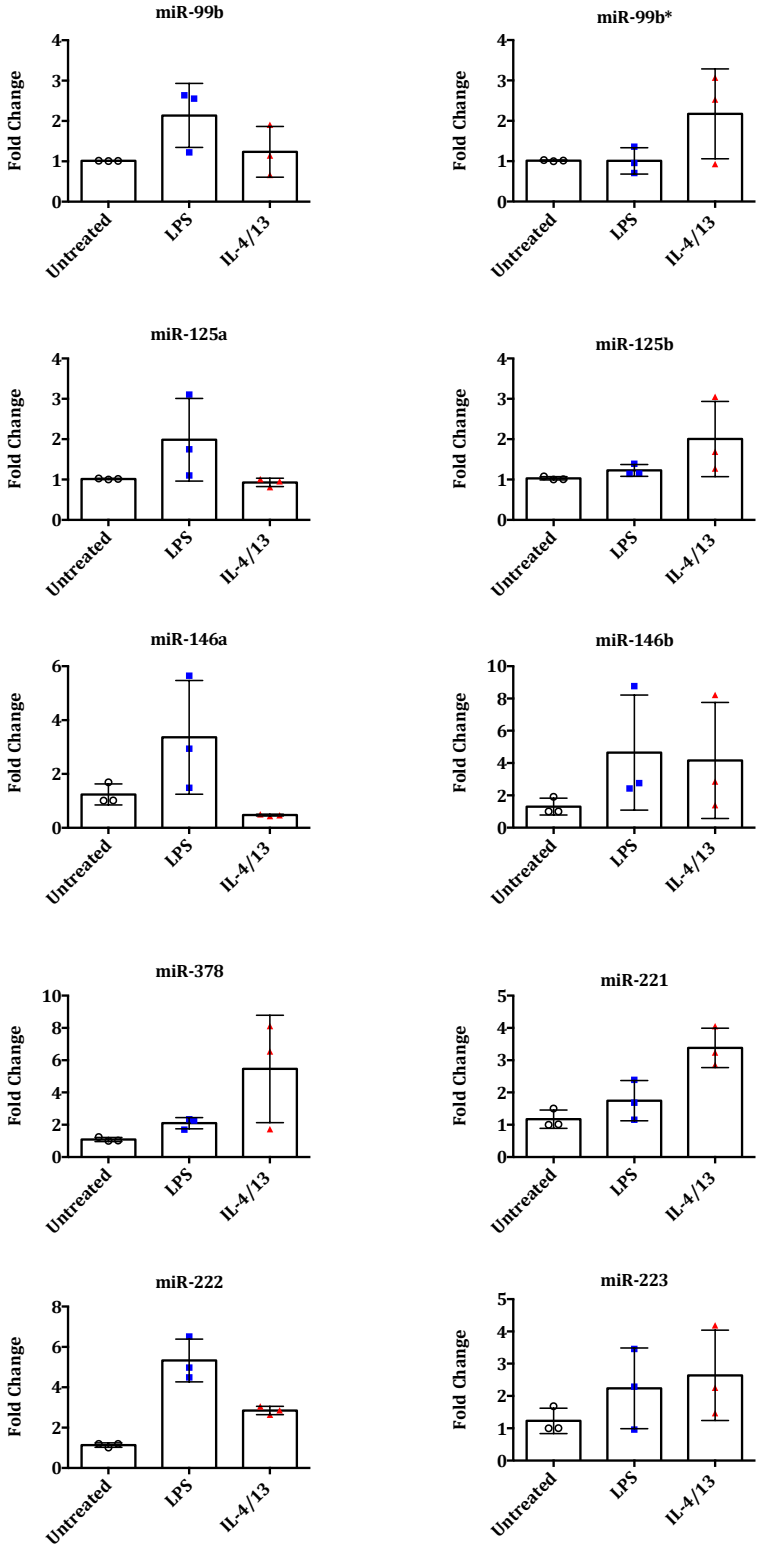

8.4 Appendix 4: Expression profiles of miR-146/b up to 48 hours post stimulation with IL-4 and IL-13 in RAW 264.7 cells

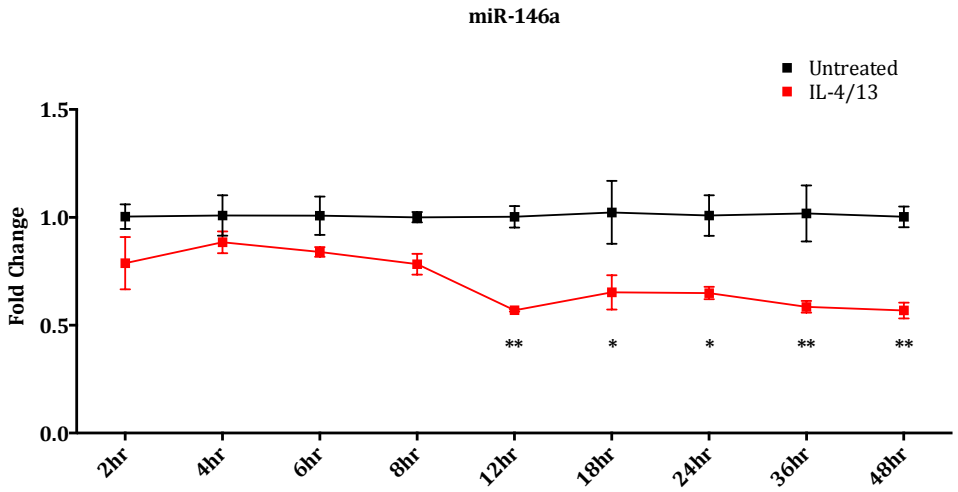

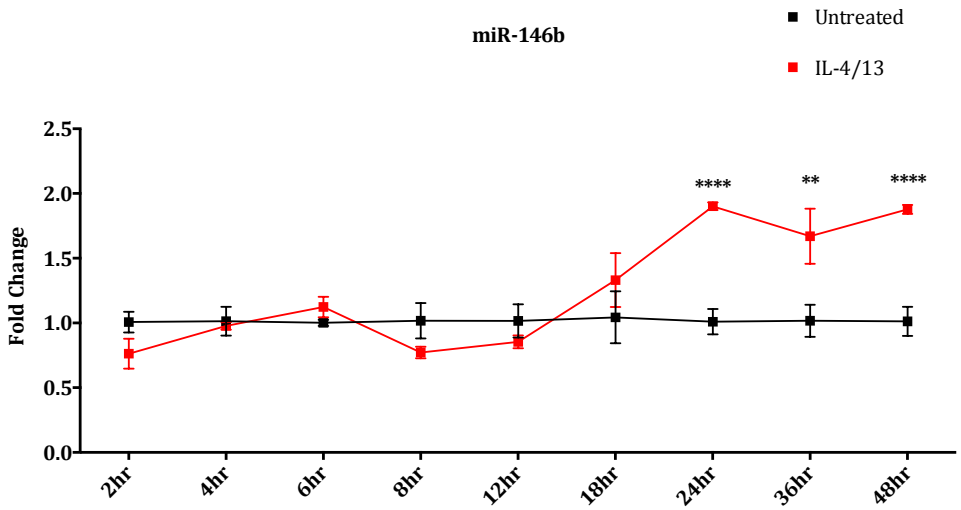

8.5 Appendix 5: Specificity of primers for the real time quantification of miR-146a and miR-146b using synthetic microRNA serial dilutions

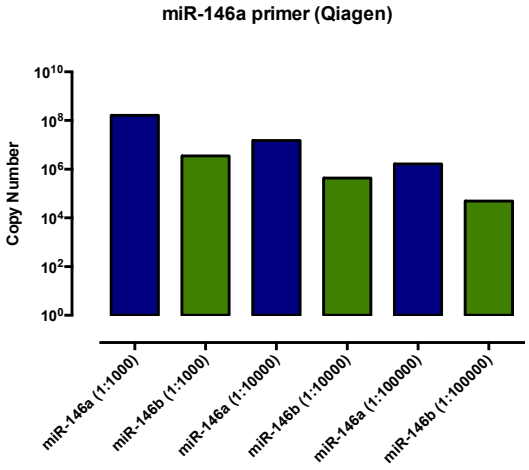

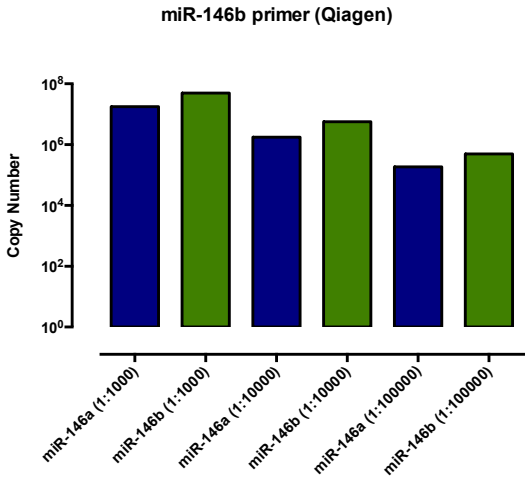

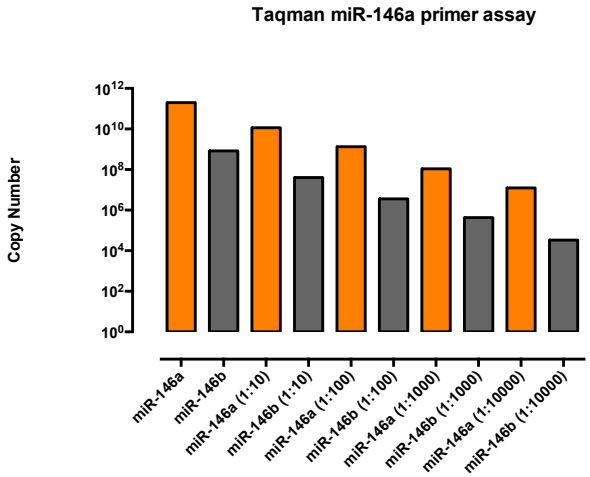

8.6 Appendix 6: Examples of standard curves generated using synthetic microRNA dilutions for the determination of microRNA copy numbers using C_t values

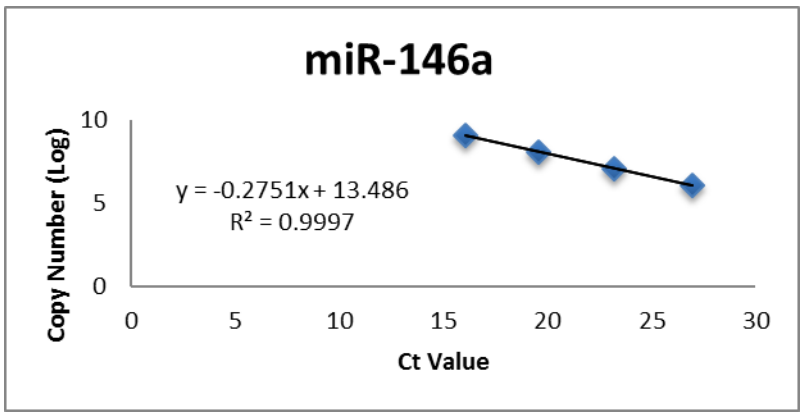

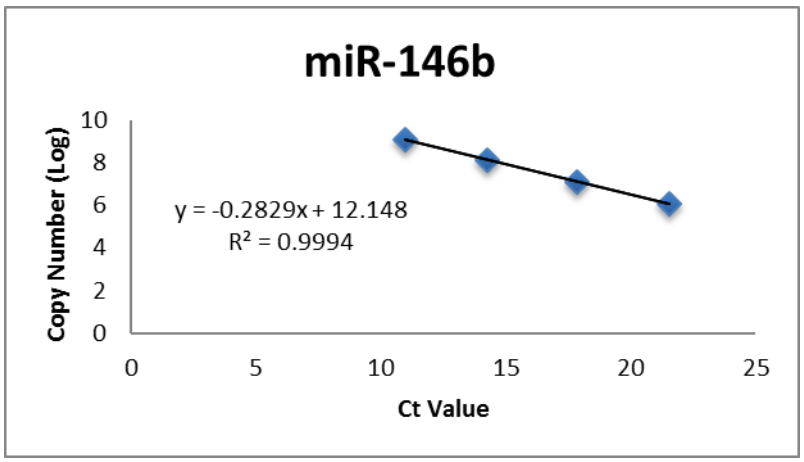

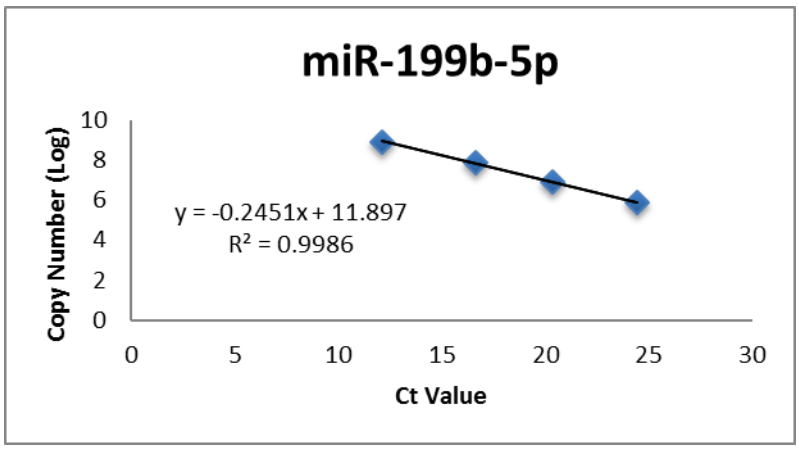

References

ADAMS, T. E., MCKERN, N. M. & WARD, C. W. 2004. Signalling by the type 1 insulin-like growth factor receptor: interplay with the epidermal growth factor receptor. *Growth Factors,* 22**,** 89-95.

AILLES, L., SCHMIDT, M., SANTONI DE SIO, F. R., GLIMM, H., CAVALIERI, S., BRUNO, S., PIACIBELLO, W., VON KALLE, C. & NALDINI, L. 2002. Molecular evidence of lentiviral vector-mediated gene transfer into human self-renewing, multi-potent, long-term NOD/SCID repopulating hematopoietic cells. *Molecular Therapy,* 6**,** 615-626.

AL-QAOUD, K. M., TAUBERT, A., ZAHNER, H., FLEISCHER, B. & HOERAUF, A. 1997. Infection of BALB/c mice with the filarial nematode Litomosoides sigmodontis: role of CD4+ T cells in controlling larval development. *Infect Immun,* 65**,** 2457-61.

ALAM, M. M. & O'NEILL, L. A. 2011. MicroRNAs and the resolution phase of inflammation in macrophages. *Eur J Immunol,* 41**,** 2482-5.

ALBINA, J. E., ABATE, J. A. & MASTROFRANCESCO, B. 1993. Role of ornithine as a proline precursor in healing wounds. *J Surg Res,* 55**,** 97-102.

ALEXANDER, M., HU, R. Z., RUNTSCH, M. C., KAGELE, D. A., MOSBRUGER, T. L., TOLMACHOVA, T., SEABRA, M. C., ROUND, J. L., WARD, D. M. & O'CONNELL, R. M. 2015. Exosome-delivered microRNAs modulate the inflammatory response to endotoxin. *Nature Communications,* 6.

ALEXANDER, M. S., KAWAHARA, G., MOTOHASHI, N., CASAR, J. C., EISENBERG, I., MYERS, J. A., GASPERINI, M. J., ESTRELLA, E. A., KHO, A. T., MITSUHASHI, S., SHAPIRO, F., KANG, P. B. & KUNKEL, L. M. 2013. MicroRNA-199a is induced in dystrophic muscle and affects WNT signaling, cell proliferation, and myogenic differentiation. *Cell Death Differ,* 20**,** 1194-208.

ALLEN, J. E. & MAIZELS, R. M. 2011. Diversity and dialogue in immunity to helminths. *Nat Rev Immunol,* 11**,** 375-88.

ALLEN, J. E. & SUTHERLAND, T. E. 2014. Host protective roles of type 2 immunity: parasite killing and tissue repair, flip sides of the same coin. *Semin Immunol,* 26**,** 329-40.

ALLEN, J. E. & WYNN, T. A. 2011. Evolution of Th2 immunity: a rapid repair response to tissue destructive pathogens. *PLoS Pathog,* 7**,** e1002003.

ALTUVIA, Y., LANDGRAF, P., LITHWICK, G., ELEFANT, N., PFEFFER, S., ARAVIN, A., BROWNSTEIN, M. J., TUSCHL, T. & MARGALIT, H. 2005. Clustering and conservation patterns of human microRNAs. *Nucleic Acids Res,* 33**,** 2697-706.

AMAYA, M. J., OLIVEIRA, A. G., GUIMARAES, E. S., CASTELUBER, M. C., CARVALHO, S. M., ANDRADE, L. M., PINTO, M. C., MENNONE, A., OLIVEIRA, C. A., RESENDE, R. R., MENEZES, G. B., NATHANSON, M. H. & LEITE, M. F. 2014. The insulin receptor translocates to the nucleus to regulate cell proliferation in liver. *Hepatology,* 59**,** 274-83.

AMERES, S. L., MARTINEZ, J. & SCHROEDER, R. 2007. Molecular basis for target RNA recognition and cleavage by human RISC. *Cell,* 130**,** 101-12.

AMERES, S. L. & ZAMORE, P. D. 2013. Diversifying microRNA sequence and function. *Nat Rev Mol Cell Biol,* 14**,** 475-88.

AMIR, S., MA, A. H., SHI, X. B., XUE, L., KUNG, H. J. & DEVERE WHITE, R. W. 2013. Oncomir miR-125b suppresses p14(ARF) to modulate p53-dependent and p53-independent apoptosis in prostate cancer. *PLoS One,* 8**,** e61064.

ANDROULIDAKI, A., ILIOPOULOS, D., ARRANZ, A., DOXAKI, C., SCHWORER, S., ZACHARIOUDAKI, V., MARGIORIS, A. N., TSICHLIS, P. N. & TSATSANIS, C. 2009. The kinase Akt1 controls macrophage response to lipopolysaccharide by regulating microRNAs. *Immunity,* 31**,** 220-31.

ANTHONY, R. M., RUTITZKY, L. I., URBAN, J. F., JR., STADECKER, M. J. & GAUSE, W. C. 2007. Protective immune mechanisms in helminth infection. *Nat Rev Immunol,* 7**,** 975-87.

ANTHONY, R. M., URBAN, J. F., JR., ALEM, F., HAMED, H. A., ROZO, C. T., BOUCHER, J. L., VAN ROOIJEN, N. & GAUSE, W. C. 2006. Memory T(H)2 cells induce alternatively activated macrophages to mediate protection against nematode parasites. *Nat Med,* 12**,** 955-60.

ARAKI, E., LIPES, M. A., PATTI, M. E., BRUNING, J. C., HAAG, B., 3RD, JOHNSON, R. S. & KAHN, C. R. 1994. Alternative pathway of insulin signalling in mice with targeted disruption of the IRS-1 gene. *Nature,* 372**,** 186-90.

ARANDA, J. F., CANFRAN-DUQUE, A., GOEDEKE, L., SUAREZ, Y. & FERNANDEZ-HERNANDO, C. 2015. The miR-199-dynamin regulatory axis controls receptor-mediated endocytosis. *J Cell Sci,* 128**,** 3197-209.

ARGIROPOULOS, B. & HUMPHRIES, R. K. 2007. Hox genes in hematopoiesis and leukemogenesis. *Oncogene,* 26**,** 6766-76.

BABAYAN, S., UNGEHEUER, M. N., MARTIN, C., ATTOUT, T., BELNOUE, E., SNOUNOU, G., RENIA, L., KORENAGA, M. & BAIN, O. 2003a. Resistance and susceptibility to filarial infection with Litomosoides sigmodontis are associated with early differences in parasite development and in localized immune reactions. *Infection and Immunity,* 71**,** 6820-6829.

BABAYAN, S., UNGEHEUER, M. N., MARTIN, C., ATTOUT, T., BELNOUE, E., SNOUNOU, G., RENIA, L., KORENAGA, M. & BAIN, O. 2003b. Resistance and susceptibility to filarial infection with Litomosoides sigmodontis are associated with early differences in parasite development and in localized immune reactions. *Infect Immun,* 71**,** 6820-9.

BABIARZ, J. E., HSU, R., MELTON, C., THOMAS, M., ULLIAN, E. M. & BLELLOCH, R. 2011. A role for noncanonical microRNAs in the mammalian brain revealed by phenotypic differences in Dgcr8 versus Dicer1 knockouts and small RNA sequencing. *RNA,* 17**,** 1489-501.

BALKHI, M. Y., IWENOFU, O. H., BAKKAR, N., LADNER, K. J., CHANDLER, D. S., HOUGHTON, P. J., LONDON, C. A., KRAYBILL, W., PERROTTI, D., CROCE, C. M., KELLER, C. & GUTTRIDGE, D. C. 2013. miR-29 acts as a decoy in sarcomas to protect the tumor suppressor A20 mRNA from degradation by HuR. *Sci Signal,* 6**,** ra63.

BANERJEE, S., CUI, H., XIE, N., TAN, Z., YANG, S., ICYUZ, M., THANNICKAL, V. J., ABRAHAM, E. & LIU, G. 2013a. miR-125a-5p regulates differential activation of macrophages and inflammation. *J Biol Chem,* 288**,** 35428-36.

BANERJEE, S., CUI, H., XIE, N., TAN, Z., YANG, S., ICYUZ, M., THANNICKAL, V. J., ABRAHAM, E. & LIU, G. 2013b. miR-125a-5p regulates differential activation of macrophages and inflammation. *Journal of Biological Chemistry,* 288**,** 35428-36.

BARTEL, D. P. 2004. MicroRNAs: genomics, biogenesis, mechanism, and function. *Cell,* 116**,** 281-97.

BARTEL, D. P. 2009. MicroRNAs: target recognition and regulatory functions. *Cell,* 136**,** 215-33.

BARTH, M. W., HENDRZAK, J. A., MELNICOFF, M. J. & MORAHAN, P. S. 1995. Review of the macrophage disappearance reaction. *J Leukoc Biol,* 57**,** 361-7.

BASERGA, R., PERUZZI, F. & REISS, K. 2003. The IGF-1 receptor in cancer biology. *Int J Cancer,* 107**,** 873-7.

BASKERVILLE, S. & BARTEL, D. P. 2005. Microarray profiling of microRNAs reveals frequent coexpression with neighboring miRNAs and host genes. *RNA,* 11**,** 241-7.

BAUMJOHANN, D. & ANSEL, K. M. 2013. MicroRNA-mediated regulation of T helper cell differentiation and plasticity. *Nat Rev Immunol,* 13**,** 666-78.

BAZZINI, A. A., LEE, M. T. & GIRALDEZ, A. J. 2012. Ribosome profiling shows that miR-430 reduces translation before causing mRNA decay in zebrafish. *Science,* 336**,** 233-7.

BAZZONI, F., ROSSATO, M., FABBRI, M., GAUDIOSI, D., MIROLO, M., MORI, L., TAMASSIA, N., MANTOVANI, A., CASSATELLA, M. A. & LOCATI, M. 2009. Induction and regulatory function of miR-9 in human monocytes and neutrophils exposed to proinflammatory signals. *Proc Natl Acad Sci U S A,* 106**,** 5282-7.

BEHM, C. A. & OVINGTON, K. S. 2000. The role of eosinophils in parasitic helminth infections: insights from genetically modified mice. *Parasitol Today,* 16**,** 202-9.

BEHM-ANSMANT, I., REHWINKEL, J., DOERKS, T., STARK, A., BORK, P. & IZAURRALDE, E. 2006. mRNA degradation by miRNAs and GW182 requires both CCR4:NOT deadenylase and DCP1:DCP2 decapping complexes. *Genes Dev,* 20**,** 1885-98.

BELFIORE, A. & MALAGUARNERA, R. 2011. Insulin receptor and cancer. *Endocr Relat Cancer,* 18**,** R125-47.

BENEZECH, C., LUU, N. T., WALKER, J. A., KRUGLOV, A. A., LOO, Y., NAKAMURA, K., ZHANG, Y., NAYAR, S., JONES, L. H., FLORES-LANGARICA, A., MCINTOSH, A., MARSHALL, J., BARONE, F., BESRA, G., MILES, K., ALLEN, J. E.,

GRAY, M., KOLLIAS, G., CUNNINGHAM, A. F., WITHERS, D. R., TOELLNER, K. M., JONES, N. D., VELDHOEN, M., NEDOSPASOV, S. A., MCKENZIE, A. N. & CAAMANO, J. H. 2015. Inflammation-induced formation of fat-associated lymphoid clusters. *Nat Immunol,* 16**,** 819-28.

BEREZIKOV, E., CHUNG, W. J., WILLIS, J., CUPPEN, E. & LAI, E. C. 2007. Mammalian mirtron genes. *Mol Cell,* 28**,** 328-36.

BERNSTEIN, E., CAUDY, A. A., HAMMOND, S. M. & HANNON, G. J. 2001. Role for a bidentate ribonuclease in the initiation step of RNA interference. *Nature,* 409**,** 363-6.

BERNSTEIN, E., KIM, S. Y., CARMELL, M. A., MURCHISON, E. P., ALCORN, H., LI, M. Z., MILLS, A. A., ELLEDGE, S. J., ANDERSON, K. V. & HANNON, G. J. 2003. Dicer is essential for mouse development. *Nat Genet,* 35**,** 215-7.

BETHUNE, J., ARTUS-REVEL, C. G. & FILIPOWICZ, W. 2012. Kinetic analysis reveals successive steps leading to miRNA-mediated silencing in mammalian cells. *EMBO Rep,* 13**,** 716-23.

BETTELLI, E., CARRIER, Y., GAO, W., KORN, T., STROM, T. B., OUKKA, M., WEINER, H. L. & KUCHROO, V. K. 2006. Reciprocal developmental pathways for the generation of pathogenic effector TH17 and regulatory T cells. *Nature,* 441**,** 235-8.

BHATTACHARJEE, A., SHUKLA, M., YAKUBENKO, V. P., MULYA, A., KUNDU, S. & CATHCART, M. K. 2013. IL-4 and IL-13 employ discrete signaling pathways for target gene expression in alternatively activated monocytes/macrophages. *Free Radic Biol Med,* 54**,** 1-16.

BHAUMIK, D., SCOTT, G. K., SCHOKRPUR, S., PATIL, C. K., ORJALO, A. V., RODIER, F., LITHGOW, G. J. & CAMPISI, J. 2009. MicroRNAs miR-146a/b negatively modulate the senescence-associated inflammatory mediators IL-6 and IL-8. *Aging (Albany NY),* 1**,** 402-11.

BISSELS, U., BOSIO, A. & WAGNER, W. 2012. MicroRNAs are shaping the hematopoietic landscape. *Haematologica,* 97**,** 160-7.

BISWAS, S. K. & MANTOVANI, A. 2010. Macrophage plasticity and interaction with lymphocyte subsets: cancer as a paradigm. *Nat Immunol,* 11**,** 889-96.

BISWAS, S. K. & MANTOVANI, A. 2012. Orchestration of metabolism by macrophages. *Cell Metab,* 15**,** 432-7.

BLANC, M., HSIEH, W. Y., ROBERTSON, K. A., KROPP, K. A., FORSTER, T., SHUI, G., LACAZE, P., WATTERSON, S., GRIFFITHS, S. J., SPANN, N. J., MELJON, A., TALBOT, S., KRISHNAN, K., COVEY, D. F., WENK, M. R., CRAIGON, M., RUZSICS, Z., HAAS, J., ANGULO, A., GRIFFITHS, W. J., GLASS, C. K., WANG, Y. & GHAZAL, P. 2013. The transcription factor STAT-1 couples macrophage synthesis of 25-hydroxycholesterol to the interferon antiviral response. *Immunity,* 38**,** 106-18.

BOHNSACK, M. T., CZAPLINSKI, K. & GORLICH, D. 2004. Exportin 5 is a RanGTP-dependent dsRNA-binding protein that mediates nuclear export of pre-miRNAs. *RNA,* 10**,** 185-91.

BOLDIN, M. P., GONCHAROV, T. M., GOLTSEV, Y. V. & WALLACH, D. 1996. Involvement of MACH, a novel MORT1/FADD-interacting protease, in Fas/APO-1- and TNF receptor-induced cell death. *Cell,* 85**,** 803-15.

BOLDIN, M. P., TAGANOV, K. D., RAO, D. S., YANG, L., ZHAO, J. L., KALWANI, M., GARCIA-FLORES, Y., LUONG, M., DEVREKANLI, A., XU, J., SUN, G., TAY, J., LINSLEY, P. S. & BALTIMORE, D. 2011. miR-146a is a significant brake on autoimmunity, myeloproliferation, and cancer in mice. *J Exp Med,* 208**,** 1189-201.

BORCHERT, G. M., LANIER, W. & DAVIDSON, B. L. 2006. RNA polymerase III transcribes human microRNAs. *Nat Struct Mol Biol,* 13**,** 1097-101.

BOWDRIDGE, S. & GAUSE, W. C. 2010. Regulation of alternative macrophage activation by chromatin remodeling. *Nat Immunol,* 11**,** 879-81.

BOYD, A., KILLORAN, K., MITRE, E. & NUTMAN, T. B. 2015. Pleural cavity type 2 innate lymphoid cells precede Th2 expansion in murine Litomosoides sigmodontis infection. *Exp Parasitol,* 159**,** 118-126.

BRACKEN, C. P., SZUBERT, J. M., MERCER, T. R., DINGER, M. E., THOMSON, D. W., MATTICK, J. S., MICHAEL, M. Z. & GOODALL, G. J. 2011. Global analysis of the mammalian RNA degradome reveals widespread miRNA-dependent and miRNA-independent endonucleolytic cleavage. *Nucleic Acids Res,* 39**,** 5658-68.

BRENNECKE, J., STARK, A., RUSSELL, R. B. & COHEN, S. M. 2005. Principles of microRNA-target recognition. *PLoS Biol,* 3**,** e85.

BROADHURST, M. J., LEUNG, J. M., LIM, K. C., GIRGIS, N. M., GUNDRA, U. M., FALLON, P. G., PREMENKO-LANIER, M., MCKERROW, J. H., MCCUNE, J. M. & LOKE, P. 2012. Upregulation of retinal dehydrogenase 2 in alternatively activated macrophages during retinoid-dependent type-2 immunity to helminth infection in mice. *PLoS Pathog,* 8**,** e1002883.

BRONTE, V. & ZANOVELLO, P. 2005. Regulation of immune responses by L-arginine metabolism. *Nat Rev Immunol,* 5**,** 641-54.

BUCK, A. H., COAKLEY, G., SIMBARI, F., MCSORLEY, H. J., QUINTANA, J. F., LE BIHAN, T., KUMAR, S., ABREU-GOODGER, C., LEAR, M., HARCUS, Y., CERONI, A., BABAYAN, S. A., BLAXTER, M., IVENS, A. & MAIZELS, R. M. 2014. Exosomes secreted by nematode parasites transfer small RNAs to mammalian cells and modulate innate immunity. *Nat Commun,* 5**,** 5488.

BUENO, M. J. & MALUMBRES, M. 2011. MicroRNAs and the cell cycle. *Biochim Biophys Acta,* 1812**,** 592-601.

BURROUGHS, A. M., ANDO, Y., DE HOON, M. J., TOMARU, Y., SUZUKI, H., HAYASHIZAKI, Y. & DAUB, C. O. 2011. Deep-sequencing of human Argonaute-associated small RNAs provides insight into miRNA sorting and reveals Argonaute association with RNA fragments of diverse origin. *RNA Biol,* 8**,** 158-77.

CABAIL, M. Z., LI, S., LEMMON, E., BOWEN, M. E., HUBBARD, S. R. & MILLER, W. T. 2015. The insulin and IGF1 receptor kinase domains are functional dimers in the activated state. *Nat Commun,* 6**,** 6406.

CAI, X., HAGEDORN, C. H. & CULLEN, B. R. 2004. Human microRNAs are processed from capped, polyadenylated transcripts that can also function as mRNAs. *RNA,* 10**,** 1957-66.

CANELLA, D., PRAZ, V., REINA, J. H., COUSIN, P. & HERNANDEZ, N. 2010. Defining the RNA polymerase III transcriptome: Genome-wide localization of the RNA polymerase III transcription machinery in human cells. *Genome Res,* 20**,** 710-21.

CARRER, M., LIU, N., GRUETER, C. E., WILLIAMS, A. H., FRISARD, M. I., HULVER, M. W., BASSEL-DUBY, R. & OLSON, E. N. 2012. Control of mitochondrial metabolism and systemic energy homeostasis by microRNAs 378 and 378*. *Proc Natl Acad Sci U S A,* 109**,** 15330-5.

CASTILLA-LLORENTE, V., NICASTRO, G. & RAMOS, A. 2013. Terminal loop-mediated regulation of miRNA biogenesis: selectivity and mechanisms. *Biochem Soc Trans,* 41**,** 861-5.

CECCHINI, M. G., DOMINGUEZ, M. G., MOCCI, S., WETTERWALD, A., FELIX, R., FLEISCH, H., CHISHOLM, O., HOFSTETTER, W., POLLARD, J. W. & STANLEY, E. R. 1994. Role of colony stimulating factor-1 in the establishment and regulation of tissue macrophages during postnatal development of the mouse. *Development,* 120**,** 1357-72.

CEPPI, M., PEREIRA, P. M., DUNAND-SAUTHIER, I., BARRAS, E., REITH, W., SANTOS, M. A. & PIERRE, P. 2009. MicroRNA-155 modulates the interleukin-1 signaling pathway in activated human monocyte-derived dendritic cells. *Proc Natl Acad Sci U S A,* 106**,** 2735-40.

CERIBELLI, A., SATOH, M. & CHAN, E. K. 2012. MicroRNAs and autoimmunity. *Curr Opin Immunol,* 24**,** 686-91.

CHAN, J. K., KIET, T. K., BLANSIT, K., RAMASUBBAIAH, R., HILTON, J. F., KAPP, D. S. & MATEI, D. 2014. MiR-378 as a biomarker for response to anti-angiogenic treatment in ovarian cancer. *Gynecol Oncol,* 133**,** 568-74.

CHANG, N. C., HUNG, S. I., HWA, K. Y., KATO, I., CHEN, J. E., LIU, C. H. & CHANG, A. C. 2001. A macrophage protein, Ym1, transiently expressed during inflammation is a novel mammalian lectin. *J Biol Chem,* 276**,** 17497-506.

CHANG, Y. H., HUANG, C. N. & SHIAU, M. Y. 2012. Association of IL-4 receptor gene polymorphisms with high density lipoprotein cholesterol. *Cytokine,* 59**,** 309-12.

CHARO, I. F. 2007. Macrophage polarization and insulin resistance: PPARgamma in control. *Cell Metab,* 6**,** 96-8.

CHAUDHURI, A. A., SO, A. Y., MEHTA, A., MINISANDRAM, A., SINHA, N., JONSSON, V. D., RAO, D. S., O'CONNELL, R. M. & BALTIMORE, D. 2012. Oncomir miR-125b regulates hematopoiesis by targeting the gene Lin28A. *Proc Natl Acad Sci U S A,* 109**,** 4233-8.

CHAUDHURI, A. A., SO, A. Y., SINHA, N., GIBSON, W. S., TAGANOV, K. D., O'CONNELL, R. M. & BALTIMORE, D. 2011. MicroRNA-125b potentiates macrophage activation. *J Immunol,* 187**,** 5062-8.

CHAWLA, A. 2010. Control of macrophage activation and function by PPARs. *Circ Res,* 106**,** 1559-69.

CHAWLA, A., BARAK, Y., NAGY, L., LIAO, D., TONTONOZ, P. & EVANS, R. M. 2001. PPAR-gamma dependent and independent effects on macrophage-gene expression in lipid metabolism and inflammation. *Nat Med,* 7**,** 48-52.

CHEKULAEVA, M., MATHYS, H., ZIPPRICH, J. T., ATTIG, J., COLIC, M., PARKER, R. & FILIPOWICZ, W. 2011. miRNA repression involves GW182-mediated recruitment of CCR4-NOT through conserved W-containing motifs. *Nat Struct Mol Biol,* 18**,** 1218-26.

CHEN, B. F., GU, S., SUEN, Y. K., LI, L. & CHAN, W. Y. 2014a. microRNA-199a-3p, DNMT3A, and aberrant DNA methylation in testicular cancer. *Epigenetics,* 9**,** 119-28.

CHEN, C. Z., SCHAFFERT, S., FRAGOSO, R. & LOH, C. 2013. Regulation of immune responses and tolerance: the microRNA perspective. *Immunol Rev,* 253**,** 112-28.

CHEN, F., LIU, Z., WU, W., ROZO, C., BOWDRIDGE, S., MILLMAN, A., VAN ROOIJEN, N., URBAN, J. F., JR., WYNN, T. A. & GAUSE, W. C. 2012a. An essential role for TH2-type responses in limiting acute tissue damage during experimental helminth infection. *Nat Med,* 18**,** 260-6.

CHEN, J., LIU, Z. & YANG, Y. 2014b. In vitro screening of LPS-induced miRNAs in leukocytes derived from cord blood and their possible roles in regulating TLR signals. *Pediatr Res,* 75**,** 595-602.

CHEN, L., DAI, Y. M., JI, C. B., YANG, L., SHI, C. M., XU, G. F., PANG, L. X., HUANG, F. Y., ZHANG, C. M. & GUO, X. R. 2014c. MiR-146b is a regulator of human visceral preadipocyte proliferation and differentiation and its expression is altered in human obesity. *Mol Cell Endocrinol,* 393**,** 65-74.

CHEN, L. T., XU, S. D., XU, H., ZHANG, J. F., NING, J. F. & WANG, S. F. 2012b. MicroRNA-378 is associated with non-small cell lung cancer brain metastasis by promoting cell migration, invasion and tumor angiogenesis. *Med Oncol,* 29**,** 1673-80.

CHEN, R., ALVERO, A. B., SILASI, D. A., KELLY, M. G., FEST, S., VISINTIN, I., LEISER, A., SCHWARTZ, P. E., RUTHERFORD, T. & MOR, G. 2008. Regulation of IKKbeta by miR-199a affects NF-kappaB activity in ovarian cancer cells. *Oncogene,* 27**,** 4712-23.

CHEN, T., MARGARITI, A., KELAINI, S., COCHRANE, A., GUHA, S. T., HU, Y., STITT, A. W., ZHANG, L. & XU, Q. 2015. MicroRNA-199b Modulates Vascular Cell Fate During iPS Cell Differentiation by Targeting the Notch Ligand Jagged1 and Enhancing VEGF Signaling. *Stem Cells,* 33**,** 1405-18.

CHENDRIMADA, T. P., GREGORY, R. I., KUMARASWAMY, E., NORMAN, J., COOCH, N., NISHIKURA, K. & SHIEKHATTAR, R. 2005. TRBP recruits the Dicer complex to Ago2 for microRNA processing and gene silencing. *Nature,* 436**,** 740-4.

CHI, S. W., HANNON, G. J. & DARNELL, R. B. 2012. An alternative mode of microRNA target recognition. *Nat Struct Mol Biol,* 19**,** 321-7.

CHITSULO, L., ENGELS, D., MONTRESOR, A. & SAVIOLI, L. 2000. The global status of schistosomiasis and its control. *Acta Trop,* 77**,** 41-51.

CHOI, Y. S., CHO, H. Y., HOYT, K. R., NAEGELE, J. R. & OBRIETAN, K. 2008. IGF-1 receptor-mediated ERK/MAPK signaling couples status epilepticus to progenitor cell proliferation in the subgranular layer of the dentate gyrus. *Glia,* 56**,** 791-800.

CHONG, M. M., RASMUSSEN, J. P., RUDENSKY, A. Y. & LITTMAN, D. R. 2008. The RNAseIII enzyme Drosha is critical in T cells for preventing lethal inflammatory disease. *J Exp Med,* 205**,** 2005-17.

CHOU, C. K., CHEN, R. F., CHOU, F. F., CHANG, H. W., CHEN, Y. J., LEE, Y. F., YANG, K. D., CHENG, J. T., HUANG, C. C. & LIU, R. T. 2010. miR-146b is highly expressed in adult papillary thyroid carcinomas with high risk features including extrathyroidal invasion and the BRAF(V600E) mutation. *Thyroid,* 20**,** 489-94.

CLOONAN, N. 2015. Re-thinking miRNA-mRNA interactions: intertwining issues confound target discovery. *Bioessays,* 37**,** 379-88.

COBB, B. S., NESTEROVA, T. B., THOMPSON, E., HERTWECK, A., O'CONNOR, E., GODWIN, J., WILSON, C. B., BROCKDORFF, N., FISHER, A. G., SMALE, S. T. & MERKENSCHLAGER, M. 2005. T cell lineage choice and differentiation in the absence of the RNase III enzyme Dicer. *J Exp Med,* 201**,** 1367-73.

COHEN, P. 2006. Timeline - The twentieth century struggle to decipher insulin signalling. *Nature Reviews Molecular Cell Biology,* 7**,** 867-873.

CORCORAN, D. L., PANDIT, K. V., GORDON, B., BHATTACHARJEE, A., KAMINSKI, N. & BENOS, P. V. 2009. Features of mammalian microRNA promoters emerge from polymerase II chromatin immunoprecipitation data. *PLoS One,* 4**,** e5279.

COSTA ROSA, L. F., SAFI, D. A., CURY, Y. & CURI, R. 1996. The effect of insulin on macrophage metabolism and function. *Cell Biochem Funct,* 14**,** 33-42.

COSTINEAN, S., SANDHU, S. K., PEDERSEN, I. M., TILI, E., TROTTA, R., PERROTTI, D., CIARLARIELLO, D., NEVIANI, P., HARB, J., KAUFFMAN, L. R., SHIDHAM, A. & CROCE, C. M. 2009. Src homology 2 domain-containing inositol-5-phosphatase and CCAAT enhancer-binding protein beta are targeted by miR-155 in B cells of Emicro-MiR-155 transgenic mice. *Blood,* 114**,** 1374-82.

CSOKA, B., SELMECZY, Z., KOSCSO, B., NEMETH, Z. H., PACHER, P., MURRAY, P. J., KEPKA-LENHART, D., MORRIS, S. M., JR., GAUSE, W. C., LEIBOVICH, S. J. & HASKO, G. 2012. Adenosine promotes alternative macrophage activation via A2A and A2B receptors. *FASEB J,* 26**,** 376-86.

CURTALE, G., CITARELLA, F., CARISSIMI, C., GOLDONI, M., CARUCCI, N., FULCI, V., FRANCESCHINI, D., MELONI, F., BARNABA, V. & MACINO, G. 2010. An emerging player in the adaptive immune response: microRNA-146a is a modulator of IL-2 expression and activation-induced cell death in T lymphocytes. *Blood,* 115**,** 265-73.

CURTALE, G., RENZI, T. A. & LOCATI, M. 2012. miR-146b: IL-10-dependent negative regulator of inflammation. *Cytokine,* 59**,** 565-565.

CZECH, B. & HANNON, G. J. 2011. Small RNA sorting: matchmaking for Argonautes. *Nat Rev Genet,* 12**,** 19-31.

DA COSTA MARTINS, P. A., SALIC, K., GLADKA, M. M., ARMAND, A. S., LEPTIDIS, S., EL AZZOUZI, H., HANSEN, A., COENEN-DE ROO, C. J., BIERHUIZEN, M. F., VAN DER NAGEL, R., VAN KUIK, J., DE WEGER, R., DE BRUIN, A., CONDORELLI, G., ARBONES, M. L., ESCHENHAGEN, T. & DE WINDT, L. J. 2010. MicroRNA-199b targets the nuclear kinase Dyrk1a in an auto-amplification loop promoting calcineurin/NFAT signalling. *Nat Cell Biol,* 12**,** 1220-7.

DALTON, D. K., PITTS-MEEK, S., KESHAV, S., FIGARI, I. S., BRADLEY, A. & STEWART, T. A. 1993. Multiple defects of immune cell function in mice with disrupted interferon-gamma genes. *Science,* 259**,** 1739-42.

DAVIES, J. B. 1994. Sixty years of onchocerciasis vector control: a chronological summary with comments on eradication, reinvasion, and insecticide resistance. *Annu Rev Entomol,* 39**,** 23-45.

DAVIES, L. C., JENKINS, S. J., ALLEN, J. E. & TAYLOR, P. R. 2013a. Tissue-resident macrophages. *Nat Immunol,* 14**,** 986-95.

DAVIES, L. C., ROSAS, M., JENKINS, S. J., LIAO, C. T., SCURR, M. J., BROMBACHER, F., FRASER, D. J., ALLEN, J. E., JONES, S. A. & TAYLOR, P. R. 2013b. Distinct bone marrow-derived and tissue-resident macrophage lineages proliferate at key stages during inflammation. *Nat Commun,* 4**,** 1886.

DAVIES, L. C. & TAYLOR, P. R. 2015. Tissue-resident macrophages: then and now. *Immunology,* 144**,** 541-8.

DAVISON, Z., DE BLACQUIERE, G. E., WESTLEY, B. R. & MAY, F. E. 2011. Insulin-like growth factor-dependent proliferation and survival of triple-negative breast cancer cells: implications for therapy. *Neoplasia,* 13**,** 504-15.

DE MEYTS, P. & WHITTAKER, J. 2002. Structural biology of insulin and IGF1 receptors: implications for drug design. *Nat Rev Drug Discov,* 1**,** 769-83.

DEMPSEY, P. W., VAIDYA, S. A. & CHENG, G. 2003. The art of war: Innate and adaptive immune responses. *Cell Mol Life Sci,* 60**,** 2604-21.

DENDULURI, S. K., IDOWU, O., WANG, Z., LIAO, Z., YAN, Z., MOHAMMED, M. K., YE, J., WEI, Q., WANG, J., ZHAO, L. & LUU, H. H. 2015. Insulin-like growth factor (IGF) signaling in tumorigenesis and the development of cancer drug resistance. *Genes Dis,* 2**,** 13-25.

DENG, X., WU, B., XIAO, K., KANG, J., XIE, J., ZHANG, X. & FAN, Y. 2015. MiR-146b-5p promotes metastasis and induces epithelial-mesenchymal transition in thyroid cancer by targeting ZNRF3. *Cell Physiol Biochem,* 35**,** 71-82.

DENLI, A. M., TOPS, B. B., PLASTERK, R. H., KETTING, R. F. & HANNON, G. J. 2004. Processing of primary microRNAs by the Microprocessor complex. *Nature,* 432**,** 231-5.

DERRY, M. C., YANAGIYA, A., MARTINEAU, Y. & SONENBERG, N. 2006. Regulation of poly(A)-binding protein through PABP-interacting proteins. *Cold Spring Harb Symp Quant Biol,* 71**,** 537-43.

DIEDERICHS, S. & HABER, D. A. 2007. Dual role for argonautes in microRNA processing and posttranscriptional regulation of microRNA expression. *Cell,* 131**,** 1097-108.

DING, A. H., NATHAN, C. F. & STUEHR, D. J. 1988. Release of reactive nitrogen intermediates and reactive oxygen intermediates from mouse peritoneal macrophages. Comparison of activating cytokines and evidence for independent production. *J Immunol,* 141**,** 2407-12.

DJURANOVIC, S., NAHVI, A. & GREEN, R. 2012. miRNA-mediated gene silencing by translational repression followed by mRNA deadenylation and decay. *Science,* 336**,** 237-40.

DOENCH, J. G. & SHARP, P. A. 2004. Specificity of microRNA target selection in translational repression. *Genes Dev,* 18**,** 504-11.

DONG, X., PARK, S., LIN, X., COPPS, K., YI, X. & WHITE, M. F. 2006. Irs1 and Irs2 signaling is essential for hepatic glucose homeostasis and systemic growth. *J Clin Invest,* 116**,** 101-14.

DROR, N., ALTER-KOLTUNOFF, M., AZRIEL, A., AMARIGLIO, N., JACOB-HIRSCH, J., ZELIGSON, S., MORGENSTERN, A., TAMURA, T., HAUSER, H., RECHAVI, G., OZATO, K. & LEVI, B. Z. 2007. Identification of IRF-8 and IRF-1 target genes in activated macrophages. *Mol Immunol,* 44**,** 338-46.

DU, C., LIU, C., KANG, J., ZHAO, G., YE, Z., HUANG, S., LI, Z., WU, Z. & PEI, G. 2009. MicroRNA miR-326 regulates TH-17 differentiation and is associated with the pathogenesis of multiple sclerosis. *Nat Immunol,* 10**,** 1252-9.

DU, L., RONG, H., CHENG, Y., GUO, S., SHI, Q., JIA, X., ZHU, H., HAO, Y., XU, K., ZHANG, J., JIAO, H., ZHAO, T., ZHANG, H., CHEN, C. & WANG, F. 2014. Identification of microRNAs dysregulated in CD14 gene silencing RAW264.7 macrophage cells. *Inflammation,* 37**,** 287-94.

DUECK, A., EICHNER, A., SIXT, M. & MEISTER, G. 2014. A miR-155-dependent microRNA hierarchy in dendritic cell maturation and macrophage activation. *FEBS Lett,* 588**,** 632-40.

EBERT, M. S., NEILSON, J. R. & SHARP, P. A. 2007. MicroRNA sponges: competitive inhibitors of small RNAs in mammalian cells. *Nat Methods,* 4**,** 721-6.

EBERT, M. S. & SHARP, P. A. 2010. MicroRNA sponges: progress and possibilities. *Rna-a Publication of the Rna Society,* 16**,** 2043-50.

EBERT, P. J., JIANG, S., XIE, J., LI, Q. J. & DAVIS, M. M. 2009. An endogenous positively selecting peptide enhances mature T cell responses and becomes an autoantigen in the absence of microRNA miR-181a. *Nat Immunol,* 10**,** 1162-9.

EDWARDS, J. P., ZHANG, X., FRAUWIRTH, K. A. & MOSSER, D. M. 2006. Biochemical and functional characterization of three activated macrophage populations. *J Leukoc Biol,* 80**,** 1298-307.

EICHHORN, S. W., GUO, H., MCGEARY, S. E., RODRIGUEZ-MIAS, R. A., SHIN, C., BAEK, D., HSU, S. H., GHOSHAL, K., VILLEN, J. & BARTEL, D. P. 2014. mRNA destabilization is the dominant effect of mammalian microRNAs by the time substantial repression ensues. *Mol Cell,* 56**,** 104-15.

EICHNER, L. J., PERRY, M. C., DUFOUR, C. R., BERTOS, N., PARK, M., ST-PIERRE, J. & GIGUERE, V. 2010. miR-378(*) mediates metabolic shift in breast cancer cells via the PGC-1beta/ERRgamma transcriptional pathway. *Cell Metab,* 12**,** 352-61.

EIRING, A. M., HARB, J. G., NEVIANI, P., GARTON, C., OAKS, J. J., SPIZZO, R., LIU, S., SCHWIND, S., SANTHANAM, R., HICKEY, C. J., BECKER, H., CHANDLER, J. C., ANDINO, R., CORTES, J., HOKLAND, P., HUETTNER, C. S., BHATIA, R., ROY, D. C., LIEBHABER, S. A., CALIGIURI, M. A., MARCUCCI, G., GARZON, R., CROCE, C. M., CALIN, G. A. & PERROTTI, D. 2010. miR-328 functions as an RNA decoy to modulate hnRNP E2 regulation of mRNA translation in leukemic blasts. *Cell,* 140**,** 652-65.

EL KASMI, K. C., QUALLS, J. E., PESCE, J. T., SMITH, A. M., THOMPSON, R. W., HENAO-TAMAYO, M., BASARABA, R. J., KONIG, T., SCHLEICHER, U., KOO, M. S., KAPLAN, G., FITZGERALD, K. A., TUOMANEN, E. I., ORME, I. M., KANNEGANTI, T. D., BOGDAN, C., WYNN, T. A. & MURRAY, P. J. 2008. Toll-like receptor-induced arginase 1 in macrophages thwarts effective immunity against intracellular pathogens. *Nat Immunol,* 9**,** 1399-406.

ELKAYAM, E., KUHN, C. D., TOCILJ, A., HAASE, A. D., GREENE, E. M., HANNON, G. J. & JOSHUA-TOR, L. 2012. The structure of human argonaute-2 in complex with miR-20a. *Cell,* 150**,** 100-10.

ENGERT, J. C., BERGLUND, E. B. & ROSENTHAL, N. 1996. Proliferation precedes differentiation in IGF-I-stimulated myogenesis. *J Cell Biol,* 135**,** 431-40.

EPELMAN, S., LAVINE, K. J. & RANDOLPH, G. J. 2014. Origin and functions of tissue macrophages. *Immunity,* 41**,** 21-35.

ESCRIBANO, O., GOMEZ-HERNANDEZ, A., DIAZ-CASTROVERDE, S., NEVADO, C., GARCIA, G., OTERO, Y. F., PERDOMO, L., BENEIT, N. & BENITO, M. 2015. Insulin receptor isoform A confers a higher proliferative capability to pancreatic beta cells enabling glucose availability and IGF-I signaling. *Mol Cell Endocrinol,* 409**,** 82-91.

ESSER-VON BIEREN, J., MOSCONI, I., GUIET, R., PIERSGILLI, A., VOLPE, B., CHEN, F., GAUSE, W. C., SEITZ, A., VERBEEK, J. S. & HARRIS, N. L. 2013. Antibodies trap tissue migrating helminth larvae and prevent tissue damage by driving IL-4Ralpha-independent alternative differentiation of macrophages. *PLoS Pathog,* 9**,** e1003771.

ETZRODT, M., CORTEZ-RETAMOZO, V., NEWTON, A., ZHAO, J., NG, A., WILDGRUBER, M., ROMERO, P., WURDINGER, T., XAVIER, R., GEISSMANN, F., MEYLAN, E., NAHRENDORF, M., SWIRSKI, F. K., BALTIMORE, D., WEISSLEDER, R. & PITTET, M. J. 2012. Regulation of monocyte functional heterogeneity by miR-146a and Relb. *Cell Rep,* 1**,** 317-24.

EULALIO, A., REHWINKEL, J., STRICKER, M., HUNTZINGER, E., YANG, S. F., DOERKS, T., DORNER, S., BORK, P., BOUTROS, M. & IZAURRALDE, E. 2007. Target-specific requirements for enhancers of decapping in miRNA-mediated gene silencing. *Genes Dev,* 21**,** 2558-70.

EVANS, D. B., GELBAND, H. & VLASSOFF, C. 1993. Social and economic factors and the control of lymphatic filariasis: a review. *Acta Trop,* 53**,** 1-26.

FABBRI, M., IVAN, M., CIMMINO, A., NEGRINI, M. & CALIN, G. A. 2007. Regulatory mechanisms of microRNAs involvement in cancer. *Expert Opin Biol Ther,* 7**,** 1009-19.

FABIAN, M. R., MATHONNET, G., SUNDERMEIER, T., MATHYS, H., ZIPPRICH, J. T., SVITKIN, Y. V., RIVAS, F., JINEK, M., WOHLSCHLEGEL, J., DOUDNA, J. A., CHEN, C. Y., SHYU, A. B., YATES, J. R., 3RD, HANNON, G. J., FILIPOWICZ, W., DUCHAINE, T. F. & SONENBERG, N. 2009. Mammalian miRNA RISC recruits CAF1 and PABP to affect PABP-dependent deadenylation. *Molecular Cell,* 35**,** 868-80.

FABIAN, M. R. & SONENBERG, N. 2012. The mechanics of miRNA-mediated gene silencing: a look under the hood of miRISC. *Nat Struct Mol Biol,* 19**,** 586-93.

FABIAN, M. R., SONENBERG, N. & FILIPOWICZ, W. 2010. Regulation of mRNA translation and stability by microRNAs. *Annu Rev Biochem,* 79**,** 351-79.

FAIRWEATHER, D. & CIHAKOVA, D. 2009. Alternatively activated macrophages in infection and autoimmunity. *J Autoimmun,* 33**,** 222-30.

FALKENBERG, N., ANASTASOV, N., RAPPL, K., BRASELMANN, H., AUER, G., WALCH, A., HUBER, M., HOFIG, I., SCHMITT, M., HOFLER, H., ATKINSON, M. J. & AUBELE, M. 2013. MiR-221/-222 differentiate prognostic groups in advanced breast cancers and influence cell invasion. *Br J Cancer,* 109**,** 2714-23.

FARAONI, I., ANTONETTI, F. R., CARDONE, J. & BONMASSAR, E. 2009. miR-155 gene: a typical multifunctional microRNA. *Biochim Biophys Acta,* 1792**,** 497-505.

FAZI, F., ROSA, A., FATICA, A., GELMETTI, V., DE MARCHIS, M. L., NERVI, C. & BOZZONI, I. 2005. A minicircuitry comprised of microRNA-223 and transcription factors NFI-A and C/EBPalpha regulates human granulopoiesis. *Cell,* 123**,** 819-31.

FELLI, N., FONTANA, L., PELOSI, E., BOTTA, R., BONCI, D., FACCHIANO, F., LIUZZI, F., LULLI, V., MORSILLI, O., SANTORO, S., VALTIERI, M., CALIN, G. A., LIU, C. G., SORRENTINO, A., CROCE, C. M. & PESCHLE, C. 2005. MicroRNAs 221 and 222 inhibit normal erythropoiesis and erythroleukemic cell growth via kit receptor down-modulation. *Proc Natl Acad Sci U S A,* 102**,** 18081-6.

FERNANDEZ-HERNANDO, C., SUAREZ, Y., RAYNER, K. J. & MOORE, K. J. 2011. MicroRNAs in lipid metabolism. *Curr Opin Lipidol,* 22**,** 86-92.

FERRARA, N. 2001. Role of vascular endothelial growth factor in regulation of physiological angiogenesis. *Am J Physiol Cell Physiol,* 280**,** C1358-66.

FERRARA, N. & GERBER, H. P. 2001. The role of vascular endothelial growth factor in angiogenesis. *Acta Haematol,* 106**,** 148-56.

FILBEY, K. J., GRAINGER, J. R., SMITH, K. A., BOON, L., VAN ROOIJEN, N., HARCUS, Y., JENKINS, S., HEWITSON, J. P. & MAIZELS, R. M. 2014. Innate and adaptive type 2 immune cell responses in genetically controlled resistance to intestinal helminth infection. *Immunol Cell Biol,* 92**,** 436-48.

FINDLAY, E. G. & HUSSELL, T. 2012. Macrophage-Mediated Inflammation and Disease: A Focus on the Lung. *Mediators of Inflammation*.

FINKELMAN, F. D., SHEA-DONOHUE, T., MORRIS, S. C., GILDEA, L., STRAIT, R., MADDEN, K. B., SCHOPF, L. & URBAN, J. F., JR. 2004. Interleukin-4- and interleukin-13-mediated host protection against intestinal nematode parasites. *Immunol Rev,* 201**,** 139-55.

FONTANA, L., PELOSI, E., GRECO, P., RACANICCHI, S., TESTA, U., LIUZZI, F., CROCE, C. M., BRUNETTI, E., GRIGNANI, F. & PESCHLE, C. 2007. MicroRNAs 17-5p-20a-106a control monocytopoiesis through AML1 targeting and M-CSF receptor upregulation. *Nat Cell Biol,* 9**,** 775-87.

FORBES, S. J. & ROSENTHAL, N. 2014. Preparing the ground for tissue regeneration: from mechanism to therapy. *Nat Med,* 20**,** 857-69.

FRIEDMAN, R. C., FARH, K. K., BURGE, C. B. & BARTEL, D. P. 2009. Most mammalian mRNAs are conserved targets of microRNAs. *Genome Res,* 19**,** 92-105.

FUKAO, T., FUKUDA, Y., KIGA, K., SHARIF, J., HINO, K., ENOMOTO, Y., KAWAMURA, A., NAKAMURA, K., TAKEUCHI, T. & TANABE, M. 2007. An evolutionarily conserved mechanism for microRNA-223 expression revealed by microRNA gene profiling. *Cell,* 129**,** 617-31.

GALVAN-PENA, S. & O'NEILL, L. A. 2014. Metabolic reprograming in macrophage polarization. *Front Immunol,* 5**,** 420.

GAN, R., YANG, Y., YANG, X., ZHAO, L., LU, J. & MENG, Q. H. 2014. Downregulation of miR-221/222 enhances sensitivity of breast cancer cells to tamoxifen through upregulation of TIMP3. *Cancer Gene Ther,* 21**,** 290-6.

GARCIA, A. I., BUISSON, M., BERTRAND, P., RIMOKH, R., ROULEAU, E., LOPEZ, B. S., LIDEREAU, R., MIKAELIAN, I. & MAZOYER, S. 2011. Down-regulation of BRCA1 expression by miR-146a and miR-146b-5p in triple negative sporadic breast cancers. *EMBO Mol Med,* 3**,** 279-90.

GAROFALO, M., QUINTAVALLE, C., ROMANO, G., CROCE, C. M. & CONDORELLI, G. 2012. miR221/222 in cancer: their role in tumor progression and response to therapy. *Curr Mol Med,* 12**,** 27-33.

GARZON, R., GAROFALO, M., MARTELLI, M. P., BRIESEWITZ, R., WANG, L., FERNANDEZ-CYMERING, C., VOLINIA, S., LIU, C. G., SCHNITTGER, S., HAFERLACH, T., LISO, A., DIVERIO, D., MANCINI, M., MELONI, G., FOA, R., MARTELLI, M. F., MECUCCI, C., CROCE, C. M. & FALINI, B. 2008. Distinctive microRNA signature of acute myeloid leukemia bearing cytoplasmic mutated nucleophosmin. *Proc Natl Acad Sci U S A,* 105**,** 3945-50.

GATTO, G., ROSSI, A., ROSSI, D., KROENING, S., BONATTI, S. & MALLARDO, M. 2008. Epstein-Barr virus latent membrane protein 1 trans-activates miR-155 transcription through the NF-kappaB pathway. *Nucleic Acids Res,* 36**,** 6608-19.

GERALDO, M. V., YAMASHITA, A. S. & KIMURA, E. T. 2012. MicroRNA miR-146b-5p regulates signal transduction of TGF-beta by repressing SMAD4 in thyroid cancer. *Oncogene,* 31**,** 1910-22.

GERIN, I., BOMMER, G. T., MCCOIN, C. S., SOUSA, K. M., KRISHNAN, V. & MACDOUGALD, O. A. 2010. Roles for miRNA-378/378* in adipocyte gene expression and lipogenesis. *Am J Physiol Endocrinol Metab,* 299**,** E198-206.

GHANI, S., RIEMKE, P., SCHONHEIT, J., LENZE, D., STUMM, J., HOOGENKAMP, M., LAGENDIJK, A., HEINZ, S., BONIFER, C., BAKKERS, J., ABDELILAH-SEYFRIED, S., HUMMEL, M. & ROSENBAUER, F. 2011. Macrophage development from HSCs requires PU.1-coordinated microRNA expression. *Blood,* 118**,** 2275-84.

GOCHEVA, V., WANG, H. W., GADEA, B. B., SHREE, T., HUNTER, K. E., GARFALL, A. L., BERMAN, T. & JOYCE, J. A. 2010. IL-4 induces cathepsin protease activity in tumor-associated macrophages to promote cancer growth and invasion. *Genes Dev,* 24**,** 241-55.

GOENKA, S. & KAPLAN, M. H. 2011. Transcriptional regulation by STAT6. *Immunol Res,* 50**,** 87-96.

GOKHALE, S. A. & GADGIL, C. J. 2012. Analysis of miRNA regulation suggests an explanation for 'unexpected' increase in target protein levels. *Mol Biosyst,* 8**,** 760-5.

GOMEZ PERDIGUERO, E., KLAPPROTH, K., SCHULZ, C., BUSCH, K., AZZONI, E., CROZET, L., GARNER, H., TROUILLET, C., DE BRUIJN, M. F., GEISSMANN, F. & RODEWALD, H. R. 2015. Tissue-resident macrophages originate from yolk-sac-derived erythro-myeloid progenitors. *Nature,* 518**,** 547-51.

GORDON, S. 2003. Alternative activation of macrophages. *Nat Rev Immunol,* 3**,** 23-35.

GORDON, S. 2007. The macrophage: past, present and future. *Eur J Immunol,* 37 Suppl 1**,** S9-17.

GORDON, S. & MARTINEZ, F. O. 2010. Alternative activation of macrophages: mechanism and functions. *Immunity,* 32**,** 593-604.

GRAFF, J. W., DICKSON, A. M., CLAY, G., MCCAFFREY, A. P. & WILSON, M. E. 2012a. Identifying functional microRNAs in macrophages with polarized phenotypes. *Journal of Biological Chemistry,* 287**,** 21816-25.

GRAFF, J. W., DICKSON, A. M., CLAY, G., MCCAFFREY, A. P. & WILSON, M. E. 2012b. Identifying functional microRNAs in macrophages with polarized phenotypes. *J Biol Chem,* 287**,** 21816-25.

GRAHAM, A. L., ALLEN, J. E. & READ, A. F. 2005a. Evolutionary causes and consequences of immunopathology. *Annual Review of Ecology Evolution and Systematics,* 36**,** 373-397.

GRAHAM, A. L., TAYLOR, M. D., LE GOFF, L., LAMB, T. J., MAGENNIS, M. & ALLEN, J. E. 2005b. Quantitative appraisal of murine filariasis confirms host strain differences but reveals that BALB/c females are more susceptible than males to Litomosoides sigmodontis. *Microbes Infect,* 7**,** 612-8.

GREGORY, R. I., YAN, K. P., AMUTHAN, G., CHENDRIMADA, T., DORATOTAJ, B., COOCH, N. & SHIEKHATTAR, R. 2004. The Microprocessor complex mediates the genesis of microRNAs. *Nature,* 432**,** 235-40.

GRIFFITHS-JONES, S., SAINI, H. K., VAN DONGEN, S. & ENRIGHT, A. J. 2008. miRBase: tools for microRNA genomics. *Nucleic Acids Res,* 36**,** D154-8.

GRIMSON, A., FARH, K. K., JOHNSTON, W. K., GARRETT-ENGELE, P., LIM, L. P. & BARTEL, D. P. 2007. MicroRNA targeting specificity in mammals: determinants beyond seed pairing. *Mol Cell,* 27**,** 91-105.

GRISHOK, A., PASQUINELLI, A. E., CONTE, D., LI, N., PARRISH, S., HA, I., BAILLIE, D. L., FIRE, A., RUVKUN, G. & MELLO, C. C. 2001. Genes and mechanisms related to RNA interference regulate expression of the small temporal RNAs that control C. elegans developmental timing. *Cell,* 106**,** 23-34.

GUAL, P., LE MARCHAND-BRUSTEL, Y. & TANTI, J. F. 2005. Positive and negative regulation of insulin signaling through IRS-1 phosphorylation. *Biochimie,* 87**,** 99-109.

GUILLIAMS, M., DE KLEER, I., HENRI, S., POST, S., VANHOUTTE, L., DE PRIJCK, S., DESWARTE, K., MALISSEN, B., HAMMAD, H. & LAMBRECHT, B. N. 2013. Alveolar macrophages develop from fetal monocytes that differentiate into long-lived cells in the first week of life via GM-CSF. *J Exp Med,* 210**,** 1977-92.

GUNDRA, U. M., GIRGIS, N. M., RUCKERL, D., JENKINS, S., WARD, L. N., KURTZ, Z. D., WIENS, K. E., TANG, M. S., BASU-ROY, U., MANSUKHANI, A., ALLEN, J. E. & LOKE, P. 2014. Alternatively activated macrophages derived from monocytes and tissue macrophages are phenotypically and functionally distinct. *Blood,* 123**,** e110-22.

GUNTHNER, R. & ANDERS, H. J. 2013. Interferon-regulatory factors determine macrophage phenotype polarization. *Mediators Inflamm,* 2013**,** 731023.

GUO, H., INGOLIA, N. T., WEISSMAN, J. S. & BARTEL, D. P. 2010. Mammalian microRNAs predominantly act to decrease target mRNA levels. *Nature,* 466**,** 835-40.

HA, M. & KIM, V. N. 2014. Regulation of microRNA biogenesis. *Nat Rev Mol Cell Biol,* 15**,** 509-24.

HAASE, A. D., JASKIEWICZ, L., ZHANG, H., LAINE, S., SACK, R., GATIGNOL, A. & FILIPOWICZ, W. 2005. TRBP, a regulator of cellular PKR and HIV-1 virus expression, interacts with Dicer and functions in RNA silencing. *EMBO Rep,* 6**,** 961-7.

HAGHIKIA, A., MISSOL-KOLKA, E., TSIKAS, D., VENTURINI, L., BRUNDIERS, S., CASTOLDI, M., MUCKENTHALER, M. U., EDER, M., STAPEL, B., THUM, T., HAGHIKIA, A., PETRASCH-PARWEZ, E., DREXLER, H., HILFIKER-KLEINER, D. & SCHERR, M. 2011. Signal transducer and activator of transcription 3-mediated regulation of

miR-199a-5p links cardiomyocyte and endothelial cell function in the heart: a key role for ubiquitin-conjugating enzymes. *Eur Heart J,* 32**,** 1287-97.

HAN, J., LEE, Y., YEOM, K. H., KIM, Y. K., JIN, H. & KIM, V. N. 2004. The Drosha-DGCR8 complex in primary microRNA processing. *Genes Dev,* 18**,** 3016-27.

HANSEN, T. B., JENSEN, T. I., CLAUSEN, B. H., BRAMSEN, J. B., FINSEN, B., DAMGAARD, C. K. & KJEMS, J. 2013. Natural RNA circles function as efficient microRNA sponges. *Nature,* 495**,** 384-8.

HASHEMI GHEINANI, A., BURKHARD, F. C., REHRAUER, H., AQUINO FOURNIER, C. & MONASTYRSKAYA, K. 2015. MicroRNA MiR-199a-5p regulates smooth muscle cell proliferation and morphology by targeting WNT2 signaling pathway. *J Biol Chem,* 290**,** 7067-86.

HASHIMOTO, D., CHOW, A., NOIZAT, C., TEO, P., BEASLEY, M. B., LEBOEUF, M., BECKER, C. D., SEE, P., PRICE, J., LUCAS, D., GRETER, M., MORTHA, A., BOYER, S. W., FORSBERG, E. C., TANAKA, M., VAN ROOIJEN, N., GARCIA-SASTRE, A., STANLEY, E. R., GINHOUX, F., FRENETTE, P. S. & MERAD, M. 2013. Tissue-resident macrophages self-maintain locally throughout adult life with minimal contribution from circulating monocytes. *Immunity,* 38**,** 792-804.

HASKO, G. & CRONSTEIN, B. 2013. Regulation of inflammation by adenosine. *Front Immunol,* 4**,** 85.

HAUSSER, J., SYED, A. P., BILEN, B. & ZAVOLAN, M. 2013. Analysis of CDS-located miRNA target sites suggests that they can effectively inhibit translation. *Genome Res,* 23**,** 604-15.

HAUSSER, J. & ZAVOLAN, M. 2014. Identification and consequences of miRNA-target interactions--beyond repression of gene expression. *Nat Rev Genet,* 15**,** 599-612.

HAYES, J., PERUZZI, P. P. & LAWLER, S. 2014. MicroRNAs in cancer: biomarkers, functions and therapy. *Trends Mol Med,* 20**,** 460-9.

HE, L., HE, X., LIM, L. P., DE STANCHINA, E., XUAN, Z., LIANG, Y., XUE, W., ZENDER, L., MAGNUS, J., RIDZON, D., JACKSON, A. L., LINSLEY, P. S., CHEN, C., LOWE, S. W., CLEARY, M. A. & HANNON, G. J. 2007. A microRNA component of the p53 tumour suppressor network. *Nature,* 447**,** 1130-4.

HE, X., JING, Z. & CHENG, G. 2014a. MicroRNAs: new regulators of Toll-like receptor signalling pathways. *Biomed Res Int,* 2014**,** 945169.

HE, X. J., MA, Y. Y., YU, S., JIANG, X. T., LU, Y. D., TAO, L., WANG, H. P., HU, Z. M. & TAO, H. Q. 2014b. Up-regulated miR-199a-5p in gastric cancer functions as an oncogene and targets klotho. *BMC Cancer,* 14**,** 218.

HE, Y., SUN, X., HUANG, C., LONG, X. R., LIN, X., ZHANG, L., LV, X. W. & LI, J. 2014c. MiR-146a regulates IL-6 production in lipopolysaccharide-induced RAW264.7 macrophage cells by inhibiting Notch1. *Inflammation,* 37**,** 71-82.

HELLER, N. M., QI, X., JUNTTILA, I. S., SHIREY, K. A., VOGEL, S. N., PAUL, W. E. & KEEGAN, A. D. 2008. Type I IL-4Rs selectively activate IRS-2 to induce target gene expression in macrophages. *Sci Signal,* 1**,** ra17.

HELWAK, A., KUDLA, G., DUDNAKOVA, T. & TOLLERVEY, D. 2013. Mapping the human miRNA interactome by CLASH reveals frequent noncanonical binding. *Cell,* 153**,** 654-65.

HELWAK, A. & TOLLERVEY, D. 2014. Mapping the miRNA interactome by cross-linking ligation and sequencing of hybrids (CLASH). *Nat Protoc,* 9**,** 711-28.

HERBERT, D. R., HOLSCHER, C., MOHRS, M., ARENDSE, B., SCHWEGMANN, A., RADWANSKA, M., LEETO, M., KIRSCH, R., HALL, P., MOSSMANN, H., CLAUSSEN, B., FORSTER, I. & BROMBACHER, F. 2004. Alternative macrophage activation is essential for survival during schistosomiasis and downmodulates T helper 1 responses and immunopathology. *Immunity,* 20**,** 623-35.

HESSE, M., MODOLELL, M., LA FLAMME, A. C., SCHITO, M., FUENTES, J. M., CHEEVER, A. W., PEARCE, E. J. & WYNN, T. A. 2001. Differential regulation of nitric oxide synthase-2 and arginase-1 by type 1/type 2 cytokines in vivo: granulomatous pathology is shaped by the pattern of L-arginine metabolism. *J Immunol,* 167**,** 6533-44.

HIGASHI, Y., SHAI, S. Y., SUKHANOV, S., KIM, C. & DELAFONTAINE, P. 2011. Monocyte/Macrophage Specific Knockout of Insulin-like Growth Factor-1 Receptor Promotes Atherosclerosis and Induces an Unstable Plaque Phenotype. *Circulation,* 124.

HOCK, H., HAMBLEN, M. J., ROOKE, H. M., TRAVER, D., BRONSON, R. T., CAMERON, S. & ORKIN, S. H. 2003. Intrinsic requirement for zinc finger transcription factor Gfi-1 in neutrophil differentiation. *Immunity,* 18**,** 109-20.

HOFFMANN, W., PETIT, G., SCHULZ-KEY, H., TAYLOR, D., BAIN, O. & LE GOFF, L. 2000. Litomosoides sigmodontis in mice: reappraisal of an old model for filarial research. *Parasitol Today,* 16**,** 387-9.

HOLCOMB, I. N., KABAKOFF, R. C., CHAN, B., BAKER, T. W., GURNEY, A., HENZEL, W., NELSON, C., LOWMAN, H. B., WRIGHT, B. D., SKELTON, N. J., FRANTZ, G. D., TUMAS, D. B., PEALE, F. V., JR., SHELTON, D. L. & HEBERT, C. C. 2000. FIZZ1, a novel cysteine-rich secreted protein associated with pulmonary inflammation, defines a new gene family. *EMBO J,* 19**,** 4046-55.

HON, L. S. & ZHANG, Z. 2007. The roles of binding site arrangement and combinatorial targeting in microRNA repression of gene expression. *Genome Biol,* 8**,** R166.

HOTEZ, P. J., BRINDLEY, P. J., BETHONY, J. M., KING, C. H., PEARCE, E. J. & JACOBSON, J. 2008. Helminth infections: the great neglected tropical diseases. *J Clin Invest,* 118**,** 1311-21.

HOU, J., LIN, L., ZHOU, W., WANG, Z., DING, G., DONG, Q., QIN, L., WU, X., ZHENG, Y., YANG, Y., TIAN, W., ZHANG, Q., WANG, C., ZHANG, Q., ZHUANG, S. M., ZHENG, L., LIANG, A., TAO, W. & CAO, X. 2011. Identification of miRNomes in human liver and hepatocellular carcinoma reveals miR-199a/b-3p as therapeutic target for hepatocellular carcinoma. *Cancer Cell,* 19**,** 232-43.

HOU, J., SCHINDLER, U., HENZEL, W. J., HO, T. C., BRASSEUR, M. & MCKNIGHT, S. L. 1994. An interleukin-4-induced transcription factor: IL-4 Stat. *Science,* 265**,** 1701-6.

HOU, J., WANG, P., LIN, L., LIU, X., MA, F., AN, H., WANG, Z. & CAO, X. 2009. MicroRNA-146a feedback inhibits RIG-I-dependent Type I IFN production in macrophages by targeting TRAF6, IRAK1, and IRAK2. *J Immunol,* 183**,** 2150-8.

HOY, A. M., LUNDIE, R. J., IVENS, A., QUINTANA, J. F., NAUSCH, N., FORSTER, T., JONES, F., KABATEREINE, N. B., DUNNE, D. W., MUTAPI, F., MACDONALD, A. S. & BUCK, A. H. 2014. Parasite-derived microRNAs in host serum as novel biomarkers of helminth infection. *PLoS Negl Trop Dis,* 8**,** e2701.

HU, X., CHAKRAVARTY, S. D. & IVASHKIV, L. B. 2008. Regulation of interferon and Toll-like receptor signaling during macrophage activation by opposing feedforward and feedback inhibition mechanisms. *Immunol Rev,* 226**,** 41-56.

HUA, Z., LV, Q., YE, W., WONG, C. K., CAI, G., GU, D., JI, Y., ZHAO, C., WANG, J., YANG, B. B. & ZHANG, Y. 2006. MiRNA-directed regulation of VEGF and other angiogenic factors under hypoxia. *PLoS One,* 1**,** e116.

HUANG, Y., LIU, X. & WANG, Y. 2015. MicroRNA-378 regulates neural stem cell proliferation and differentiation in vitro by modulating Tailless expression. *Biochem Biophys Res Commun,* 466**,** 214-20.

HUAT, T. J., KHAN, A. A., PATI, S., MUSTAFA, Z., ABDULLAH, J. M. & JAAFAR, H. 2014. IGF-1 enhances cell proliferation and survival during early differentiation of mesenchymal stem cells to neural progenitor-like cells. *BMC Neurosci,* 15**,** 91.

HUBER, S., HOFFMANN, R., MUSKENS, F. & VOEHRINGER, D. 2010. Alternatively activated macrophages inhibit T-cell proliferation by Stat6-dependent expression of PD-L2. *Blood,* 116**,** 3311-20.

HUBNER, M. P., TORRERO, M. N., MCCALL, J. W. & MITRE, E. 2009. Litomosoides sigmodontis: a simple method to infect mice with L3 larvae obtained from the pleural space of recently infected jirds (Meriones unguiculatus). *Exp Parasitol,* 123**,** 95-8.

HUME, D. A. & MACDONALD, K. P. 2012. Therapeutic applications of macrophage colony-stimulating factor-1 (CSF-1) and antagonists of CSF-1 receptor (CSF-1R) signaling. *Blood,* 119**,** 1810-20.

HUME, D. A., PAVLI, P., DONAHUE, R. E. & FIDLER, I. J. 1988. The effect of human recombinant macrophage colony-stimulating factor (CSF-1) on the murine mononuclear phagocyte system in vivo. *J Immunol,* 141**,** 3405-9.

HUMPHREYS, D. T., WESTMAN, B. J., MARTIN, D. I. & PREISS, T. 2005. MicroRNAs control translation initiation by inhibiting eukaryotic initiation factor 4E/cap and poly(A) tail function. *Proc Natl Acad Sci U S A,* 102**,** 16961-6.

HUNG, S. I., CHANG, A. C., KATO, I. & CHANG, N. C. 2002. Transient expression of Ym1, a heparin-binding lectin, during developmental hematopoiesis and inflammation. *J Leukoc Biol,* 72**,** 72-82.

HUNTZINGER, E. & IZAURRALDE, E. 2011. Gene silencing by microRNAs: contributions of translational repression and mRNA decay. *Nat Rev Genet,* 12**,** 99-110.

HUTVAGNER, G., MCLACHLAN, J., PASQUINELLI, A. E., BALINT, E., TUSCHL, T. & ZAMORE, P. D. 2001. A cellular function for the RNA-interference enzyme Dicer in the maturation of the let-7 small temporal RNA. *Science,* 293**,** 834-8.

HUTVAGNER, G. & SIMARD, M. J. 2008. Argonaute proteins: key players in RNA silencing. *Nat Rev Mol Cell Biol,* 9**,** 22-32.

HWANG, H. W. & MENDELL, J. T. 2006. MicroRNAs in cell proliferation, cell death, and tumorigenesis. *Br J Cancer,* 94**,** 776-80.

IGARASHI, K. & KASHIWAGI, K. 2000. Polyamines: mysterious modulators of cellular functions. *Biochem Biophys Res Commun,* 271**,** 559-64.

ISHII, M., WEN, H., CORSA, C. A., LIU, T., COELHO, A. L., ALLEN, R. M., CARSON, W. F. T., CAVASSANI, K. A., LI, X., LUKACS, N. W., HOGABOAM, C. M., DOU, Y. & KUNKEL, S. L. 2009. Epigenetic regulation of the alternatively activated macrophage phenotype. *Blood,* 114**,** 3244-54.

IWAMA, A., YAMAGUCHI, N. & SUDA, T. 1996. STK/RON receptor tyrosine kinase mediates both apoptotic and growth signals via the multifunctional docking site conserved among the HGF receptor family. *EMBO J,* 15**,** 5866-75.

JACKSON, A. L. & LINSLEY, P. S. 2010. Recognizing and avoiding siRNA off-target effects for target identification and therapeutic application. *Nat Rev Drug Discov,* 9**,** 57-67.

JACKSON, R. J. & STANDART, N. 2007. How do microRNAs regulate gene expression? *Sci STKE,* 2007**,** re1.

JANSSEN, H. L., REESINK, H. W., LAWITZ, E. J., ZEUZEM, S., RODRIGUEZ-TORRES, M., PATEL, K., VAN DER MEER, A. J., PATICK, A. K., CHEN, A., ZHOU, Y., PERSSON, R., KING, B. D., KAUPPINEN, S., LEVIN, A. A. & HODGES, M. R. 2013. Treatment of HCV infection by targeting microRNA. *N Engl J Med,* 368**,** 1685-94.

JANSSON, M. D. & LUND, A. H. 2012. MicroRNA and cancer. *Mol Oncol,* 6**,** 590-610.

JENKINS, S. J. & ALLEN, J. E. 2010. Similarity and diversity in macrophage activation by nematodes, trematodes, and cestodes. *J Biomed Biotechnol,* 2010**,** 262609.

JENKINS, S. J., RUCKERL, D., COOK, P. C., JONES, L. H., FINKELMAN, F. D., VAN ROOIJEN, N., MACDONALD, A. S. & ALLEN, J. E. 2011. Local macrophage proliferation, rather than recruitment from the blood, is a signature of TH2 inflammation. *Science,* 332**,** 1284-8.

JENKINS, S. J., RUCKERL, D., THOMAS, G. D., HEWITSON, J. P., DUNCAN, S., BROMBACHER, F., MAIZELS, R. M., HUME, D. A. & ALLEN, J. E. 2013. IL-4 directly signals tissue-resident macrophages to proliferate beyond homeostatic levels controlled by CSF-1. *J Exp Med,* 210**,** 2477-91.

JENS, M. & RAJEWSKY, N. 2015. Competition between target sites of regulators shapes post-transcriptional gene regulation. *Nat Rev Genet,* 16**,** 113-26.

JIANG, H., HARRIS, M. B. & ROTHMAN, P. 2000. IL-4/IL-13 signaling beyond JAK/STAT. *J Allergy Clin Immunol,* 105**,** 1063-70.

JIN, H. M., COPELAND, N. G., GILBERT, D. J., JENKINS, N. A., KIRKPATRICK, R. B. & ROSENBERG, M. 1998. Genetic characterization of the murine Ym1 gene and identification of a cluster of highly homologous genes. *Genomics,* 54**,** 316-22.

JINDRA, P. T., BAGLEY, J., GODWIN, J. G. & IACOMINI, J. 2010. Costimulation-dependent expression of microRNA-214 increases the ability of T cells to proliferate by targeting Pten. *J Immunol,* 185**,** 990-7.

JINEK, M. & DOUDNA, J. A. 2009. A three-dimensional view of the molecular machinery of RNA interference. *Nature,* 457**,** 405-12.

JOHNNIDIS, J. B., HARRIS, M. H., WHEELER, R. T., STEHLING-SUN, S., LAM, M. H., KIRAK, O., BRUMMELKAMP, T. R., FLEMING, M. D. & CAMARGO, F. D. 2008. Regulation of progenitor cell proliferation and granulocyte function by microRNA-223. *Nature,* 451**,** 1125-9.

JOSEFOWICZ, S. Z., LU, L. F. & RUDENSKY, A. Y. 2012. Regulatory T cells: mechanisms of differentiation and function. *Annu Rev Immunol,* 30**,** 531-64.

KAIKO, G. E., HORVAT, J. C., BEAGLEY, K. W. & HANSBRO, P. M. 2008. Immunological decision-making: how does the immune system decide to mount a helper T-cell response? *Immunology,* 123**,** 326-38.

KANG, K., REILLY, S. M., KARABACAK, V., GANGL, M. R., FITZGERALD, K., HATANO, B. & LEE, C. H. 2008. Adipocyte-derived Th2 cytokines and myeloid PPARdelta regulate macrophage polarization and insulin sensitivity. *Cell Metab,* 7**,** 485-95.

KAPP, L. D. & LORSCH, J. R. 2004. The molecular mechanics of eukaryotic translation. *Annu Rev Biochem,* 73**,** 657-704.

KARGINOV, F. V., CHELOUFI, S., CHONG, M. M., STARK, A., SMITH, A. D. & HANNON, G. J. 2010. Diverse endonucleolytic cleavage sites in the mammalian transcriptome depend upon microRNAs, Drosha, and additional nucleases. *Mol Cell,* 38**,** 781-8.

KATAKOWSKI, M., BULLER, B., ZHENG, X., LU, Y., ROGERS, T., OSOBAMIRO, O., SHU, W., JIANG, F. & CHOPP, M. 2013. Exosomes from marrow stromal cells expressing miR-146b inhibit glioma growth. *Cancer Lett,* 335**,** 201-4.

KATAKOWSKI, M., ZHENG, X., JIANG, F., ROGERS, T., SZALAD, A. & CHOPP, M. 2010. MiR-146b-5p suppresses EGFR expression and reduces in vitro migration and invasion of glioma. *Cancer Invest,* 28**,** 1024-30.

KEDDE, M. & AGAMI, R. 2008. Interplay between microRNAs and RNA-binding proteins determines developmental processes. *Cell Cycle,* 7**,** 899-903.

KETTING, R. F., FISCHER, S. E., BERNSTEIN, E., SIJEN, T., HANNON, G. J. & PLASTERK, R. H. 2001. Dicer functions in RNA interference and in synthesis of small RNA involved in developmental timing in C. elegans. *Genes Dev,* 15**,** 2654-9.

KHAN, A. A., BETEL, D., MILLER, M. L., SANDER, C., LESLIE, C. S. & MARKS, D. S. 2009. Transfection of small RNAs globally perturbs gene regulation by endogenous microRNAs. *Nat Biotechnol,* 27**,** 549-55.

KHVOROVA, A., REYNOLDS, A. & JAYASENA, S. D. 2003. Functional siRNAs and miRNAs exhibit strand bias. *Cell,* 115**,** 209-16.

KIDD, P. 2003. Th1/Th2 balance: the hypothesis, its limitations, and implications for health and disease. *Altern Med Rev,* 8**,** 223-46.

KIM, B. K., YOO, H. I., KIM, I., PARK, J. & KIM YOON, S. 2015. FZD6 expression is negatively regulated by miR-199a-5p in human colorectal cancer. *BMB Rep,* 48**,** 360-6.

KIM, S. W., RAMASAMY, K., BOUAMAR, H., LIN, A. P., JIANG, D. & AGUIAR, R. C. 2012. MicroRNAs miR-125a and miR-125b constitutively activate the NF-kappaB pathway by targeting the tumor necrosis factor alpha-induced protein 3 (TNFAIP3, A20). *Proc Natl Acad Sci U S A,* 109**,** 7865-70.

KLUSMANN, J. H., LI, Z., BOHMER, K., MAROZ, A., KOCH, M. L., EMMRICH, S., GODINHO, F. J., ORKIN, S. H. & REINHARDT, D. 2010. miR-125b-2 is a potential oncomir on human chromosome 21 in megakaryoblastic leukemia. *Genes Dev,* 24**,** 478-90.

KNIPPER, J. A., WILLENBORG, S., BRINCKMANN, J., BLOCH, W., MAASS, T., WAGENER, R., KRIEG, T., SUTHERLAND, T., MUNITZ, A., ROTHENBERG, M. E., NIEHOFF, A., RICHARDSON, R., HAMMERSCHMIDT, M., ALLEN, J. E. & EMING, S. A. 2015. Interleukin-4 Receptor alpha Signaling in Myeloid Cells Controls Collagen Fibril Assembly in Skin Repair. *Immunity,* 43**,** 803-16.

KOBAYASHI, K., SAKURAI, K., HIRAMATSU, H., INADA, K., SHIOGAMA, K., NAKAMURA, S., SUEMASA, F., KOBAYASHI, K., IMOTO, S., HARAGUCHI, T., ITO, H., ISHIZAKA, A., TSUTSUMI, Y. & IBA, H. 2015. The miR-199a/Brm/EGR1 axis is a determinant of anchorage-independent growth in epithelial tumor cell lines. *Sci Rep,* 5**,** 8428.

KONIG, J., ZARNACK, K., LUSCOMBE, N. M. & ULE, J. 2011. Protein-RNA interactions: new genomic technologies and perspectives. *Nat Rev Genet,* 13**,** 77-83.

KORALOV, S. B., MULJO, S. A., GALLER, G. R., KREK, A., CHAKRABORTY, T., KANELLOPOULOU, C., JENSEN, K., COBB, B. S., MERKENSCHLAGER, M., RAJEWSKY, N. & RAJEWSKY, K. 2008. Dicer ablation affects antibody diversity and cell survival in the B lymphocyte lineage. *Cell,* 132**,** 860-74.

KORN, T., BETTELLI, E., OUKKA, M. & KUCHROO, V. K. 2009. IL-17 and Th17 Cells. *Annu Rev Immunol,* 27**,** 485-517.

KOZOMARA, A. & GRIFFITHS-JONES, S. 2011. miRBase: integrating microRNA annotation and deep-sequencing data. *Nucleic Acids Res,* 39**,** D152-7.

KOZOMARA, A. & GRIFFITHS-JONES, S. 2014. miRBase: annotating high confidence microRNAs using deep sequencing data. *Nucleic Acids Res,* 42**,** D68-73.

KREK, A., GRUN, D., POY, M. N., WOLF, R., ROSENBERG, L., EPSTEIN, E. J., MACMENAMIN, P., DA PIEDADE, I., GUNSALUS, K. C., STOFFEL, M. & RAJEWSKY, N. 2005. Combinatorial microRNA target predictions. *Nat Genet,* 37**,** 495-500.

KUEHBACHER, A., URBICH, C., ZEIHER, A. M. & DIMMELER, S. 2007. Role of Dicer and Drosha for endothelial microRNA expression and angiogenesis. *Circ Res,* 101**,** 59-68.

KULYTE, A., LORENTE-CEBRIAN, S., GAO, H., MEJHERT, N., AGUSTSSON, T., ARNER, P., RYDEN, M. & DAHLMAN, I. 2014. MicroRNA profiling links miR-378 to enhanced adipocyte lipolysis in human cancer cachexia. *Am J Physiol Endocrinol Metab,* 306**,** E267-74.

KUROWSKA-STOLARSKA, M., ALIVERNINI, S., BALLANTINE, L. E., ASQUITH, D. L., MILLAR, N. L., GILCHRIST, D. S., REILLY, J., IERNA, M., FRASER, A. R., STOLARSKI, B., MCSHARRY, C., HUEBER, A. J., BAXTER, D., HUNTER, J., GAY, S., LIEW, F. Y. & MCINNES, I. B. 2011. MicroRNA-155 as a proinflammatory regulator in clinical and experimental arthritis. *Proc Natl Acad Sci U S A,* 108**,** 11193-8.

KUROWSKA-STOLARSKA, M., STOLARSKI, B., KEWIN, P., MURPHY, G., CORRIGAN, C. J., YING, S., PITMAN, N., MIRCHANDANI, A., RANA, B., VAN ROOIJEN, N., SHEPHERD, M., MCSHARRY, C., MCINNES, I. B., XU, D. & LIEW, F. Y. 2009. IL-33 Amplifies the Polarization of Alternatively Activated Macrophages That Contribute to Airway Inflammation. *Journal of Immunology,* 183**,** 6469-6477.

KUTTY, R. K., NAGINENI, C. N., SAMUEL, W., VIJAYASARATHY, C., JAWORSKI, C., DUNCAN, T., CAMERON, J. E., FLEMINGTON, E. K., HOOKS, J. J. & REDMOND, T. M. 2013. Differential regulation of microRNA-146a and microRNA-146b-5p in human retinal pigment epithelial cells by interleukin-1beta, tumor necrosis factor-alpha, and interferon-gamma. *Mol Vis,* 19**,** 737-50.

KUZUOGLU-OZTURK, D., HUNTZINGER, E., SCHMIDT, S. & IZAURRALDE, E. 2012. The Caenorhabditis elegans GW182 protein AIN-1 interacts with PAB-1 and subunits of the PAN2-PAN3 and CCR4-NOT deadenylase complexes. *Nucleic Acids Res,* 40**,** 5651-65.

LABBAYE, C. & TESTA, U. 2012. The emerging role of MIR-146A in the control of hematopoiesis, immune function and cancer. *J Hematol Oncol,* 5**,** 13.

LAMAGNA, C., AURRAND-LIONS, M. & IMHOF, B. A. 2006. Dual role of macrophages in tumor growth and angiogenesis. *J Leukoc Biol,* 80**,** 705-13.

LANDTHALER, M., YALCIN, A. & TUSCHL, T. 2004. The human DiGeorge syndrome critical region gene 8 and Its D. melanogaster homolog are required for miRNA biogenesis. *Curr Biol,* 14**,** 2162-7.

LANGRISH, C. L., CHEN, Y., BLUMENSCHEIN, W. M., MATTSON, J., BASHAM, B., SEDGWICK, J. D., MCCLANAHAN, T., KASTELEIN, R. A. & CUA, D. J. 2005. IL-23

drives a pathogenic T cell population that induces autoimmune inflammation. *J Exp Med,* 201**,** 233-40.

LAVIOLA, L., NATALICCHIO, A. & GIORGINO, F. 2007. The IGF-I signaling pathway. *Current Pharmaceutical Design,* 13**,** 663-669.

LAWRENCE, T. 2009. The nuclear factor NF-kappaB pathway in inflammation. *Cold Spring Harb Perspect Biol,* 1**,** a001651.

LE GOFF, L., LAMB, T. J., GRAHAM, A. L., HARCUS, Y. & ALLEN, J. E. 2002. IL-4 is required to prevent filarial nematode development in resistant but not susceptible strains of mice. *Int J Parasitol,* 32**,** 1277-84.

LEE, D. Y., DENG, Z., WANG, C. H. & YANG, B. B. 2007. MicroRNA-378 promotes cell survival, tumor growth, and angiogenesis by targeting SuFu and Fus-1 expression. *Proc Natl Acad Sci U S A,* 104**,** 20350-5.

LEE, I., AJAY, S. S., YOOK, J. I., KIM, H. S., HONG, S. H., KIM, N. H., DHANASEKARAN, S. M., CHINNAIYAN, A. M. & ATHEY, B. D. 2009. New class of microRNA targets containing simultaneous 5'-UTR and 3'-UTR interaction sites. *Genome Res,* 19**,** 1175-83.

LEE, R. C., FEINBAUM, R. L. & AMBROS, V. 1993. The C. elegans heterochronic gene lin-4 encodes small RNAs with antisense complementarity to lin-14. *Cell,* 75**,** 843-54.

LEE, Y., AHN, C., HAN, J., CHOI, H., KIM, J., YIM, J., LEE, J., PROVOST, P., RADMARK, O., KIM, S. & KIM, V. N. 2003. The nuclear RNase III Drosha initiates microRNA processing. *Nature,* 425**,** 415-9.

LEE, Y., HUR, I., PARK, S. Y., KIM, Y. K., SUH, M. R. & KIM, V. N. 2006. The role of PACT in the RNA silencing pathway. *EMBO J,* 25**,** 522-32.

LEE, Y., KIM, M., HAN, J., YEOM, K. H., LEE, S., BAEK, S. H. & KIM, V. N. 2004. MicroRNA genes are transcribed by RNA polymerase II. *EMBO J,* 23**,** 4051-60.

LEE, Y. S. & DUTTA, A. 2009. MicroRNAs in cancer. *Annu Rev Pathol,* 4**,** 199-227.

LEYVA, F. J., ANZINGER, J. J., MCCOY, J. P., JR. & KRUTH, H. S. 2011. Evaluation of transduction efficiency in macrophage colony-stimulating factor differentiated human macrophages using HIV-1 based lentiviral vectors. *BMC Biotechnol,* 11**,** 13.

LI, D., FERNANDEZ, L. G., DODD-O, J., LANGER, J., WANG, D. & LAUBACH, V. E. 2005. Upregulation of hypoxia-induced mitogenic factor in compensatory lung growth after pneumonectomy. *Am J Respir Cell Mol Biol,* 32**,** 185-91.

LI, J., KIM, T., NUTIU, R., RAY, D., HUGHES, T. R. & ZHANG, Z. 2014. Identifying mRNA sequence elements for target recognition by human Argonaute proteins. *Genome Res,* 24**,** 775-85.

LI, Q. J., CHAU, J., EBERT, P. J., SYLVESTER, G., MIN, H., LIU, G., BRAICH, R., MANOHARAN, M., SOUTSCHEK, J., SKARE, P., KLEIN, L. O., DAVIS, M. M. &

CHEN, C. Z. 2007. miR-181a is an intrinsic modulator of T cell sensitivity and selection. *Cell,* 129**,** 147-61.

LI, Z., LU, J., SUN, M., MI, S., ZHANG, H., LUO, R. T., CHEN, P., WANG, Y., YAN, M., QIAN, Z., NEILLY, M. B., JIN, J., ZHANG, Y., BOHLANDER, S. K., ZHANG, D. E., LARSON, R. A., LE BEAU, M. M., THIRMAN, M. J., GOLUB, T. R., ROWLEY, J. D. & CHEN, J. 2008. Distinct microRNA expression profiles in acute myeloid leukemia with common translocations. *Proc Natl Acad Sci U S A,* 105**,** 15535-40.

LIAN, J. B., STEIN, G. S., VAN WIJNEN, A. J., STEIN, J. L., HASSAN, M. Q., GAUR, T. & ZHANG, Y. 2012. MicroRNA control of bone formation and homeostasis. *Nat Rev Endocrinol,* 8**,** 212-27.

LICATALOSI, D. D., MELE, A., FAK, J. J., ULE, J., KAYIKCI, M., CHI, S. W., CLARK, T. A., SCHWEITZER, A. C., BLUME, J. E., WANG, X., DARNELL, J. C. & DARNELL, R. B. 2008. HITS-CLIP yields genome-wide insights into brain alternative RNA processing. *Nature,* 456**,** 464-9.

LIM, L. P., LAU, N. C., GARRETT-ENGELE, P., GRIMSON, A., SCHELTER, J. M., CASTLE, J., BARTEL, D. P., LINSLEY, P. S. & JOHNSON, J. M. 2005. Microarray analysis shows that some microRNAs downregulate large numbers of target mRNAs. *Nature,* 433**,** 769-73.

LIN, H. S., GONG, J. N., SU, R., CHEN, M. T., SONG, L., SHEN, C., WANG, F., MA, Y. N., ZHAO, H. L., YU, J., LI, W. W., HUANG, L. X., XU, X. H. & ZHANG, J. W. 2014. miR-199a-5p inhibits monocyte/macrophage differentiation by targeting the activin A type 1B receptor gene and finally reducing C/EBPalpha expression. *J Leukoc Biol,* 96**,** 1023-35.

LIN, S. & GREGORY, R. I. 2015. MicroRNA biogenesis pathways in cancer. *Nat Rev Cancer,* 15**,** 321-33.

LINDSAY, M. A. 2008. microRNAs and the immune response. *Trends Immunol,* 29**,** 343-51.

LISTON, A., LU, L. F., O'CARROLL, D., TARAKHOVSKY, A. & RUDENSKY, A. Y. 2008. Dicer-dependent microRNA pathway safeguards regulatory T cell function. *J Exp Med,* 205**,** 1993-2004.

LIU, G. & ABRAHAM, E. 2013a. MicroRNAs in Immune Response and Macrophage Polarization. *Arteriosclerosis Thrombosis and Vascular Biology,* 33**,** 170-177.

LIU, G. & ABRAHAM, E. 2013b. MicroRNAs in immune response and macrophage polarization. *Arterioscler Thromb Vasc Biol,* 33**,** 170-7.

LIU, G., FRIGGERI, A., YANG, Y., PARK, Y. J., TSURUTA, Y. & ABRAHAM, E. 2009a. miR-147, a microRNA that is induced upon Toll-like receptor stimulation, regulates murine macrophage inflammatory responses. *Proc Natl Acad Sci U S A,* 106**,** 15819-24.

LIU, J., CARMELL, M. A., RIVAS, F. V., MARSDEN, C. G., THOMSON, J. M., SONG, J. J., HAMMOND, S. M., JOSHUA-TOR, L. & HANNON, G. J. 2004a. Argonaute2 is the catalytic engine of mammalian RNAi. *Science,* 305**,** 1437-41.

LIU, J., VALENCIA-SANCHEZ, M. A., HANNON, G. J. & PARKER, R. 2005. MicroRNA-dependent localization of targeted mRNAs to mammalian P-bodies. *Nat Cell Biol,* 7**,** 719-23.

LIU, J. P., BAKER, J., PERKINS, A. S., ROBERTSON, E. J. & EFSTRATIADIS, A. 1993. Mice carrying null mutations of the genes encoding insulin-like growth factor I (Igf-1) and type 1 IGF receptor (Igf1r). *Cell,* 75**,** 59-72.

LIU, Q. P., FRUIT, K., WARD, J. & CORRELL, P. H. 1999. Negative regulation of macrophage activation in response to IFN-gamma and lipopolysaccharide by the STK/RON receptor tyrosine kinase. *J Immunol,* 163**,** 6606-13.

LIU, T., DHANASEKARAN, S. M., JIN, H., HU, B., TOMLINS, S. A., CHINNAIYAN, A. M. & PHAN, S. H. 2004b. FIZZ1 stimulation of myofibroblast differentiation. *Am J Pathol,* 164**,** 1315-26.

LIU, T., HU, B., CHOI, Y. Y., CHUNG, M., ULLENBRUCH, M., YU, H., LOWE, J. B. & PHAN, S. H. 2009b. Notch1 signaling in FIZZ1 induction of myofibroblast differentiation. *Am J Pathol,* 174**,** 1745-55.

LIU, W., CAO, H., YE, C., CHANG, C., LU, M., JING, Y., ZHANG, D., YAO, X., DUAN, Z., XIA, H., WANG, Y. C., JIANG, J., LIU, M. F., YAN, J. & YING, H. 2014. Hepatic miR-378 targets p110alpha and controls glucose and lipid homeostasis by modulating hepatic insulin signalling. *Nat Commun,* 5**,** 5684.

LLAVE, C., KASSCHAU, K. D., RECTOR, M. A. & CARRINGTON, J. C. 2002. Endogenous and silencing-associated small RNAs in plants. *Plant Cell,* 14**,** 1605-19.

LOIS, C., REFAELI, Y., QIN, X. F. & VAN PARIJS, L. 2001. Retroviruses as tools to study the immune system. *Current Opinion in Immunology,* 13**,** 496-504.

LOKE, P., GALLAGHER, I., NAIR, M. G., ZANG, X., BROMBACHER, F., MOHRS, M., ALLISON, J. P. & ALLEN, J. E. 2007. Alternative activation is an innate response to injury that requires CD4+ T cells to be sustained during chronic infection. *J Immunol,* 179**,** 3926-36.

LOKE, P., NAIR, M. G., PARKINSON, J., GUILIANO, D., BLAXTER, M. & ALLEN, J. E. 2002. IL-4 dependent alternatively-activated macrophages have a distinctive in vivo gene expression phenotype. *BMC Immunol,* 3**,** 7.

LONG, E., HUYNH, H. T. & ZHAO, X. 1998. Involvement of insulin-like growth factor-1 and its binding proteins in proliferation and differentiation of murine bone marrow-derived macrophage precursors. *Endocrine,* 9**,** 185-192.

LOSMAN, J. A., CHEN, X. P., HILTON, D. & ROTHMAN, P. 1999. Cutting edge: SOCS-1 is a potent inhibitor of IL-4 signal transduction. *J Immunol,* 162**,** 3770-4.

LU, H., HUANG, D., SAEDERUP, N., CHARO, I. F., RANSOHOFF, R. M. & ZHOU, L. 2011. Macrophages recruited via CCR2 produce insulin-like growth factor-1 to repair acute skeletal muscle injury. *FASEB J,* 25**,** 358-69.

LU, L. F., BOLDIN, M. P., CHAUDHRY, A., LIN, L. L., TAGANOV, K. D., HANADA, T., YOSHIMURA, A., BALTIMORE, D. & RUDENSKY, A. Y. 2010. Function of miR-146a in controlling Treg cell-mediated regulation of Th1 responses. *Cell,* 142**,** 914-29.

LU, L. F. & LISTON, A. 2009. MicroRNA in the immune system, microRNA as an immune system. *Immunology,* 127**,** 291-8.

LUCAS, T., WAISMAN, A., RANJAN, R., ROES, J., KRIEG, T., MULLER, W., ROERS, A. & EMING, S. A. 2010. Differential roles of macrophages in diverse phases of skin repair. *J Immunol,* 184**,** 3964-77.

LUND, E., GUTTINGER, S., CALADO, A., DAHLBERG, J. E. & KUTAY, U. 2004. Nuclear export of microRNA precursors. *Science,* 303**,** 95-8.

MA, X., BECKER BUSCAGLIA, L. E., BARKER, J. R. & LI, Y. 2011. MicroRNAs in NF-kappaB signaling. *J Mol Cell Biol,* 3**,** 159-66.

MAARSINGH, H., ZAAGSMA, J. & MEURS, H. 2009. Arginase: a key enzyme in the pathophysiology of allergic asthma opening novel therapeutic perspectives. *Br J Pharmacol,* 158**,** 652-64.

MACDONALD, A. S., ARAUJO, M. I. & PEARCE, E. J. 2002. Immunology of parasitic helminth infections. *Infect Immun,* 70**,** 427-33.

MACDONALD, A. S., MAIZELS, R. M., LAWRENCE, R. A., DRANSFIELD, I. & ALLEN, J. E. 1998. Requirement for in vivo production of IL-4, but not IL-10, in the induction of proliferative suppression by filarial parasites. *J Immunol,* 160**,** 1304-12.

MACDONALD, K. P., PALMER, J. S., CRONAU, S., SEPPANEN, E., OLVER, S., RAFFELT, N. C., KUNS, R., PETTIT, A. R., CLOUSTON, A., WAINWRIGHT, B., BRANSTETTER, D., SMITH, J., PAXTON, R. J., CERRETTI, D. P., BONHAM, L., HILL, G. R. & HUME, D. A. 2010. An antibody against the colony-stimulating factor 1 receptor depletes the resident subset of monocytes and tissue- and tumor-associated macrophages but does not inhibit inflammation. *Blood,* 116**,** 3955-63.

MACMICKING, J., XIE, Q. W. & NATHAN, C. 1997. Nitric oxide and macrophage function. *Annu Rev Immunol,* 15**,** 323-50.

MADSEN, D. H., LEONARD, D., MASEDUNSKAS, A., MOYER, A., JURGENSEN, H. J., PETERS, D. E., AMORNPHIMOLTHAM, P., SELVARAJ, A., YAMADA, S. S., BRENNER, D. A., BURGDORF, S., ENGELHOLM, L. H., BEHRENDT, N., HOLMBECK, K., WEIGERT, R. & BUGGE, T. H. 2013. M2-like macrophages are responsible for collagen degradation through a mannose receptor-mediated pathway. *J Cell Biol,* 202**,** 951-66.

MALMGAARD, L. 2004. Induction and regulation of IFNs during viral infections. *J Interferon Cytokine Res,* 24**,** 439-54.

MALMGAARD, L., MELCHJORSEN, J., BOWIE, A. G., MOGENSEN, S. C. & PALUDAN, S. R. 2004. Viral activation of macrophages through TLR-dependent and -independent pathways. *J Immunol,* 173**,** 6890-8.

MANICASSAMY, S. & PULENDRAN, B. 2009. Retinoic acid-dependent regulation of immune responses by dendritic cells and macrophages. *Semin Immunol,* 21**,** 22-7.

MANTOVANI, A., BISWAS, S. K., GALDIERO, M. R., SICA, A. & LOCATI, M. 2013. Macrophage plasticity and polarization in tissue repair and remodelling. *J Pathol,* 229**,** 176-85.

MANTOVANI, A., SICA, A. & LOCATI, M. 2005. Macrophage polarization comes of age. *Immunity,* 23**,** 344-6.

MANTOVANI, A., SICA, A., SOZZANI, S., ALLAVENA, P., VECCHI, A. & LOCATI, M. 2004. The chemokine system in diverse forms of macrophage activation and polarization. *Trends Immunol,* 25**,** 677-86.

MARECHAL, P., LE GOFF, L., HOFFMAN, W., RAPP, J., OSWALD, I. P., OMBROUCK, C., TAYLOR, D. W., BAIN, O. & PETIT, G. 1997. Immune response to the filaria Litomosoides sigmodontis in susceptible and resistant mice. *Parasite Immunol,* 19**,** 273-9.

MARONEY, P. A., YU, Y., FISHER, J. & NILSEN, T. W. 2006. Evidence that microRNAs are associated with translating messenger RNAs in human cells. *Nature Structural & Molecular Biology,* 13**,** 1102-1107.

MARTIN, H. C., WANI, S., STEPTOE, A. L., KRISHNAN, K., NONES, K., NOURBAKHSH, E., VLASSOV, A., GRIMMOND, S. M. & CLOONAN, N. 2014. Imperfect centered miRNA binding sites are common and can mediate repression of target mRNAs. *Genome Biol,* 15**,** R51.

MARTINEZ, F. O. 2011. Regulators of macrophage activation. *Eur J Immunol,* 41**,** 1531-4.

MARTINEZ, F. O. & GORDON, S. 2014. The M1 and M2 paradigm of macrophage activation: time for reassessment. *F1000Prime Rep,* 6**,** 13.

MARTINEZ, F. O., HELMING, L. & GORDON, S. 2009. Alternative activation of macrophages: an immunologic functional perspective. *Annu Rev Immunol,* 27**,** 451-83.

MARTINEZ-NUNEZ, R. T., LOUAFI, F., FRIEDMANN, P. S. & SANCHEZ-ELSNER, T. 2009. MicroRNA-155 modulates the pathogen binding ability of dendritic cells (DCs) by down-regulation of DC-specific intercellular adhesion molecule-3 grabbing non-integrin (DC-SIGN). *J Biol Chem,* 284**,** 16334-42.

MATHONNET, G., FABIAN, M. R., SVITKIN, Y. V., PARSYAN, A., HUCK, L., MURATA, T., BIFFO, S., MERRICK, W. C., DARZYNKIEWICZ, E., PILLAI, R. S., FILIPOWICZ, W., DUCHAINE, T. F. & SONENBERG, N. 2007. MicroRNA inhibition of translation initiation in vitro by targeting the cap-binding complex eIF4F. *Science,* 317**,** 1764-7.

MCSORLEY, H. J. & MAIZELS, R. M. 2012. Helminth infections and host immune regulation. *Clin Microbiol Rev,* 25**,** 585-608.

MEIJER, H. A., KONG, Y. W., LU, W. T., WILCZYNSKA, A., SPRIGGS, R. V., ROBINSON, S. W., GODFREY, J. D., WILLIS, A. E. & BUSHELL, M. 2013. Translational

repression and eIF4A2 activity are critical for microRNA-mediated gene regulation. *Science,* 340**,** 82-5.

MENDOZA, N., LI, A., GILL, A. & TYRING, S. 2009. Filariasis: diagnosis and treatment. *Dermatol Ther,* 22**,** 475-90.

MIGLIACCIO, C. T., BUFORD, M. C., JESSOP, F. & HOLIAN, A. 2008. The IL-4R alpha pathway in macrophages and its potential role in silica-induced pulmonary fibrosis. *Journal of Leukocyte Biology,* 83**,** 630-639.

MODOLELL, M., CORRALIZA, I. M., LINK, F., SOLER, G. & EICHMANN, K. 1995. Reciprocal regulation of the nitric oxide synthase/arginase balance in mouse bone marrow-derived macrophages by TH1 and TH2 cytokines. *Eur J Immunol,* 25**,** 1101-4.

MONTAGNER, S., DEHO, L. & MONTICELLI, S. 2014. MicroRNAs in hematopoietic development. *BMC Immunol,* 15**,** 14.

MONTICELLI, S., ANSEL, K. M., XIAO, C., SOCCI, N. D., KRICHEVSKY, A. M., THAI, T. H., RAJEWSKY, N., MARKS, D. S., SANDER, C., RAJEWSKY, K., RAO, A. & KOSIK, K. S. 2005. MicroRNA profiling of the murine hematopoietic system. *Genome Biol,* 6**,** R71.

MORI, M. & GOTOH, T. 2000. Regulation of nitric oxide production by arginine metabolic enzymes. *Biochem Biophys Res Commun,* 275**,** 715-9.

MORIMOTO, K., NISHIKAWA, M., KAWAKAMI, S., NAKANO, T., HATTORI, Y., FUMOTO, S., YAMASHITA, F. & HASHIDA, M. 2003. Molecular weight-dependent gene transfection activity of unmodified and galactosylated polyethyleneimine on hepatoma cells and mouse liver. *Mol Ther,* 7**,** 254-61.

MORRIS, S. M., JR. 2007. Arginine metabolism: boundaries of our knowledge. *J Nutr,* 137**,** 1602S-1609S.

MOSMANN, T. R., CHERWINSKI, H., BOND, M. W., GIEDLIN, M. A. & COFFMAN, R. L. 1986. Two types of murine helper T cell clone. I. Definition according to profiles of lymphokine activities and secreted proteins. *J Immunol,* 136**,** 2348-57.

MOSSER, D. M. 2003. The many faces of macrophage activation. *J Leukoc Biol,* 73**,** 209-12.

MOSSER, D. M. & EDWARDS, J. P. 2008. Exploring the full spectrum of macrophage activation. *Nat Rev Immunol,* 8**,** 958-69.

MOSSER, D. M. & ZHANG, X. 2008. Activation of murine macrophages. *Curr Protoc Immunol,* Chapter 14**,** Unit 14 2.

MOURELATOS, Z. 2008. Small RNAs: The seeds of silence. *Nature,* 455**,** 44-5.

MULJO, S. A., ANSEL, K. M., KANELLOPOULOU, C., LIVINGSTON, D. M., RAO, A. & RAJEWSKY, K. 2005. Aberrant T cell differentiation in the absence of Dicer. *J Exp Med,* 202**,** 261-9.

MUNDER, M. 2009. Arginase: an emerging key player in the mammalian immune system. *Br J Pharmacol,* 158**,** 638-51.

MUNDER, M., EICHMANN, K. & MODOLELL, M. 1998. Alternative metabolic states in murine macrophages reflected by the nitric oxide synthase/arginase balance: competitive regulation by CD4+ T cells correlates with Th1/Th2 phenotype. *J Immunol,* 160**,** 5347-54.

MUNDER, M., EICHMANN, K., MORAN, J. M., CENTENO, F., SOLER, G. & MODOLELL, M. 1999. Th1/Th2-regulated expression of arginase isoforms in murine macrophages and dendritic cells. *J Immunol,* 163**,** 3771-7.

MUNN, D. H., BEALL, A. C., SONG, D., WRENN, R. W. & THROCKMORTON, D. C. 1995. Activation-induced apoptosis in human macrophages: developmental regulation of a novel cell death pathway by macrophage colony-stimulating factor and interferon gamma. *J Exp Med,* 181**,** 127-36.

MURAKAMI, Y., TOYODA, H., TANAKA, M., KURODA, M., HARADA, Y., MATSUDA, F., TAJIMA, A., KOSAKA, N., OCHIYA, T. & SHIMOTOHNO, K. 2011. The progression of liver fibrosis is related with overexpression of the miR-199 and 200 families. *PLoS One,* 6**,** e16081.

MURRAY, P. J., ALLEN, J. E., BISWAS, S. K., FISHER, E. A., GILROY, D. W., GOERDT, S., GORDON, S., HAMILTON, J. A., IVASHKIV, L. B., LAWRENCE, T., LOCATI, M., MANTOVANI, A., MARTINEZ, F. O., MEGE, J. L., MOSSER, D. M., NATOLI, G., SAEIJ, J. P., SCHULTZE, J. L., SHIREY, K. A., SICA, A., SUTTLES, J., UDALOVA, I., VAN GINDERACHTER, J. A., VOGEL, S. N. & WYNN, T. A. 2014. Macrophage activation and polarization: nomenclature and experimental guidelines. *Immunity,* 41**,** 14-20.

MURRAY, P. J. & WYNN, T. A. 2011. Protective and pathogenic functions of macrophage subsets. *Nat Rev Immunol,* 11**,** 723-37.

MUSSNICH, P., ROSA, R., BIANCO, R., FUSCO, A. & D'ANGELO, D. 2015. MiR-199a-5p and miR-375 affect colon cancer cell sensitivity to cetuximab by targeting PHLPP1. *Expert Opin Ther Targets,* 19**,** 1017-26.

MYLONAS, K. J., NAIR, M. G., PRIETO-LAFUENTE, L., PAAPE, D. & ALLEN, J. E. 2009. Alternatively activated macrophages elicited by helminth infection can be reprogrammed to enable microbial killing. *J Immunol,* 182**,** 3084-94.

NAGATA, S. & GOLSTEIN, P. 1995. The Fas death factor. *Science,* 267**,** 1449-56.

NAHID, M. A., PAULEY, K. M., SATOH, M. & CHAN, E. K. 2009. miR-146a is critical for endotoxin-induced tolerance: IMPLICATION IN INNATE IMMUNITY. *J Biol Chem,* 284**,** 34590-9.

NAHID, M. A., SATOH, M. & CHAN, E. K. L. 2011. MicroRNA in TLR signaling and endotoxin tolerance. *Cellular & Molecular Immunology,* 8**,** 388-403.

NAIR, M. G., COCHRANE, D. W. & ALLEN, J. E. 2003. Macrophages in chronic type 2 inflammation have a novel phenotype characterized by the abundant expression of Ym1 and Fizz1 that can be partly replicated in vitro. *Immunol Lett,* 85**,** 173-80.

NAIR, M. G., DU, Y., PERRIGOUE, J. G., ZAPH, C., TAYLOR, J. J., GOLDSCHMIDT, M., SWAIN, G. P., YANCOPOULOS, G. D., VALENZUELA, D. M., MURPHY, A., KAROW, M., STEVENS, S., PEARCE, E. J. & ARTIS, D. 2009. Alternatively activated macrophage-derived RELM-{alpha} is a negative regulator of type 2 inflammation in the lung. *J Exp Med,* 206**,** 937-52.

NAIR, M. G., GALLAGHER, I. J., TAYLOR, M. D., LOKE, P., COULSON, P. S., WILSON, R. A., MAIZELS, R. M. & ALLEN, J. E. 2005. Chitinase and Fizz family members are a generalized feature of nematode infection with selective upregulation of Ym1 and Fizz1 by antigen-presenting cells. *Infect Immun,* 73**,** 385-94.

NAKANISHI, H., HORII, Y., TERASHIMA, K. & FUJITA, K. 1989. Effect of macrophage blockade on the resistance to a primary Brugia pahangi infection of female BALB/c mice. *Trop Med Parasitol,* 40**,** 75-6.

NALDINI, L., BLOMER, U., GALLAY, P., ORY, D., MULLIGAN, R., GAGE, F. H., VERMA, I. M. & TRONO, D. 1996. In vivo gene delivery and stable transduction of nondividing cells by a lentiviral vector. *Science,* 272**,** 263-267.

NATHAN, C. 1991. Mechanisms and modulation of macrophage activation. *Behring Inst Mitt***,** 200-7.

NATHAN, C. F., MURRAY, H. W., WIEBE, M. E. & RUBIN, B. Y. 1983. Identification of interferon-gamma as the lymphokine that activates human macrophage oxidative metabolism and antimicrobial activity. *J Exp Med,* 158**,** 670-89.

NELMS, K., O'NEILL, T. J., LI, S., HUBBARD, S. R., GUSTAFSON, T. A. & PAUL, W. E. 1999. Alternative splicing, gene localization, and binding of SH2-B to the insulin receptor kinase domain. *Mamm Genome,* 10**,** 1160-7.

NGUYEN, K. D., QIU, Y., CUI, X., GOH, Y. P., MWANGI, J., DAVID, T., MUKUNDAN, L., BROMBACHER, F., LOCKSLEY, R. M. & CHAWLA, A. 2011. Alternatively activated macrophages produce catecholamines to sustain adaptive thermogenesis. *Nature,* 480**,** 104-8.

NISHIHARA, T., ZEKRI, L., BRAUN, J. E. & IZAURRALDE, E. 2013. miRISC recruits decapping factors to miRNA targets to enhance their degradation. *Nucleic Acids Res,* 41**,** 8692-705.

NOACK, M. & MIOSSEC, P. 2014. Th17 and regulatory T cell balance in autoimmune and inflammatory diseases. *Autoimmun Rev,* 13**,** 668-77.

NOTTROTT, S., SIMARD, M. J. & RICHTER, J. D. 2006. Human let-7a miRNA blocks protein production on actively translating polyribosomes. *Nature Structural & Molecular Biology,* 13**,** 1108-1114.

NOY, R. & POLLARD, J. W. 2014. Tumor-associated macrophages: from mechanisms to therapy. *Immunity,* 41**,** 49-61.

NUCERA, S., BIZIATO, D. & DE PALMA, M. 2011. The interplay between macrophages and angiogenesis in development, tissue injury and regeneration. *Int J Dev Biol,* 55**,** 495-503.

O'CARROLL, D., MECKLENBRAUKER, I., DAS, P. P., SANTANA, A., KOENIG, U., ENRIGHT, A. J., MISKA, E. A. & TARAKHOVSKY, A. 2007. A Slicer-independent role for Argonaute 2 in hematopoiesis and the microRNA pathway. *Genes Dev,* 21**,** 1999-2004.

O'CARROLL, D. & SCHAEFER, A. 2013. General principals of miRNA biogenesis and regulation in the brain. *Neuropsychopharmacology,* 38**,** 39-54.

O'CONNELL, R. M., CHAUDHURI, A. A., RAO, D. S. & BALTIMORE, D. 2009. Inositol phosphatase SHIP1 is a primary target of miR-155. *Proc Natl Acad Sci U S A,* 106**,** 7113-8.

O'CONNELL, R. M., KAHN, D., GIBSON, W. S., ROUND, J. L., SCHOLZ, R. L., CHAUDHURI, A. A., KAHN, M. E., RAO, D. S. & BALTIMORE, D. 2010. MicroRNA-155 promotes autoimmune inflammation by enhancing inflammatory T cell development. *Immunity,* 33**,** 607-19.

O'CONNELL, R. M., RAO, D. S., CHAUDHURI, A. A., BOLDIN, M. P., TAGANOV, K. D., NICOLL, J., PAQUETTE, R. L. & BALTIMORE, D. 2008. Sustained expression of microRNA-155 in hematopoietic stem cells causes a myeloproliferative disorder. *J Exp Med,* 205**,** 585-94.

O'CONNELL, R. M., TAGANOV, K. D., BOLDIN, M. P., CHENG, G. & BALTIMORE, D. 2007. MicroRNA-155 is induced during the macrophage inflammatory response. *Proc Natl Acad Sci U S A,* 104**,** 1604-9.

O'NEILL, L. A., SHEEDY, F. J. & MCCOY, C. E. 2011. MicroRNAs: the fine-tuners of Toll-like receptor signalling. *Nat Rev Immunol,* 11**,** 163-75.

OBATA-NINOMIYA, K., ISHIWATA, K., TSUTSUI, H., NEI, Y., YOSHIKAWA, S., KAWANO, Y., MINEGISHI, Y., OHTA, N., WATANABE, N., KANUKA, H. & KARASUYAMA, H. 2013. The skin is an important bulwark of acquired immunity against intestinal helminths. *J Exp Med,* 210**,** 2583-95.

OBERNOSTERER, G., TAFER, H. & MARTINEZ, J. 2008. Target site effects in the RNA interference and microRNA pathways. *Biochem Soc Trans,* 36**,** 1216-9.

ODEGAARD, J. I. & CHAWLA, A. 2011. Alternative macrophage activation and metabolism. *Annu Rev Pathol,* 6**,** 275-97.

ODEGAARD, J. I., RICARDO-GONZALEZ, R. R., GOFORTH, M. H., MOREL, C. R., SUBRAMANIAN, V., MUKUNDAN, L., RED EAGLE, A., VATS, D., BROMBACHER, F., FERRANTE, A. W. & CHAWLA, A. 2007. Macrophage-specific PPARgamma controls alternative activation and improves insulin resistance. *Nature,* 447**,** 1116-20.

OERTLI, M., ENGLER, D. B., KOHLER, E., KOCH, M., MEYER, T. F. & MULLER, A. 2011. MicroRNA-155 is essential for the T cell-mediated control of Helicobacter pylori infection and for the induction of chronic Gastritis and Colitis. *J Immunol,* 187**,** 3578-86.

OKABE, Y. & MEDZHITOV, R. 2014. Tissue-specific signals control reversible program of localization and functional polarization of macrophages. *Cell,* 157**,** 832-44.

OKOYE, I. S., COOMES, S. M., PELLY, V. S., CZIESO, S., PAPAYANNOPOULOS, V., TOLMACHOVA, T., SEABRA, M. C. & WILSON, M. S. 2014. MicroRNA-containing T-

regulatory-cell-derived exosomes suppress pathogenic T helper 1 cells. *Immunity,* 41**,** 89-103.

OLEFSKY, J. M. & GLASS, C. K. 2010. Macrophages, inflammation, and insulin resistance. *Annu Rev Physiol,* 72**,** 219-46.

OLSEN, P. H. & AMBROS, V. 1999. The lin-4 regulatory RNA controls developmental timing in Caenorhabditis elegans by blocking LIN-14 protein synthesis after the initiation of translation. *Dev Biol,* 216**,** 671-80.

ORBAN, T. I. & IZAURRALDE, E. 2005. Decay of mRNAs targeted by RISC requires XRN1, the Ski complex, and the exosome. *RNA,* 11**,** 459-69.

ORTEGA, F. J., MORENO-NAVARRETE, J. M., PARDO, G., SABATER, M., HUMMEL, M., FERRER, A., RODRIGUEZ-HERMOSA, J. I., RUIZ, B., RICART, W., PERAL, B. & FERNANDEZ-REAL, J. M. 2010. MiRNA expression profile of human subcutaneous adipose and during adipocyte differentiation. *PLoS One,* 5**,** e9022.

OUYANG, W., KOLLS, J. K. & ZHENG, Y. 2008. The biological functions of T helper 17 cell effector cytokines in inflammation. *Immunity,* 28**,** 454-67.

OWHASHI, M., ARITA, H. & NIWA, A. 1998. Production of eosinophil chemotactic factor by CD8+ T-cells in Toxocara canis-infected mice. *Parasitol Res,* 84**,** 136-8.

PALUDAN, S. R., ELLERMANN-ERIKSEN, S., KRUYS, V. & MOGENSEN, S. C. 2001. Expression of TNF-alpha by herpes simplex virus-infected macrophages is regulated by a dual mechanism: transcriptional regulation by NF-kappa B and activating transcription factor 2/Jun and translational regulation through the AU-rich region of the 3' untranslated region. *J Immunol,* 167**,** 2202-8.

PALUDAN, S. R. & MOGENSEN, S. C. 2001. Virus-cell interactions regulating induction of tumor necrosis factor alpha production in macrophages infected with herpes simplex virus. *J Virol,* 75**,** 10170-8.

PAN, D., MAO, C., QUATTROCHI, B., FRIEDLINE, R. H., ZHU, L. J., JUNG, D. Y., KIM, J. K., LEWIS, B. & WANG, Y. X. 2014. MicroRNA-378 controls classical brown fat expansion to counteract obesity. *Nat Commun,* 5**,** 4725.

PANDINI, G., FRASCA, F., MINEO, R., SCIACCA, L., VIGNERI, R. & BELFIORE, A. 2002. Insulin/insulin-like growth factor I hybrid receptors have different biological characteristics depending on the insulin receptor isoform involved. *J Biol Chem,* 277**,** 39684-95.

PARAMESWARAN, N. & PATIAL, S. 2010. Tumor necrosis factor-alpha signaling in macrophages. *Crit Rev Eukaryot Gene Expr,* 20**,** 87-103.

PARKIN, J. & COHEN, B. 2001. An overview of the immune system. *Lancet,* 357**,** 1777-89.

PASQUINELLI, A. E., REINHART, B. J., SLACK, F., MARTINDALE, M. Q., KURODA, M. I., MALLER, B., HAYWARD, D. C., BALL, E. E., DEGNAN, B., MULLER, P., SPRING, J., SRINIVASAN, A., FISHMAN, M., FINNERTY, J., CORBO, J., LEVINE, M.,

LEAHY, P., DAVIDSON, E. & RUVKUN, G. 2000. Conservation of the sequence and temporal expression of let-7 heterochronic regulatory RNA. *Nature,* 408**,** 86-9.

PAUL, W. E. 2011. Bridging innate and adaptive immunity. *Cell,* 147**,** 1212-5.

PAULEY, K. M., CHA, S. & CHAN, E. K. 2009. MicroRNA in autoimmunity and autoimmune diseases. *J Autoimmun,* 32**,** 189-94.

PECK, A. & MELLINS, E. D. 2010. Plasticity of T-cell phenotype and function: the T helper type 17 example. *Immunology,* 129**,** 147-53.

PEDERSEN, I. & DAVID, M. 2008. MicroRNAs in the immune response. *Cytokine,* 43**,** 391-4.

PERRY, M. M., MOSCHOS, S. A., WILLIAMS, A. E., SHEPHERD, N. J., LARNER-SVENSSON, H. M. & LINDSAY, M. A. 2008. Rapid changes in microRNA-146a expression negatively regulate the IL-1beta-induced inflammatory response in human lung alveolar epithelial cells. *J Immunol,* 180**,** 5689-98.

PERRY, M. M., WILLIAMS, A. E., TSITSIOU, E., LARNER-SVENSSON, H. M. & LINDSAY, M. A. 2009. Divergent intracellular pathways regulate interleukin-1beta-induced miR-146a and miR-146b expression and chemokine release in human alveolar epithelial cells. *FEBS Lett,* 583**,** 3349-55.

PESCE, J., KAVIRATNE, M., RAMALINGAM, T. R., THOMPSON, R. W., URBAN, J. F., JR., CHEEVER, A. W., YOUNG, D. A., COLLINS, M., GRUSBY, M. J. & WYNN, T. A. 2006. The IL-21 receptor augments Th2 effector function and alternative macrophage activation. *J Clin Invest,* 116**,** 2044-55.

PESCE, J. T., RAMALINGAM, T. R., MENTINK-KANE, M. M., WILSON, M. S., EL KASMI, K. C., SMITH, A. M., THOMPSON, R. W., CHEEVER, A. W., MURRAY, P. J. & WYNN, T. A. 2009a. Arginase-1-expressing macrophages suppress Th2 cytokine-driven inflammation and fibrosis. *PLoS Pathog,* 5**,** e1000371.

PESCE, J. T., RAMALINGAM, T. R., WILSON, M. S., MENTINK-KANE, M. M., THOMPSON, R. W., CHEEVER, A. W., URBAN, J. F., JR. & WYNN, T. A. 2009b. Retnla (relmalpha/fizz1) suppresses helminth-induced Th2-type immunity. *PLoS Pathog,* 5**,** e1000393.

PETERSEN, C. P., BORDELEAU, M. E., PELLETIER, J. & SHARP, P. A. 2006. Short RNAs repress translation after initiation in mammalian cells. *Molecular Cell,* 21**,** 533-542.

PFEFFER, S., SEWER, A., LAGOS-QUINTANA, M., SHERIDAN, R., SANDER, C., GRASSER, F. A., VAN DYK, L. F., HO, C. K., SHUMAN, S., CHIEN, M., RUSSO, J. J., JU, J., RANDALL, G., LINDENBACH, B. D., RICE, C. M., SIMON, V., HO, D. D., ZAVOLAN, M. & TUSCHL, T. 2005. Identification of microRNAs of the herpesvirus family. *Nat Methods,* 2**,** 269-76.

PIEHLER, D., ESCHKE, M., SCHULZE, B., PROTSCHKA, M., MULLER, U., GRAHNERT, A., RICHTER, T., HEYEN, L., KOHLER, G., BROMBACHER, F. & ALBER, G. 2015. The IL-33 receptor (ST2) regulates early IL-13 production in fungus-induced allergic airway inflammation. *Mucosal Immunol*.

PILLAI, R. S., BHATTACHARYYA, S. N., ARTUS, C. G., ZOLLER, T., COUGOT, N., BASYUK, E., BERTRAND, E. & FILIPOWICZ, W. 2005. Inhibition of translational initiation by Let-7 MicroRNA in human cells. *Science,* 309**,** 1573-6.

PITETTI, J. L., CALVEL, P., ZIMMERMANN, C., CONNE, B., PAPAIOANNOU, M. D., AUBRY, F., CEDERROTH, C. R., URNER, F., FUMEL, B., CRAUSAZ, M., DOCQUIER, M., HERRERA, P. L., PRALONG, F., GERMOND, M., GUILLOU, F., JEGOU, B. & NEF, S. 2013. An essential role for insulin and IGF1 receptors in regulating sertoli cell proliferation, testis size, and FSH action in mice. *Mol Endocrinol,* 27**,** 814-27.

PIXLEY, F. J. & STANLEY, E. R. 2004. CSF-1 regulation of the wandering macrophage: complexity in action. *Trends Cell Biol,* 14**,** 628-38.

PLACE, R. F., LI, L. C., POOKOT, D., NOONAN, E. J. & DAHIYA, R. 2008. MicroRNA-373 induces expression of genes with complementary promoter sequences. *Proc Natl Acad Sci U S A,* 105**,** 1608-13.

PODSHIVALOVA, K. & SALOMON, D. R. 2013. MicroRNA regulation of T-lymphocyte immunity: modulation of molecular networks responsible for T-cell activation, differentiation, and development. *Crit Rev Immunol,* 33**,** 435-76.

POLLARD, J. W. 2004. Tumour-educated macrophages promote tumour progression and metastasis. *Nat Rev Cancer,* 4**,** 71-8.

POPOVIC, R., RIESBECK, L. E., VELU, C. S., CHAUBEY, A., ZHANG, J., ACHILLE, N. J., ERFURTH, F. E., EATON, K., LU, J., GRIMES, H. L., CHEN, J., ROWLEY, J. D. & ZELEZNIK-LE, N. J. 2009. Regulation of mir-196b by MLL and its overexpression by MLL fusions contributes to immortalization. *Blood,* 113**,** 3314-3322.

PRIDANS, C., LILLICO, S., WHITELAW, B. & HUME, D. A. 2014. Lentiviral vectors containing mouse Csf1r control elements direct macrophage-restricted expression in multiple species of birds and mammals. *Mol Ther Methods Clin Dev,* 1**,** 14010.

QU, Z., LI, W. & FU, B. 2014. MicroRNAs in autoimmune diseases. *Biomed Res Int,* 2014**,** 527895.

QUINN, S. R. & O'NEILL, L. A. 2011. A trio of microRNAs that control Toll-like receptor signalling. *Int Immunol,* 23**,** 421-5.

RAES, G., DE BAETSELIER, P., NOEL, W., BESCHIN, A., BROMBACHER, F. & HASSANZADEH GH, G. 2002. Differential expression of FIZZ1 and Ym1 in alternatively versus classically activated macrophages. *J Leukoc Biol,* 71**,** 597-602.

RALPH, P., MOORE, M. A. & NILSSON, K. 1976. Lysozyme synthesis by established human and murine histiocytic lymphoma cell lines. *J Exp Med,* 143**,** 1528-33.

RAMALINGAM, P., PALANICHAMY, J. K., SINGH, A., DAS, P., BHAGAT, M., KASSAB, M. A., SINHA, S. & CHATTOPADHYAY, P. 2014. Biogenesis of intronic miRNAs located in clusters by independent transcription and alternative splicing. *RNA,* 20**,** 76-87.

RAO, U. R., VICKERY, A. C., KWA, B. H., NAYAR, J. K. & SUBRAHMANYAM, D. 1992. Effect of carrageenan on the resistance of congenitally athymic nude and normal BALB/c mice to infective larvae of Brugia malayi. *Parasitol Res,* 78**,** 235-40.

RASCHKE, W. C., BAIRD, S., RALPH, P. & NAKOINZ, I. 1978. Functional macrophage cell lines transformed by Abelson leukemia virus. *Cell,* 15**,** 261-7.

REHWINKEL, J., BEHM-ANSMANT, I., GATFIELD, D. & IZAURRALDE, E. 2005. A crucial role for GW182 and the DCP1:DCP2 decapping complex in miRNA-mediated gene silencing. *RNA,* 11**,** 1640-7.

REINHART, B. J., SLACK, F. J., BASSON, M., PASQUINELLI, A. E., BETTINGER, J. C., ROUGVIE, A. E., HORVITZ, H. R. & RUVKUN, G. 2000. The 21-nucleotide let-7 RNA regulates developmental timing in Caenorhabditis elegans. *Nature,* 403**,** 901-6.

RENZI, T., CURTALE, G. & LOCATI, M. 2012. Negative regulation of Toll-like receptor 4 signaling by the IL-10-dependent miR-146b. *Immunology,* 137**,** 160-161.

RHOADES, M. W., REINHART, B. J., LIM, L. P., BURGE, C. B., BARTEL, B. & BARTEL, D. P. 2002. Prediction of plant microRNA targets. *Cell,* 110**,** 513-20.

RIBATTI, D., NICO, B., CRIVELLATO, E. & VACCA, A. 2007. Macrophages and tumor angiogenesis. *Leukemia,* 21**,** 2085-9.

RICARDO-GONZALEZ, R. R., RED EAGLE, A., ODEGAARD, J. I., JOUIHAN, H., MOREL, C. R., HEREDIA, J. E., MUKUNDAN, L., WU, D., LOCKSLEY, R. M. & CHAWLA, A. 2010. IL-4/STAT6 immune axis regulates peripheral nutrient metabolism and insulin sensitivity. *Proc Natl Acad Sci U S A,* 107**,** 22617-22.

RODRIGUEZ, A., VIGORITO, E., CLARE, S., WARREN, M. V., COUTTET, P., SOOND, D. R., VAN DONGEN, S., GROCOCK, R. J., DAS, P. P., MISKA, E. A., VETRIE, D., OKKENHAUG, K., ENRIGHT, A. J., DOUGAN, G., TURNER, M. & BRADLEY, A. 2007. Requirement of bic/microRNA-155 for normal immune function. *Science,* 316**,** 608-11.

ROMAGNANI, S. 1997. The Th1/Th2 paradigm. *Immunol Today,* 18**,** 263-6.

ROSA, A., BALLARINO, M., SORRENTINO, A., STHANDIER, O., DE ANGELIS, F. G., MARCHIONI, M., MASELLA, B., GUARINI, A., FATICA, A., PESCHLE, C. & BOZZONI, I. 2007. The interplay between the master transcription factor PU.1 and miR-424 regulates human monocyte/macrophage differentiation. *Proc Natl Acad Sci U S A,* 104**,** 19849-54.

ROSAS, M., DAVIES, L. C., GILES, P. J., LIAO, C. T., KHARFAN, B., STONE, T. C., O'DONNELL, V. B., FRASER, D. J., JONES, S. A. & TAYLOR, P. R. 2014. The transcription factor Gata6 links tissue macrophage phenotype and proliferative renewal. *Science,* 344**,** 645-8.

RUCKERL, D. & ALLEN, J. E. 2014. Macrophage proliferation, provenance, and plasticity in macroparasite infection. *Immunol Rev,* 262**,** 113-33.

RUCKERL, D., JENKINS, S. J., LAQTOM, N. N., GALLAGHER, I. J., SUTHERLAND, T. E., DUNCAN, S., BUCK, A. H. & ALLEN, J. E. 2012. Induction of IL-4Ralpha-dependent microRNAs identifies PI3K/Akt signaling as essential for IL-4-driven murine macrophage proliferation in vivo. *Blood,* 120**,** 2307-16.

RUNTSCH, M. C., ROUND, J. L. & O'CONNELL, R. M. 2014. MicroRNAs and the regulation of intestinal homeostasis. *Front Genet,* 5**,** 347.

RUSCA, N. & MONTICELLI, S. 2011. MiR-146a in Immunity and Disease. *Mol Biol Int,* 2011**,** 437301.

SAITO, S., NAKASHIMA, A., SHIMA, T. & ITO, M. 2010. Th1/Th2/Th17 and regulatory T-cell paradigm in pregnancy. *Am J Reprod Immunol,* 63**,** 601-10.

SAKURAI, K., FURUKAWA, C., HARAGUCHI, T., INADA, K., SHIOGAMA, K., TAGAWA, T., FUJITA, S., UENO, Y., OGATA, A., ITO, M., TSUTSUMI, Y. & IBA, H. 2011. MicroRNAs miR-199a-5p and -3p target the Brm subunit of SWI/SNF to generate a double-negative feedback loop in a variety of human cancers. *Cancer Res,* 71**,** 1680-9.

SANDBERG, R., NEILSON, J. R., SARMA, A., SHARP, P. A. & BURGE, C. B. 2008. Proliferating cells express mRNAs with shortened 3' untranslated regions and fewer microRNA target sites. *Science,* 320**,** 1643-7.

SANDLER, N. G., MENTINK-KANE, M. M., CHEEVER, A. W. & WYNN, T. A. 2003. Global gene expression profiles during acute pathogen-induced pulmonary inflammation reveal divergent roles for Th1 and Th2 responses in tissue repair. *J Immunol,* 171**,** 3655-67.

SATOH, T., TAKEUCHI, O., VANDENBON, A., YASUDA, K., TANAKA, Y., KUMAGAI, Y., MIYAKE, T., MATSUSHITA, K., OKAZAKI, T., SAITOH, T., HONMA, K., MATSUYAMA, T., YUI, K., TSUJIMURA, T., STANDLEY, D. M., NAKANISHI, K., NAKAI, K. & AKIRA, S. 2010. The Jmjd3-Irf4 axis regulates M2 macrophage polarization and host responses against helminth infection. *Nat Immunol,* 11**,** 936-44.

SCHANEN, B. C. & LI, X. 2011. Transcriptional regulation of mammalian miRNA genes. *Genomics,* 97**,** 1-6.

SCHERR, M., BATTMER, K., BLOMER, U., SCHIEDLMEIER, B., GANSER, A., GREZ, M. & EDER, M. 2002. Lentiviral gene transfer into peripheral blood-derived CD34(+) NOD/SCID-repopulating cells. *Blood,* 99**,** 709-712.

SCHIAFFINO, S. & MAMMUCARI, C. 2011. Regulation of skeletal muscle growth by the IGF1-Akt/PKB pathway: insights from genetic models. *Skelet Muscle,* 1**,** 4.

SCHIRLE, N. T. & MACRAE, I. J. 2012. The crystal structure of human Argonaute2. *Science,* 336**,** 1037-40.

SCHUG, T. T. & LI, X. 2009. PPARdelta-mediated macrophage activation: a matter of fat. *Dis Model Mech,* 2**,** 421-2.

SCHULZ, C., GOMEZ PERDIGUERO, E., CHORRO, L., SZABO-ROGERS, H., CAGNARD, N., KIERDORF, K., PRINZ, M., WU, B., JACOBSEN, S. E., POLLARD, J.

W., FRAMPTON, J., LIU, K. J. & GEISSMANN, F. 2012. A lineage of myeloid cells independent of Myb and hematopoietic stem cells. *Science,* 336**,** 86-90.

SCHWARZ, D. S., HUTVAGNER, G., DU, T., XU, Z., ARONIN, N. & ZAMORE, P. D. 2003. Asymmetry in the assembly of the RNAi enzyme complex. *Cell,* 115**,** 199-208.

SEGGERSON, K., TANG, L. & MOSS, E. G. 2002. Two genetic circuits repress the Caenorhabditis elegans heterochronic gene lin-28 after translation initiation. *Dev Biol,* 243**,** 215-25.

SELBACH, M., SCHWANHAUSSER, B., THIERFELDER, N., FANG, Z., KHANIN, R. & RAJEWSKY, N. 2008. Widespread changes in protein synthesis induced by microRNAs. *Nature,* 455**,** 58-63.

SELL, C., PTASZNIK, A., CHANG, C. D., SWANTEK, J., CRISTOFALO, V. J. & BASERGA, R. 1993. Igf-1 Receptor Levels and the Proliferation of Young and Senescent Human Fibroblasts. *Biochemical and Biophysical Research Communications,* 194**,** 259-265.

SEO, K. H., ZHOU, L., MENG, D., XU, J., DONG, Z. & MI, Q. S. 2010. Loss of microRNAs in thymus perturbs invariant NKT cell development and function. *Cell Mol Immunol,* 7**,** 447-53.

SHAH, M. Y. & CALIN, G. A. 2011. MicroRNAs miR-221 and miR-222: a new level of regulation in aggressive breast cancer. *Genome Med,* 3**,** 56.

SHATSEVA, T., LEE, D. Y., DENG, Z. & YANG, B. B. 2011. MicroRNA miR-199a-3p regulates cell proliferation and survival by targeting caveolin-2. *J Cell Sci,* 124**,** 2826-36.

SHAWL, A. I., PARK, K. H. & KIM, U. H. 2009. Insulin receptor signaling for the proliferation of pancreatic beta-cells: involvement of Ca2+ second messengers, IP3, NAADP and cADPR. *Islets,* 1**,** 216-23.

SHEEDY, F. J. & O'NEILL, L. A. 2008. Adding fuel to fire: microRNAs as a new class of mediators of inflammation. *Ann Rheum Dis,* 67 Suppl 3**,** iii50-5.

SHEEDY, F. J., PALSSON-MCDERMOTT, E., HENNESSY, E. J., MARTIN, C., O'LEARY, J. J., RUAN, Q., JOHNSON, D. S., CHEN, Y. & O'NEILL, L. A. 2010. Negative regulation of TLR4 via targeting of the proinflammatory tumor suppressor PDCD4 by the microRNA miR-21. *Nat Immunol,* 11**,** 141-7.

SHIN, C., NAM, J. W., FARH, K. K., CHIANG, H. R., SHKUMATAVA, A. & BARTEL, D. P. 2010. Expanding the microRNA targeting code: functional sites with centered pairing. *Mol Cell,* 38**,** 789-802.

SHIN, V. Y., SIU, J. M., CHEUK, I., NG, E. K. & KWONG, A. 2015. Circulating cell-free miRNAs as biomarker for triple-negative breast cancer. *Br J Cancer,* 112**,** 1751-9.

SICA, A. & MANTOVANI, A. 2012. Macrophage plasticity and polarization: in vivo veritas. *J Clin Invest,* 122**,** 787-95.

SIDDLE, K. 2011. Signalling by insulin and IGF receptors: supporting acts and new players. *Journal of Molecular Endocrinology,* 47**,** R1-R10.

SIMPSON, L. J. & ANSEL, K. M. 2015. MicroRNA regulation of lymphocyte tolerance and autoimmunity. *J Clin Invest,* 125**,** 2242-9.

SINDRILARU, A. & SCHARFFETTER-KOCHANEK, K. 2013. Disclosure of the Culprits: Macrophages-Versatile Regulators of Wound Healing. *Adv Wound Care (New Rochelle),* 2**,** 357-368.

SINGH, R. P., MASSACHI, I., MANICKAVEL, S., SINGH, S., RAO, N. P., HASAN, S., MC CURDY, D. K., SHARMA, S., WONG, D., HAHN, B. H. & REHIMI, H. 2013. The role of miRNA in inflammation and autoimmunity. *Autoimmun Rev,* 12**,** 1160-5.

SISSONS, J. R., PESCHON, J. J., SCHMITZ, F., SUEN, R., GILCHRIST, M. & ADEREM, A. 2012. Cutting edge: microRNA regulation of macrophage fusion into multinucleated giant cells. *J Immunol,* 189**,** 23-7.

SLY, L. M., RAUH, M. J., KALESNIKOFF, J., SONG, C. H. & KRYSTAL, G. 2004. LPS-induced upregulation of SHIP is essential for endotoxin tolerance. *Immunity,* 21**,** 227-39.

SMITH, J. R., BENGHUZZI, H., TUCCI, M., PUCKETT, A. & HUGHES, J. L. 2000. The effects of growth hormone and insulinlike growth factor on the proliferation rate and morphology of RAW 264.7 macrophages. *Biomedical Sciences Instrumentation, Vol 36,* 395**,** 111-116.

SO, A. Y., SOOKRAM, R., CHAUDHURI, A. A., MINISANDRAM, A., CHENG, D., XIE, C., LIM, E. L., FLORES, Y. G., JIANG, S., KIM, J. T., KEOWN, C., RAMAKRISHNAN, P. & BALTIMORE, D. 2014. Dual mechanisms by which miR-125b represses IRF4 to induce myeloid and B-cell leukemias. *Blood,* 124**,** 1502-12.

SOLINAS, G., GERMANO, G., MANTOVANI, A. & ALLAVENA, P. 2009. Tumor-associated macrophages (TAM) as major players of the cancer-related inflammation. *J Leukoc Biol,* 86**,** 1065-73.

SONG, G. & WANG, L. 2008. MiR-433 and miR-127 arise from independent overlapping primary transcripts encoded by the miR-433-127 locus. *PLoS One,* 3**,** e3574.

SONG, G., ZENG, H., LI, J., XIAO, L., HE, Y., TANG, Y. & LI, Y. 2010. miR-199a regulates the tumor suppressor mitogen-activated protein kinase kinase kinase 11 in gastric cancer. *Biol Pharm Bull,* 33**,** 1822-7.

SONG, J., GAO, L., YANG, G., TANG, S., XIE, H., WANG, Y., WANG, J., ZHANG, Y., JIN, J., GOU, Y., YANG, Z., CHEN, Z., WU, K., LIU, J. & FAN, D. 2014. MiR-199a regulates cell proliferation and survival by targeting FZD7. *Plos One,* 9**,** e110074.

SONG, J. J., SMITH, S. K., HANNON, G. J. & JOSHUA-TOR, L. 2004. Crystal structure of Argonaute and its implications for RISC slicer activity. *Science,* 305**,** 1434-7.

SONKOLY, E. & PIVARCSI, A. 2011. MicroRNAs in inflammation and response to injuries induced by environmental pollution. *Mutat Res,* 717**,** 46-53.

SQUADRITO, M. L., BAER, C., BURDET, F., MADERNA, C., GILFILLAN, G. D., LYLE, R., IBBERSON, M. & DE PALMA, M. 2014. Endogenous RNAs modulate microRNA sorting to exosomes and transfer to acceptor cells. *Cell Rep,* 8**,** 1432-46.

SQUADRITO, M. L., ETZRODT, M., DE PALMA, M. & PITTET, M. J. 2013. MicroRNA-mediated control of macrophages and its implications for cancer. *Trends Immunol,* 34**,** 350-9.

SQUADRITO, M. L., PUCCI, F., MAGRI, L., MOI, D., GILFILLAN, G. D., RANGHETTI, A., CASAZZA, A., MAZZONE, M., LYLE, R., NALDINI, L. & DE PALMA, M. 2012. miR-511-3p modulates genetic programs of tumor-associated macrophages. *Cell Rep,* 1**,** 141-54.

STEIN, M., KESHAV, S., HARRIS, N. & GORDON, S. 1992. Interleukin 4 potently enhances murine macrophage mannose receptor activity: a marker of alternative immunologic macrophage activation. *J Exp Med,* 176**,** 287-92.

STEINMAN, L. 2007. A brief history of T(H)17, the first major revision in the T(H)1/T(H)2 hypothesis of T cell-mediated tissue damage. *Nat Med,* 13**,** 139-45.

STENVANG, J., PETRI, A., LINDOW, M., OBAD, S. & KAUPPINEN, S. 2012. Inhibition of microRNA function by antimiR oligonucleotides. *Silence,* 3**,** 1.

STITTRICH, A. B., HAFTMANN, C., SGOUROUDIS, E., KUHL, A. A., HEGAZY, A. N., PANSE, I., RIEDEL, R., FLOSSDORF, M., DONG, J., FUHRMANN, F., HEINZ, G. A., FANG, Z., LI, N., BISSELS, U., HATAM, F., JAHN, A., HAMMOUD, B., MATZ, M., SCHULZE, F. M., BAUMGRASS, R., BOSIO, A., MOLLENKOPF, H. J., GRUN, J., THIEL, A., CHEN, W., HOFER, T., LODDENKEMPER, C., LOHNING, M., CHANG, H. D., RAJEWSKY, N., RADBRUCH, A. & MASHREGHI, M. F. 2010. The microRNA miR-182 is induced by IL-2 and promotes clonal expansion of activated helper T lymphocytes. *Nat Immunol,* 11**,** 1057-62.

STOUT, R. D. & SUTTLES, J. 2004. Functional plasticity of macrophages: reversible adaptation to changing microenvironments. *J Leukoc Biol,* 76**,** 509-13.

STOUT, R. D., WATKINS, S. K. & SUTTLES, J. 2009. Functional plasticity of macrophages: in situ reprogramming of tumor-associated macrophages. *J Leukoc Biol,* 86**,** 1105-9.

STUTZ, A. M., PICKART, L. A., TRIFILIEFF, A., BAUMRUKER, T., PRIESCHL-STRASSMAYR, E. & WOISETSCHLAGER, M. 2003. The Th2 cell cytokines IL-4 and IL-13 regulate found in inflammatory zone 1/resistin-like molecule alpha gene expression by a STAT6 and CCAAT/enhancer-binding protein-dependent mechanism. *J Immunol,* 170**,** 1789-96.

SU, H., TROMBLY, M. I., CHEN, J. & WANG, X. 2009. Essential and overlapping functions for mammalian Argonautes in microRNA silencing. *Genes Dev,* 23**,** 304-17.

SUAREZ, Y., FERNANDEZ-HERNANDO, C., YU, J., GERBER, S. A., HARRISON, K. D., POBER, J. S., IRUELA-ARISPE, M. L., MERKENSCHLAGER, M. & SESSA, W. C. 2008. Dicer-dependent endothelial microRNAs are necessary for postnatal angiogenesis. *Proc Natl Acad Sci U S A,* 105**,** 14082-7.

SUAREZ, Y. & SESSA, W. C. 2009. MicroRNAs as novel regulators of angiogenesis. *Circ Res,* 104**,** 442-54.

SUGANAMI, T. & OGAWA, Y. 2010. Adipose tissue macrophages: their role in adipose tissue remodeling. *J Leukoc Biol,* 88**,** 33-9.

SUN, Y. M., LIN, K. Y. & CHEN, Y. Q. 2013. Diverse functions of miR-125 family in different cell contexts. *J Hematol Oncol,* 6**,** 6.

SUNDERKOTTER, C., STEINBRINK, K., GOEBELER, M., BHARDWAJ, R. & SORG, C. 1994. Macrophages and angiogenesis. *J Leukoc Biol,* 55**,** 410-22.

SUTHERLAND, T. E., LOGAN, N., RUCKERL, D., HUMBLES, A. A., ALLAN, S. M., PAPAYANNOPOULOS, V., STOCKINGER, B., MAIZELS, R. M. & ALLEN, J. E. 2014. Chitinase-like proteins promote IL-17-mediated neutrophilia in a tradeoff between nematode killing and host damage. *Nat Immunol,* 15**,** 1116-25.

SVEGLIATI-BARONI, G., RIDOLFI, F., DI SARIO, A., CASINI, A., MARUCCI, L., GAGGIOTTI, G., ORLANDONI, P., MACARRI, G., PEREGO, L., BENEDETTI, A. & FOLLI, F. 1999. Insulin and insulin-like growth factor-1 stimulate proliferation and type I collagen accumulation by human hepatic stellate cells: Differential effects on signal transduction pathways. *Hepatology,* 29**,** 1743-1751.

SZANTO, A., BALINT, B. L., NAGY, Z. S., BARTA, E., DEZSO, B., PAP, A., SZELES, L., POLISKA, S., OROS, M., EVANS, R. M., BARAK, Y., SCHWABE, J. & NAGY, L. 2010. STAT6 transcription factor is a facilitator of the nuclear receptor PPARgamma-regulated gene expression in macrophages and dendritic cells. *Immunity,* 33**,** 699-712.

TAFER, H., AMERES, S. L., OBERNOSTERER, G., GEBESHUBER, C. A., SCHROEDER, R., MARTINEZ, J. & HOFACKER, I. L. 2008. The impact of target site accessibility on the design of effective siRNAs. *Nat Biotechnol,* 26**,** 578-83.

TAGANOV, K. D., BOLDIN, M. P., CHANG, K. J. & BALTIMORE, D. 2006. NF-kappaB-dependent induction of microRNA miR-146, an inhibitor targeted to signaling proteins of innate immune responses. *Proc Natl Acad Sci U S A,* 103**,** 12481-6.

TAGLIANI, E., SHI, C., NANCY, P., TAY, C. S., PAMER, E. G. & ERLEBACHER, A. 2011. Coordinate regulation of tissue macrophage and dendritic cell population dynamics by CSF-1. *J Exp Med,* 208**,** 1901-16.

TAMEMOTO, H., KADOWAKI, T., TOBE, K., YAGI, T., SAKURA, H., HAYAKAWA, T., TERAUCHI, Y., UEKI, K., KABURAGI, Y., SATOH, S. & ET AL. 1994. Insulin resistance and growth retardation in mice lacking insulin receptor substrate-1. *Nature,* 372**,** 182-6.

TANIGUCHI, C. M., EMANUELLI, B. & KAHN, C. R. 2006. Critical nodes in signalling pathways: insights into insulin action. *Nature Reviews Molecular Cell Biology,* 7**,** 85-96.

TAYLOR, M. D., VAN DER WERF, N., HARRIS, A., GRAHAM, A. L., BAIN, O., ALLEN, J. E. & MAIZELS, R. M. 2009. Early recruitment of natural CD4+ Foxp3+ Treg cells by infective larvae determines the outcome of filarial infection. *Eur J Immunol,* 39**,** 192-206.

TENG, X., LI, D., CHAMPION, H. C. & JOHNS, R. A. 2003. FIZZ1/RELMalpha, a novel hypoxia-induced mitogenic factor in lung with vasoconstrictive and angiogenic properties. *Circ Res,* 92**,** 1065-7.

TESCHENDORF, C., WARRINGTON, K. H., JR., SIEMANN, D. W. & MUZYCZKA, N. 2002. Comparison of the EF-1 alpha and the CMV promoter for engineering stable tumor cell lines using recombinant adeno-associated virus. *Anticancer Res,* 22**,** 3325-30.

THAI, T. H., CALADO, D. P., CASOLA, S., ANSEL, K. M., XIAO, C., XUE, Y., MURPHY, A., FRENDEWEY, D., VALENZUELA, D., KUTOK, J. L., SCHMIDT-SUPPRIAN, M., RAJEWSKY, N., YANCOPOULOS, G., RAO, A. & RAJEWSKY, K. 2007. Regulation of the germinal center response by microRNA-155. *Science,* 316**,** 604-8.

THIEU, V. T., NGUYEN, E. T., MCCARTHY, B. P., BRUNS, H. A., KAPUR, R., CHANG, C. H. & KAPLAN, M. H. 2007. IL-4-stimulated NF-kappaB activity is required for Stat6 DNA binding. *J Leukoc Biol,* 82**,** 370-9.

THOMAS, G. D., RUCKERL, D., MASKREY, B. H., WHITFIELD, P. D., BLAXTER, M. L. & ALLEN, J. E. 2012. The biology of nematode- and IL4Ralpha-dependent murine macrophage polarization in vivo as defined by RNA-Seq and targeted lipidomics. *Blood,* 120**,** e93-e104.

THOMSON, D. W., BRACKEN, C. P. & GOODALL, G. J. 2011. Experimental strategies for microRNA target identification. *Nucleic Acids Res,* 39**,** 6845-53.

TIDBALL, J. G. & WELC, S. S. 2015. Macrophage-Derived IGF-1 Is a Potent Coordinator of Myogenesis and Inflammation in Regenerating Muscle. *Mol Ther,* 23**,** 1134-5.

TILI, E., MICHAILLE, J. J., CIMINO, A., COSTINEAN, S., DUMITRU, C. D., ADAIR, B., FABBRI, M., ALDER, H., LIU, C. G., CALIN, G. A. & CROCE, C. M. 2007. Modulation of miR-155 and miR-125b levels following lipopolysaccharide/TNF-alpha stimulation and their possible roles in regulating the response to endotoxin shock. *J Immunol,* 179**,** 5082-9.

TOMARI, Y. & ZAMORE, P. D. 2005. MicroRNA biogenesis: drosha can't cut it without a partner. *Curr Biol,* 15**,** R61-4.

TONKIN, J., TEMMERMAN, L., SAMPSON, R. D., GALLEGO-COLON, E., BARBERI, L., BILBAO, D., SCHNEIDER, M. D., MUSARO, A. & ROSENTHAL, N. 2015. Monocyte/Macrophage-derived IGF-1 Orchestrates Murine Skeletal Muscle Regeneration and Modulates Autocrine Polarization. *Mol Ther,* 23**,** 1189-200.

TREADWAY, J. L., MORRISON, B. D., GOLDFINE, I. D. & PESSIN, J. E. 1989. Assembly of insulin/insulin-like growth factor-1 hybrid receptors in vitro. *J Biol Chem,* 264**,** 21450-3.

UEKI, K., KONDO, T. & KAHN, C. R. 2004. Suppressor of cytokine signaling 1 (SOCS-1) and SOCS-3 cause insulin resistance through inhibition of tyrosine phosphorylation of insulin receptor substrate proteins by discrete mechanisms. *Mol Cell Biol,* 24**,** 5434-46.

ULE, J., JENSEN, K. B., RUGGIU, M., MELE, A., ULE, A. & DARNELL, R. B. 2003. CLIP identifies Nova-regulated RNA networks in the brain. *Science,* 302**,** 1212-5.

UMESHITA-SUYAMA, R., SUGIMOTO, R., AKAIWA, M., ARIMA, K., YU, B., WADA, M., KUWANO, M., NAKAJIMA, K., HAMASAKI, N. & IZUHARA, K. 2000. Characterization of IL-4 and IL-13 signals dependent on the human IL-13 receptor alpha chain 1: redundancy of requirement of tyrosine residue for STAT3 activation. *Int Immunol,* 12**,** 1499-509.

UNANUE, E. R. 1984. Antigen-presenting function of the macrophage. *Annu Rev Immunol,* 2**,** 395-428.

UNDI, R. B., KANDI, R. & GUTTI, R. K. 2013. MicroRNAs as Haematopoiesis Regulators. *Adv Hematol,* 2013**,** 695754.

URBAN, J. F., JR., NOBEN-TRAUTH, N., DONALDSON, D. D., MADDEN, K. B., MORRIS, S. C., COLLINS, M. & FINKELMAN, F. D. 1998. IL-13, IL-4Ralpha, and Stat6 are required for the expulsion of the gastrointestinal nematode parasite Nippostrongylus brasiliensis. *Immunity,* 8**,** 255-64.

URBICH, C., KUEHBACHER, A. & DIMMELER, S. 2008. Role of microRNAs in vascular diseases, inflammation, and angiogenesis. *Cardiovasc Res,* 79**,** 581-8.

VASUDEVAN, S., TONG, Y. & STEITZ, J. A. 2007. Switching from repression to activation: microRNAs can up-regulate translation. *Science,* 318**,** 1931-4.

VATS, D., MUKUNDAN, L., ODEGAARD, J. I., ZHANG, L., SMITH, K. L., MOREL, C. R., WAGNER, R. A., GREAVES, D. R., MURRAY, P. J. & CHAWLA, A. 2006. Oxidative metabolism and PGC-1beta attenuate macrophage-mediated inflammation. *Cell Metab,* 4**,** 13-24.

VELDHOEN, M., HOCKING, R. J., ATKINS, C. J., LOCKSLEY, R. M. & STOCKINGER, B. 2006. TGFbeta in the context of an inflammatory cytokine milieu supports de novo differentiation of IL-17-producing T cells. *Immunity,* 24**,** 179-89.

VELU, C. S., BAKTULA, A. M. & GRIMES, H. L. 2009. Gfi1 regulates miR-21 and miR-196b to control myelopoiesis. *Blood,* 113**,** 4720-8.

VENTURA, A., YOUNG, A. G., WINSLOW, M. M., LINTAULT, L., MEISSNER, A., ERKELAND, S. J., NEWMAN, J., BRONSON, R. T., CROWLEY, D., STONE, J. R., JAENISCH, R., SHARP, P. A. & JACKS, T. 2008. Targeted deletion reveals essential and overlapping functions of the miR-17 through 92 family of miRNA clusters. *Cell,* 132**,** 875-86.

VEREMEYKO, T., SIDDIQUI, S., SOTNIKOV, I., YUNG, A. & PONOMAREV, E. D. 2013. IL-4/IL-13-dependent and independent expression of miR-124 and its contribution to M2 phenotype of monocytic cells in normal conditions and during allergic inflammation. *PLoS One,* 8**,** e81774.

VIGNALI, D. A., COLLISON, L. W. & WORKMAN, C. J. 2008. How regulatory T cells work. *Nat Rev Immunol,* 8**,** 523-32.

VIGORITO, E., PERKS, K. L., ABREU-GOODGER, C., BUNTING, S., XIANG, Z., KOHLHAAS, S., DAS, P. P., MISKA, E. A., RODRIGUEZ, A., BRADLEY, A., SMITH, K. G., RADA, C., ENRIGHT, A. J., TOELLNER, K. M., MACLENNAN, I. C. &

TURNER, M. 2007. microRNA-155 regulates the generation of immunoglobulin class-switched plasma cells. *Immunity,* 27**,** 847-59.

VOLKMANN, L., SAEFTEL, M., BAIN, O., FISCHER, K., FLEISCHER, B. & HOERAUF, A. 2001. Interleukin-4 is essential for the control of microfilariae in murine infection with the filaria Litomosoides sigmodontis. *Infect Immun,* 69**,** 2950-6.

WAITE, J. C. & SKOKOS, D. 2012. Th17 response and inflammatory autoimmune diseases. *Int J Inflam,* 2012**,** 819467.

WAJANT, H., PFIZENMAIER, K. & SCHEURICH, P. 2003. Tumor necrosis factor signaling. *Cell Death Differ,* 10**,** 45-65.

WAKIYAMA, M., TAKIMOTO, K., OHARA, O. & YOKOYAMA, S. 2007. Let-7 microRNA-mediated mRNA deadenylation and translational repression in a mammalian cell-free system. *Genes Dev,* 21**,** 1857-62.

WANG, H. W. & JOYCE, J. A. 2010. Alternative activation of tumor-associated macrophages by IL-4: priming for protumoral functions. *Cell Cycle,* 9**,** 4824-35.

WANG, L. M., KEEGAN, A., FRANKEL, M., PAUL, W. E. & PIERCE, J. H. 1995. Signal transduction through the IL-4 and insulin receptor families. *Stem Cells,* 13**,** 360-8.

WANG, L. M., KEEGAN, A. D., LI, W., LIENHARD, G. E., PACINI, S., GUTKIND, J. S., MYERS, M. G., JR., SUN, X. J., WHITE, M. F., AARONSON, S. A. & ET AL. 1993a. Common elements in interleukin 4 and insulin signaling pathways in factor-dependent hematopoietic cells. *Proc Natl Acad Sci U S A,* 90**,** 4032-6.

WANG, L. M., MYERS, M. G., JR., SUN, X. J., AARONSON, S. A., WHITE, M. & PIERCE, J. H. 1993b. IRS-1: essential for insulin- and IL-4-stimulated mitogenesis in hematopoietic cells. *Science,* 261**,** 1591-4.

WANG, S. & OLSON, E. N. 2009. AngiomiRs--key regulators of angiogenesis. *Curr Opin Genet Dev,* 19**,** 205-11.

WANG, X. 2014. Composition of seed sequence is a major determinant of microRNA targeting patterns. *Bioinformatics,* 30**,** 1377-83.

WANG, Y. & BLELLOCH, R. 2011. Cell cycle regulation by microRNAs in stem cells. *Results Probl Cell Differ,* 53**,** 459-72.

WANG, Y., MEDVID, R., MELTON, C., JAENISCH, R. & BLELLOCH, R. 2007. DGCR8 is essential for microRNA biogenesis and silencing of embryonic stem cell self-renewal. *Nat Genet,* 39**,** 380-5.

WANG, Y., SZRETTER, K. J., VERMI, W., GILFILLAN, S., ROSSINI, C., CELLA, M., BARROW, A. D., DIAMOND, M. S. & COLONNA, M. 2012. IL-34 is a tissue-restricted ligand of CSF1R required for the development of Langerhans cells and microglia. *Nat Immunol,* 13**,** 753-60.

WEBB, D. C., MCKENZIE, A. N. & FOSTER, P. S. 2001. Expression of the Ym2 lectin-binding protein is dependent on interleukin (IL)-4 and IL-13 signal transduction: identification of a novel allergy-associated protein. *J Biol Chem,* 276**,** 41969-76.

WEISCHENFELDT, J. & PORSE, B. 2008. Bone Marrow-Derived Macrophages (BMM): Isolation and Applications. *CSH Protoc,* 2008**,** pdb prot5080.

WELCH, J. S., ESCOUBET-LOZACH, L., SYKES, D. B., LIDDIARD, K., GREAVES, D. R. & GLASS, C. K. 2002. TH2 cytokines and allergic challenge induce Ym1 expression in macrophages by a STAT6-dependent mechanism. *J Biol Chem,* 277**,** 42821-9.

WERNER, H. & BRUCHIM, I. 2009. The insulin-like growth factor-I receptor as an oncogene. *Arch Physiol Biochem,* 115**,** 58-71.

WERY-ZENNARO, S., LETOURNEUR, M., DAVID, M., BERTOGLIO, J. & PIERRE, J. 1999. Binding of IL-4 to the IL-13Ralpha(1)/IL-4Ralpha receptor complex leads to STAT3 phosphorylation but not to its nuclear translocation. *FEBS Lett,* 464**,** 91-6.

WHERRY, J. C., SCHREIBER, R. D. & UNANUE, E. R. 1991. Regulation of gamma interferon production by natural killer cells in scid mice: roles of tumor necrosis factor and bacterial stimuli. *Infect Immun,* 59**,** 1709-15.

WHYTE, C. S., BISHOP, E. T., RUCKERL, D., GASPAR-PEREIRA, S., BARKER, R. N., ALLEN, J. E., REES, A. J. & WILSON, H. M. 2011. Suppressor of cytokine signaling (SOCS)1 is a key determinant of differential macrophage activation and function. *J Leukoc Biol,* 90**,** 845-54.

WIGHTMAN, B., HA, I. & RUVKUN, G. 1993. Posttranscriptional regulation of the heterochronic gene lin-14 by lin-4 mediates temporal pattern formation in C. elegans. *Cell,* 75**,** 855-62.

WILCZYNSKA, A. & BUSHELL, M. 2015. The complexity of miRNA-mediated repression. *Cell Death Differ,* 22**,** 22-33.

WILLEAUME, V., KRUYS, V., MIJATOVIC, T. & HUEZ, G. 1995. Tumor necrosis factor-alpha production induced by viruses and by lipopolysaccharides in macrophages: similarities and differences. *J Inflamm,* 46**,** 1-12.

WINTER, J., JUNG, S., KELLER, S., GREGORY, R. I. & DIEDERICHS, S. 2009. Many roads to maturity: microRNA biogenesis pathways and their regulation. *Nat Cell Biol,* 11**,** 228-34.

WISSINGER, E., GOULDING, J. & HUSSELL, T. 2009. Immune homeostasis in the respiratory tract and its impact on heterologous infection. *Semin Immunol,* 21**,** 147-55.

WITKOS, T. M., KOSCIANSKA, E. & KRZYZOSIAK, W. J. 2011. Practical Aspects of microRNA Target Prediction. *Curr Mol Med,* 11**,** 93-109.

WURSTER, A. L., WITHERS, D. J., UCHIDA, T., WHITE, M. F. & GRUSBY, M. J. 2002. Stat6 and IRS-2 cooperate in interleukin 4 (IL-4)-induced proliferation and differentiation but are dispensable for IL-4-dependent rescue from apoptosis. *Mol Cell Biol,* 22**,** 117-26.

WYNES, M. W. & RICHES, D. W. 2003. Induction of macrophage insulin-like growth factor-I expression by the Th2 cytokines IL-4 and IL-13. *J Immunol,* 171**,** 3550-9.

WYNN, T. A. 2004. Fibrotic disease and the T(H)1/T(H)2 paradigm. *Nat Rev Immunol,* 4**,** 583-94.

WYNN, T. A. & BARRON, L. 2010. Macrophages: master regulators of inflammation and fibrosis. *Semin Liver Dis,* 30**,** 245-57.

WYNN, T. A., CHAWLA, A. & POLLARD, J. W. 2013. Macrophage biology in development, homeostasis and disease. *Nature,* 496**,** 445-55.

XIA, H., QI, Y., NG, S. S., CHEN, X., LI, D., CHEN, S., GE, R., JIANG, S., LI, G., CHEN, Y., HE, M. L., KUNG, H. F., LAI, L. & LIN, M. C. 2009. microRNA-146b inhibits glioma cell migration and invasion by targeting MMPs. *Brain Res,* 1269**,** 158-65.

XIANG, M., BIRKBAK, N. J., VAFAIZADEH, V., WALKER, S. R., YEH, J. E., LIU, S., KROLL, Y., BOLDIN, M., TAGANOV, K., GRONER, B., RICHARDSON, A. L. & FRANK, D. A. 2014. STAT3 induction of miR-146b forms a feedback loop to inhibit the NF-kappaB to IL-6 signaling axis and STAT3-driven cancer phenotypes. *Sci Signal,* 7**,** ra11.

XIAO, C., CALADO, D. P., GALLER, G., THAI, T. H., PATTERSON, H. C., WANG, J., RAJEWSKY, N., BENDER, T. P. & RAJEWSKY, K. 2007. MiR-150 controls B cell differentiation by targeting the transcription factor c-Myb. *Cell,* 131**,** 146-59.

XIAO, C. & RAJEWSKY, K. 2009. MicroRNA control in the immune system: basic principles. *Cell,* 136**,** 26-36.

XIAO, C., SRINIVASAN, L., CALADO, D. P., PATTERSON, H. C., ZHANG, B., WANG, J., HENDERSON, J. M., KUTOK, J. L. & RAJEWSKY, K. 2008. Lymphoproliferative disease and autoimmunity in mice with increased miR-17-92 expression in lymphocytes. *Nat Immunol,* 9**,** 405-14.

XU, J., LI, C. X., LI, Y. S., LV, J. Y., MA, Y., SHAO, T. T., XU, L. D., WANG, Y. Y., DU, L., ZHANG, Y. P., JIANG, W., LI, C. Q., XIAO, Y. & LI, X. 2011. MiRNA-miRNA synergistic network: construction via co-regulating functional modules and disease miRNA topological features. *Nucleic Acids Res,* 39**,** 825-36.

XU, N., ZHANG, J., SHEN, C., LUO, Y., XIA, L., XUE, F. & XIA, Q. 2012. Cisplatin-induced downregulation of miR-199a-5p increases drug resistance by activating autophagy in HCC cell. *Biochem Biophys Res Commun,* 423**,** 826-31.

YANG, J., SUNDRUD, M. S., SKEPNER, J. & YAMAGATA, T. 2014. Targeting Th17 cells in autoimmune diseases. *Trends Pharmacol Sci,* 35**,** 493-500.

YANG, L., BOLDIN, M. P., YU, Y., LIU, C. S., EA, C. K., RAMAKRISHNAN, P., TAGANOV, K. D., ZHAO, J. L. & BALTIMORE, D. 2012. miR-146a controls the resolution of T cell responses in mice. *J Exp Med,* 209**,** 1655-70.

YANG, Z. H., GRINCHUK, V., URBAN, J. F., BOHL, J., SUN, R., NOTARI, L., YAN, S., RAMALINGAM, T., KEEGAN, A. D., WYNN, T. A., SHEA-DONOHUE, T. & ZHAO, A.

P. 2013. Macrophages as IL-25/IL-33-Responsive Cells Play an Important Role in the Induction of Type 2 Immunity. *Plos One,* 8.

YEKTA, S., SHIH, I. H. & BARTEL, D. P. 2004. MicroRNA-directed cleavage of HOXB8 mRNA. *Science,* 304**,** 594-6.

YERAMIAN, A., MARTIN, L., SERRAT, N., ARPA, L., SOLER, C., BERTRAN, J., MCLEOD, C., PALACIN, M., MODOLELL, M., LLOBERAS, J. & CELADA, A. 2006. Arginine transport via cationic amino acid transporter 2 plays a critical regulatory role in classical or alternative activation of macrophages. *J Immunol,* 176**,** 5918-24.

YI, H., LIANG, B., JIA, J., LIANG, N., XU, H., JU, G., MA, S. & LIU, X. 2013. Differential roles of miR-199a-5p in radiation-induced autophagy in breast cancer cells. *FEBS Lett,* 587**,** 436-43.

YIN, Q., WANG, X., MCBRIDE, J., FEWELL, C. & FLEMINGTON, E. 2008. B-cell receptor activation induces BIC/miR-155 expression through a conserved AP-1 element. *J Biol Chem,* 283**,** 2654-62.

YING, W., TSENG, A., CHANG, R. C., MORIN, A., BREHM, T., TRIFF, K., NAIR, V., ZHUANG, G., SONG, H., KANAMENI, S., WANG, H., GOLDING, M. C., BAZER, F. W., CHAPKIN, R. S., SAFE, S. & ZHOU, B. 2015. MicroRNA-223 is a crucial mediator of PPARgamma-regulated alternative macrophage activation. *J Clin Invest,* 125**,** 4149-59.

YU, H. & ROHAN, T. 2000. Role of the insulin-like growth factor family in cancer development and progression. *Journal of the National Cancer Institute,* 92**,** 1472-1489.

YU, M., WANG, H., XU, Y., YU, D., LI, D., LIU, X. & DU, W. 2015. Insulin-like growth factor-1 (IGF-1) promotes myoblast proliferation and skeletal muscle growth of embryonic chickens via the PI3K/Akt signalling pathway. *Cell Biol Int,* 39**,** 910-22.

YUE, D., LIU, H. & HUANG, Y. 2009. Survey of Computational Algorithms for MicroRNA Target Prediction. *Curr Genomics,* 10**,** 478-92.

ZAMORANO, J., WANG, H. Y., WANG, L. M., PIERCE, J. H. & KEEGAN, A. D. 1996. IL-4 protects cells from apoptosis via the insulin receptor substrate pathway and a second independent signaling pathway. *J Immunol,* 157**,** 4926-34.

ZENG, Y., YI, R. & CULLEN, B. R. 2005. Recognition and cleavage of primary microRNA precursors by the nuclear processing enzyme Drosha. *EMBO J,* 24**,** 138-48.

ZHAI, P. F., WANG, F., SU, R., LIN, H. S., JIANG, C. L., YANG, G. H., YU, J. & ZHANG, J. W. 2014. The regulatory roles of microRNA-146b-5p and its target platelet-derived growth factor receptor alpha (PDGFRA) in erythropoiesis and megakaryocytopoiesis. *J Biol Chem,* 289**,** 22600-13.

ZHANG, B., PAN, X., COBB, G. P. & ANDERSON, T. A. 2007. microRNAs as oncogenes and tumor suppressors. *Dev Biol,* 302**,** 1-12.

ZHANG, C., ZHANG, J., ZHANG, A., WANG, Y., HAN, L., YOU, Y., PU, P. & KANG, C. 2010a. PUMA is a novel target of miR-221/222 in human epithelial cancers. *Int J Oncol,* 37**,** 1621-6.

ZHANG, C. Z., ZHANG, J. X., ZHANG, A. L., SHI, Z. D., HAN, L., JIA, Z. F., YANG, W. D., WANG, G. X., JIANG, T., YOU, Y. P., PU, P. Y., CHENG, J. Q. & KANG, C. S. 2010b. MiR-221 and miR-222 target PUMA to induce cell survival in glioblastoma. *Mol Cancer,* 9**,** 229.

ZHANG, H., FAGAN, D. H., ZENG, X., FREEMAN, K. T., SACHDEV, D. & YEE, D. 2010c. Inhibition of cancer cell proliferation and metastasis by insulin receptor downregulation. *Oncogene,* 29**,** 2517-27.

ZHANG, H., ZHU, S., ZHANG, C., LIU, W. & ZHU, J. 2015. [miR-199a-5p inhibits the proliferation of rat airway smooth muscle cells and the expression of hypoxia inducible factor 1 alpha under hypoxia conditions]. *Xi Bao Yu Fen Zi Mian Yi Xue Za Zhi,* 31**,** 1183-8.

ZHANG, J., HAN, L., GE, Y., ZHOU, X., ZHANG, A., ZHANG, C., ZHONG, Y., YOU, Y., PU, P. & KANG, C. 2010d. miR-221/222 promote malignant progression of glioma through activation of the Akt pathway. *Int J Oncol,* 36**,** 913-20.

ZHANG, N. & BEVAN, M. J. 2010. Dicer controls CD8+ T-cell activation, migration, and survival. *Proc Natl Acad Sci U S A,* 107**,** 21629-34.

ZHANG, X., EDWARDS, J. P. & MOSSER, D. M. 2009. The expression of exogenous genes in macrophages: obstacles and opportunities. *Methods Mol Biol,* 531**,** 123-43.

ZHANG, X. & MOSSER, D. M. 2008. Macrophage activation by endogenous danger signals. *J Pathol,* 214**,** 161-78.

ZHAO, A., URBAN, J. F., JR., ANTHONY, R. M., SUN, R., STILTZ, J., VAN ROOIJEN, N., WYNN, T. A., GAUSE, W. C. & SHEA-DONOHUE, T. 2008. Th2 cytokine-induced alterations in intestinal smooth muscle function depend on alternatively activated macrophages. *Gastroenterology,* 135**,** 217-225 e1.

ZHAO, J. L., RAO, D. S., BOLDIN, M. P., TAGANOV, K. D., O'CONNELL, R. M. & BALTIMORE, D. 2011. NF-kappaB dysregulation in microRNA-146a-deficient mice drives the development of myeloid malignancies. *Proc Natl Acad Sci U S A,* 108**,** 9184-9.

ZHAO, Q. Q., CHEN, J. L., LV, T. F., HE, C. X., TANG, G. P., LIANG, W. Q., TABATA, Y. & GAO, J. Q. 2009. N/P ratio significantly influences the transfection efficiency and cytotoxicity of a polyethylenimine/chitosan/DNA complex. *Biol Pharm Bull,* 32**,** 706-10.

ZHOU, B., WANG, S., MAYR, C., BARTEL, D. P. & LODISH, H. F. 2007. miR-150, a microRNA expressed in mature B and T cells, blocks early B cell development when expressed prematurely. *Proc Natl Acad Sci U S A,* 104**,** 7080-5.

ZHOU, R., O'HARA, S. P. & CHEN, X. M. 2011. MicroRNA regulation of innate immune responses in epithelial cells. *Cell Mol Immunol,* 8**,** 371-9.

ZHOU, X., DUAN, X., QIAN, J. & LI, F. 2009. Abundant conserved microRNA target sites in the 5'-untranslated region and coding sequence. *Genetica,* 137**,** 159-64.

ZHOU, X., JEKER, L. T., FIFE, B. T., ZHU, S., ANDERSON, M. S., MCMANUS, M. T. & BLUESTONE, J. A. 2008. Selective miRNA disruption in T reg cells leads to uncontrolled autoimmunity. *J Exp Med,* 205**,** 1983-91.

ZHU, X., PRIBIS, J. P., RODRIGUEZ, P. C., MORRIS, S. M., JR., VODOVOTZ, Y., BILLIAR, T. R. & OCHOA, J. B. 2014. The central role of arginine catabolism in T-cell dysfunction and increased susceptibility to infection after physical injury. *Ann Surg*, 259**,** 171-8.

ZHU, Z., ZHENG, T., HOMER, R. J., KIM, Y. K., CHEN, N. Y., COHN, L., HAMID, Q. & ELIAS, J. A. 2004. Acidic mammalian chitinase in asthmatic Th2 inflammation and IL-13 pathway activation. *Science*, 304**,** 1678-82.

ZHUANG, G., MENG, C., GUO, X., CHERUKU, P. S., SHI, L., XU, H., LI, H., WANG, G., EVANS, A. R., SAFE, S., WU, C. & ZHOU, B. 2012. A novel regulator of macrophage activation: miR-223 in obesity-associated adipose tissue inflammation. *Circulation*, 125**,** 2892-903.